THE UNIVERSITY OF ALBERTA

"LANDSLIDES IN LAYERED VOLCANIC SUCCESSIONS WITH PARTICULAR REFERENCE TO
THE TERTIARY ROCKS OF SOUTH CENTRAL BRITISH COLUMBIA"

by

Stephen George Evans

A THESIS

SUBMITTED TO THE FACULTY OF GRADUATE STUDIES AND RESEARCH

IN PARTIAL FULFILMENT OF THE REQUIREMENTS FOR THE DEGREE

OF DOCTOR OF PHILOSOPHY

Department of Geology

EDMONTON, ALBERTA

FALL 1983

Dedication

To my wife Dale, for her sacrifices, and to my children, Sarah and Matthew, who spent long childhood hours without their father during his pre-occupation with this work.

iv

Abstract

The results of a literature review indicated that slopes developed in layered volcanic successions are particularly susceptible to slope movements. Landsliding is related to the presence of a weak layer beneath a rigid capping of lavas and breccias. The weak layer is frequently volcaniclastic material. The effect of geological structure is evident in lateral and headscarp geometries, and movement is frequently in a direction at some angle to the direction of true dip. Movement direction is governed by the orientation of release surfaces in the cap, rather than by the orientation of the weak layer, or discontinuities within it. Initial slope movements are generally of the block type and are successive in nature. The morphology of the landslides is suggestive of two types of slope movement, viz. sliding or spreading.

To investigate the nature of geological controls on landslides, and the kinematics of slope movements, a regional landslide study was carried out in slopes developed in Paleogene and Neogene volcanic successions in two areas of the Interior Plateau, British Columbia.

The distribution of landslides was mapped using aerial photographs, and landslides were classified on the basis of morphology. The morphology and geological setting of the landslide sites were discussed in detail. Detailed geological mappping and field observations were carried out on four massive landslides in the Salmon River valley, sothwest of Westwold. The volumes of these movements are in excess of $10^8 m^3$. Movement has taken place where weak volcaniclastic layers were exposed at the base of pre-movement slopes, and the relationship between geological structure was examined.

The microstructure of the volcaniclastic layers was analysed by polarising and scanning electron microscopes, in addition to X-ray diffraction. The microstructure was described using a hierarchy of microsructural domains. The clay mineralogy was found to be dominated by montmorillonite, which occurs at grain and matrix sites in each domain as an alteration product of volcanic glass particles and feldspar crystals. The microfabric is characterised by an open, porous structure at the inter-, intra-, and trans-assemblage scales.

A range of geotechnical properties was established for selected volcaniclastic materials. They are characterised by low dry density (13.98–21.92 KN/m³) and high

porosity (9.0–43.3%); low uniaxial compressive strength, q_u ≤13.5 MPa; low angles of ultimate shear resistance, <20°, which are found to be higher in the presesnce of significant amounts of authigenic or pyroclastic silica.

An evaluation of sliding and spreading models was carried out. The sliding mechanism was analysed using a simple wedge analysis under a variety of geometries and groundwater conditions. The analysis indicates that conditions for sliding could have existed in the slopes analysed.

In the spreading model, the stability of the loading produced by the weight of the cap was analysed as an analogue to a bearing capacity problem, and is estimated from the theory of Mandel and Salençon. The analysis shows that only undrained spreading is possible in the slopes analysed. It is unlikely that undrained conditions resulted directly from cap loading, but undrained conditions may have existed as a result of the structural breakdown of the porous rock mass in the subjacent layer. Although this is suggested by microstructural observations , detailed laboratory test results are not available to confirm this possibility.

It is probable that the slope movements resulted from a general progressive failure initiated by local structural breakdown in the spreading layer.

Although no absolute dates were obtained for the slope movements examined, first–time slope movemenets are thought to have occurred in the early post–glacial period prior to the onset of the Altithermal at approximately 8200 years B.P. Evidence does exist at some landslide sites, however, for subsequent movement having taken place since that date.

Acknowledgements

Table of Contents

List of Tables

List of Figures

List of Plates

xxiii

1. LANDSLIDES IN VOLCANIC SUCCESSIONS

1.1 Introduction

The observation that slopes developed in volcanic successions are particularly susceptible to landslides has been made in many parts of the world. The purpose of this introductory chapter is to review this observation, to evaluate the geological factors contributing to this susceptibility and to broadly review the range of movement mechanisms which may be operative in these slopes. It also serves as an introduction to the regional landslide study of volcanic successions in south-central British Columbia which makes up the remainder of this work.

Widespread instability in volcanic successions was first reported by geologists of the United States Geological Survey working in the American Cordillera. Observations on landslides on the Columbia River Plateau and the Snake River Plains were made, for example, by I.C. Russell (1893; 1898; 1899; 1901; 1902). He described what he called "unusually favorable conditions" in the volcanic successions of this region including stratigraphical controls, structural relations and slope geometry. In addition to Russell, Lindgren (1901) in Oregon and Howe (1909) in Colorado contributed other observations on landslides in volcanic successions. It is remarkable that their contemporaries working in Canada, in similar terrain, made no comment on the widespread instability associated with volcanic successions in the Interior Plateau of British Columbia which is described in the following chapters of this work for the first time.

A volcanic succession can consist of lava flows, pyroclastic flows, airfall pyroclastics and mudflow units as well as those deposited by "normal" sedimentary processes. The heterogeneity exhibited in such successions reflects the episodic nature of volcanic processes, the variability of eruptive products and the spatial variability of processes in the volcanic environment, well documented in the volcanological literature (Macdonald, 1972; Williams and McBirney, 1979; Parsons, 1974). In addition to variability between units, the properties of individual units in the succession can also vary both in vertical and horizontal directions. This may include variations in lithology, alteration or diagenesis, all of which significantly affect the geotechnical properties of a given unit. Volcanic successions are good examples, therefore, of a geotechnical complexity which

"arises when the properties that govern the geotechnical behaviour of the project vary rapidly across a wide range within a site[1]" (Morgenstern and Cruden, 1977, p. 3).

Heterogeneity in geotechnical properties in volcanic successions has led to severe problems in the design, construction and maintenance of engineering projects (e.g., Rands, 1915; Bryan, 1929; Banks and Saucier, 1965; Niccum, 1967; Dreyer, 1926; Tryggvason, 1957; Rocha *et al.*, 1974; Flyngenring *et al.*, 1976; Lutton *et al.*, 1979).

1.2 Landslides and Geological Environments in Volcanic Successions

A review of instability in volcanic successions has led to the conclusion that landslides occur in four geological environments, or types of successions, which are illustrated in Fig. 1.1.

1.2.1 Type 1 - Landslides in Interlayered Volcanic Successions

The most common geological conditions for instability are on slopes where massive resistant flow rocks, which may be interstratified with other types of rock, overlie a soft layer, or zone, of weak pyroclastic rocks, or tuffaceous or poorly lithified sediments. The upper resistant rock unit (or units) is an essential component of this environment and is termed the *cap* (Fig. 1.1).

These geological conditions are reported in the Cenozoic rocks of the Cordillera of the United States by Liang and Belcher (1958), Baker and Chieruzzi (1959), Ray (1960), Rib and Liang (1978) and Radbruch-Hall *et al.* (1976).

In the Intermontane area of the United States, Russell (1898) noted that where soft rocks consisting of lapilli, tephra, clays or lacustrine sediments, occurred beneath cliff-forming layers of basalt, widespread instability was observed. He also noted that where these soft layers were absent, no evidence for landsliding was observed (*cf.* Chapter 3,). In commenting on landslides in Nez Perce Co., Idaho, he noted that,

> "...so constant is the relation between landslides and the presence of (soft interbeds) ... that the landslides furnish an indication of the extent and thickness of soft layers." (Russell, 1901, p. 79)

. Stearns *et al.* (1938) point to the importance of lacustrine sediments and tuffs in

----

[1]A site is meant to embrace extended routes for projects such as tunnels, highways or pipelines, as well as the more local situations such as those which arise with dam and building foundations (Morgenstern and Cruden, 1977).
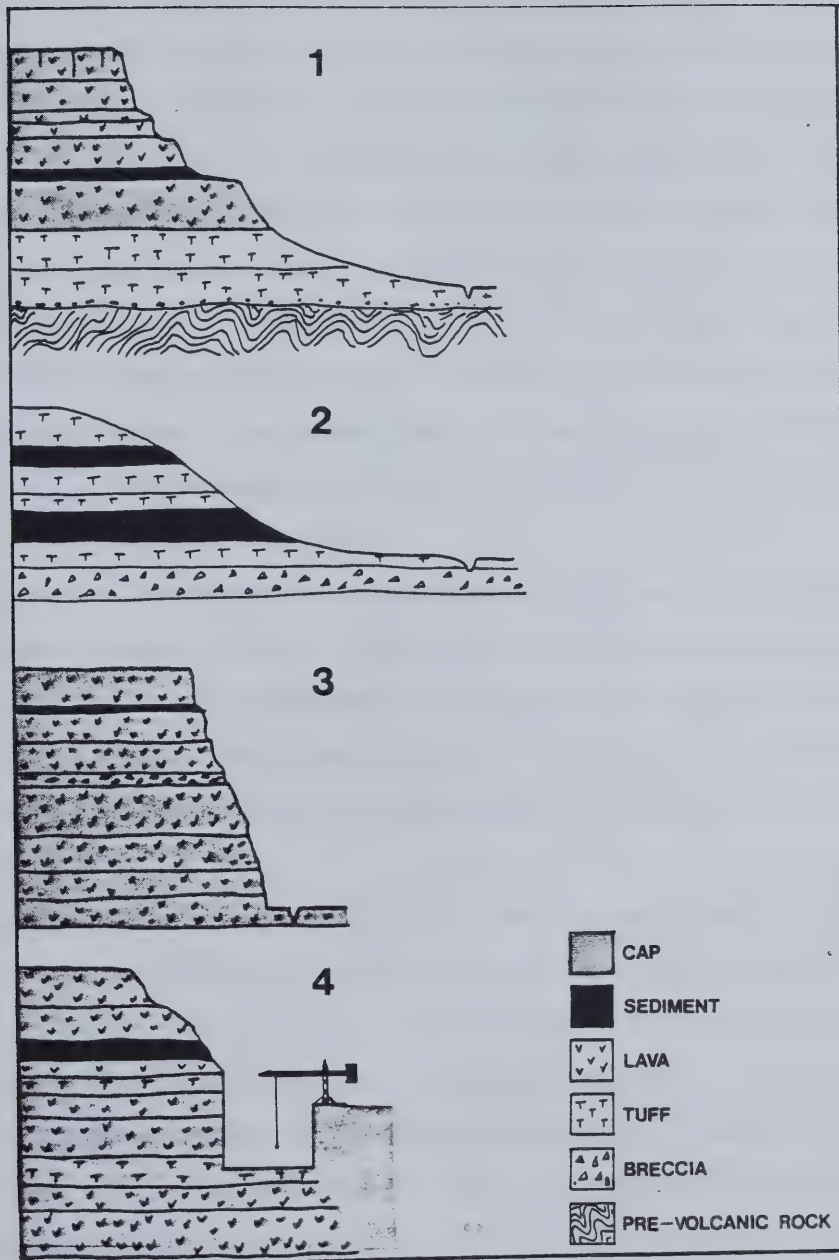
Figure 1.1 Types of volcanic successions, (for details see text).

landslides in the Snake River Plain and mention recent movements and failures resulting from irrigation. Griggs (1976) noted widespread landslides where claystones and siltstones of the Tertiary Latah Formation underlay Columbia River Basalts in the Spokane quadrangle, and noted their re-activation by stream erosion. Hogensen (1964) describes the sliding of basalt on tuffaceous sandy shale in the Umatilla River basin, and landslides in the vicinity of The Dalles along the Columbia River have been noted by Piper (1932). More detailed work by Anderson and Schuster (1970), Waters (1973) and Palmer (1977) describe large landslides in the Lower Columbia River. Whilst Anderson and Schuster (1970) were concerned with the engineering properties of altered clay-rich pyroclastic units, Waters (1973) followed by Palmer (1977) identified a clay-rich saprolite horizon developed in Lower Tertiary volcaniclastic rocks which have undergone hydrothermal alteration as a major zone of weakness on the northern slopes of the Columbia River Gorge in the vicinity of the Bonneville Dam.

This type of succession and associated landsliding has been described in the vicinity of Portland, Oregon, by Trimble (1964), who noted that landslides composed the entire slopes of the tuffaceous sediments of the Scappoose Formation. Also in Oregon, Lawrence (1979) describes massive block sliding of the basalts of the Columbia River Group, resting on top of the tuffaceous John Day Formation, down the dip slope of the Ochoco Mountains.

In Wyoming, Pierce (1968) described the Carter Mountain landslide complex in which the Eocene Cody Shale, as Pierce notes, "gave way" under the load of 915 m of cliff-forming volcanic flows and sediments. Shroder (1971) in his regional landslide study of Utah found that the lithological combination of Tertiary basalt over limestone or tuffaceous sediments accounted for 16% of the landslide areas in the state.

In Colorado, Howe (1909), Attwood (1919), Attwood and Mather (1932), Hinds (1938) and Yeend (1969, 1973) have reported on instability of steep slopes in horizontal to sub-horizontal bedded volcanics where shales, tuffs and pyroclastic beds occur beneath caps composed mainly of lava. Van Horn (1972) reported on the failure of the tuffaceous Eocene Denver Formation beneath latite flows on Table Mountain at Golden. In New Mexico, Kelley (1979) reported instability along the Rio Grande where basalt flows overlie the tuffaceous shales and sandstones of the Mio-Pliocene Santa Fe Formation in

the Espanola Basin.

Although conditions for similar instability appear to exist in parts of Central and South America, the writer is not aware of their report. Excellent documentation of the engineering geology of damsites in volcanic successions in Mexico (UNAM, 1976) and Brazil (e.g. Nieble *et al.*, 1979) mention local instability associated with construction, but no mention is made of natural instability on the scale that would be anticipated. Similar remarks apply to slopes developed in volcanic successions in the Patagonia plateau of Argentina.

Landslides occurring in this type of volcanic succession have been reported from the Tertiary volcanic successions of the Brito–Arctic (Thulean) volcanic province in the North Atlantic. Thorarinssen *et al.* (1959), Asai (1968), and Ollier (1969) report extensive landsliding along sedimentary interbeds in the plateau basalts of Iceland. In the Faeroe Islands, Jorgensen (1978) reports detailed observations on landslides, first noted by Geikie (1880), which involve the movement of a basalt cap on altered pyroclastic breccias and tuffs.

In Eastern Europe, landslides in this type of geological environment have been studied in Czechoslovakia (*e.g.*, Nemcok, 1964; Zaruba and Mencl, 1969; Pasek and Kostak, 1977; Malgot and Otepka, 1977). The problem is marked around the Handlova depression where a cap of andesite overlies soft Tertiary tuffs and claystones (Malgot and Otepka, 1977).

Perhaps one of the better documented failures in this type of succession is the 1956 failure of Gradot Ridge in Yugoslavia (Suklje and Vidmar, 1961). A rib of a tableland catastrophically failed through clayey lacustrine sediment and bedded silt which were part of a Cenozoic volcanic succession. The cap was composed of more indurated rocks consisting of tuffs, sediments and lava flows. The landslide involved 20×10^6 m^3 and occurred in the Vatasha valley where older and similar landslides had occurred with their basal failure plane located in the same clay layer as it was successively exposed by erosion.

Slope movements in similar geological environments are also reported from Japan. Large scale slope movements are reported around the Tertiary basalt plateau in western Kyushu by the Japan Society of Landslide (1972). A recent example involving an area of

64 ha. is described where movement of a basalt cap took place along tuff seams within Neogene coal-bearing sediments dipping 4^0 downslope. Miyagi (1979) describes large landslides in north-east Honshu where lava cappings overlying pyroclastic rocks have undergone movement. Sharma (1975) reports the occurrence of large scale landslides in the Deccan Plateau, India.

A related environment which is highly susceptible to slope movement exists where a capping of massive volcanic rocks overlies weak material, below the base of the volcanic succession in pre-volcanic rocks. The weak material may consist of (a) the weathered unconformity between underlying resistant rocks and an overlying volcanic succession or (b) of a greater thickness of weak material in the form of older sediments. In the former category, Smith (1903) noted that landslides were common where Columbia River Basalt overlies pre-Tertiary schist or granite in Central Washington. Griggs (1976) also noted that some landslides involving the Columbia River Basalt have moved on the surface of the Pre-Cambrian Belt Supergroup in the Spokane area.

In the latter category, instability also arises where older, weak, pre-volcanic sediments underly lava caps. Instability in these circumstances has been described in the vicinity of Yellowstone National Park by Keefer and Love (1956), Hall (1960) and Waldrop and Hyden (1963), and in Colorado by Howe (1909). Along the Snake River, south of Yellowstone Park, Bailey (1971) observes that the entire area where Tertiary volcanics rest upon Mesozoic mudrocks which contain bentonitic seams, is characterised by numerous and extensive slope movements. In Colorado, Howe (1909) and Attwood and Mather (1932) noted similar slope movements in the San Juan Mountains where the underlying weak rock is the Mancos Shale. Koons (1945) has described instability in the Uinkaret Plateau of northern Arizona where basalt cappings overlay soft Triassic shales and marls, and Wright (1946) has a spectacular aerial photograph of an unstable mesa margin where basalt overlies similar Triassic shale in the Lower Rio Puerco area of New Mexico.

Large landslides have occurred in the Tertiary volcanic rocks of the Western Isles of Scotland and the Antrim Plateau of Northern Ireland. In coastal slopes on the Western Isles, where basalt flows overlie weaker Mesozoic mudrocks, large slumps have commonly occurred (Sissons, 1967). On Skye the geological environment of large landslides was first reported by Geikie (1904) and is described in detail by Anderson and

Durham (1966). Similar movements are common on Mull (Bailey *et al.*, 1924), Raasay and Eigg (Sissons, 1967).

In Northern Ireland large landslides have occurred along the rim of Antrim Plateau (Charlesworth, 1953; Manning *et al.* 1970) where the Tertiary basalts are underlain by weaker Jurassic mudrocks and Triassic marls. Stephens (1958) and Prior *et al.* (1968) describe block movements in which rotation has taken place in a zone which is between 1 and 4 km in width.

G.Jorgensen (pers. comm.) reports similar movements in the Tertiary Province of West Greenland which are also mapped by the Geological Survey of Greenland (1976).

1.2.2 Type 2 - Landslides in Weak Volcanic Successions in the Absence of a Cap

A second, less common, unstable environment exists where weak volcanic rocks exist in slopes without a substantial cap of more resistant material. These rocks may be rich in clay as a result of alteration (weathering, diagenesis, hydrothermal activity) , or they may be loose pyroclastic material or soft sediments. Landslides occurring in such environments are frequently flows, defined after Varnes (1978), and do not exhibit the block morphology of the groups previously described. Examples are described by Waters (1973) and Palmer (1977) in the vicinity of the Bonneville Dam in the Columbia River Gorge where the debris from one such failure constitutes the foundation of the dam itself. Photographs of classical flows in the same region are shown by Anderson and Schuster (1970) and Varnes (1978), both movements involving altered volcanic rock. Debris flows in the western Cascade Range in Oregon have occurred in altered clay rich soils developed on Tertiary volcaniclastic rock. These soils have a high concentration of expandable clay minerals and have been the subject of much investigation by Dyrness (1967), Paeth *et al.* (1971), Swanson and James (1975), Swanston and Swanson (1976) and Swanson and Swanston (1977). Patton (1976), and Mokievsky–Zubok (1977) have discussed a massive mobile slide of clay–rich hydrothermally altered acidic flows and tuff breccia from the slopes of the Meager Creek Complex in British Columbia. The slide occurred in 1975 and involved 29×10^6 m^3. In the Yellowstone National Park, Hall (1960) and Witkind (1969) have described large landslides in altered rhyolite and rhyolitic welded tuffs, and Attwood and Mather (1932) have given a full description of two large slope

movements in altered acidic lavas and tuffs at the Slumgullion and Cimarron flow slides in the San Juan Mountains of Colorado.

Slides of poorly lithified material from the slopes of volcanoes should also be mentioned in this category of failures (Kuenen, 1935; Dishaw, 1967; Voight et al., 1981.) These may contribute to lahars as discussed by Crandell (1971).

Gibb (1979) has an excellent description of a flow slide on the coast of the Bay of Plenty, New Zealand, in porous volcanic ash. This type of landslide is also common in pyroclastic debris in Japan and examples of these landslides are described by Yatsu (1966), Watari (1967), Miyagi (1979), Nakamura (1976) and the Japan Society of Landslide (1972). Harp et al. (1981) document extensive landsliding resulting from the 1976 Guatemala Earthquake, in Pleistocene pyroclastic deposits.

These types of slope movements are transitional to those occurring in residual soils (e.g., Simonett, 1967; and it is not the intent to pursue this class of landslide further.

1.2.3 Type 3 - Landslides in Volcanic Successions Consisting of a Cap Only

The third type of unstable geological environment involves the collapse of a slope consisting of cap material only, due to shear along existing discontinuities within a comparatively resistant rock mass. This category of failure is transitional to rock slope movements in other rock types. Slope movement originates in oversteepened slopes which result from erosion or ice–contact process such as those described by Mathews (1952). The resultant landslide is usually highly mobile and initial failure may be triggered by seismic forces. Examples are described by Mathews (1952), Crandell and Fahnestock (1965), Moore and Mathews (1977), and Clague and Souther (1982) from volcanic complexes in the coastal ranges of the North American Cordillera.

1.2.4 Type 4 - Landslides Associated with Construction Activity in Volcanic Successions

Construction–related failure as a result of rapid geometry changes associated with excavation comprise the fourth category or environment of slope movement in volcanic successions since the special conditions imposed by construction make it difficult to treat them in other environments. It is with reference to these failures that a large body of

detailed geological and geotechnical work has been undertaken in highway and dam construction. Many of the documented construction failures have occurred within old slide masses associated with a Type 1 geological environment.

Pope and Anderson (1960) have given detailed engineering data on the behaviour of montmorillonite-rich soils derived from pyroclastic sediments encountered in dam construction in the Willamette Basin, Oregon, and Staples (1957) described an abutment failure at the Point Lookout Dam in the same project. Anderson (1971) has described the engineering behaviour of altered pyroclastic rocks in the Columbia River Valley where construction failures occurred in old landslide masses during a highway relocation project. Squier and Vesteeg (1971) describe the well-known OMSI-Zoo slide in Portland, Oregon, where movement involved decomposed basalt within an old landslide mass. In the same city, Clarke (1908, 1918) has described a slide in weathered volcanic rock triggered by reservoir construction. Bryan (1929) described an abutment failure at the Zuni Dam in New Mexico, and Nobles (1973) has described a failure in a highway cut in Colorado.

An extensive body of data exists for construction projects in Central and South America. UNAM (1976) includes several case histories of the engineering geology of dams in Mexico developed mostly in acid volcanic successions, and Lutton *et al.* (1979) have summarised the landslide experiences in the Gaillard Cut of the Panama Canal. Much information exists on the engineering behaviour of the Plateau Basalts of the Parana Basin in Brazil which has been extensively developed for hydro-electricity (Nieble and Cruz, 1971; Nieble *et al.*, 1974; Ruiz *et al.*, 1968; Kanji *et al.*, 1977; Ruiz *et al.*, 1979; Rocha *et al.*, 1974; Kanji, 1979).

This work is concerned with evaluating the landslide reponse of interlayered volcanic successions such as those described in the discussion of Type 1 environments above. As a result, attention will now be focussed on the development of this type of slope movement.

1.3 Development of Landslides in Layered Volcanic Successions

The development of landslides in layered volcanic successions is not well understood. The role of the weak layers in the mechanics of movement is also complex and will be examined in detail in Chapter 7. However, from the observations recorded in the literature, it is possible to identify phases in landslide development, the types of landslides, the role of structural relations and the role of conductivity contrasts in developing groundwater flow systems conducive to slope movement.

1.3.1 Phases in Landslide Development

Based on a literature review, there are several phases in the development of these landslides which appear to be common to all types of movement encountered in this environment, (Fig. 1.2).

Phase I: Erosion and Slope Formation in the Volcanic Succession.

This phase consists of erosion (which may be joint controlled, *e.g.*, Lawrence, 1979; Pasek and Kostak, 1977) through the cap into the underlying weak sediments. Frequently this erosion is rapid, *e.g.*, meltwater channel development from drainage of glacial lakes, which produces oversteepened slopes in both the cap and the weak layers. Where erosion is less rapid, slope development is more gradual and other processes (*e.g.*, rockfall and slope wash) may be active in modifying slope geometry to the extent that slope angles are not as high. The speed of initial erosion may also be important in determining the strain energy release pattern of the underlying weak material which itself is an important contributor to instability.

Phase II: Cap Separation.

Stress relief generated by rapid erosion results in the lateral movement of the cap away from its parent sheet. Movement of this type is well documented in artificial excavations in other rock types where a rigid cap overlies a softer layer (*e.g.*, Underwood, 1964; Resendiz and Zonana 1969; Stimpson and Walton, 1970) and in excavations in volcanic successions (*e.g.*, Niccum, 1967). Cracking and cap separation parallels existing slopes and an excellent example is given by Stearns *et al.* (1938) from the Snake River
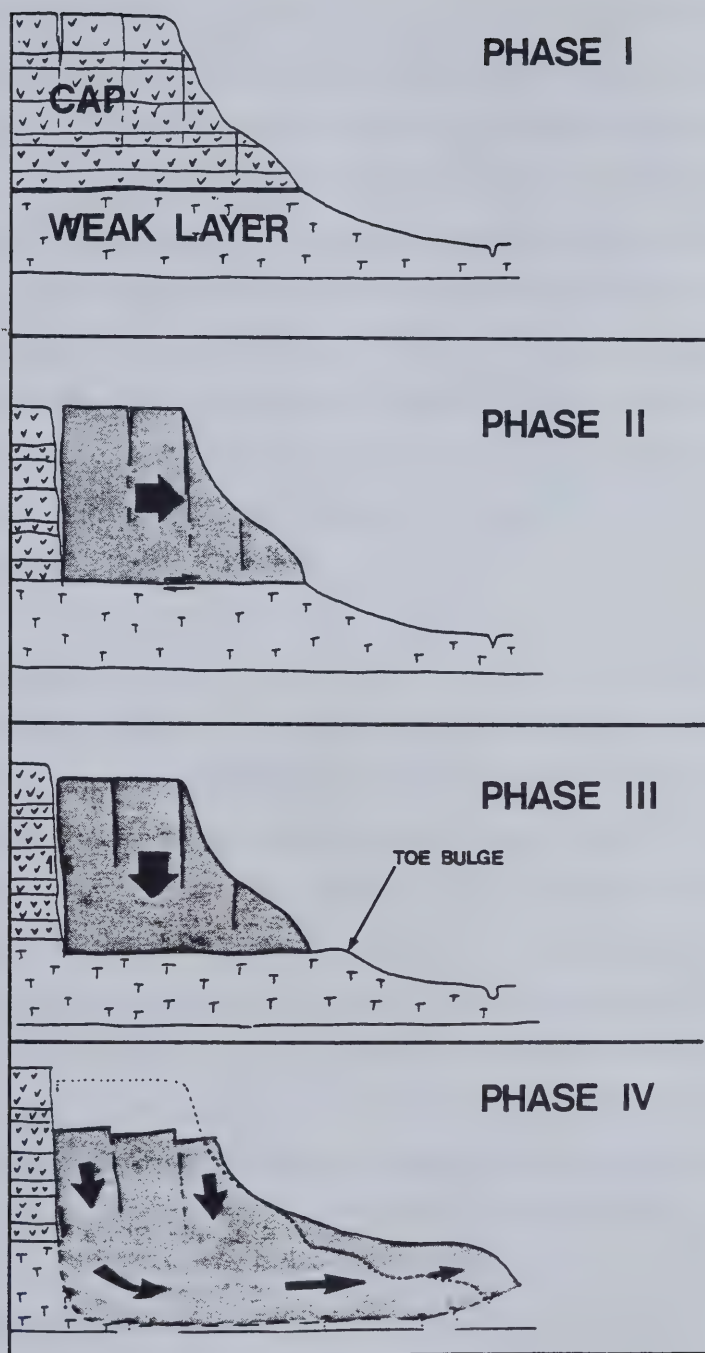
Figure 1.2 Phases in the development of landslides in layered volcanic successions. Phase I-erosion and slope formation; Phase II-cap separation; Phase III- cap loading; Phase IV-failure.

Plains, Idaho.

Movements during the separation phase involve vertical as well as horizontal movements (Suklje and Vidmar, 1961; Yeend, 1969, 1973). Yeend (1969) reported that vertical movements exceeded horizontal movements, "as would be expected with this type of vertical fissure". Waldrop and Hyden (1963) reported that vertical slickensides were present on tension crack surfaces on Sepulchre Mountain in Yellowstone National Park, suggesting that vertical sliding movements occurred before separation took place as a result of displacement in the underlying soft material. The separation phase is vital in the development of the failure mechanism since it creates a discrete block which is free to load the subjacent strata in the slope. In addition, the separation and cracking behind it may allow the ingress of water deep into the slope, allowing softening processes to be activated in the weak layer.

Phase III: Cap Loading.

Documented landslides of this type indicate a considerable time gap between separation and mass movement of the slope (Suklje and Vidmar, 1961; Yeend, 1973). The process is probably analogous to softening–related, delayed failure in cuttings of overconsolidated clay (Vaughan and Walbancke, 1973; Lutton *et al.*, 1979). Failure results from the termination of creep initiated by the loading of the weak layer by the separated cap block. During this phase some movement of the subjacent weak material might take place by being squeezed (e.g., Lee and Lo, 1976) out from under the cap as a response to block loading. This process has been postulated by Waters (1973) to account for heaves and mud–boils which have appeared beneath high (and, as yet, unfailed) cliffs in the Columbia River Basalt on the south side of the Columbia River. These heaves consist of soft clayey material from the underlying Ohanapecosh Formation. Indeed, many geologists have alluded to this type of loading mechanism to account for landslides in layered volcanic successions (Attwood and Mather, 1932; Koons, 1945; Trimble, 1963; Pierce, 1968) and the process has been extensively studied by workers in Czechoslovakia (Nemcok, 1968; Pasek and Kostak, 1977).

Phase IV: Failure.

Initial general failure of the slope may occur catastrophically (Russell, 1898; Stearns *et al.*, 1932; Suklje and Vidmar, 1961; Japan Society of Landslide, 1972). However, as mentioned above, the precise mechanism is in doubt.

In this work two possible mechanisms for such movement are examined: (a) movement along a discrete shear surface, or in a well-defined shear zone (sliding) or (b) movement by load-induced plastic flow (spreading).

1.3.2 Landslide types

The classification of these movements is made difficult both by their complexity and the vagaries of existing classification systems (*e.g.*, Pasek *et al.*, 1973). However, using the terminology of Varnes (1978) a landslide developed in slopes in volcanic successions may exhibit the five primary modes of movement, viz. falls, topples, slides, lateral spreads and flows. Taken as a whole, they are classed under the term complex where "movement is by a combination of one or more of the five principal types of movement described above" (Varnes, 1978).

Under certain conditions, the cap is preserved as a block or strip after movement occurs. Successive blocks or strips can be traced upslope in a landslide complex of this type. If the rotated blocks or strips are preserved and have not undergone advanced degradation, the slide may be termed a rotational slide or rock slump (Varnes, 1978). The lateral continuity of unbroken strips of rotated blocks along the rims of some mesa landforms in the United States, for example, is striking. Wright (1946) reproduces a remarkable aerial photograph of such strips and records their unbroken continuity over 4.8 km. Similarly, Yeend (1969) reports unbroken strips over 3.2 km in width. Although these landslides have occurred in horizontal bedrock, this continuity implies a great uniformity in movement conditions and time of movement.

The behaviour of the failed cap is determined by the character of the cap itself and the thickness of the weak layer. The character of the cap determines whether the cap is preserved or fragments on failure. If the cap is resistant, block landslides (Pasek and Kostak, 1977) are the result. If the cap disintegrates, as at Gradot Ridge, then blocks are not preserved. If the subjacent weak layer is thin, translation takes place along a basal shear surface which results in the formation of a graben beneath the scarp, or separation

surface. This type of landslide has been described by Attwood and Mather (1932), Pasek and Kostak (1977), Trollope (1980), and with reference to a sandstone cap, by Wright and Watson (1965). In cases where the weak layer is thicker, slope movement may be of the lateral spread type although it may be difficult to distinguish the two movement types. The geological and geotechnical factors controlling the sliding—spreading threshold are not well understood and are addressed in later parts of this work.

The result of successive slope movements in this environment is the development of a landslide complex that at the head consists of well-defined blocks (which may be the result of toppling, translational or rotational sliding, or lateral spread movements) and degraded slump blocks at the toe which may grade into flows (*e.g.*, Pierce, 1968; Mahr and Malgot, 1977).

1.3.3 The Role of Structural Relations

With respect to the basal shear surface (or zone), many block landslides appear to occur independently of what Attwood and Mather (1932) refer to as "larger structural relations". They observed in their study of landslides in volcanic rocks in the San Juan Mountains of Colorado that only two landslides had moved along bedding planes, the remainder moving in directions not related to the attitude of a basal weak layer. These observations were also made by later workers (*e.g.*, Suklje and Vidmar, 1961). This suggests that existing discontinuities in the weak zone (*e.g.*, bedding planes or bedding plane slips) are not important in determining the attitude of the basal shear, or that discontinuities existed prior to movement that were not detected afterwards. Jointing and fault patterns do, however, appear to control the plan geometry of the cap block.

Where interlayered volcanic successions have been tilted or folded so that the strike of such deformation is parallel to an eroded valley slope, simple translation along weak layers is the dominant mode of initial movement. The best documented cases exist for landslides in the Columbia River Group. Russell (1893) reported sliding of Columbia River Basalt on the tuffaceous rocks of the John Day Formation. The relation between structure and sliding in the Lower Columbia River has also been examined by Anderson (1971), Waters (1973) and Palmer (1977).

During folding or tilting, strain is preferentially taken up in weak strata between
more resistant units (e.g., Anderson, 1971) and leads to the development of flexural slip
structures. These may consist of rubbly mylonite zones or discrete planar shear surfaces
along existing bedding planes within units, or unit boundaries. In the Columbia River
Basalts, Waters (1955) notes the "local smearing out and slickensiding of thin sedimentary
beds and intercalated residual soils" (p. 676) and Newcomb (1969) notes the development
of a mylonite breccia between basalt units in Central Washington. Corns and Nesbit (1967)
encountered extensive interbed shearing at the Green Peter Dam Site in the Willamette
Basin, Oregon, where shearing in tuffaceous interbeds was so intense in some cases that
the sheared material had to be mined out and replaced by concrete to provide adequate
foundations and abutments for the dam structure. Anderson (1971) has also looked at the
relationship between structure and mass failure in the Columbia River Valley and reported
on the nature of bedding plane slips in tuffaceous interbeds.

In addition to these structures associated with tectonic activity, shear zones may
also be caused by valley formation in volcanic successions. Features which may be
attributable to stress relief have been reported from the Green Peter Dam (Corns and
Nesbit, 1967) and the McNary Dam (Gullixson, 1958). These features include vertical
shear zones parallel to the valley walls and complex fault patterns in valley bottoms, and
compare to similar features encountered in dam sites in the Plains, e.g., Underwood *et al.*
(1964), Matheson and Thomson (1973).

In the North American Cordillera the area of exposure of Cenozoic volcanic
successions is typified by Basin and Range structure (Stewart, 1979) and associated
normal block faulting. The generally steep faults control the plan geometry of landslides in
providing planes of low shear strength in the separation phase and also control the
stratigraphical continuity of the weak layers at the base of slopes (Fig. 1.3). Low-angle
faults, such as antithetic faults accompanying normal faulting, or thrust faulting
accompanying strike slip along normal fault planes, may be important locally in slope
stability but their role is not well documented.

LATERAL MARGINS DEFINED
BY FAULT PLANES

HEADSCARP DEFINED BY
STRIKE-SLIP FAULT PLANE

FAULT DISPLACEMENT ASSURES
CONTINUITY OF WEAK MATERIAL
AT SLOPE BASE

WEAK LAYER
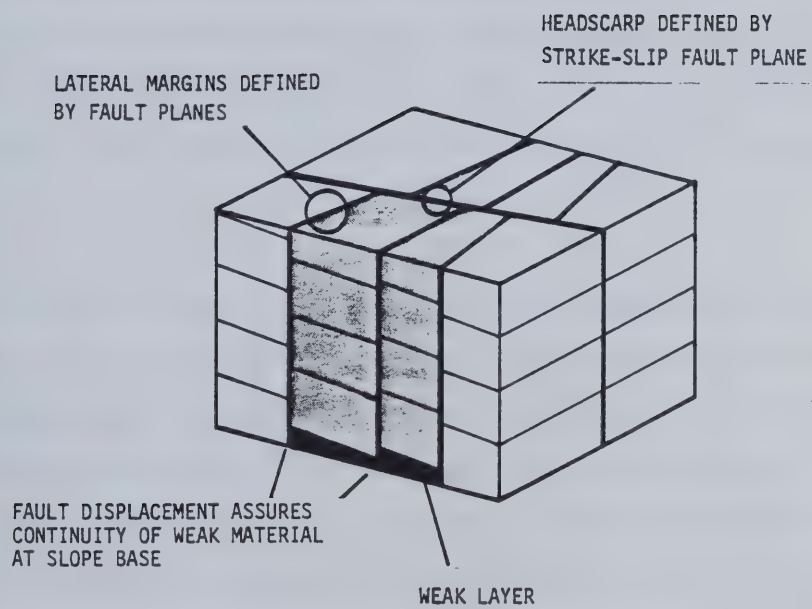
Figure 1.3 Effect of steep faults in controlling landslide geometry and occurrence.

1.3.4 The Role of Groundwater Flow Systems

The groundwater conditions attending the occurrence of large landslides in interlayered volcanic sequences is largely unknown for several reasons:

(a) Initial slope movements, with the few exceptions noted above, have taken place at various times in post–Pleistocene time. The landslides in the Intermontane region of the United States, for example, are thought to have resulted from much wetter climates which have occurred in Pleistocene and Holocene times.

(b) Landslide complexes frequently result from several movement phases over time and the role of groundwater in these different phases is difficult to assess.

(c) Groundwater flow patterns are highly complex because of the heterogeneity of conductivity within a volcanic succession (*cf.* Davis, 1969; Atlantic Richfield Hanford Co., 1976). Hence the estimation of groundwater pressures on potential failure planes is very difficult.

The various structural features that produce permeability and porosity in volcanic successions are well documented by Davis and de Wiest (1966), and Davis (1969). The nature of groundwater flow systems and large–scale features are less well known, however. Newcomb (1959, 1966, 1969) has investigated groundwater in the Columbia River Basalt and recent observations were made by Atlantic Richfield Hanford Co. (1976). The control by tectonic structures and the occurrence of artesian horizons are stressed by these workers. Artesian horizons in rubbly interbed material are reported from dam sites by Thompson (1950) and Chandler (1966) in the northwest United States. Whilst Hodge (1977) did not model groundwater flow systems in volcanic successions specifically, his model of interstratified sandstones and shales exhibiting stress relief features is worthy of note. He concluded that because of conductivity contrasts in the interlayered beds and the occurrence of horizontal gouge zones due to interbed slip that the resultant flow regime was detrimental to the stability of the valley wall.

1.4 A Regional Landslide Framework for the Study of Landslides in Volcanic Successions in South Central British Columbia

1.4.1 Regional Landslide Studies

This work has been conducted as a regional landslide study. As Morgenstern *et al.* (1977) have pointed out, the results of the regional landslide study "are particularly useful in providing insight into the geological (and climatic) factors controlling instability and, by comparing various cases, into the likely mechanisms that contribute to instability" (p. 569). Examples are the studies of slope stability in the London Clay (Hutchinson, 1967), Lias Clay (Chandler, 1971), Leda Clay (LaRochelle *et al.* 1970), the Cretaceous argillaceous bedrock of the North American Plains (*e.g.*, Thomson and Morgenstern, 1977, 1979; Scott and Brooker, 1968; Erskine, 1973). These have been valuable in revealing many common features of landslides and are therefore suggestive of the factors that influence the style of instability (Morgenstern *et al.* 1977). They may be seen as the vital precursors to the engineering phase of slope stability investigations undertaken for major construction projects. Many of the regional landslide studies referred to in previous sections have concentrated on the variety of landslide types in various materials within a specific region or map area and, therefore, have lacked the depth which is required of an integrated regional landslide study of a defined geological environment.

1.4.2 Background to the Present Work

From the preceding review of instability in layered volcanic successions, it is evident that an integrated regional landslide study, which examines the regional occurrence of instability in relation to a set of geological factors, and also investigates a number of selected landslides with reference to landslide mechanics, has not been carried out. This work was designed to fill that gap and was begun in the fall of 1977 with the intent of investigating massive landslides in Tertiary volcanic successions in the southern Interior Plateau of British Columbia, Fig. 1.4.

Two areas within the Interior Plateau, defined in Fig. 1.5 , were investigated. The investigation was concentrated in the Thompson Study Area (16,565 km²) which included northern parts of the Thompson Plateau and the southern fringe of the Fraser Plateau. A
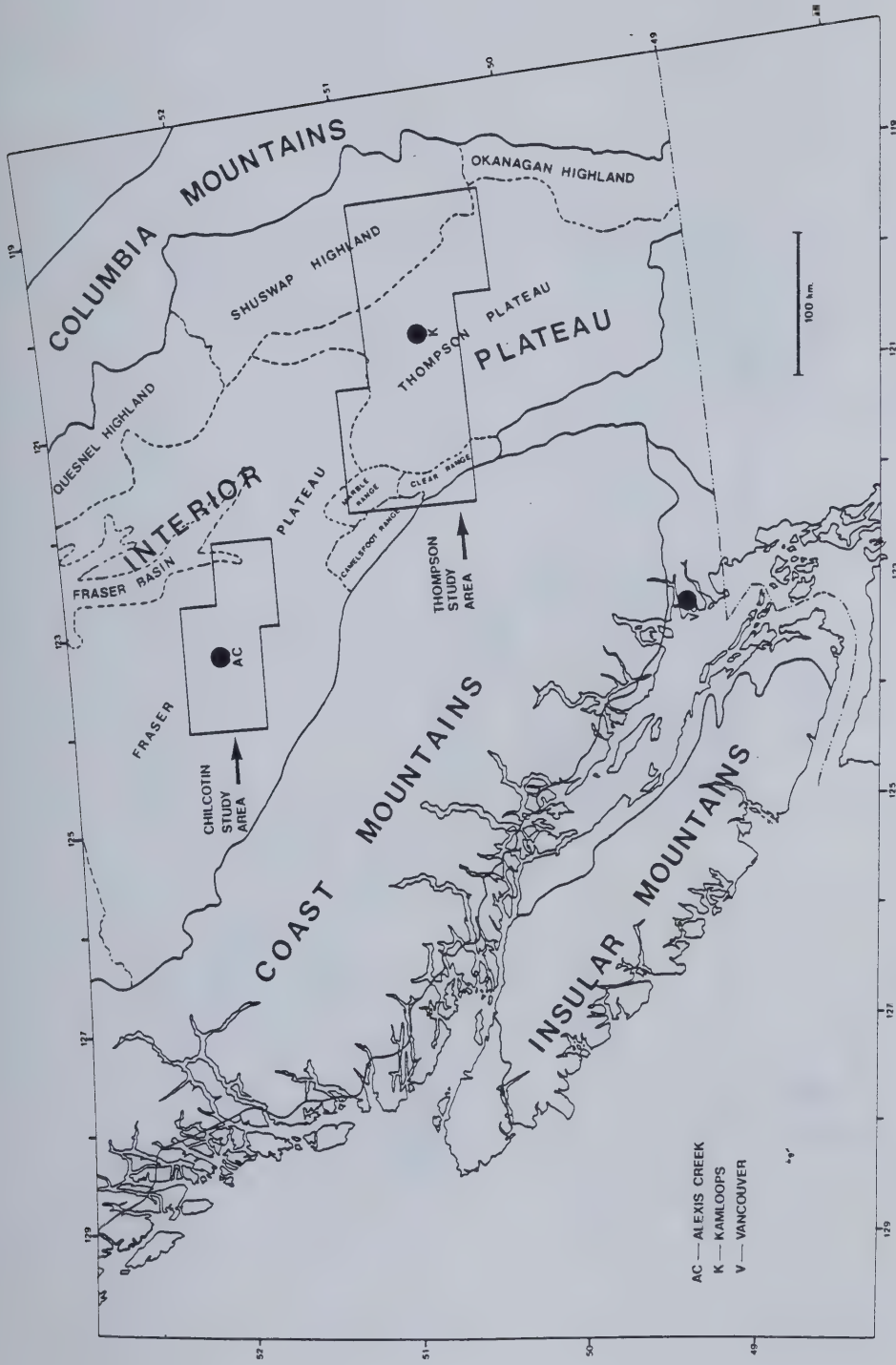
Figure 1.4 Location of study areas within the southern Canadian Cordillera. Physiographic divisions are after Holland (1964).
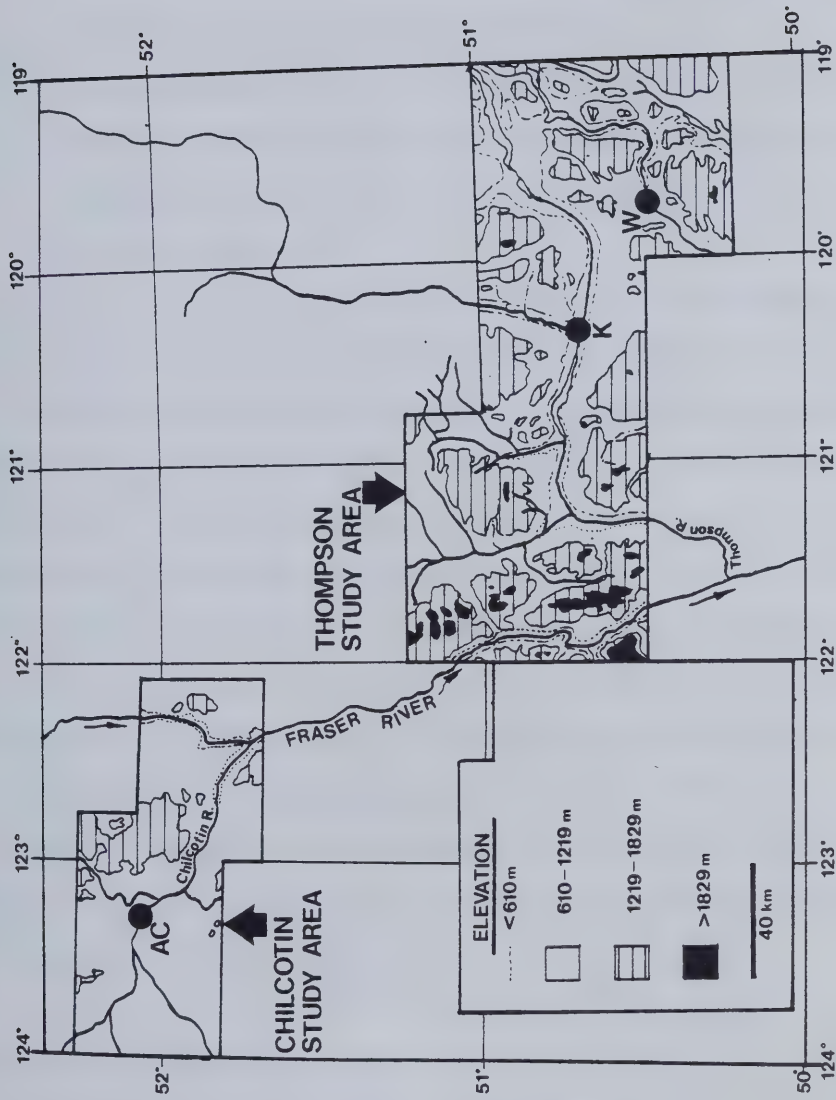
Figure 1.5 Location of study areas in central British Columbia. (AC=Alexis Creek; K=Kamloops; W=Westwold).

reconnaissance was also made into the Chilcotin River basin, within the Fraser Plateau, and landslides in an area of 6500 km² were mapped.

Two Tertiary successions are examined in this work:

a.   The Paleogene Succession: the Kamloops Group of Dawson (1899) which is of Eocene–Oligocene age, consisting of a structurally disturbed succession of lava flows, breccias and volcaniclastic rocks.

b.   The Neogene Succession: consisting of a basal series of volcaniclastic rocks overlain by a series of basaltic lava flows known as the plateau lavas (e.g., Campbell and Tipper, 1971) , which are mainly of Mio–Pliocene age and structurally undisturbed.

Landslides in both successions were investigated in the Thompson study area but work in the Chilcotin was limited to slope movements in Neogene rocks.

In the Thompson study area no indication of the landslide susceptibility of slopes developed in these successions had been given by previous workers in the region before Fulton (1975) and Ryder (1976) mapped a number of landslides in their investigations of surficial geology in the Vernon, Kamloops, Merritt, and Ashcroft areas.   In the Chilcotin area the existence of large landslides has been previously reported by Heginbottom (1972). The writer became aware of the extent of massive instability in these successions whilst in the employ of the Government of British Columbia, and this work represents the first detailed examination of these features in the Southern Interior.

Extensive landsliding in Tertiary volcanic rocks in other parts of British Columbia has been noted by Alley and Thomson (1978) on Graham Island, Queen Charlotte Islands and by the writer in the Princeton Basin.

1.4.3 Objectives of the Present Work

The present work has the following objectives;

(a) To establish the regional distribution of landslides, the variation in landslide types and the geomorphic and geological environments of landslides in Paleogene and Neogene volcanic successions in selected areas of the southern Interior Plateau of British Columbia.

(b) To isolate the geological factors contributing to slope movements within a smaller study area (including geomorphology, geological history, stratigraphy, lithology and

structure) with particular emphasis on the characteristics of weak volcaniclastic strata, and to describe landslide morphology, kinematics and movement history.

(c) To investigate the microstructure and geotechnical properties of weak volcaniclastic rocks which are associated with landsliding.

(d) To evaluate sliding and spreading models of slope movement with respect to selected landslides.

(e) To develop a geotechnical basis for the assessment of existing natural slope stability for use in natural hazard evaluations.

2. THE GEOLOGY OF TERTIARY VOLCANIC SUCCESSIONS IN SOUTH-CENTRAL BRITISH COLUMBIA

2.1 Introduction

Complex sequences of Tertiary volcanic rocks and associated volcaniclastic rocks and sediments occur throughout the Interior of British Columbia. As mentioned in Chapter 1, two volcanic successions of different ages are distinguished and are termed the Paleogene and Neogene successions.

The Paleogene succession consists of a wide variety of lava types, pyroclastic material and sediments. In contrast to the Neogene succession, it is structurally disturbed by gentle folds and a variety of faulting processes (Ewing, 1981a). The distribution of Paleogene rocks is given in Figure 2.1, and, based on K/Ar dating and palaeoenvironmental interpretation they are Eocene in age (Mathews and Rouse, 1963; Mathews, 1964; Hills and Baadsgaard, 1967; Ewing, 1981a).

The Neogene succession contrasts lithologically with the Paleogene rocks by exhibiting a narrow range of lava types. The succession is dominated by a series of basalt lava flows with associated intra-volcanic and basal sediments which are frequently tuffaceous. Only a limited amount of coarse grained pyroclastic material is present in the succession. With the exception of minor warping, the Neogene succession is structurally undisturbed. The distribution of Neogene rocks in the Interior Plateau is given in Figure 2.1. As will be seen in Chapter 3, the differences between the two successions have an important effect in determining their landslide response.

It is noted in this work that the term 'volcaniclastic' is used in the sense of Pettijohn (1975, p. 299), i.e., those materials with a preponderance of fragments of volcanic origin. Volcaniclastic materials include pyroclastic debris but also include deposits derived from volcanic source rocks by ordinary processes of weathering and redeposited pyroclastic materials.
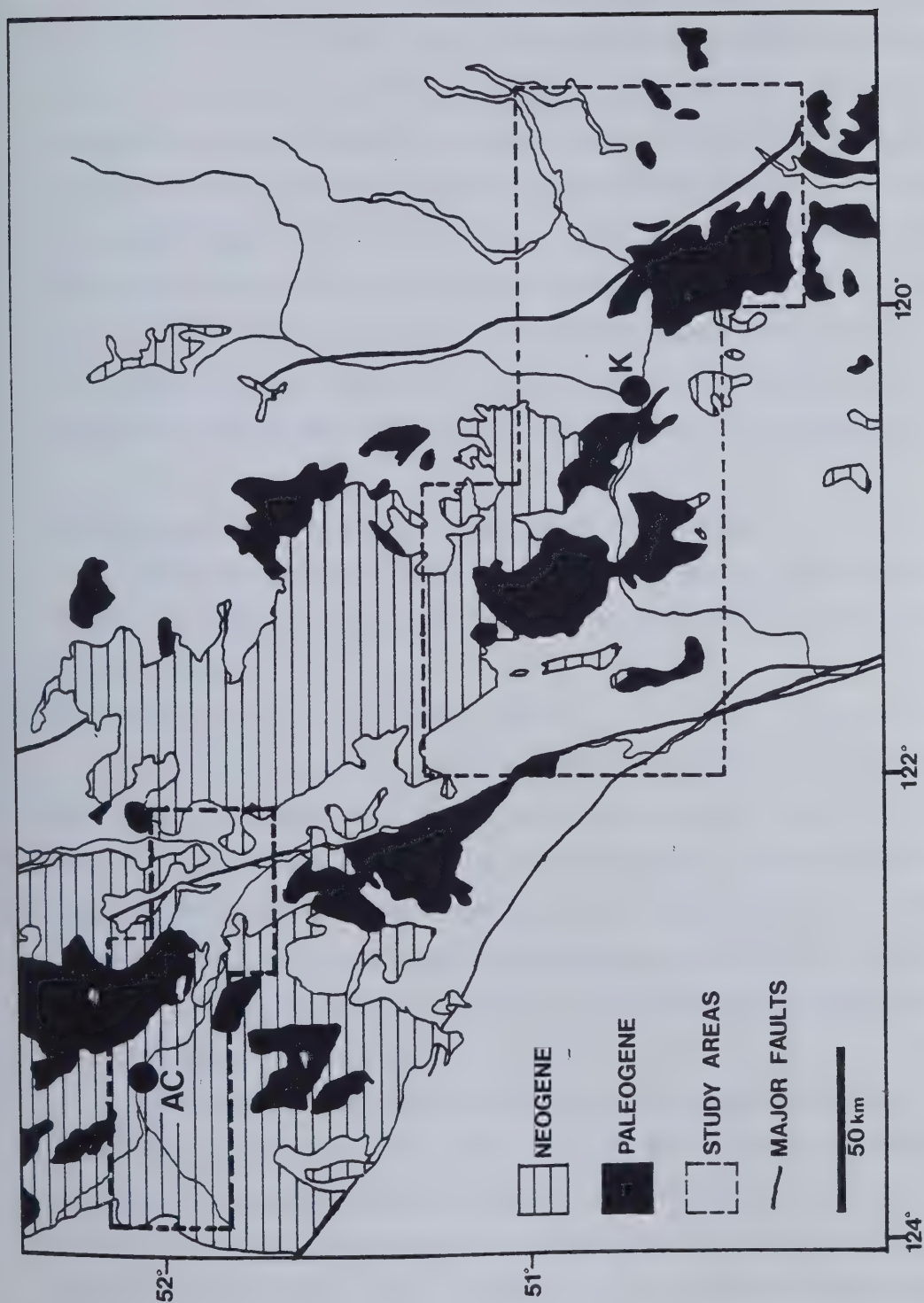
Figure 2.1 Distribution of Paleogene and Neogene volcanic rocks in the southern Interior of British Columbia. AC=Alexis Creek, K=Kamloops. (Based on Tipper *et al.* 1981).

2.2 The Paleogene Succession

The stratigraphy of the Paleogene rocks is only well known at a limited number of locations, and to date no formal regional correlation has been established. In the Thompson study area, Ewing (1981a) has suggested that the rocks contained in the Paleogene succession be named the Kamloops Group. The long history of their description and the evolution of their stratigraphical nomenclature has been discussed by Campbell and Tipper (1971), Graham and Long (1979) and Ewing (1981a). It is intended here to discuss the geology of the Kamloops Group only with reference to its engineering significance. Therefore, in this context, a three-fold division of the succession is made on the basis of material types, viz. a basal sedimentary and volcaniclastic assemblage, a volcanic rock assemblage and an intra-volcanic volcaniclastic assemblage.

2.2.1 The Basal Sedimentary and Volcaniclastic Assemblage

The form and characteristics of the sub-Paleogene unconformity are included in the basal sedimentary assemblage since it is a potential zone of weakness associated with the assemblage.

(a) *The sedimentary and volcaniclastic rocks:*

The sedimentary and volcaniclastic rocks are occasionally interbedded with lava flows and accumulated on a sub-aerial surface developed in pre-Tertiary rocks. They include conglomerates, fanglomerates, breccias, sandstones, siltstones, mudrocks and coal, which vary in their contents of pyroclastic material as well as tuffs and tuff breccias. Variations in facies show a variability consistent with the variability of depositional processes on a sub-aerial surface. Beds are thinly bedded and show rapid vertical variations in lithology (Long, 1981).

In the Bonaparte Lake area, the basal assemblage is called the Chu Chua Formation (Campbell and Tipper, 1971) and consists of a series of conglomerates, arkosic sandstones and sandy shales containing the occasional coal seam. In the Ashcroft and Nicola map-sheet areas it is known as the Coldwater Beds (Dawson, 1896; Cockfield, 1948; Duffel and McTaggart, 1951), and again consists of continental sandstones, conglomerates, shales and clays. Extensive coal seams occur within the basal assemblage in the Hat Creek, Merritt and Quilchena basins. At Hat Creek, Church (1977) has informally

subdivided the basal assemblage into the Coldwater Beds (sandstones, conglomerates, claystones and coal), the Hat Creek coal measures (thick seams of coal containing bentonitic seams, siltstone and sandstone lenses) and the Medicine Creek Formation (an alternating sequence of lacustrine siltstone and claystone). Bentonitic seams are also reported from the McAbee locality by Hills and Baadsgaard (1967). In the Vernon map-area the basal assemblage varies in thickness from a few centimetres to over one hundred metres and consists of lacustrine, fluvial and colluvial deposits and weathered detritus (Jones, 1959).

Church (1979) mapped basal beds in the Terrace Mountain area in the vicinity of Bouleau Lake as the Shorts Creek Formation, consisting of sandstones, shales and conglomerate. Ewing (1981a) applied this formation name to similar sediments found in the Falkland area.

The thick basal assemblage in the Kamloops area, the Tranquille Formation, has been studied in detail by Ewing (1979, 1981a). It consists of 450 m of lacustrine sediments and bedded tuffs, andesitic lava flows and mudflow breccias as well as other landslide deposits. Ewing's reconstruction of the filling of the Tranquille Basin is thought to be typical for the Paleogene sedimentary basins in the interior. Graham and Long (1979) have described lacustrine sediments and coal in the Tranquille beds in the vicinity of the Afton mine, west of Kamloops.

The basal assemblage thus reflects the variability of sedimentary processes acting on an uplifted early Tertiary landscape. Localised fault-bounded sedimentary basins were the foci of deposition of fluvial, lacustrine, organic accumulation and alluvial fan processes, in addition to slope processes, which included large landslides. As a result of this process pattern, the assemblage is characterised by rapid vertical and lateral facies changes which are manifested in marked changes of thickness and lithology over short distances (Long, 1981). Geotechnical properties and the engineering behaviour of the assemblage are expected to reflect this heterogeneity which is further complicated by varying airfall pyroclastic contribution to the deposits.

(b) *The basal Tertiary unconformity:*

In assessing the role of the basal assemblage as a zone of weakness within the Paleogene succession, consideration must be given to the configuration and nature of the

basal Tertiary unconformity. Exposures of the unconformity are not plentiful, however, and detailed subsurface investigations have not been carried out.

With reference to the configuration of the surface, Fulton (1975), referring to evidence at Enderby and at Shorts Creek, suggests that relief on the basal Tertiary surface was as great as 915 m. Bostock (1941) and Campbell and Tipper (1971) comment on the surface being a rock surface of steep relief. The cause of this configuration is not clear, i.e., whether it was due to primary topography or to contemporaneous, or later, faulting.

The nature of the unconformity appears to vary with location and is not related to the lithology of the pre–Tertiary rocks. Some workers have observed a depositional transition between pre–Tertiary and Tertiary rocks without a dramatic change in material properties (e.g. Uglow, 1922; Mathews, 1981), whilst others report a weathered or highly altered boundary. For example, Ross (1975) reports from the Vaseux Lake area that the basal Tertiary rocks are unaltered in contrast to the underlying metamorphic material which, within 15 m of the Tertiary contact, is highly altered. Riglin (1976) reported the contact to be weathered near Summerland, where it forms a saprolite and weathered rock zone in granodiorite. She suggests that this forms the zone of weakness on which the Crater Mountain landslide moved. The basal Tertiary unconformity is exposed in the Salmon Valley and, as described in Chapter 4, basal Tertiary volcaniclastics were found to rest on a friction breccia of unknown origin developed in Palaeozoic Chapperon schists.

2.2.2 The Volcanic Rock Assemblage

The volcanic rocks of the Paleogene succession vary throughout the study area and also vary markedly within a sequence at a given location. They include, for the purpose of this discussion, lava flows and associated flow–top breccias. The petrology and geochemistry of lava flow rocks from the study area have recently been examined by Ewing (1981b). Church and Evans (1983) have recently reported on the petrology and geochemistry of lavas from the Salmon River valley, near Westwold. Lava types ranging from basalt to rhyolite occur and scoriaceous horizons and vesicular lavas are common. Columnar jointing is rare but, in general, the rocks are dominated by persistent vertical joints. Accumulation of the volcanic rock assemblage was episodic and spatially variable between about 53 Ma and 45 Ma. The sequence contains unconformities which separate

phases of deformation and indicate periods of continental erosion and deposition during which intra—volcanic volcaniclastic rocks accumulated.

The thickness of the volcanic rock assemblage varies considerably according to the vagaries of original accumulation patterns and subsequent erosion. Individual flows may be up to 16 m in thickness. Basaltic lavas are predominant in the Thompson study area with andesites being of secondary importance, whilst flow—banded siliceous lavas are frequently found near the base of the assemblage.

2.2.3 Intra-Volcanic Volcaniclastic Assemblage

Rocks included in this assemblage are agglomerates, pyroclastic breccia and tuffs, fragmental rocks (such as laharic breccias) resulting from mass movement processes, and localised interbeds of sedimentary material. Where present, these beds form an important zone of weakness in slopes developed in the volcanic rock assemblage. As discussed in Chapter 5, alteration processes are important in the development of smectite clays in these materials resulting in further degradation of mechanical properties. Accumulation of these deposits varies locally, giving rise to rapid changes in horizontal and vertical facies.

Ewing (1981a) has described in detail the intra—volcanic assemblage within the Tranquille Basin near Kamloops, where it consists mainly of breccia and tuffs.

2.3 Structural Geology of the Paleogene Succession

The structural complexity of the Paleogene succession in the study area was not realised by earlier workers. In geological maps by Duffel and McTaggart (1951), Cockfield (1948) and Jones (1959), no faults are indicated within the Kamloops Group. Campbell and Tipper (1971), Church (1973) and Ewing (1980, 1981a) have discussed structural features within the succession in some detail. Paleogene tectonic events were dominated by dextral strike—slip faulting forming a wide transcurrent shear zone through the Cordillera (Ewing, 1980; Long, 1981). Within this shear zone we may define the Interior strike—slip shear zone situated between two very marked vertical to steeply—dipping converging principal displacement shears, i.e., the Pinchi Lake — Louis Creek Fault and the Fraser River Fault zone (Fig. 2.2). The structure of the Interior Shear Zone has a marked similarity to the structure of shear zones of various magnitudes reported by Skempton (1966) and
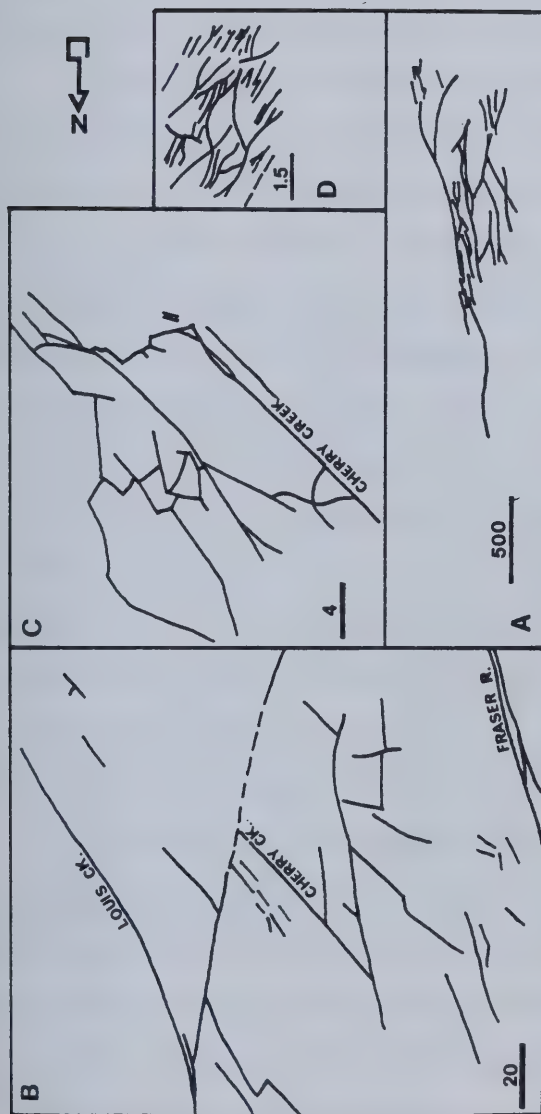
A. PATTERN OF SHEARS ASSOCIATED WITH INTERCONNECTING DEXTRAL STRIKE-SLIP FAULTS IN THE CORDILLERA (LONG, 1981).

B. STRIKE-SLIP FAULT NETWORK IN THE KAMLOOPS AREA WITHIN INTERIOR SHEAR ZONE (AFTER EWING, 1981).

C. LOCAL STRUCTURAL PATTERN AT KAMLOOPS LAKE (AFTER EWING, 1981). NOTE SHEAR LENSES AND SLICES.

D. LINEAMENT PATTERN FROM AERIAL PHOTOGRAPHS OF SALMON VALLEY STUDY AREA SUGGESTIVE OF SHEAR LENSES DEVELOPED ALONG REIDEL SHEARS WITHIN INTERIOR SHEAR ZONE. DIP-SLIP FAULTS ARE APPROXIMATELY AT RIGHT ANGLES TO THESE LINEAMENTS SUGGESTIVE OF PULL APART TENSIONAL STRUCTURES ALONG CONJUGATE REIDEL SHEARS.

Figure 2.2 Structural framework of Paleogene rocks in the southern Interior. Scale on bars is in kilometres.

Tchalenko (1972). The result of these shearing processes was to cut the rocks into shear lenses and slices of varying shapes and sizes, and a hierarchical series of structural features is evident. Deformation is also seen within the blocks as shown in Figure 2.2C from Ewing (1981a), and lineament patterns from the Salmon River study area (Fig. 2.2D) suggest even smaller scale features perhaps indicative of strike–slip movement along closely–spaced, steeply–dipping shear surfaces.

Locally, complex variations in structural pattern exist due to a number of factors. Strike–slip movement on buried normal faults can produce reverse faults (Church, 1979; Brown, 1928). Further, normal dip–slip movement can take place transverse to the direction of strike slip (Lensen, 1958; Ewing, 1981a), giving rise to horst and graben structures. Grabens formed in this way became loci for the deposition of the basal assemblage. The margins of the grabens are not simple dip–slip structures but may be a jumble of faults and slump blocks, e.g., at the southern margin of the Tranquille Basin at the Afton mine (Preto, 1973; Carr and Reid, 1976; Ewing, 1981a).

Low angle normal faults occur within the succession. One such feature was examined at Teakettle Creek, southwest of Monte Lake, and is seen in Plate 2.1. It is not related to any present surface instability and is interpreted as the shear surface of a large landslide which occurred contemporaneously with the accumulation of the sequence. The presence of such shear surfaces within the succession would have considerable significance in slope stability considerations.

Further mention must be made of the presence of contemporaneous Tertiary landslides within the succession. Their presence is important since they provide pre–sheared surfaces within the succession, and they also complicate the interpretation of exposures in the vicinity of present day landslides. During the accumulation of a sub–aerial volcanic succession, slopes frequently become unstable due to erosion, seismicity, the growth of fault scarps and volcanic loading. Large contemporaneous landslides are characteristic of the Kamloops Group and its equivalents throughout the Cordillera (Pearson and Obradovich, 1977), and may involve pre–Tertiary rocks as well as rocks of the volcanic succession. Slump blocks are described by Preto (1973) at Afton mine near Kamloops, and Church (1973) describes rock avalanche deposits within the Skaha Formation in the White Lake Basin near Penticton.

Plate 2.1 Low angle fault exposed in volcaniclastic rocks at Teakettle Creek, near Monte Lake.

The operation of these various shearing processes has resulted in a complex structural pattern in which the Paleogene rocks are frequently broken up into small blocks or panels of varying orientation (Ewing, 1979). Campbell and Tipper (1971) reported that around Bridge Lake the Skull Hill Formation has no consistent dip direction and is cut by closely spaced faults that have produced disoriented, tilted fault blocks. Similar structural features were found in the Salmon River valley as discussed in Chapter 4 and are important controls on the plan geometry of landslides.

A schematic diagram of a block of valley side slope developed within the Paleogene succession which illustrates the lithological and structural features that determine its landslide response is shown in Figure 2.3. The role of these features in controlling slope movements will be discussed on a regional scale in Chapter 3 and with specific reference to the Salmon Valley landslides in Chapter 4.

2.4 The Neogene Succession

As mentioned above, the Neogene succession in the study area differs from the Paleogene succession in many respects and is less complex in lithology and structure. Two distinct assemblages are identified and consist of a basal sedimentary assemblage and a volcanic rock assemblage.

2.4.1 The Neogene Basal Sedimentary-Volcaniclastic Assemblage

The basal sedimentary–volcaniclastic assemblage was deposited on the eroded surface of older rocks which includes for the most part eroded Paleogene rocks. Their deposition was preceded by a period of erosion lasting approximately 32 Ma, during which time a marked erosion surface developed in the Interior Plateau (Mathews, 1968). The Neogene basal sedimentary–volcaniclastic assemblage represents the initiation of the Miocene sedimentary–volcanic cycle.

The basal sedimentary–volcaniclastic assemblage has been examined in most detail by Campbell and Tipper (1971) in the upper Deadman River valley and they have named these rocks the Deadman River Formation. Equivalent strata are found at Chasm Creek and throughout the Chilcotin River valley (Tipper, 1959; 1963). Some sediments interfinger with the overlying plateau lavas near Big Bar Creek (Trettin, 1961) and along the Chilcotin
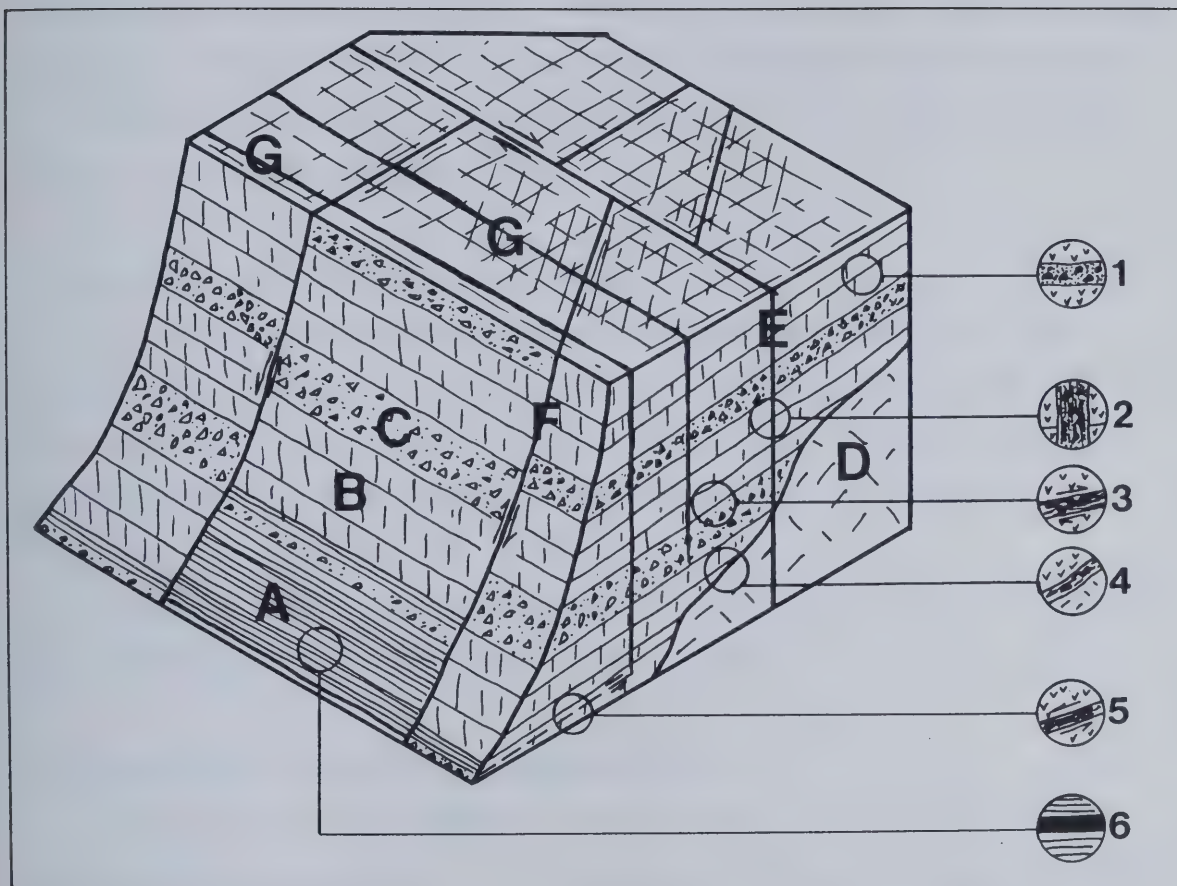
KEY TO GEOLOGICAL FEATURES.

A. LAYERED VOLCANICLASTIC MATERIAL AT BASE OF SUCCESSION
B. LAVA FLOW UNITS
C. VOLCANIC BRECCIA WITHIN SEQUENCE
D. PRE-TERTIARY ROCK
E. STRIKE-SLIP FAULT
F. NORMAL FAULT
G. TENSION CRACKS AT SLOPE CREST DUE TO VALLEY STRESS RELIEF

1. INTER-FLOW BRECCIA
2. SHEAR ZONE ALONG STRIKE-SLIP FAULT
3. INTER-BED SLIP BETWEEN UNITS DUE TO TILTING
4. WEATHERED ZONE OR SHEAR ZONE AT UNCONFORMITY
5. SHEAR ZONE ASSOCIATED WITH REBOUND STRUCTURES
6. WEAK ZONE WITHIN VOLCANICLASTIC STRATA

Figure 2.3 Schematic block diagram of valley side slope developed within the Paleogene succession illustrating lithological and structural features which determine its landslide response.

River (Tipper, 1963). The assemblage consists of laminated lacustrine clays and silts, diatomite, fluvial silts, and sands and gravels which vary in pyroclastic content, as well as fanglomerates, tuffs and tuff breccias. Generally the rocks are poorly indurated. Marked variations in lithology and thickness occur within the assemblage. Campbell and Tipper (1971) suggest that the sub–Miocene unconformity had a relief of at least 150 m in the vicinity of the upper Deadman River valley.

2.4.2 The Neogene Volcanic Rock Assemblage

This assemblage is dominated by a monotonous series of basalt flows. Most flows are thin, being between 1.5 m and 15 m thick (Campbell and Tipper, 1971) with thin flow top breccias. Locally breccia and pillow lavas are present proximal to major river channels and minor silicic ash layers within the assemblage may be the product of Coast Range volcanoes to the east (Bevier, 1981).

K–Ar age determinations reported by Bevier (1981) range in age from 0.6–19.8 Ma with most dates being in the range of 6–10 Ma (Miocene).

2.4.3 Structural Geology of the Neogene Succession

For the most part the Neogene succession is flat–lying or very gently tilted, as noted at the Chasm near Clinton. There is an absence of folding or faulting, and, in further contrast to the Paleogene succession, there are no marked unconformities within the succession. Some dips in the Deadman River Formation may be due to slumping or differential compaction from the weight of the overlying plateau lavas (Campbell and Tipper, 1971). Columnar jointing is common in the lavas and cooling joints are pervasive. Local structural disturbance in the vicinity of valley sides may arise from stress relief, as has been encountered in the Miocene basalts of the Columbia River Plateau (Corns and Nesbitt, 1967).

A schematic diagram of a block of valley side developed in the Neogene succession is seen in Figure 2.4 (cf. Fig. 2.3). The regional landslide study in Chapter 3 will evaluate the role of these features.
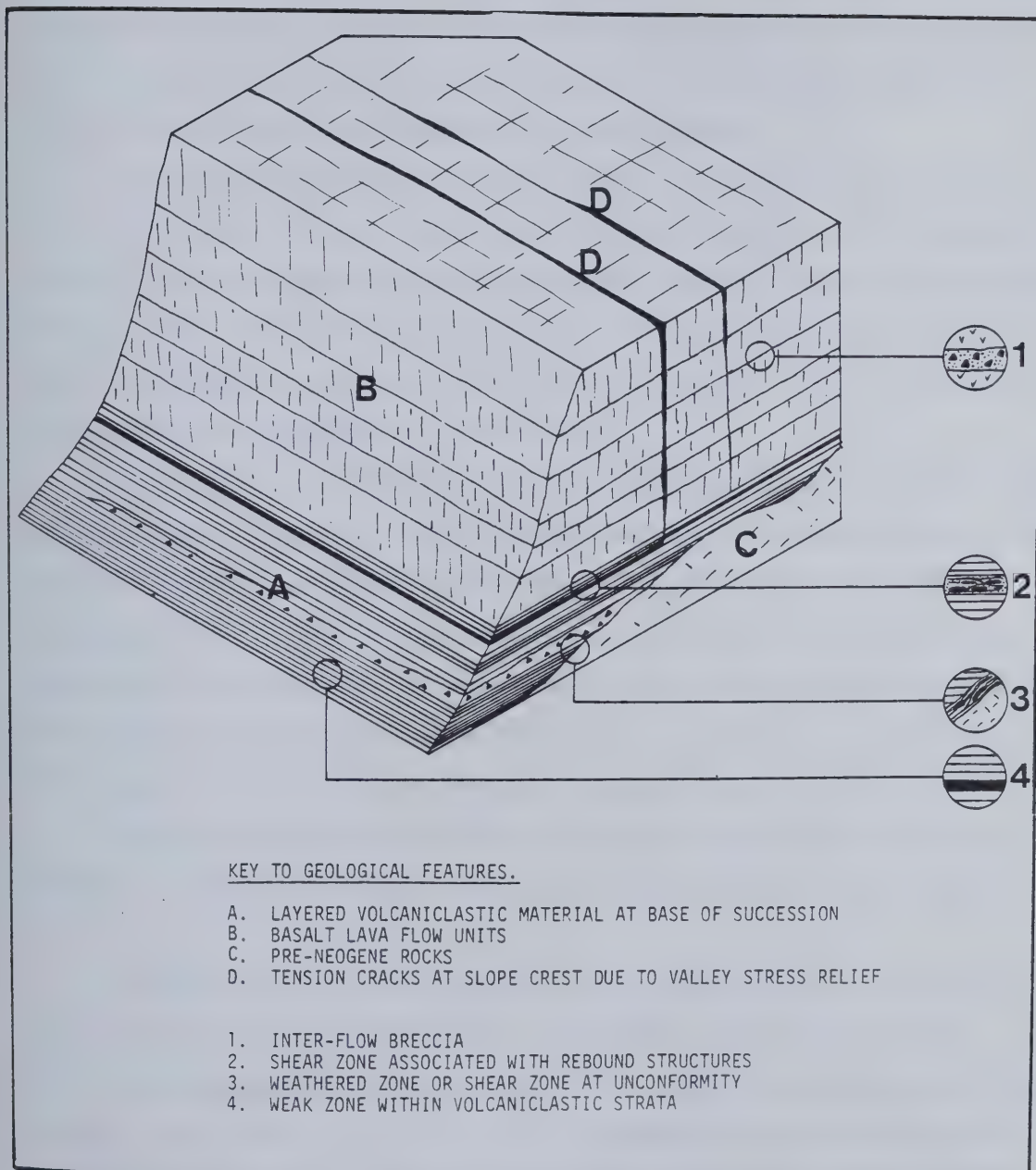
Figure 2.4 Schematic block diagram of valley side slope developed within the Neogene succession illustrating lithological and structural features which determine its landslide response.

2.5 History of Slope Development

The land surface of the Southern Interior of British Columbia has been subject to slope development processes since the early Tertiary. As a result certain features of the landscape are inherited from that era, having persisted in the landscape to the present. In addition, because of a succession of deposition, uplift and erosion stages, the stress history of materials making up the slopes in the area is complex.

Although unconformities within the Paleogene succession reflect periods of erosion during accumulation, the oldest inherited feature is thought to be the Paleogene erosion surface or the "upland erosion surface" which is found in the northern Thompson Plateau and southern Fraser Plateau. It resulted from the uplift and dissection of the Paleogene succession, the structure of which it truncates. In the 30 Ma of its formation, an unknown depth of Paleogene rocks was eroded.

Dissection of this surface had already begun before the deposition of the Neogene basal assemblage in the Miocene. At the cessation of Neogene vulcanism, another erosion surface was formed, the Neogene surface, during which an indeterminate thickness of Neogene volcanics was eroded. The Neogene surface was then dissected by Pliocene uplift, during which the current main valley system was excavated (Mathews, 1968). Some of these valleys were exhumed from the pre-Miocene surface since many present river valleys appear to follow old Tertiary drainages, particularly in major fault zones.

At the onset of glaciation, therefore, slopes in the study area had already been subject to a complex series of geomorphic events over an interval of approximately 50 Ma.

The glacial history of the study area has been reported in detail in a number of papers by Fulton (1965, 1967, 1969, 1975, 1976), Ryder (1976, 1978) and Tipper (1971). Several glaciations affected the Interior which was covered by a continental-type ice-sheet. The ice sheets covered the summits of the Interior Plateau, and although they did not follow the valleys during their maximum extent, they appear to have been valley controlled in their stagnating phase. The Fraser glaciation and its retreat is the best documented (Fulton, 1969, 1975) and perhaps the most important effect was the formation and drainage of pro-glacial lakes during deglaciation. This gave rise to oversteepened meltwater channels which are preferred sites for many of the large scale

slope movements as discussed in Chapter 3.

The history of slope development is further complicated by stream capture and glacial drainage derangement which has led to the formation of high level water gaps and steep gorges in several places in the Thompson Plateau.

The post-glacial geomorphic history of parts of the study area has been examined in detail by Ryder (1971, 1976, 1978) and will be discussed in Chapter 7.

3. LANDSLIDES IN THE TERTIARY VOLCANIC SUCCESSIONS OF SOUTH-CENTRAL BRITISH COLUMBIA

3.1 Introduction

3.1.1 Previous Work

Prior to the work of Fulton (1975) and Ryder (1976), only Cockfield (1948) and Duffel and McTaggart (1951) briefly mention landslides in the Ashcroft and Kamloops areas.

Fulton (1975) treated landslides as post-Fraser glaciation deposits and noted that they "consist of piles of shattered bedrock lying below escarpments" (p. 30). He observed the linkage between large landslides and Tertiary bedrock and noted that "most occur where soft, clay rich sediments underlie competent volcanic rock" (p. 30). The surficial geology maps produced by Fulton (1975) were the first to locate many of the large landslides in the Nicola-Vernon area.

Ryder (1976), in the Ashcroft area, treated landslides as a terrain mapping unit and describes large-scale slumping in the Camelsfoot Range in Neogene rocks at Leon Creek as "huge crescentic blocks ... breaking away from the margins of a plateau of Tertiary volcanic rocks" (p. 11). The cause was ascribed to the presence of clay-rich sediments underlying the volcanics.

In the Taseko Lakes map-area, Heginbottom (1972) mapped large landslides in Neogene rocks along the Chilcotin River, Big Creek, and in the vicinity of Alkali Lake.

The large landslides discussed in this work involve the valley side slope unit, *i.e.*, the top of the scarp is usually the top of the valley side slope and the toe of the slide is usually at the base of the valley. As such, smaller scale movements, as discussed in detail by Riglin (1977) at Trout Creek, Summerland, and mentioned by Ewing (1979) on the south side of Kamloops Lake, are excluded. Further, mass movements in Lower Paleogene sedimentary and volcaniclastic rocks in Hat Creek currently being investigated by British Columbia Hydro and Power Authority are also excluded.

3.1.2 Objectives and Techniques of Investigation

The objectives of this part of the investigation are three-fold.

1.   to report the results of a detailed landslide inventory in both Paleogene and Neogene rocks within the study areas. This adds to the inventory already in existence in the form of the maps of Fulton (1975) and Ryder (1976) in the Thompson study area and Heginbottom (1972) in the Chilcotin.

2.   to establish the geological factors responsible for each landslide.

3.   to map the morphology of the landslides in order to classify movement type and mechanism.

In establishing the landslide inventory, aerial photographs were obtained of the areas of outcrop of the Tertiary volcanic rocks in the study areas. These photographs were interpreted and landslide sites detected. The majority of the sites were then inspected in the field during the 1978, 1979 and 1980 field seasons. Observations were made on local geology, characteristics of the landslide debris and shear zones. This chapter reports the regional aspects of this work whilst the detailed observations made in the Salmon Valley are reported in the next chapter.

The south-central part of British Columbia is amenable to extensive field work due to the presence of a network of public and private roads and trails, as well as the open nature of the forest cover.

3.2 The Landslide Inventory

3.2.1 Uncertainty in the Recognition and Delimitation of Landslides

A major problem in establishing the landslide inventory was one of recognition, both on aerial photographs and on the ground. A secondary problem was the precise delimitation of the extent of slide debris.

The problem of landslide recognition is commonly encountered in regional studies of landslide processes and surficial deposits (Flint and Denny, 1958; Bailey, 1971; Rib and Liang, 1978). In the context of this investigation uncertainty was generated by the following:

(a) Strike ridges in tilted fault blocks sometimes give the impression of being back-tilted

slide blocks (e.g., north end of Enderby Cliffs).

(b) Erosion of a slope on one side of a prominent joint or fault which gives the impression of a landslide block or scarp. This is particularly a problem because some of the landslides encountered have undergone limited movement. Thus slope disturbance is minimal (e.g., between Buse Hill and Ducks Meadow).

(c) Some meander scars along valleys in flat-lying Neogene rocks can be interpreted as landslide scars (e.g., between Hanceville and Alexis Creek).

(d) Post-failure modification of the scarp region of several landslides, by erosion, makes it difficult in some cases to precisely delimit the boundaries of the slide (e.g., Buse Hill).

(e) Post-failure channelling and in some cases deposition can also make it difficult to delimit the precise boundaries of certain slide debris.

(f) Confusion can occur due to the similarity between hummocky landslide debris and certain types of hummocky glacial debris (e.g., east of Siwash Rock Mountain).

(g) Lateral meltwater channels close to the valley rim can give the impression of being the product of block separation (e.g., along the Chilcotin River).

(h) Also, in the Chilcotin study area, valley side steps in the horizontal Neogene rocks can give the impression of landslide blocks.

(i) Erratic dips within and between fault blocks can give the impression of a slope (e.g., in the Salmon River Valley) having been subject to a partially developed slope movement.

3.2.2 The Problem of Landslide Classification

Difficulty is encountered when attempts are made to classify slope movements in volcanic successions. As described in detail below, many of the landslide sites represent the outcome of several slope movement events which occurred in complex succession, each event possibly exhibiting a different mode of movement. It is important to identify a primary slope movement event which constitutes the initial movement of a slope and which results in the production of primary landslide debris. Successive movements involving additional failure in the scarp, or re-mobilisation of debris, are termed secondary movements. Part of the difficulty associated with classifying landslide sites in the volcanic successions under study is the importance of secondary flows which are a response to the changing properties of volcaniclastic and pyroclastic debris through time during which

high strength loss associated with alteration and remolding takes place.

There are two aspects to the problem of classification, viz. the type of movement involved in the primary failure and the classification of a landslide site that has been subject to successive movement events.

It is thought that in the landslides described below, initial movement involves some type of block failure wherein the cap begins its movement as a rigid body. This precedes disintegration and later degradation. The question remains as to whether or not these initial block movements are, according to Varnes (1978), slides (involving displacement along one or several surfaces) or spreads (where the dominant movement is lateral extension owing to the liquefaction or plastic flow of subjacent material). The boundary conditions controlling the two modes of movement will be discussed in detail in Chapter 7.

In the Varnes (1978) classification, displaced material which has been subject to successive movements which exhibit different modes, would be termed complex movements. This writer feels, however, that the term is unsuitable for the present study since it is too insensitive to the wide variation in morphology exhibited by landslide sites which have been subject to secondary flows and other types of movement.

For the purpose of this study the following morphological classification will be used;

(a) *Simple Block Movements*

Discrete landslides with well-defined lateral margins. It may be interpreted to be the result of one event. Landslide blocks are preserved and well defined. Degradation of debris is minimal and secondary movements are restricted to block movements within the debris. Longitudinal grooving and low amplitude transverse ridges are absent. The movement can be a slide or a spread. Usually field criteria are absent for distinguishing these types of movement (e.g., Ducks Meadow in Fig. 3.18).

(b) *Multiple Juxtaposed Block Movements*

A contiguous area of interlocking blocks running for some distance along a valley side slope resulting from a succession of block movements through time. Age differences may be apparent in the blocks which are well defined. Degradation of older blocks may have taken place and secondary movements are restricted to block movements within the debris. The movements can be either spreads or slides (e.g., Chasm Creek in Fig. 3.22).

(c) Complex Block Movements

Individual, discrete landslides with well defined lateral margins which may be interpreted as the result of one event. Blocks are preserved near the scarp but down slope fragmentation has resulted in debris flowage. Longitudinal grooving and transverse ridges may be present in the disintegrated zone which exhibits lobate toe areas. Initial block failure may be a slide or spread (e.g., Deadman River Complex 3, Fig. 3.20).

(d) Successive Block Movements

Discrete or continuous block movements in which blocks involved in initial movement (either block movement or disintegrated block movement) undergo degradation due to the alteration of debris as a result of secondary flow processes (e.g., Enderby, Fig. 3.12).

Thus two types of complex movements are distinguished, one in which the complexity arises from one event, and one where the complexity arises from a succession of events over time consequent upon the changing mechanical properties of the debris.

3.2.3 The Results of the Landslide Inventory

(a) *Paleogene Rocks*

Approximately 50 landslide sites were identified in Paleogene rocks in the Thompson study area. As can be seen in Figure 3.1, they are concentrated in an extensive Paleogene outlier centred on Westwold. Other local concentrations occur in outliers in the Shuswap Highland at China Valley, Fly Hill, Mount Ida and Enderby. To the west of the Westwold outlier, scattered slides occur on Paleogene outcrops as far west as Hat Creek, but a large concentration of slides is found near the northern margins of the Thompson Plateau in the Deadman River Valley. Some landslide geometries, types and other properties are given in Table 3.1.

(b) *Neogene Rocks*

Figure 3.1 also shows the results of the inventory of slides in Neogene rocks in the Fraser Plateau and the Camelsfoot Range. Concentrations are found along north-south trending valleys in the upper Deadman Valley and Chasm Creek. Concentrations are also found along the west side of the Fraser River near Leon Creek (in the Camelsfoot Range). In the Chilcotin study area (Fig. 3.2) landslides occur east of Riske Creek in the vicinity of Doc English Gulch. Along the Chilcotin River large landslides occur at Big Creek, near Beaumont

Figure 3.1 Location of landslides in Tertiary volcanic rocks in the Thompson study area.

Table 3.1 Descriptions of landslides in Paleogene rocks.

LANDSLIDE	1	2	3
BOULEAU LAKE COMPLEX	VB	H/U	Figs. 3.3,3.4,3.5. Plate 3.1
BOULEAU LAKE 4	VB	H	Figs. 3.4,3.5.
TAHAETKUN MOUNTAIN	VB	H	Fig. 3.5.
PINAUS LAKE 1	SB	U	Fig. 3.6.
PINAUS LAKE 2	SB	U	Fig. 3.6.
PINAUS LAKE 3	SB	U	Fig. 3.6.
PINAUS LAKE 4	SB	U	Fig. 3.6.
PINAUS LAKE 5	SB	U	Fig. 3.6.
PINAUS LAKE 6	SB	U	Fig. 3.6.
ESTEKWALAN MOUNTAIN	CB	N	Figs. 3.7,3.8. Plate 3.3.
CHASE CREEK	MJ	U	Fig. 3.9.
CHARCOAL CREEK (CHINA VALLEY)	MJ	U	Fig. 3.9.
FLAG HILL	SB	N	Fig. 3.1.
MOUNT IDA	VB	N	Fig. 3.10.
ENDERBY CLIFFS	VB	N	Figs. 3.11-3.14, Plates 3.4-3.6.
PEMBERTON HILL COMPLEX	VB	N	Figs. 3.15,3.16.
LAVEAU CREEK	SB	U	Fig. 3.15.
BUSE HILL COMPLEX	MJ	N	Fig. 3.17, Plate 3.7.
DUCKS MEADOW	SB	M	Fig. 3.18.
GEORGE CREEK NORTH	SB	U	Fig. 3.18.
GEORGE CREEK SOUTH	SB	U	Fig. 3.18.
TEAKETTLE CREEK 1	SB	U	Fig. 3.18.
TEAKETTLE CREEK 2	SB	U	Fig. 3.18.
TEAKETTLE CREEK 3	SB	U	Fig. 3.18.
MONTE LAKE	SB	M	Fig. 3.18.
DEADMAN 1	CB/VB	M	
DEADMAN 2	CB/VB	M	
DEADMAN 3	CB/VB	M	
DEADMAN 4	CB/VB	M	
DEADMAN 5	CB/VB	M	Figs. 3.19,3.20.
DEADMAN 6	CB/VB	M	Plates 3.8-3.15.
DEADMAN 7	CB/VB	M	
DEADMAN 8	CB/VB	M	
DEADMAN 9	CB/VB	M	
DEADMAN 10	CB/VB	M	
DEADMAN 11	CB/VB	M	

KEY TO COLUMNS:
1-MORPHOLOGICAL CLASSIFICATION; SB=SIMPLE BLOCK MOVEMENT, MJ=MULTIPLE JUXTA-
POSED BLOCK MOVEMENT, CB=COMPLEX BLOCK MOVEMENT, VB=SUCCESSIVE BLOCK MOVEMENT.

2-GEOMORPHIC SETTING; H=HIGH LEVEL PASS, U=UNDERCUT BY FLUVIAL PROCESSES, M=
MELTWATER CHANNEL, N=NO EVIDENCE OF RAPID SLOPE GEOMETRY CHANGE.

3-ILLUSTRATIONS.
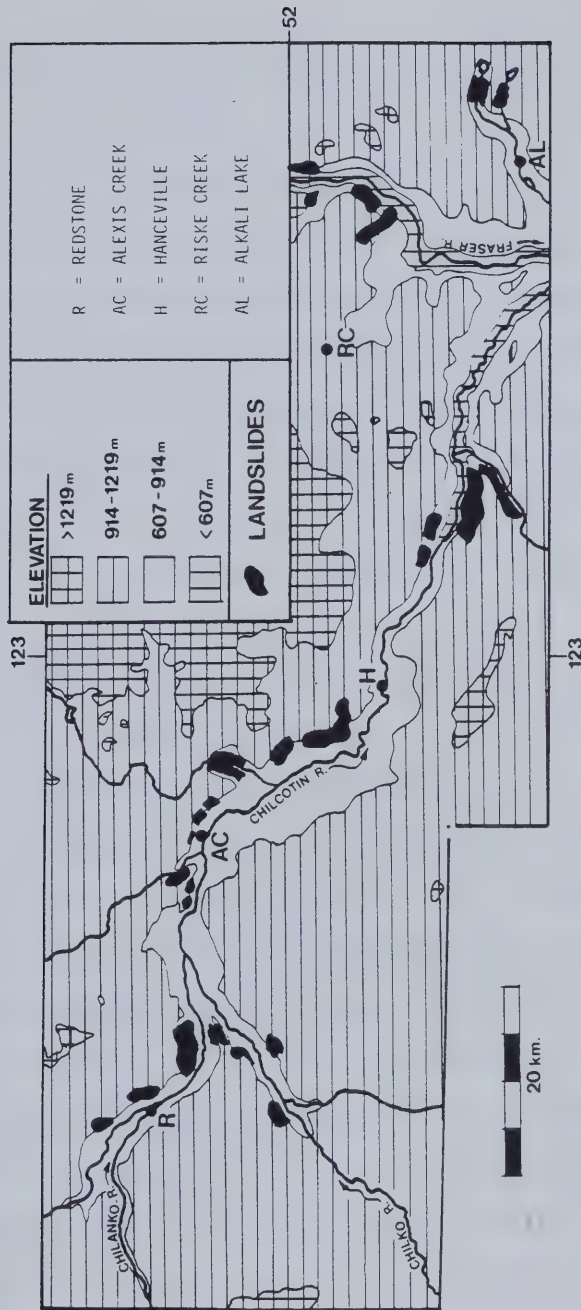
Figure 3.2 Location of landslides in Neogene rocks in the Chilcotin study area.

Creek, and sporadically for about 48 km along the north side of the Chilcotin, between Lee's Corner and Redstone. An isolated landslide area was identified east of Alkali Lake (Fig. 3.2).

3.3 Detailed Description of Landslide Sites in the Paleogene Volcanic Successions

3.3.1 Bouleau Lake and Tahaetkun Mountain

The landslides at Bouleau Lake (Plate 3.1) were first noted by Fulton (1975), and were visited by the writer in the summer of 1979. A landslide complex exists south of Bouleau Lake which, together with Little Bouleau Lake, is slide-dammed in origin. Slope movements within the slide complex involved slopes varying in height between 215 and 450 m. The landslide varies in length between 1650 and 2100 m. It consists of 3 slide masses (Fig. 3.3) which have an overall width of 4.9 Km. Profiles of the landslides are seen in Figure 3.4. Bouleau 4 is located to the west of the Bouleau Lake landslide complex (Fig. 3.5).

The clustering of slides of such large magnitude in the vicinity of Bouleau Lake suggests strong geological control of failure occurrence since other slopes developed in the Paleogene rocks of the area of similar geometries show no recognisable signs of instability. The geology of the Bouleau Lake area is reported in a preliminary map by Church (1979). From this map (Fig. 3.5) it is evident that the rocks have been cut up into irregularly shaped fault blocks by vertical faulting, and that the blocks have irregular dips. The faulting has resulted in differential vertical displacement between the blocks, and this seems to have resulted in weaker beds, probably the Shorts Creek Formation, being exposed at the base of slopes which underwent slope movement. Sediments, including a sheared black clay shale, and clay-rich debris, were found in road cuts along the base of the slide complex. The complex occurs within a triangular shaped fault block and the lateral margins of the complex are defined by persistent discontinuities which trend 324° and 054° giving a set of fractures which are conducive to northerly movement. Other fractures appear to cross the complex (Plate 3.1).

Much of the slide debris along the Bouleau Lake road is rich in a gritty clay which varies in colour from yellow through brown to red. Much of the clay is randomly
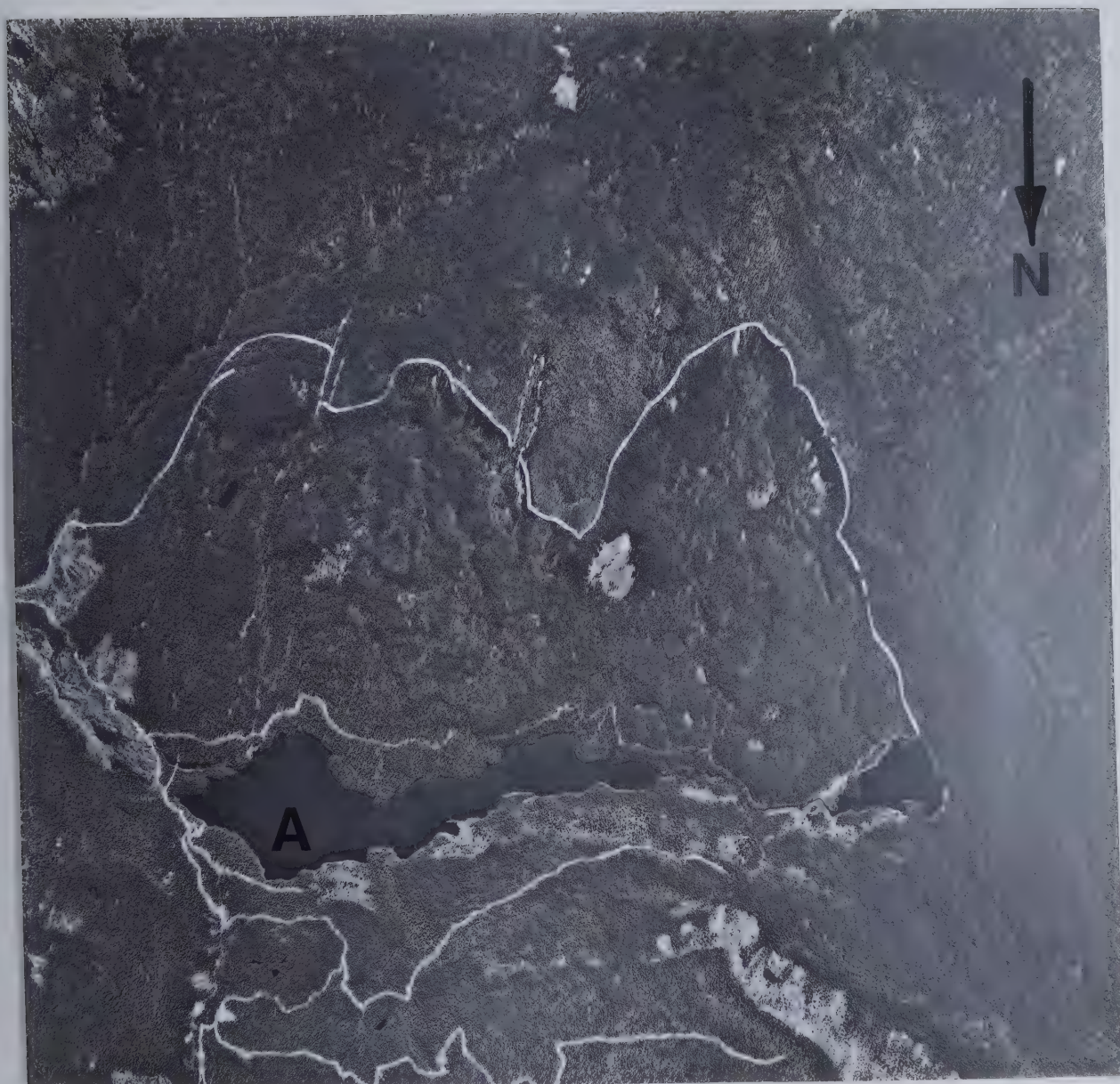
Plate 3.1 Aerial photograph of Bouleau Lake landslide complex (B.C. Air Photograph 5187–259–exposed 28 May, 1966). A = Bouleau Lake.
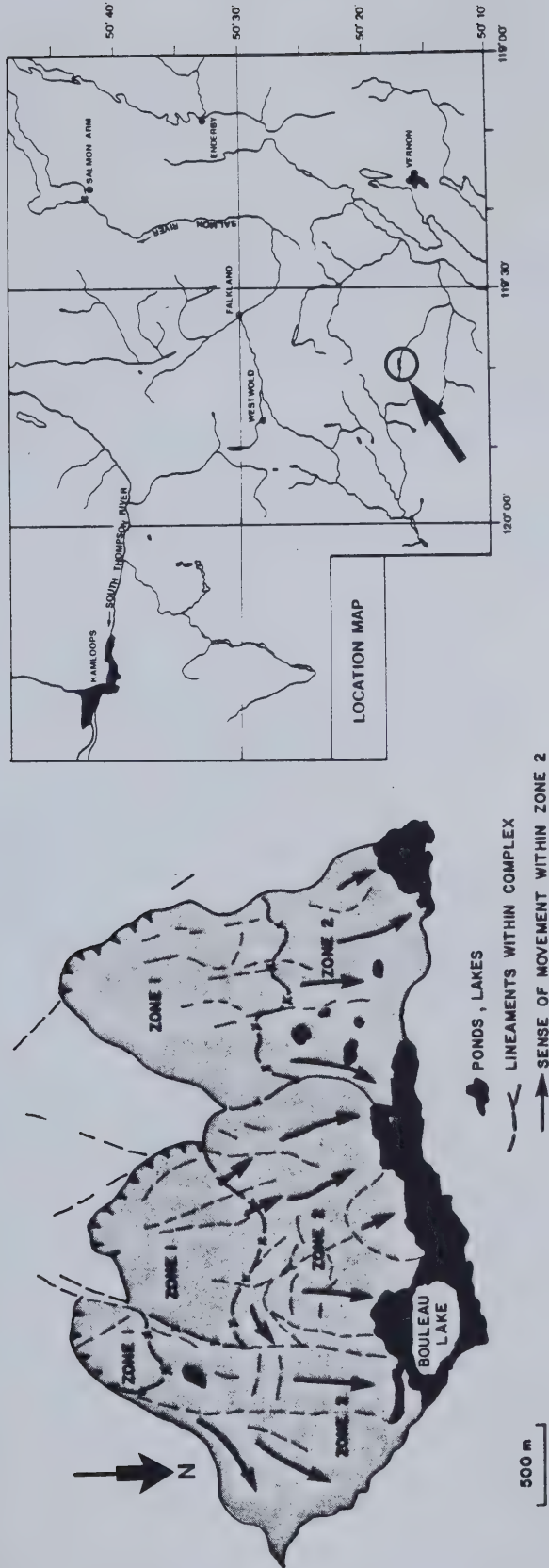
Figure 3.3 Morphology of Bouleau Lake landslide complex (from an interpretation of B.C.

Air Photograph BC 5187–259).
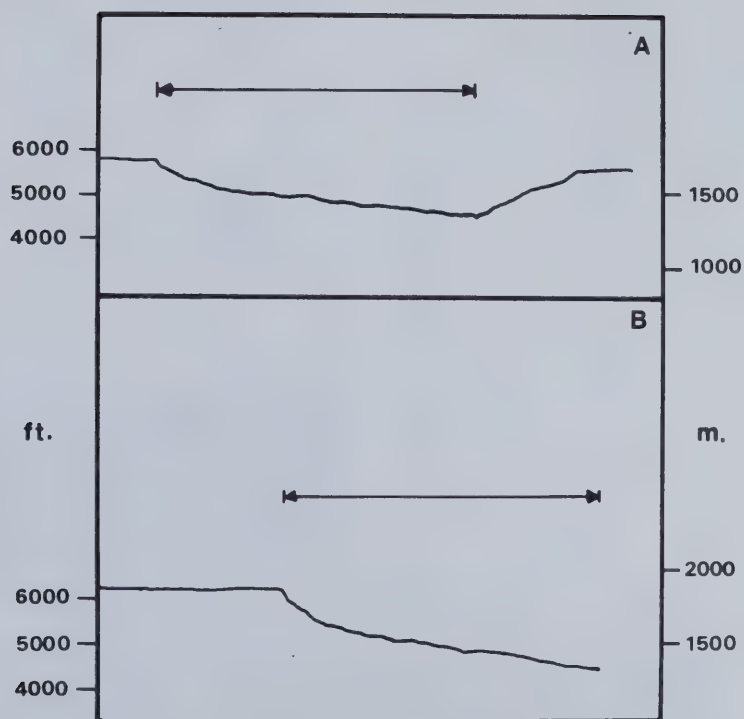
Figure 3.4 Profiles of the Bouleau Lake landslides. Drawn with no vertical exaggeration.

50
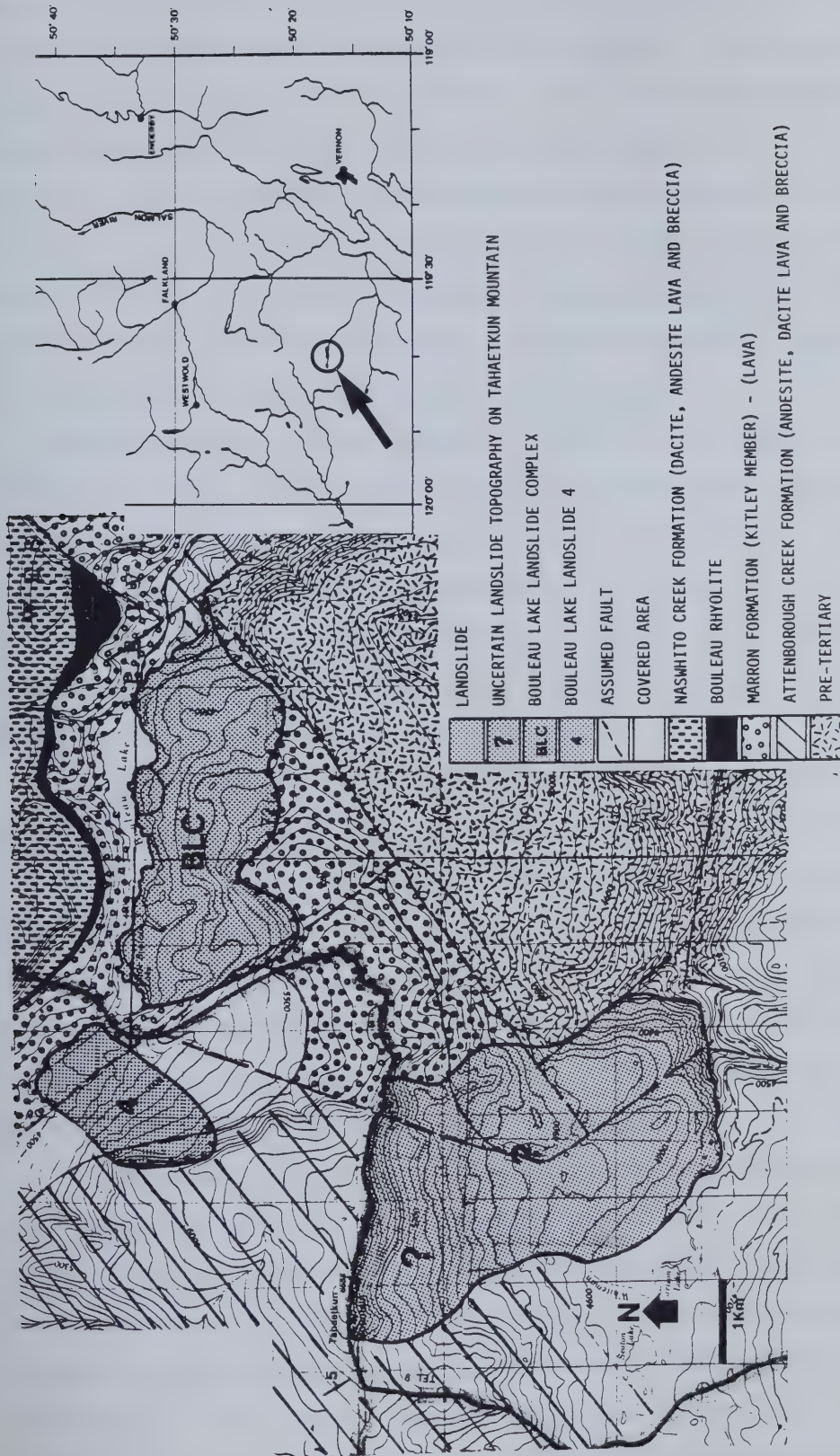
Figure 3.5 Landslides at Bouleau Lake and Tahaetkun Mountain. Geology after Church (1979).

slickensided and probably originated from the alteration of the slide mass. Heavy seepage was noted in the slide mass which contributes to this alteration. The debris within the complex can be divided into two zones (Fig. 3.3). Zone 1 is directly beneath an ill-defined irregular scarp in which degraded slide blocks are still perceptible in the debris. Downslope of this zone the debris is disaggregated, either by initial failure or secondary movements. Several small lakes within Zone 2 reflect the heavy seepage conditions within this part of the debris. Hummocky topography is also observed and longitudinal lineaments indicate the sense of movement within Zone 2. Transverse topographic features mark the site of secondary failure within these zones.

Based upon Church's (1979) succession established in the Bouleau Lake area, the failed slopes consist of andesitic lava and volcanic breccia from the lower part of the Kitley Member of the Marron Formation underlain by the Attenborough Creek Formation consisting of thinly bedded andesite and dacite lavas with breccias. Field observations of the attitude of beds within the scarps suggest a dip of $060°/5°$. The landslides have moved in a direction ranging from 000 to $020°$ suggesting movement down an apparent dip of between $3°$ and $4°$.

Uncertainty surrounds the interpretation of certain geomorphological features on the south flank of Tahaetkun Mountain. A combination of features interpreted from aerial photographs suggests the existence of a very large landslide. However, the debris is difficult to delimit and features such as the scarp and a hummocky portruberance at the foot of the slope could be explained by erosion and glacial deposition. The various ridges and transverse features on the slope beneath Tahaetkun Mountain may also have resulted from faulting. If the feature represents a landslide, then it is one of the largest in the study area, being 760 m high, 2440 m wide and 4420 m in length.

The slides described above occur in high-level gaps in the Tahaetkun upland with summit elevations of about 1370 m. According to Fulton (1975), these were the paths of glacial meltwater draining east from pro-glacial lakes known to have existed west of these gaps at various stages in deglaciation. Whilst Bouleau 4 appears to have moved without slope geometry change by basal erosion by contemporary streams, slope movements in the Bouleau Lake Complex and on Tahaetkun Mountain occurred as a result of downcutting and headward erosion by the eastward flowing Bouleau and Whiteman Creeks.

3.3.2 Pinaus Lake

Five major landslides have occurred in the vicinity of Pinaus Lake (Fig. 3.6) in similar geomorphological circumstances to the Bouleau Lake movements. Some of the slides were first recognised by Fulton (1975). Pinaus Lake and Little Pinaus Lake are also slide dammed. The area was traversed in 1978 but no detailed observations were made due to heavy vegetative cover.

The geology of the Pinaus Lake area has not been mapped in detail. Small scale maps produced by Jones (1959) and Okulitch (1979) indicate that weak rocks of the basal sedimentary assemblage occur towards the base of slopes in the vicinity of the landslides between 915 and 1070 m a. s. l., overlain with breccias and flow rocks which appear to be horizontally bedded. Therefore, it is probable that the landslides occurred in response to the presence of weak layers at the base of the valley side slopes during the headward erosion of Equesis Creek. The plan geometry of the slides appears to have been controlled by steeply dipping discontinuities which are evident in the lineament pattern near the scarp. The slides on the south side of Pinaus Lake and Little Pinaus Lake form a very large slide complex in which the topography is characterised by irregular hummocky terrain. Large flow movements also occur in this vicinity. Several are noted in the vicinity of Siwash Rock Mountain (Fig. 3.6) and a large flow occurred between 1974 and 1976 in the Salmon Valley 2.75 km to the northeast of the eastern end of Pinaus Lake. It involved a heavily altered volcanic breccia and cut a swath through forest cover about 1525 m long and 120 m wide (Fig. 3.6, Plate 3.2).

3.3.3 Estekwalan Mountain

A major complex landslide has occurred on the south side of Estekwalan Mountain (Fig. 3.7) which appears to form part of the remnants of a large volcanic edifice which is thought to have been located near the present site of Falkland in Paleogene time (Ewing, 1981a). The landslide was first noted by Fulton (1975), and is inaccessible. Because of this, it was only inspected from the summit of Tuktakamin Mountain by the present writer. Movement is again related to the base of the Paleogene succession, i.e., the presence of weak sediments at about 915 m, about 300 m above the valley floor (Fig. 3.8). However, the slide does not appear to have moved down into the Salmon Valley. Fulton (1975,
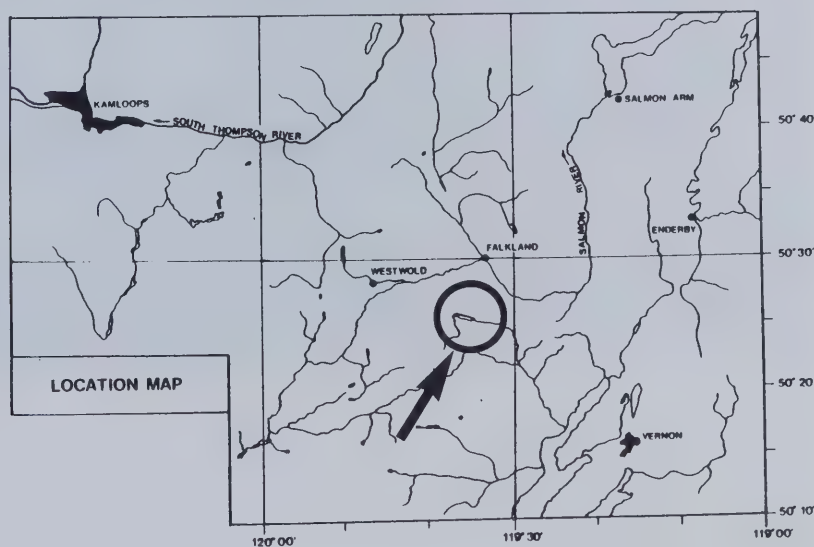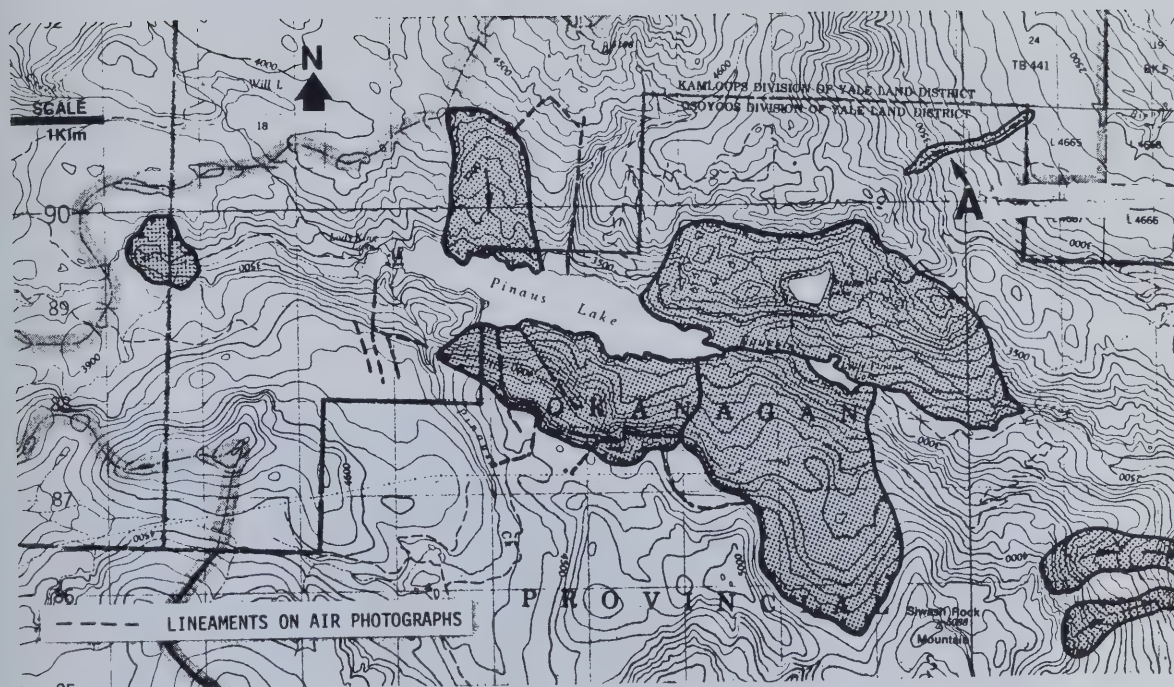
Figure 3.6 Landslides in the vicinity of Pinaus Lake. A = Falkland flow slide photographed in Plate 3.2.

Plate 3.2 The Falkland landslide which occurred between 1974 and 1976. The movement appears to be of the flow type involving altered Paleogene volcanic breccia. Note figure for scale.
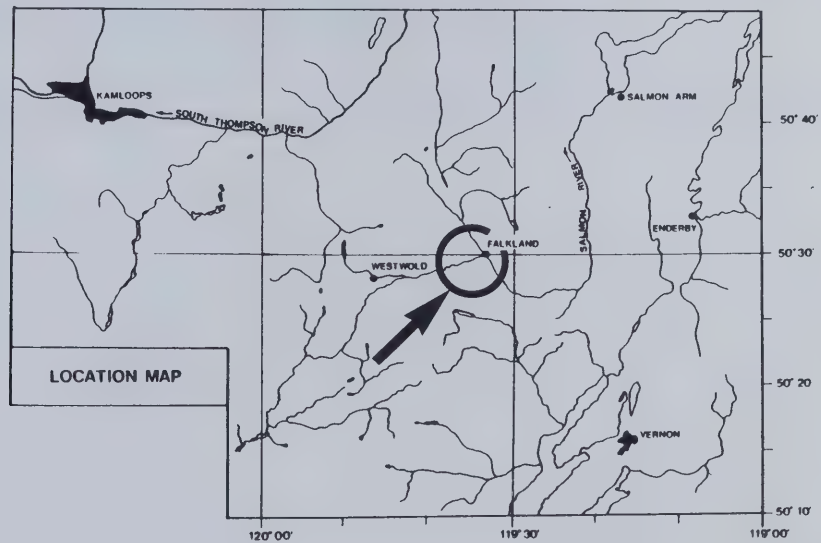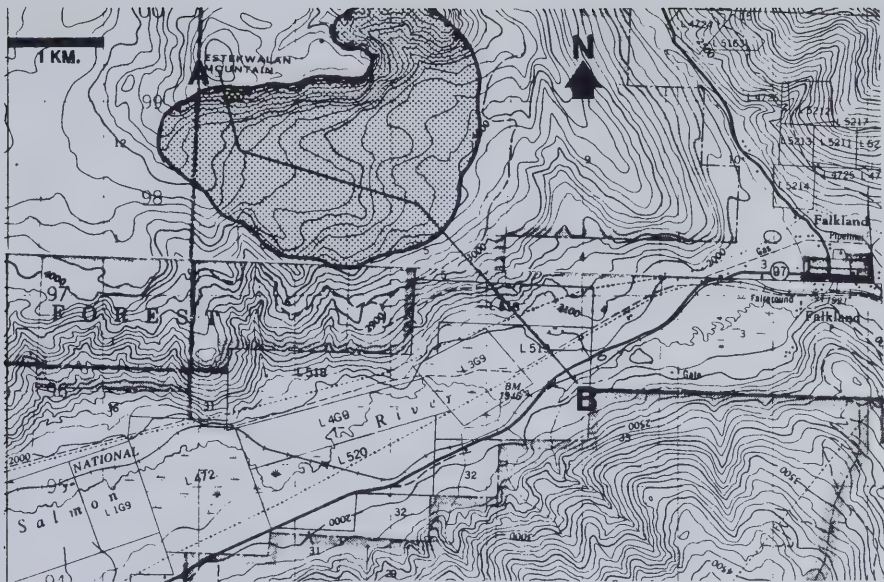
Figure 3.7 Estekwalan Mountain landslide. A–B is line of section in Fig 3.8.
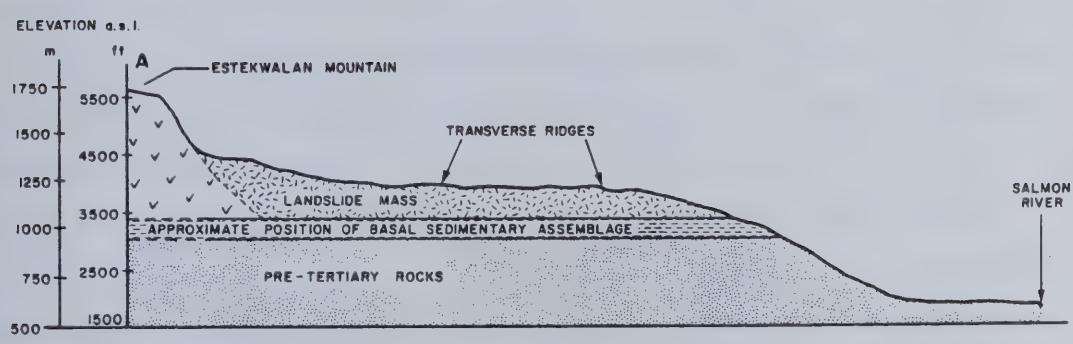
Figure 3.8 Approximate geological cross section through Estekwalan Mountain landslide.

p. 30) suggested that the slide has produced a large bog by partly damming the Salmon River. This writer suggests that the blockage is due to the development of an alluvial fan (Fig. 3.7).

The debris of the slide, though heavily vegetated, exhibits very marked transverse ridges (Plate 3.3).

3.3.4 Landslides between Falkland and Salmon Arm

Large landslides have also occurred on isolated outliers between Falkland and Salmon Arm in the Shuswap Highland. These landslides have not been examined in detail. Only the general features are recorded here.

(a) *North of Falkland*

North of Falkland, block type landslides have occurred where westward flowing streams have eroded through the Paleogene outlier at Charcoal Creek (locally called China Valley) and possibly at Chase Creek just to the south. China Valley is a flat-bottomed valley which appears to have been an old lake bed which may have formed by landslide damming (Fig. 3.9). A minor slide also occurs on the east flank of Flag Hill to the west of Salmon Arm. Again it occurs on the boundary of the Paleogene volcanics.

(b) *Mt. Ida*

A large landslide has taken place on the north face of Mt. Ida 4.8 km south of Salmon Arm over a slope width of 1770 m, the scarp corresponding to the summit of Mount Ida at the head of Rumball Creek (Fig. 3.10). The landslide was first noted by Fulton (1975), occurs near the base of the Paleogene and exhibits secondary flow features within the debris.

3.3.5 Enderby Cliffs

The landslide at Enderby Cliffs (Plates 3.4 and 3.5) was discovered by the writer in 1975 and occurs on the east flank of a Paleogene outlier about 4.8 Km north east of Enderby (Fig. 3.11). It was inspected in the field in 1979 and 1980. A traverse was made along the landslide scarp and the debris examined. The landslide debris is heavily vegetated and infested with black bears, factors which limited the extent of traverses in the debris. According to Mathews (1981) the outlier is a fault block tilted to the east within which the dips of the various strata are erratic. Mathews (1981) distinguishes three

Plate 3.3 View to the north of the Estekwalan Mountain landslide from the summit of Tuktakamin Mountain.
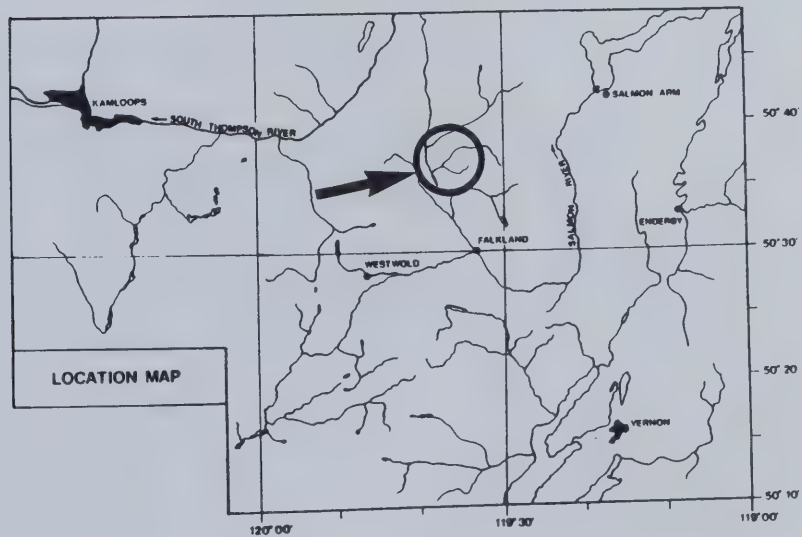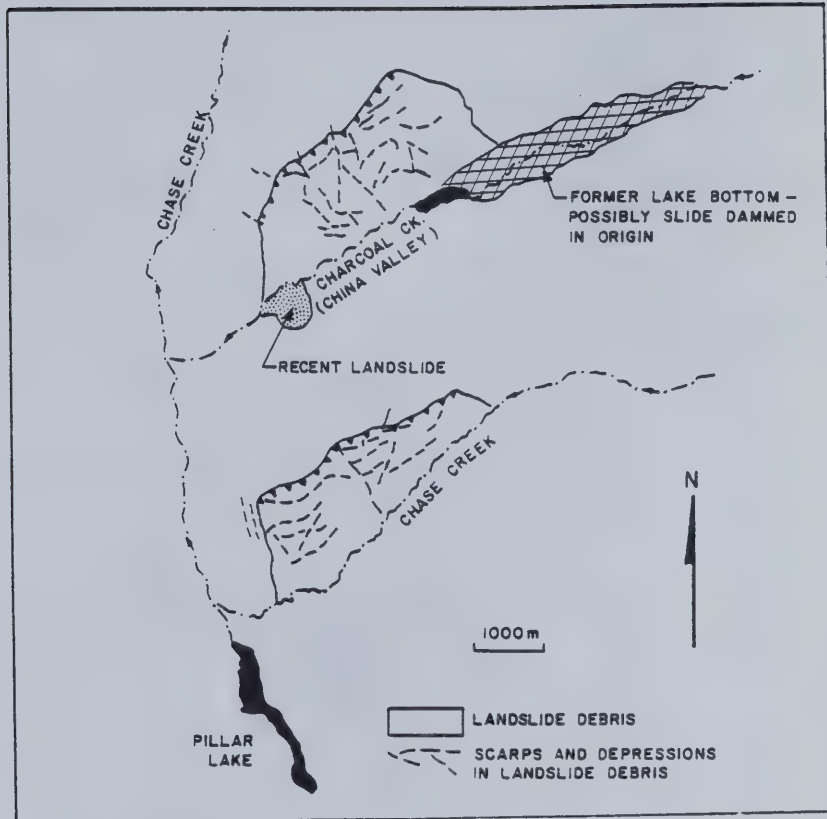
Figure 3.9 Landslides at China Valley and Chase Creek (Traced from an interpretation of B.C. Government air photograph BC 5377–127).
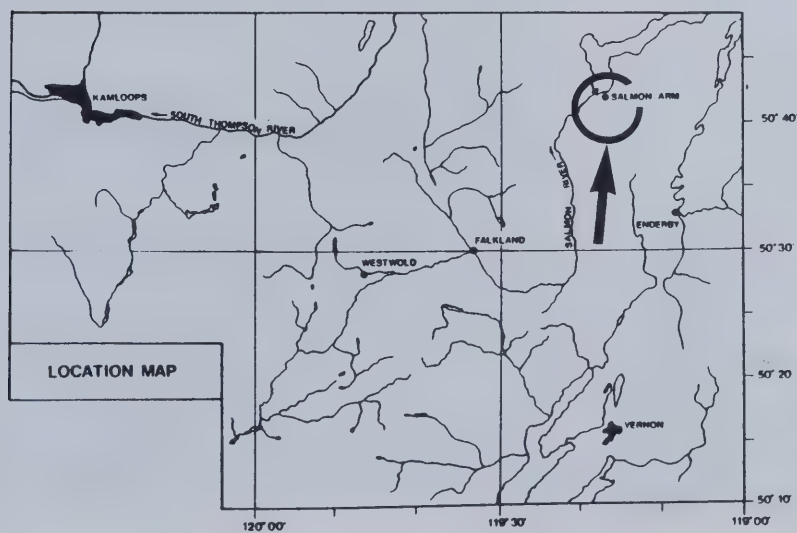
Figure 3.10 Mount Ida landslide, near Salmon Arm.

Plate 3.4 Aerial photograph of Enderby Cliffs. B.C. air photograph BC 5190-158. A =North Block; B = Active Flow Lobe.
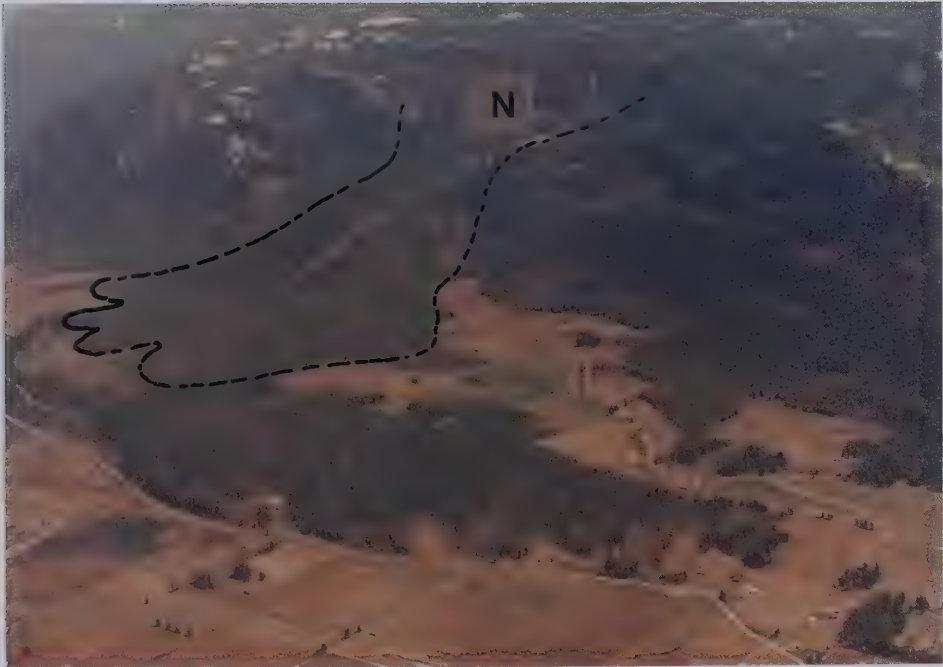
Plate 3.5 Oblique aerial photograph of the Enderby landslide. N=North Block.
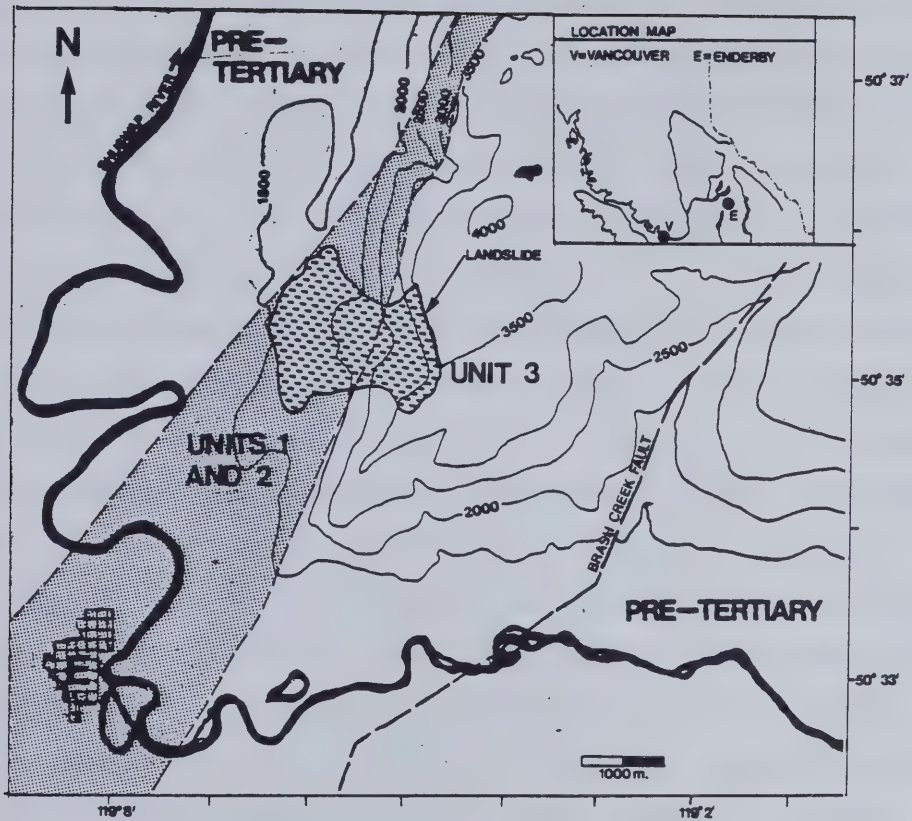
KEY TO TERTIARY UNITS (DESCRIPTION AFTER MATHEWS, 1981).
UNIT 1:   BASAL UNIT CONSISTING OF THINLY BEDDED SHALES, SANDSTONES AND
          CONGLOMERATES WITH LOCAL DEVELOPMENT OF COAL SEAMS.
UNIT 2:   COARSE INTERMEDIATE UNIT CONSISTING OF CONGLOMERATE AND
          FANGLOMERATE-CLASTIC BRECCIA WHICH IN PART APPEARS TO BE
          AN EOCENE LANDSLIDE DEPOSIT.
UNIT 3:   UPPER UNIT CONSISTING OF LAVA FLOWS AND VOLCANIC BRECCIA.

Figure 3.11 Location and geological setting of Enderby landslide. Geology after Mathews
(1981).

Paleogene units in the vicinity of Enderby Cliffs. The basal unit (Unit 1) consists of thinly bedded shales, sandstones and conglomerates with local development of coal seams. Cairnes (1932) noted that some of these sediments exhibited clay-like seams "along which it appeared that some movement had occurred" (p. 104A), in Coal Gulch to the north of Logan Gulch. The middle unit (Unit 2) consists of coarse conglomerate and fanglomerate with large clasts up to 10 m in length. Most clasts are of pre-Tertiary rocks, and according to Mathews (1981) may be in part a large landslide deposit similar to the Skaha Formation in the White Lake area (Church, 1973). Together with the observations of Cairnes (1932) on exposures in Logan and Coal Gulch, it appears that contemporaneous landsliding may have been important in determining the properties of rocks in Unit 2. Unit 3 (B in Figure 3.13) consists of flow rocks and large thicknesses of volcanic breccia.

As noted above, although the fault block is tilted generally to the southeast, dips and dip directions within it are erratic. North of Coal Gulch the dips are 20^0 to the southwest (Mathews, 1981), whilst in the landslide area they are 5^0-10^0 to the east and southeast (Fig. 3.12). This appears to be typical of observations on fault blocks elsewhere in the Paleogene succession studied (e.g., in the Salmon River). The Brash Creek Fault which forms the eastern boundary of the outlier is segmented in zig-zag fashion and the segments have orientations of 006^0-010^0 and 041^0-045^0, according to Figure 2 in Mathews (1981). The structure of the Enderby Cliffs area in the vicinity of the landslide was inferred from lineament patterns evident on large-scale aerial photographs (Fig. 3.12). As can be seen, the face of the cliffs south of the landslide, and the south scarp of the landslide itself, have developed along a vertical discontinuity which has a direction of 041^0 then doglegs to 006^0. This mirrors precisely the inferred trace of the Brash Creek Fault (Fig. 3.11) to the east noted by Mathews (1981) and it is probable that it is a smaller scale fault, or at least a persistent set of discontinuities related to the fault.

Other lineaments were observed. A set is oriented at about 165^0 and appears to correspond to the north scarp of the landslide itself and the eastern boundary of the north block. This set of lineaments is thought to correspond to joints observed at the back of the north block and forms another block east of the landslide scarp. Another set, which is limited in extent to the junction of the north and south scarps, is oriented at 075^0 and is associated with closely spaced fractures (Fig. 3.12). While some of these lineaments
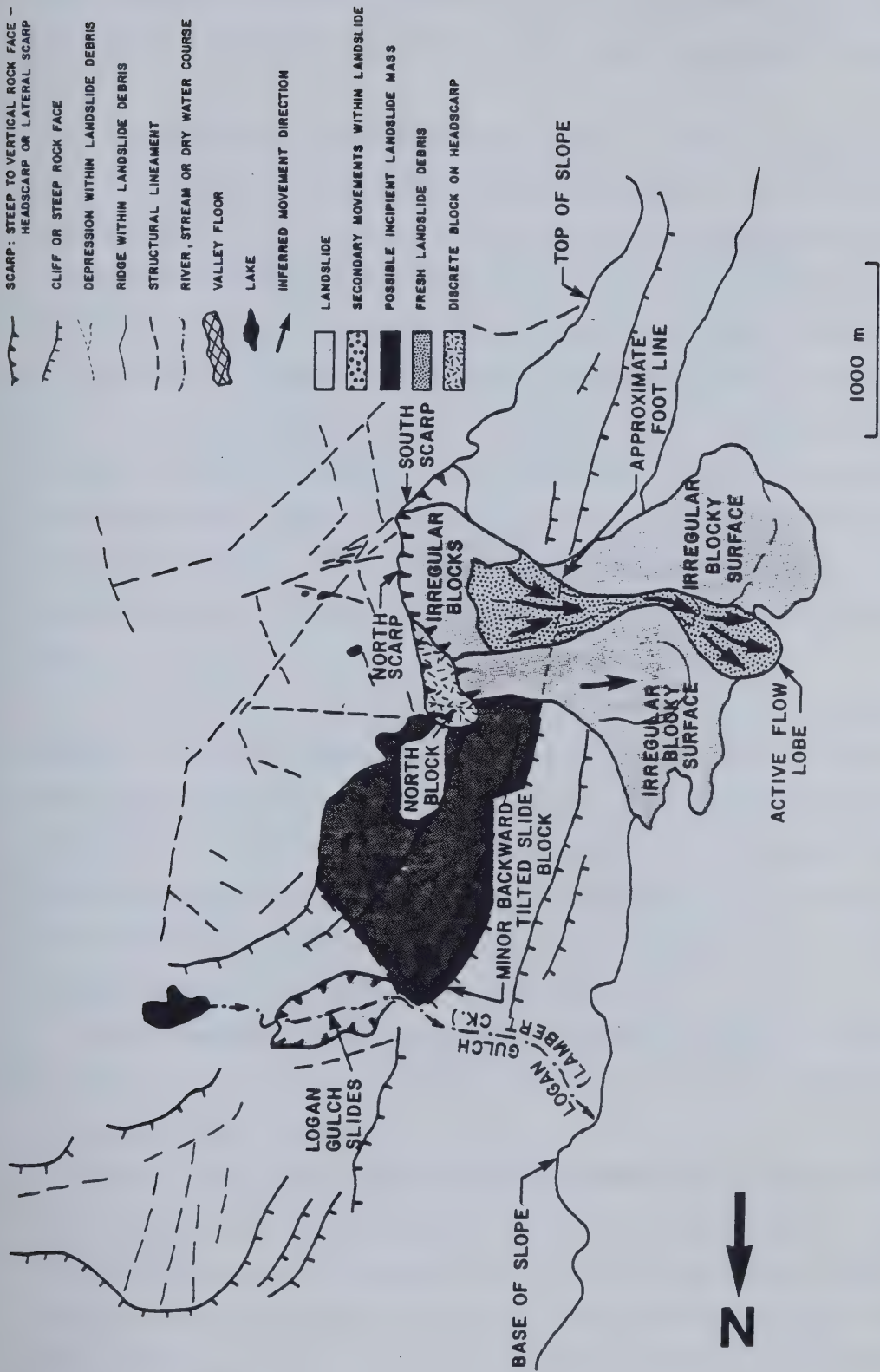
Figure 3.12 Map of Logan Gulch–Enderby landslide Area (Traced from B.C. air photographs

BC 5190–157, 158, 159).

could correspond to stress relief fractures formed by the movement itself, it would appear that they form part of a larger scale fracture system resulting from tectonic activity.

The morphology of the landslide debris appears to reflect a series of landslide events. The scarp is almost vertical and prominently displays the near vertical jointing mentioned above (Plate 3.6). Beneath the scarp is a zone of irregular blocks which are currently undergoing degradation by weathering and secondary flow. The centre of the landslide debris is the site of an active flow, the lobe of which is encroaching on farmland and a house (Fig. 3.12, Plate 3.4). The remainder of the debris appears to be irregular and blocky in nature and possibly results from the initial failure. The so-called north block is separated from the north scarp at present. An open discontinuity with an aperture of .1 m was observed from the scarp to run from its top to the lowest part exposed (Plate 3.6). However, very little if any vertical displacement has occurred. More debris would presumably have to be displaced from the upper part of the debris for movement to occur.

The structural control on the plan geometry of the failure has already been mentioned. In terms of stratigraphic units an approximate reconstruction of the unfailed slope to the north and a geological section (Fig. 3.13) indicate that the failure was located in the upper part of Unit 2, the clastic breccia, a brecciated landslide debris unit. Note is made of the fact that movement is to the west whilst the dip is to the southeast. This lack of correspondence between true structural dip and the direction of slide movement is common in landslides in the Paleogene rocks (cf. Chapter 1).

A proposed chronology of block release from the Enderby Cliffs is given in Figure 3.14. The importance of structural control can be seen in determining block shape and sequence of block supply.

In view of this reconstruction of events at Enderby Slide, questions may be raised about the stability of the rock mass between the landslide and Logan Gulch. It appears to exhibit similar stratigraphy to the landslide site. Indeed, minor landslides in Logan Gulch (Fig. 3.13) would seem to confirm this. Further, diverging lineaments appear to constitute a release set of discontinuities. This slope constitutes a problem in distinguishing the difference between backward-tilted slide blocks and strike ridges. Just below the top of
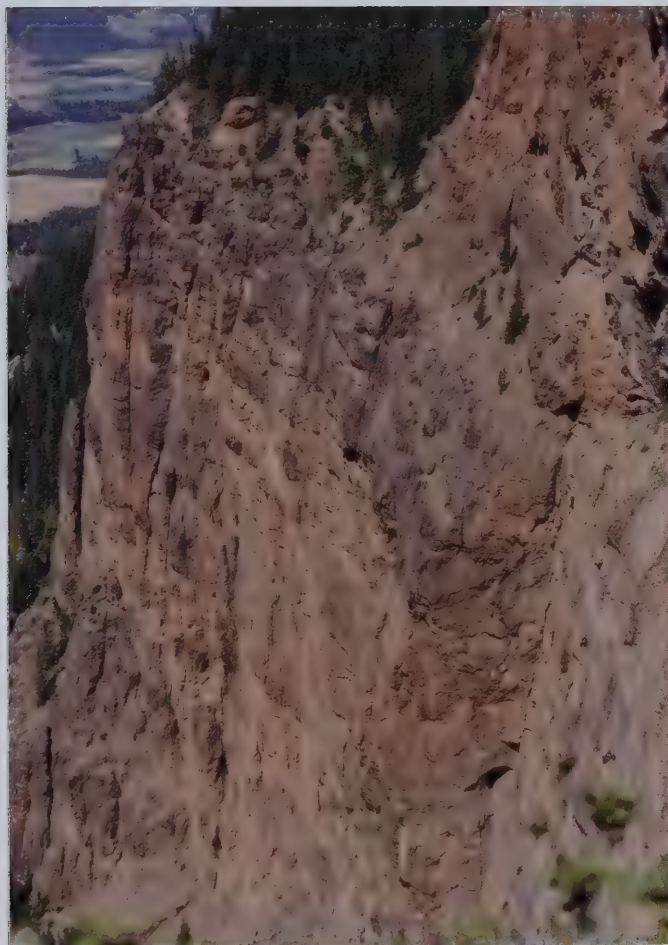
Plate 3.6 Vertical jointing observed in the scarp of Enderby landslide at the North Block.
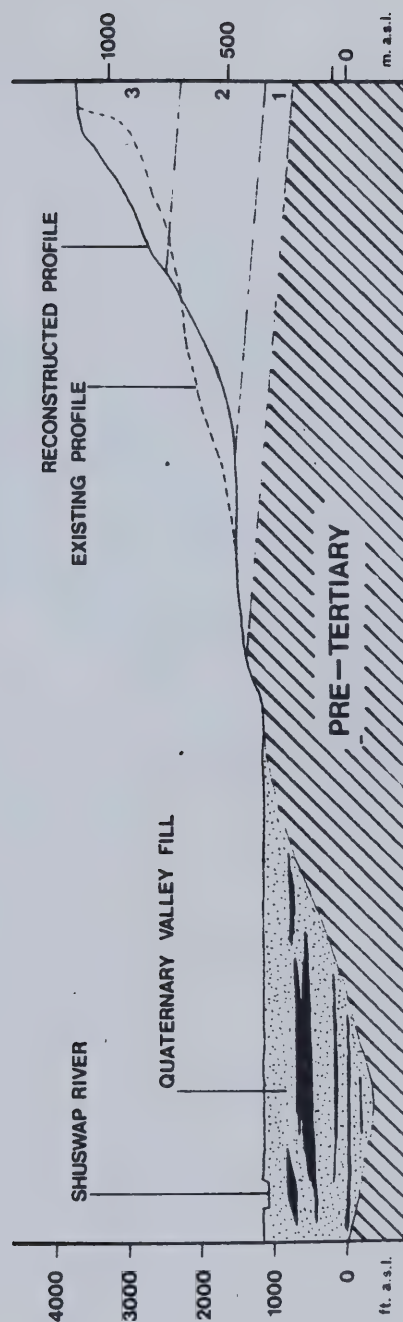
(SUBSURFACE BEDROCK TOPOGRAPHY IN SHUSWAP RIVER VALLEY BASED ON SEISMIC REFRACTION SURVEY BY McAULAY AND HOBSON (1972) . TERTIARY UNITS ARE NUMBERED AFTER MATHEWS (1981).)

Figure 3.13 Approximate geological cross section of Enderby landslide. Geology partly based on Mathews (1981).
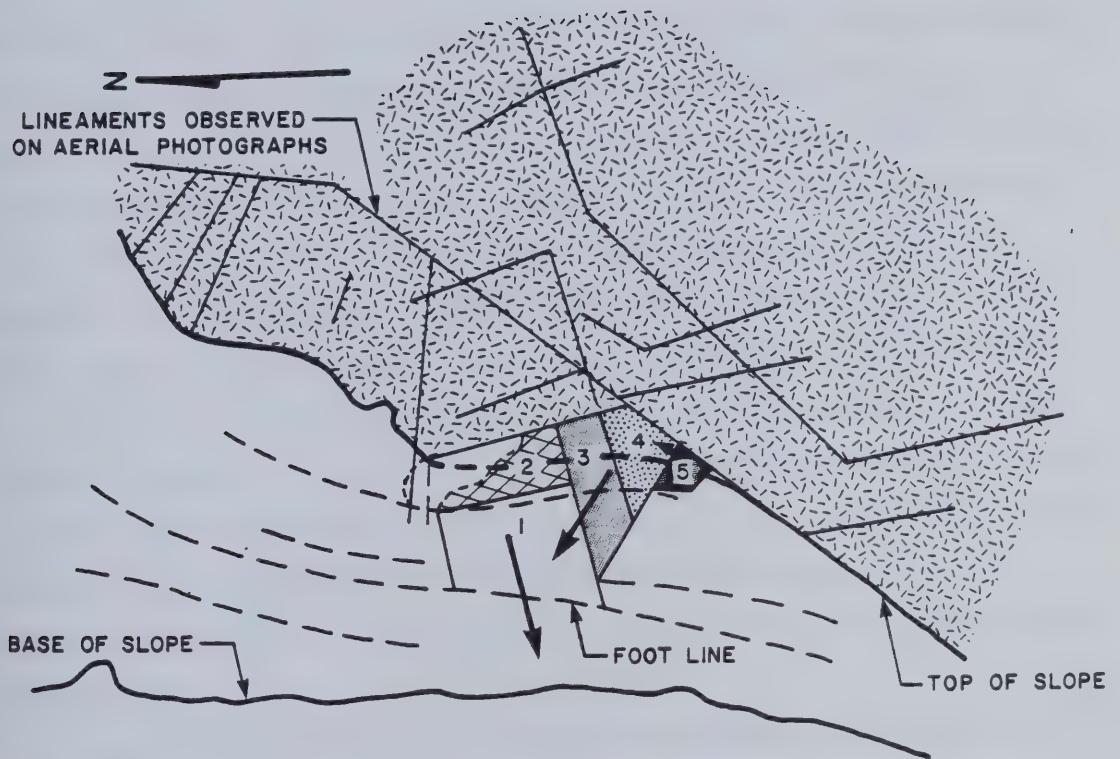
Figure 3.14 Hypothetical sequence of block movement at Enderby landslide.

the slope, an embayment and a marked reverse slope downslope strongly suggest that limited movement has already taken place.

3.3.6 Slides at Pemberton Hill and Laveau Creek

The landslide complex, which is located on the south flank of Pemberton Hill (Fig. 3.15) , was first noted by Fulton (1975). It was inspected briefly by the writer in 1978. The movements have occurred in a slope approximately 300 m in height and the toe of the more mobile part of the landslide debris extends 3000 m downslope from the scarp. It is with respect to this run-out distance that the Pemberton Hill landslides are atypical of slides in the Kamloops Group. Further, according to Jones (1959) and Okulitch (1979), the landslide did not originate in the basal part of the Paleogene but within it. The scarp consists of nearly horizontal basalt flows, yet the debris appears to be highly fragmented. Further geological mapping might indicate the presence of weaker strata beneath the flow rocks in the scarp. Where topography limited the travel of the debris, blocks from the initial movement are preserved intact. The surface of the lower part of the landslide complex is hummocky with small lakes and seepage common over its surface (Fig. 3.16). Two zones are apparent in the debris. An upper zone which contains degraded blocks and the lower zone which contains the hummocky disintegrated flow material. Note in Figure 3.16 the central part of the complex does not have a flow zone downslope of the block zone.

A second landslide is found south of the South Thompson River on the eastern side of the Lois Creek Fault Zone at Laveau Creek (Fig. 3.15); this slide was first reported by Fulton (1975). The debris shows no transverse ridges or longitudinal features and has been eroded through by Laveau Creek. This has resulted in some re-activation of the slide blocks in the debris along the creek. The scarp is well marked. The debris is about 2745 m in length and extends down from the scarp at 1400 m to about 520 m in Laveau Creek. The base of the Paleogene is at an approximate elevation of 1060-1130 m (based on Okulitch, 1979) and it was exposure of these weaker materials by headward erosion which probably led to the landslide.

71

Figure 3.15 Location map of the Pemberton Hill and Laveau Creek landslides.
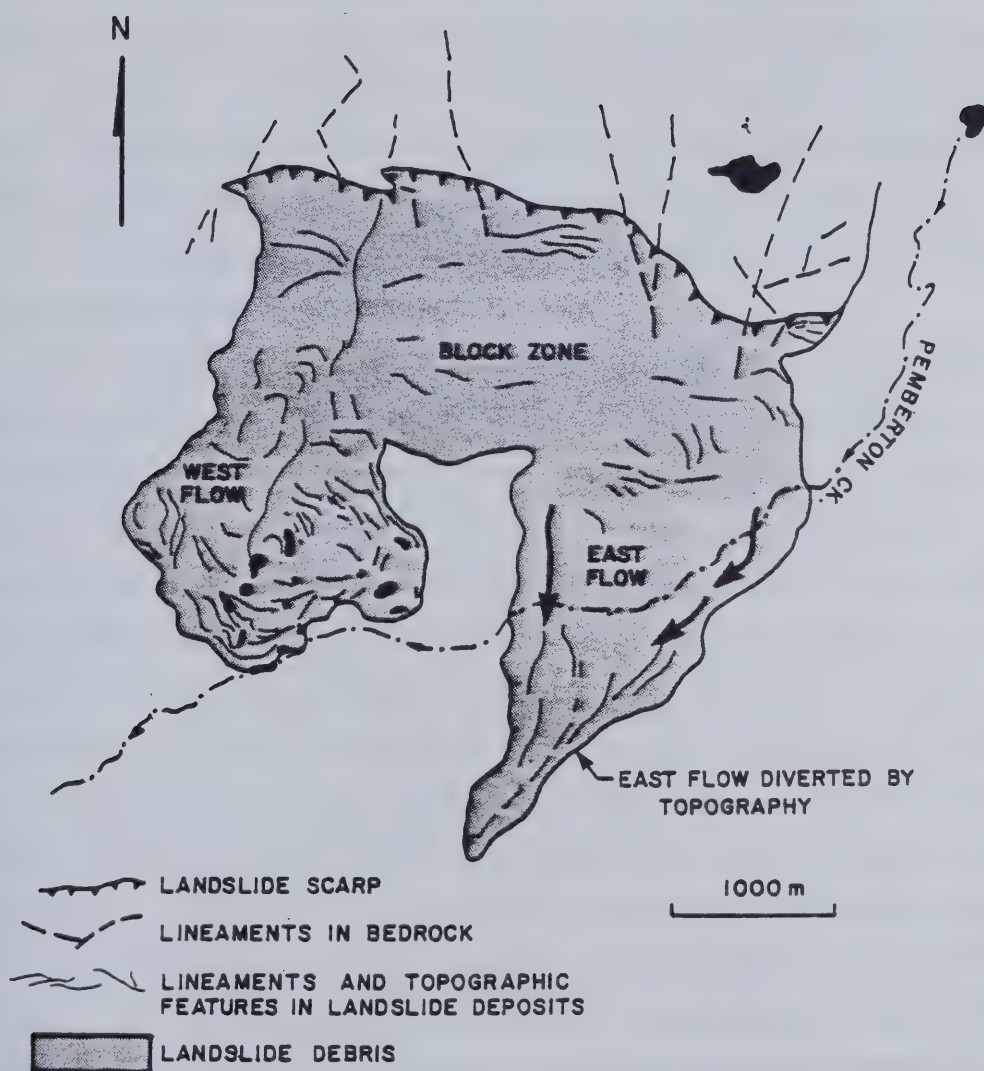
Figure 3.16 Morphological map of Pemberton Hill landslide complex (based on B.C. Air Photograph BC 5187-151).

3.3.7 Buse Hill

The Buse Hill landslide complex (Fig. 3.17) was first identified by Fulton (1975). The site was visited in 1979 and a traverse made along the scarp. The geology of the site is not known in detail but a series of lava flows and volcanic breccias appears to be interlayered with a considerable thickness of tuffaceous sediments and tuffs. The sediments include fine and coarse sandstone and shale, and the succession appears to have a 5° southerly dip. Ewing (1981a) has called these volcaniclastic sediments the Buse Hill Beds. Early observations were made by Daly (1915) in the Buse Hill area and in his descriptions of the Tertiary rocks, which were characterised by "sudden changes of dip, caused by considerable faulting and sharp upturning" (p. 128). It is likely that he was referring to landslide–disturbed rocks.

The Paleogene rocks rest on a surface of unknown configuration developed on Triassic Nicola Group limestones in which a quarry has been developed at the base of the landslide debris. This evidence suggests that the base of the Paleogene corresponds to the base of the slope. Exposures in the Paleogene are limited to the inaccessible scarps and overgrown landslide debris. However, basal tuffs and sediments are exposed along a road cut at the foot of the debris. The rocks consist of stratified siltstones and tuffs that have undergone considerable disturbance. They are cut by filled discontinuities between 2 mm and 50 mm in thickness which appear to be small normal faults (Plate 3.8). Another set of filled discontinuities is found parallel to, or at small angles to, the bedding plane traces in the material. These are much thicker, having a maximum width of about 250 mm. Both fillings are highly calcareous. In some places, steeply dipping calcite veins occur, exhibiting well–developed slickensides along their interfaces, parallel to the dip of the vein. In the Atterberg Limits test, these fillings were found to be non–plastic. Similar filled discontinuities associated with calcite veining were found in undisturbed tuffs north of Monte Lake and in the vicinity of the Jupiter Creek landslide in the Salmon Valley.

The scarp of the complex is steep and breccia exposed near its top exhibits persistent vertical jointing with apertures up to 1 m. The surface of the debris is hummocky and is more subdued than most debris examined. There is an absence of well–defined blocks, probably due to the dominance of weaker material in the failed slope. The extent of the debris is difficult to define in places because of post–movement
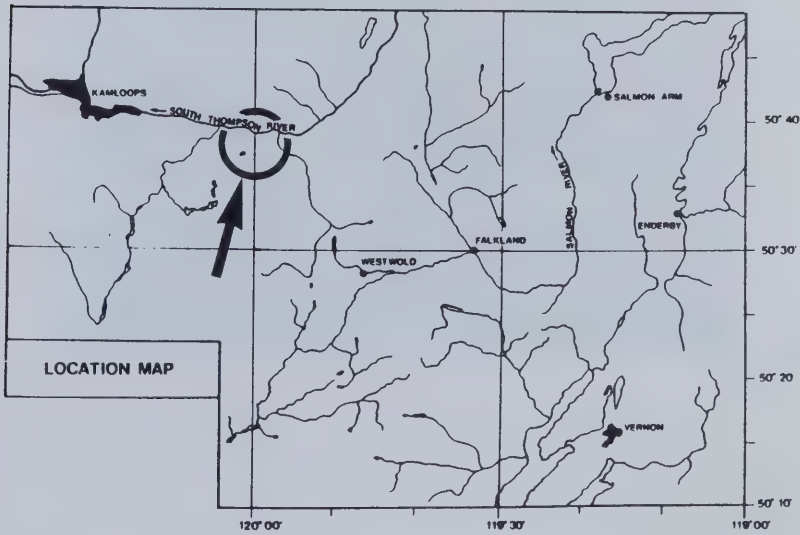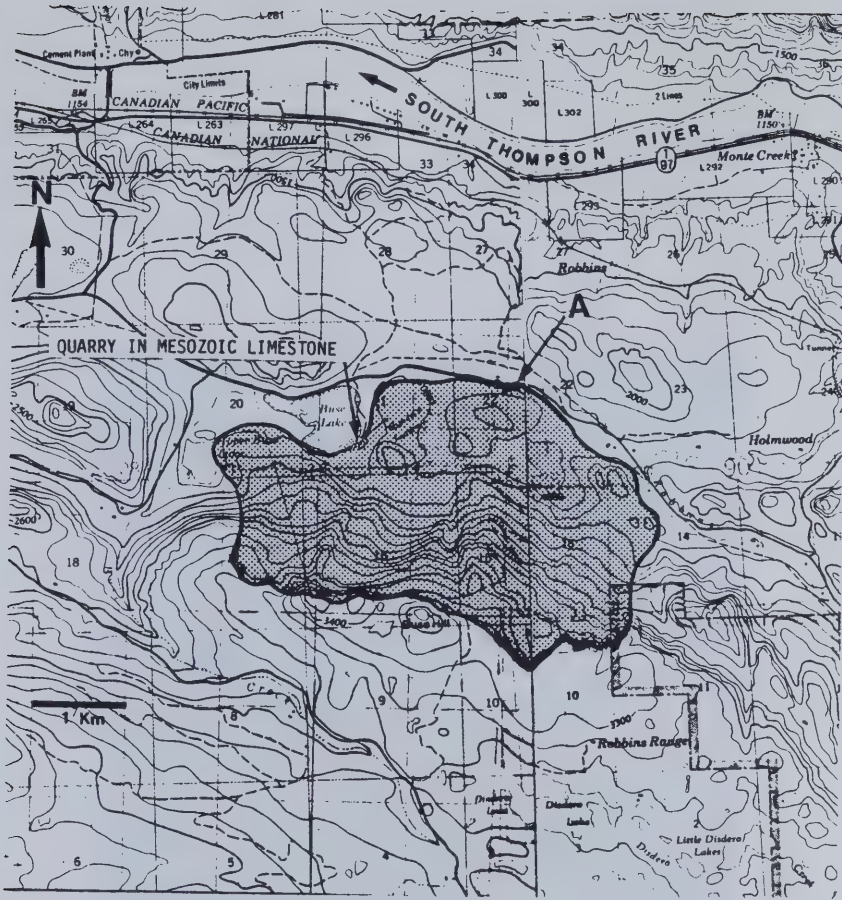
Figure 3.17 Location of Buse Hill landslide complex. A = Exposure of sheared tuff photographed in Plate 3.7.

Plate 3.7 Disturbed Paleogene tuffs at Buse Hill. Note small normal faults and filled discontinuities. The exposure, located in Fig. 3.17, is interpreted to be the shear zone of the Buse Hill landslide complex.

modification.

3.3.8 Monte Lake - Ducks Meadow

In the vicinity of Monte Lake, several landslides have been identified (Fig. 3.18). The block-type failure at Ducks Meadow was the only slide examined in the field. Sediments and tuffs, which are well exposed in road cuts along Highway 97, were also examined.

The landslides were first identified on aerial photographs. In this phase of the study of the area, uncertainty was encountered in the interpretation of certain slopes along the main Monte Creek valley. These slopes gave the impression of having undergone limited movement. Whilst showing the trace of block outlines, a marked scarp and reverse slopes within the slopes, they lack the well-defined displaced mass, scarp and debris configuration typical of other landslides in Paleogene rocks of the area. It is suggested that these ill-defined zones represent areas of stress relief. One such area at Monte Lake is outlined in Fig. 3.18 and was inspected at road level in the field. The exposed rock was a weathered tuff breccia with steeply dipping calcite veining. Slickensides were developed in pink-red clay along the interfaces. Whether these features were due to tectonic activity or to slope movements is not clear.

Structural lineaments identified on aerial photographs are shown in Fig. 3.18, and it is seen that they control the plan geometry of many of the landslides mapped.

Traverses were made of the Ducks Meadow landslide which is characterised by well-defined headwall and north lateral scarps which appear to be controlled by two sets of discontinuities trending 298^0 and 017^0 respectively (Fig. 3.18). Movement was a result of the existence of these release sets and facilitated by the erosion of the spur which the landslide affects. The scarp consists of lava flows, which has resulted in the debris being made up of well-defined blocks separated by steep-sided transverse depressions. Dips of flow units in the scarp were estimated to be in the order of $035^0/14^0$. The direction of movement of the slide is also 035^0 and a translational movement down dip is strongly suggested.

All of the landslides identified in this area are of the block-type variety. This reflects the dominance of flow rocks throughout the succession which has led to high cap mass-cohesion and thus well-preserved blocks.
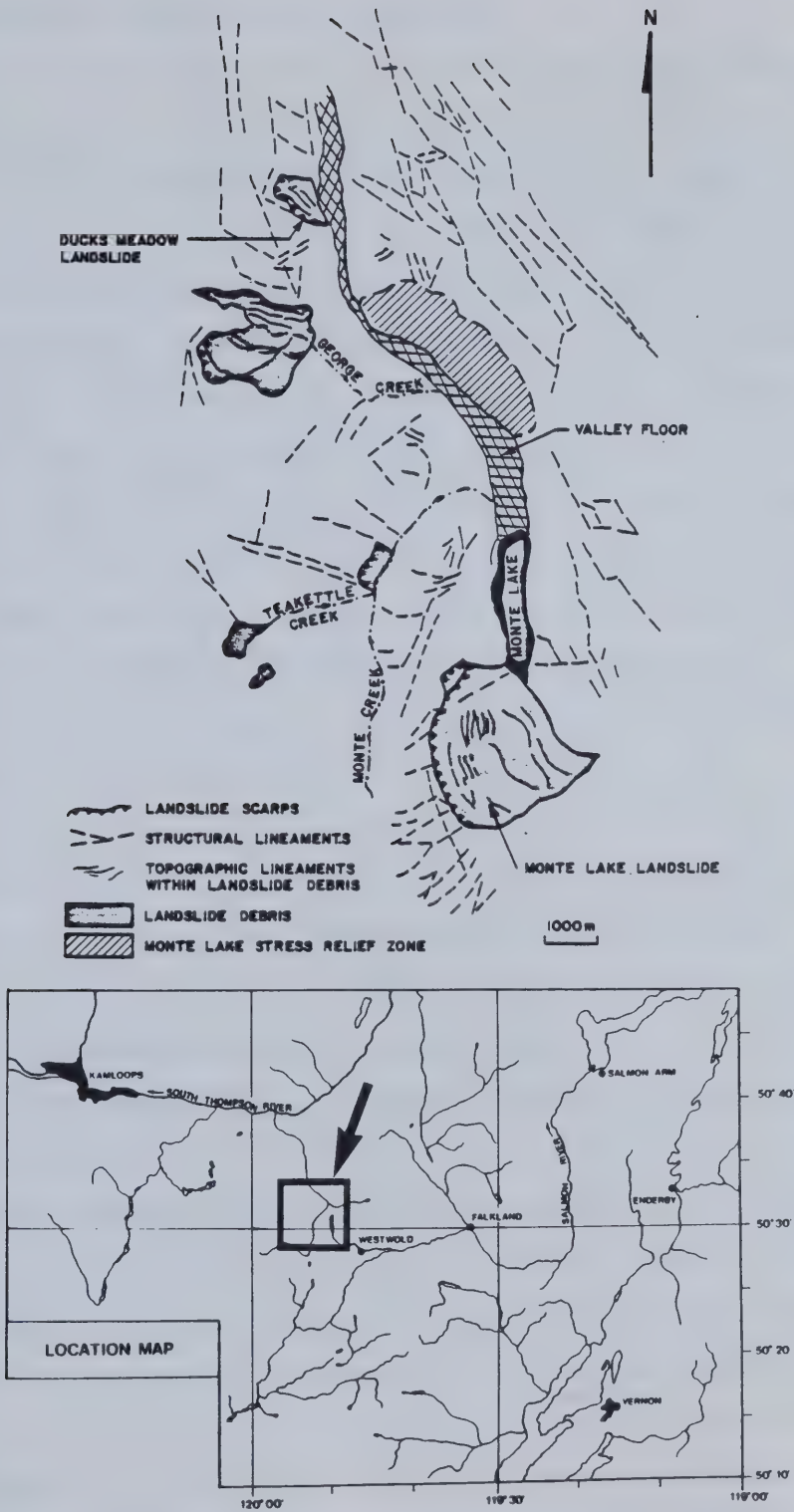
Figure 3.18 Landslides in the Monte Lake – Ducks Meadow Area (Based on B.C. aerial photograph BC 5377–049 exposed September 1, 1976).

3.3.9 Deadman River (Criss Creek to Gorge Creek)

As can be seen in Figure 3.1, only scattered landslides occur in Paleogene rocks west of Kamloops. The exception is the high concentration of large slope movements along both sides of the Deadman River valley between Gorge Creek and Criss Creek (Plates 3.8 and 3.9) which was first reported by Fulton (1975). The valley is a steep–sided trench trending almost due north, which varies in depth from 300 m at Criss Creek to 600 m at Gorge Creek. The stratigraphy and structure of this part of the valley are not completely known, largely because of the burial of exposures by landslide debris, disturbance of exposures by landslide processes and the inaccessibility of undisturbed exposures in the high vertical scarps formed by the slope movements. General observations on the geology of the Deadman Valley were reported by Dawson (1896) and Cockfield (1948) without mentioning the extensive degree of instability in the valley. The writer carried out geological reconnaissance in the valley in the summer of 1980 and data from a shallow diamond drill hole were provided by the British Columbia Ministry of Transportation and Communications.

In analysing the stratigraphical factors which are important in slope movement in the Deadman Valley, several come to light. First, the nature and configuration of the surface developed in Triassic Nicola Group rocks on which the Paleogene rocks rest unconformably; second, the nature of the Paleogene succession itself; and third, the nature of the boundary between the Paleogene rocks and the Neogene succession which overlies it and forms the headwall scarps of the landslides on the north side of Gorge Creek and landslides on the eastern side of the valley. Because of the incomplete knowledge surrounding the complex geological framework in which these movements have taken place, the following is intended as a first approximation only to that framework.

According to Dawson (1896) and Cockfield (1948), the Nicola Group rocks in the valley consist of limestones, altered chlorite–rich flow rocks (greenstones) and volcanic breccias. No data exist on their attitude in the valley, but the surface of the Nicola Group was examined in a road cut near Split Rock (at about 760 m elevation) and in the diamond drill–hole (at 562 m elevation). At both locations it consisted of heavily fractured greenstone fragments set in a creamy white to green fragmental plastic clay. Based on the two locations noted above and the character of the rocks along the river channel between

79
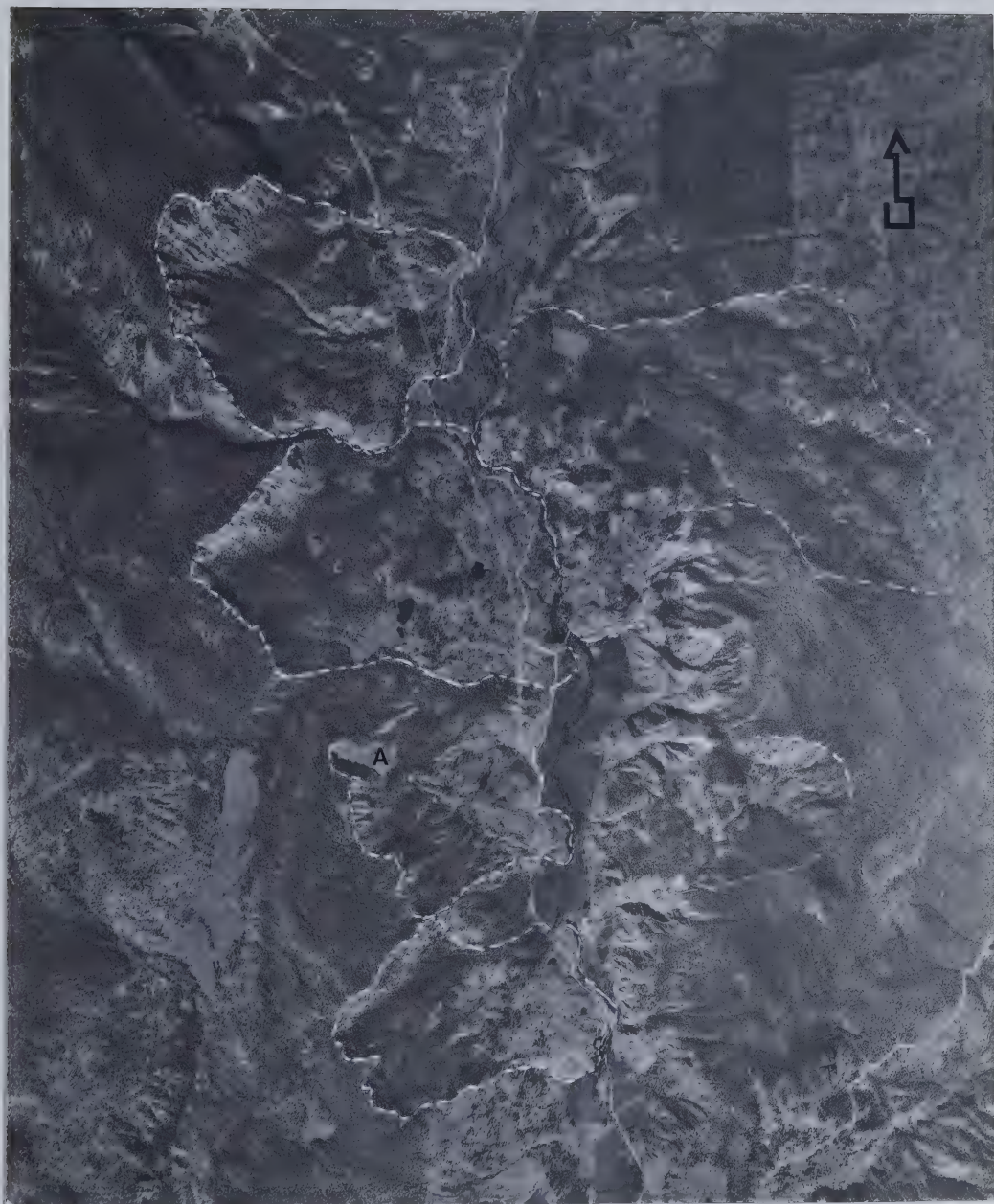
1 km

Plate 3.8 Aerial photograph of landslides in Paleogene rocks in the Deadman River valley between Criss Creek and Gorge Creek (BC air photograph 5742–049 exposed September 1, 1976). A = recent scarp failure photographed in Plate 3.15.
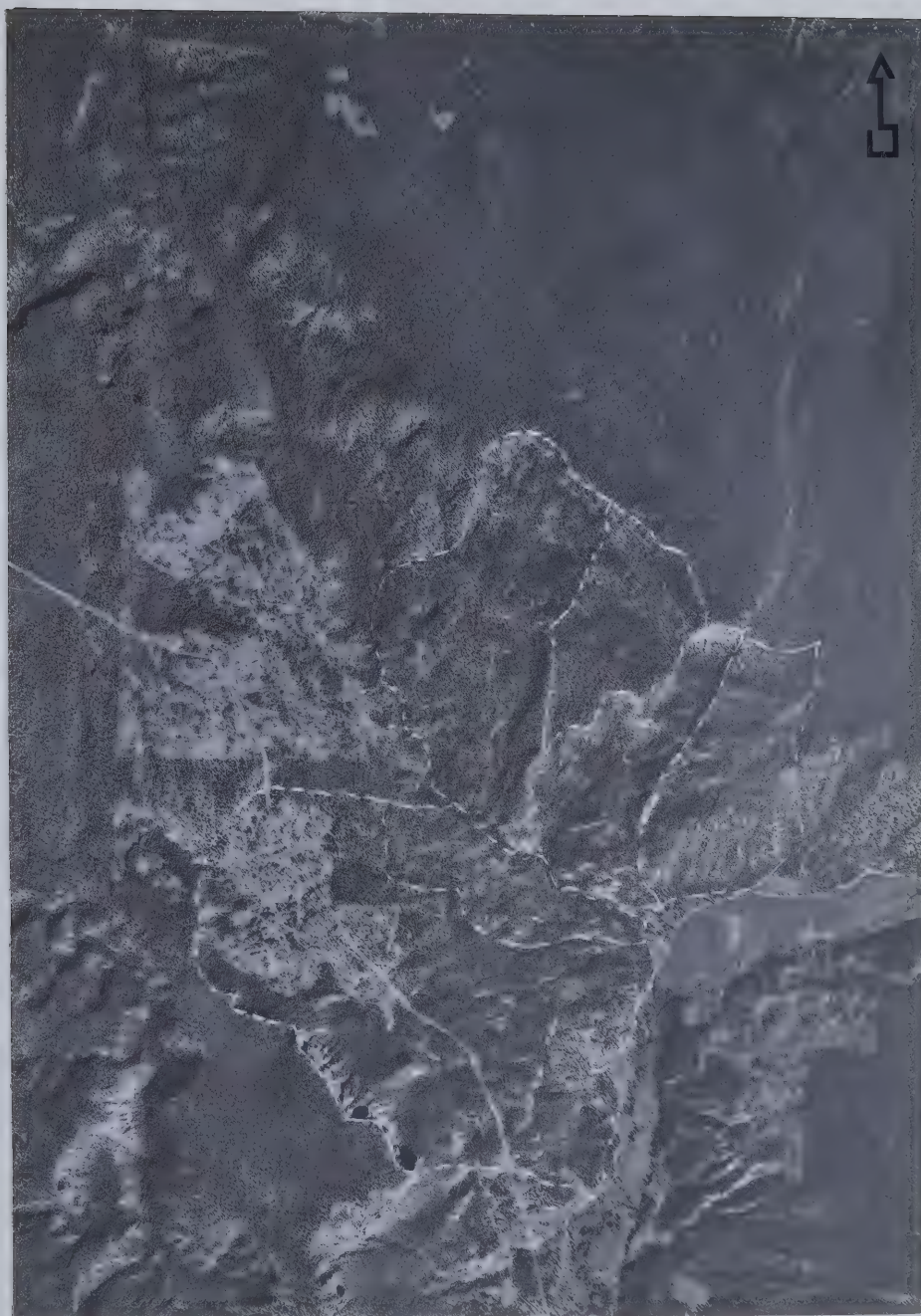
1 km

Plate 3.9 Aerial photograph of landslides in the vicinity of Gorge Creek, Deadman River valley (BC air photograph 5742-0116, exposed September 8, 1976).

them, a rough cross section may be drawn (Fig. 3.19).

Thus the surface of the Nicola Group is irregular and appears to slope into the valley from both sides. The configuration of the surface may be due to pre–Paleogene topography or later faulting.

The Paleogene succession in the Deadman is dominated by silicic volcaniclastic sediments, tuffs and breccias. Flow rocks were observed in the scarps but are subordinate in the succession as a whole. An estimated 640 m of Paleogene rocks are present in slopes on the west side of the valley, of which the upper 300 m are the buff to white, dominantly pyroclastic and volcaniclastic materials exposed in the high scarps between Silverspring Creek and Gorge Creek. All these rock types display prominent vertical jointing which is persistent across stratigraphical units (Plate 3.10). The rocks are susceptible to piping erosion and joint systems exposed on vertical faces are commonly enlarged by this process. Rocks exposed north of Criss Creek on the east side of the valley are unlike the rocks on the west side. No high scarps are formed and their colours, textures and weathering patterns are quite dissimilar (Plate 3.11).

The basal part of the Paleogene was examined near Split Rock and in the vicinity of the diamond drill hole south of Slide 1. Near Split Rock, fossiliferous shales and tuffaceous sandstones were found at an elevation of about 762 m. On an apparently undisturbed slope in the vicinity of the drill hole, stratified black plastic shales and cloddy yellow smectite–rich clays were found 45 m above the Paleogene base. Both these units were observed to have pervasive slickensides throughout. The cloddy, unstratified yellow clay has formed from the alteration (or weathering) of pyroclastic rocks. Fossiliferous shales and pyroclastic rocks were encountered up to an elevation of 714 m where a spring issued from beneath a resistant flow unit. Thus on the basis of these observations, we may suggest that the basal 150 m of the Paleogene succession consists of black plastic shales and pyroclastic rocks which are susceptible to alteration to a cloddy clay. (It may be added that these rocks were not encountered in the drill hole). This alteration appears to be most marked and extensive in seepage areas. At the so–called Bat Clay exposures beneath the spring mentioned above, slopes could only be traversed with extreme difficulty due to their slippery nature (Plate 3.12). Where tuffaceous sediments or pyroclastic rocks are exposed on slopes, a thin soil cover of clay develops and some
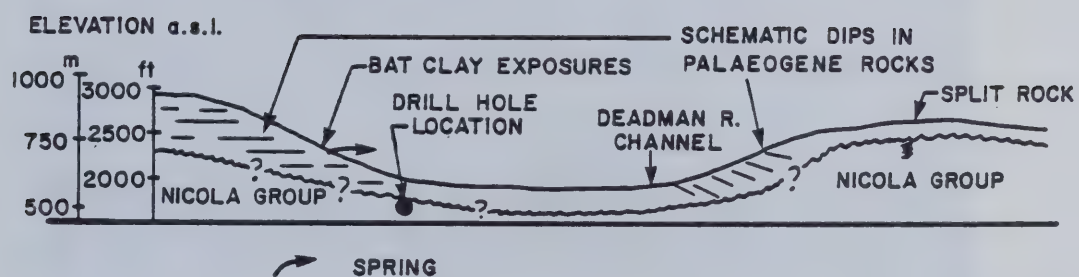
Figure 3.19 Approximate geological cross section from the Split Rock area to the Bat Clay exposures.

Plate 3.10 Pyroclastic/volcaniclastic rocks in typical cliff exposure on west side of Deadman Valley. Partly degraded block in landslide complex #4 visible in foreground.

Plate 3.11 Landslides north of Criss Creek on east side of Deadman River valley

Plate 3.12 Outcrop of weathered pyroclastic rocks at Bat Clay exposures approximately 150 m above the base of the Tertiary.

of the erosional patterns are similar to those found in badlands. Above the regional groundwater table (or perched groundwater tables) the rocks do not appear to experience this loss in strength due to water−induced alteration as evidenced by the fact that they stand up in high vertical cliffs (Plate 3.10). The yellow smectite−rich clay (see Chapter 5) is a distinctive product of the breakdown of landslide debris on slopes on the west side of the valley, and is found in all the landslide debris on the west side of the valley.

North of Gorge Creek the slopes are capped by Neogene plateau lavas which form the headwall scarp of landslides 8 and 9. Beneath the basalt cap, brown varved silts and yellow weathered breccias and tuffs were exposed. Some doubt appears to exist concerning the precise age of these rocks. Field relations are confused due to slope movements. Mathews (1964) reports a K/Ar date from a "pink ash layer" at Gorge Creek as Neogene (10±2 Ma).

On the east side of the valley, the succession is dominated by purple, red and brown coarse volcanic breccias and sedimentary interbeds.

There are eleven major landslide complexes in Paleogene rocks in the Deadman Valley. Their morphology has been mapped from aerial photographs and is seen in Figure 3.20. Three distinctive groups are distinguished, being landslides 1−7 between Clemes Creek and Gorge Creek on the west side of the valley, 8−9 on the north side of Gorge Creek, and 10−11 on the east side of the Deadman River.

According to Varnes (1978), landslides 1−7 are properly described as complex movements since the debris is the product both of multiple slope movement events and multiple modes of movement. Three major stages are envisaged for these movements, based upon an examination of the morphology of the complex. The initial stage is one of block failure whereby large blocks moved out from the slope. The plan geometry of these blocks is believed to be related to discontinuity patterns as discussed in detail below. These initial movements appear to be responsible for the high, steep headwall and lateral scarps. Due to the lack of a high−strength cap (e.g., flow rock) during this movement, the blocks partially disintegrate and continue to move downslope where the material comes to rest. Remnants of partially disintegrated blocks can be seen as high relief ridged areas of landslide debris which form a degraded block front in the landslide complexes (Plate 3.13). A second stage is marked by further degradation of the debris and involves further
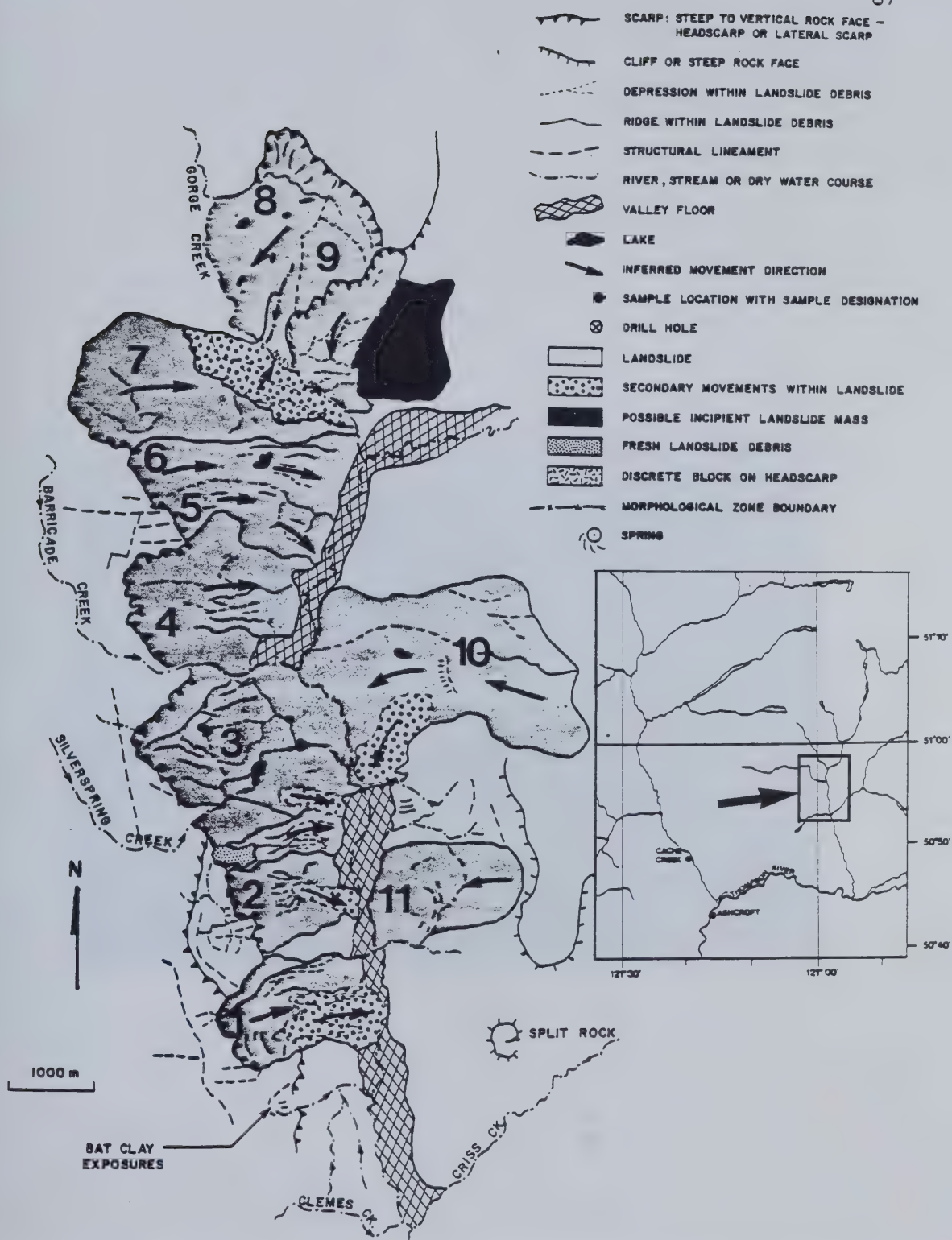
Figure 3.20 Morphology of Landslide in the Deadman River Valley between Criss Creek and Gorge Creek (Based on interpretation of aerial photographs BC 5740-049 and 5742-116).

Plate 3.13 View to the south of landslide on west side of Deadman River valley showing example of degraded block front (A).

breakdown of the initial debris. Largely through the alteration of pyroclastic material contained in the debris in contact with rainfall and seepage, the production of smectite-rich clays leads to localised reduction of shear strength and subsequent re-activation of debris by secondary flowage (Fig. 3.20). Flow movements exhibit longitudinal flow lines, marginal levees and lobe-like termini on many of the complexes (Plate 3.14). The head of these secondary flow failures appears to be related to a seepage zone within the debris at about 760 m , at the base of the degraded block front. Slope angles measured on these flows average $8^\circ-9^\circ$. A third stage which is not necessarily pre-dated by the second stage involves localised headwall scarp failure, best classified as large rockfalls. A fresh example which is described below is noted at the north end of slide 2. A large rockfall-avalanche emanating directly from the scarp is thought to have taken place on complex 4.

The recent scarp failure in complex 2 was examined in the field and traverses were made along and behind the scarp. The rock making up the scarp is a red-brown volcanic breccia with elongate slab-like masses of flow rock which lens out within the breccia. Closely spaced vertical joints are pervasive on the face which was estimated to be 106 m high. Apertures of up to 0.5 m were noted on the face (Plate 3.15) and there is an absence of horizontal discontinuities, although the breccia is crudely layered. As seen in Plate 3.15, the rockfall mass completely disintegrated upon failure, and no large blocks were preserved. The failure occurred at the head of marked, active flow, and appears to be a mechanism for its movement by loading the head of the flow.

Behind the scarp on complex 2, a series of intersecting depressions was noted. Their pattern suggested the outline of blocks which have already undergone some movement (Fig. 3.20) and is probably determined by two sets of discontinuities similar to those thought to be responsible for scarp plan geometry as discussed below.

Landslides north of Gorge Creek have not undergone the same sequence of movement processes, which reflects the different geology of the slope. Initial failure does not appear to have been of the block variety, but degradation of the debris is taking place. Failure on the east side of the valley appears to be the product of a different sequence of processes while again being affected by multiple re-activation or secondary flow failures (Fig. 3.20).

Plate 3.14 Morphology of lobe–like terminus of secondary flow on landslide complex 1, west side of Deadman River valley.
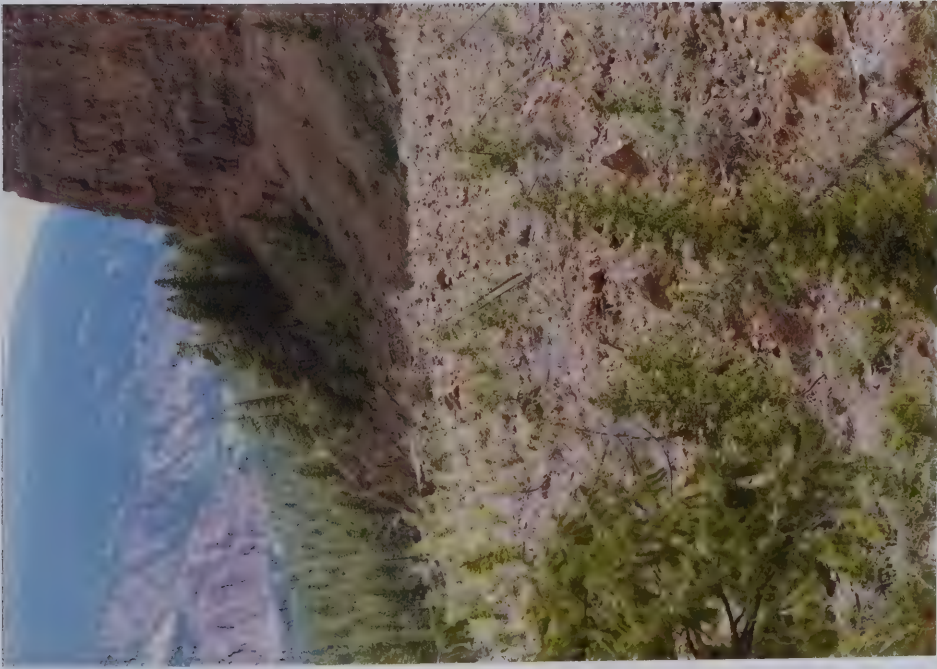
Plate 3.15 Recent scarp failure on landslide complex 2, west side of Deadman River valley.

The effects of stratigraphical and structural factors on the morphology and location of failures were examined with respect to the first group of slides, i.e., 1–7. The trace of the Deadman Valley between its mouth and Gorge Creek is noticeably straight, suggesting some degree of structural control. The orientation of the trend of the valley, neglecting the action of slope movements in pushing the river to the east side of the valley, is about 350°. The geometry of the landslide scarps also reflects some degree of structural control since both headwall and north–lateral scarps are staggered *en echelon* from slide 1 through to slide 7 (Fig. 3.20). The orientations of the headwall scarps vary in a narrow range from 330° to 338°. Similarly the north lateral scarps are oriented between 045° and 065°, almost at right angles to the headwall scarps. This suggests an initial block movement in a north–easterly direction (i.e., between 045° and 065°), controlled by a regional set of discontinuities, along a basal shear surface. However, once free of the constraining effects of the block walls, or due to block disintegration, the material involved in the movement shifted in movement direction towards 090°. This indicates the effect of the configuration of the valley side slope beneath the failure plane, i.e., the role of the plane of separation (Varnes, 1978).

The location and characteristics of the basal shear surface in the landslides is not known, since nowhere is it exposed. In the absence of a sub–surface investigation, however, it is possible to infer the location of the surface and to hypothesize on its nature.

An effort was made to locate the foot line (Varnes, 1958) of the failures by a re–construction of pre–failure contours and by locating the point where debris emerges from the scar and turns. This exercise indicates that the initial basal falure plane was located in the interval between the elevations of 600 m and 700 m. This interval is close to the elevation of the seepage line noted above and within 120 m of the estimated base of the Paleogene. Two hypotheses arise from these observations, regarding the nature of the basal shear zone:

(a) That basal failure could have taken place in smectite–rich units within the basal 120 m of the sequence. This could have been produced by the alteration of pyroclastic material by reaction with groundwater within the slope to form a diagenetic assemblage zone (cf. Walton, 1975) independent of stratigraphy, or could have been localised within a stratigraphic interval.

(b) That basal failure could have taken place along the altered sub–Paleogene unconformity which may have daylighted above the valley floor but which is now covered by slide debris.

However, since the estimate of the position of the sub–Paleogene unconformity puts it about 182 m below the inferred foot line, and very few fragments of Nicola Group rocks are found in debris, it is thought that hypothesis (a) is a more likely one, although neither is verifiable on the basis of present exposures.

3.4 Detailed Description of Landslide Sites in Neogene Volcanic Successions

Large landslides in the Neogene rocks of the Interior Plateau were examined at four localities. Reconnaissance work was conducted at Chasm Creek in 1979 and 1980. In 1980, sites in the Upper Deadman River, Leon Creek and the Chilcotin area were examined. These areas are located in Figures 3.1 and 3.2.

3.4.1 Deadman River (Mowitch Lake – Vidette Lake

The valley sides of the Deadman River between Mowitch Lake and Vidette Lake constitute a major, almost continuous, zone of landsliding. Weak volcaniclastic sediments of the Deadman River Formation underlying flow units of plateau basalt have been subject to failure, resulting in block–type failures. Landsliding has resulted in the formation of several landslide–dammed lakes (Plate 3.16).

The sediments of the Deadman River Formation are buff to yellowish, occurring as a horizontally bedded series of tuffs, breccias, siltstones and pebbly sandstones and conglomerates which are generally poorly indurated. The depth of the valley varies between 245 m and 305 m and at the type section of the Deadman River Formation at Snohoosh Lake, described by Campbell and Tipper (1971), there is at least 130 m exposed, although this section is in landslide debris. However, as Campbell and Tipper (1971) point out, the deposition of the formation took place on an irregular surface in which deep valleys were cut, and its thickness may vary from a few centimetres to 150 m throughout the Bonaparte Lake area. Variation noted in the retrogressivity of the landslide complexes may reflect this variation in the thickness of the Deadman River Formation. It is noted that landslides are absent in those parts of the valley where, according to Campbell and Tipper (1971), the plateau lavas directly overlie the Nicola Group. This observation
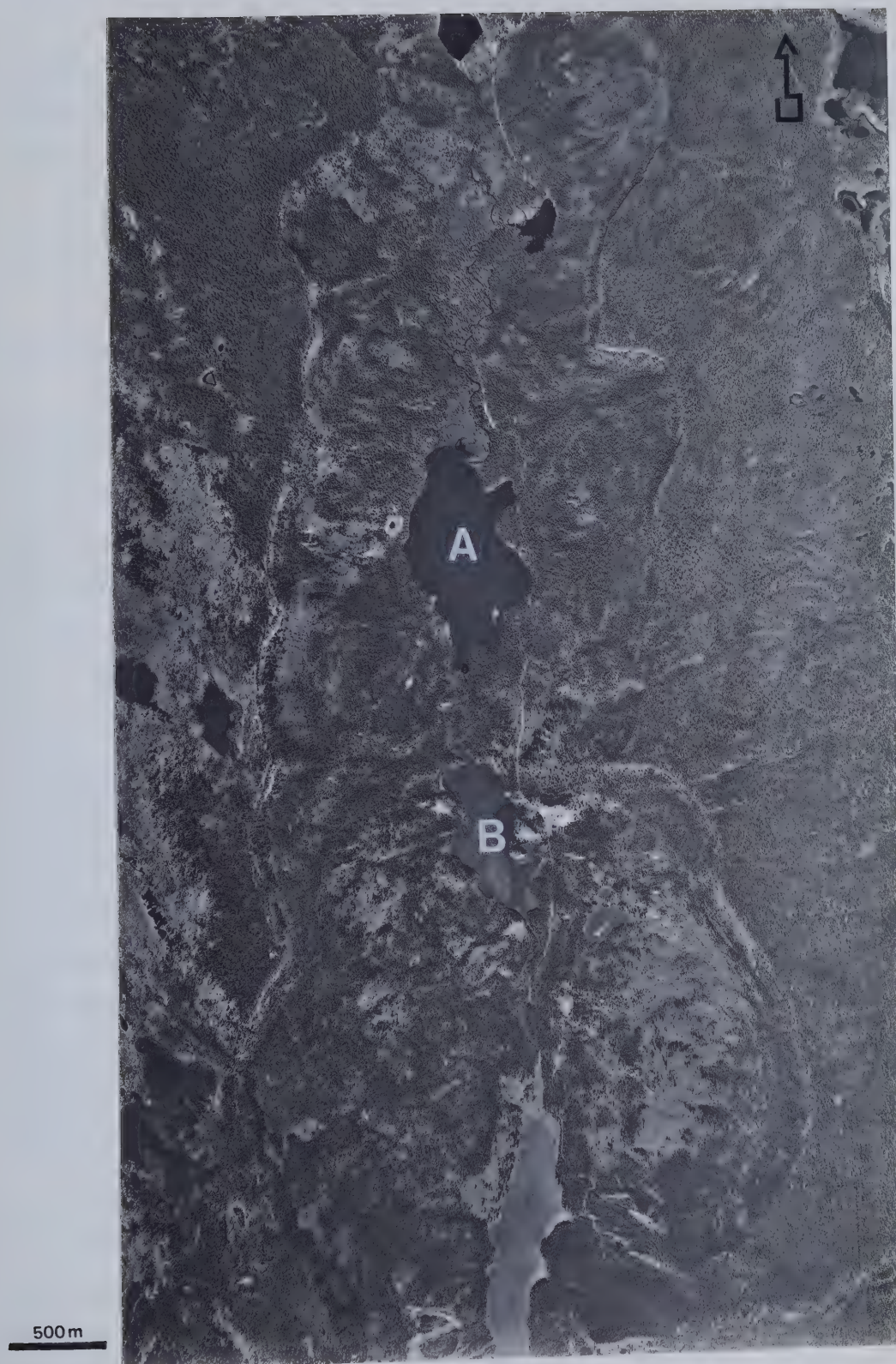
Plate 3.16 Air photograph of landslides in Neogene rocks in the vicinity of Skookum Lake, Deadman River (BC Air Photograph BC 5187-004 exposed May 18, 1966). A=Deadman Lake, B=Skookum Lake.

strongly suggests that the sub-Neogene unconformity is not the location of the basal

failure zone. Re-activation has taken place at several locations in the debris, particularly

downstream of the highest landslide dam at the outlet of Snohoosh Lake.

Glacial meltwater may have contributed to the development of slope geometry in

this straight, steep-sided valley.

3.4.2 Chasm Creek

Three landslide complexes of the block type were identified along Chasm Creek,

southeast of Clinton (Fig. 3.1, Plate 3.17). The valley of Chasm Creek is a steep-walled

notch-like valley cut into the Fraser Plateau and is about 290 m deep. Aspects of its

geometry may be the result of the passage of glacial meltwater through the valley during

deglaciation, but the very marked knick-point at the head of the Chasm also suggests that

its origin may be simply related to headward erosion by Chasm Creek.

The geological circumstances of these landslides are similar to those described

above in the upper Deadman River wherein basalt flow units and interflow breccias overlie

the relatively weak rock of the Deadman River Formation (Campbell and Tipper, 1971)

(Fig. 3.21). Dips measured along the rims of the valley indicate that the plateau lavas are

not horizontal but dip at about $330^0/3^0$. Exposures in the Deadman River were examined

north of the junction between Chasm Creek and the Bonaparte River. A thick deposit of

buff-coloured, weakly stratified breccia appears to underlie tuffs and volcaniclastic

sediments. Campbell and Tipper (1971) suggest that the breccia is a fan deposit, about

90 m in thickness. Although the configuration and extent of the Deadman River sediments

in the vicinity of Chasm Creek are uncertain, they do appear to underlie the landslide sites

where the total thickness can only be estimated.

The geometry of the landslide scarps (Fig. 3.22) appears to be controlled by closely

spaced vertical cooling and stress relief joints. There is a marked lack of preferred

orientation in the few lineaments observed on aerial photographs. Thus there is an

absence of control by major regional discontinuity patterns which was seen to be

important in the Paleogene landslides. This arises from the fact that the Neogene

successions are structurally undisturbed.
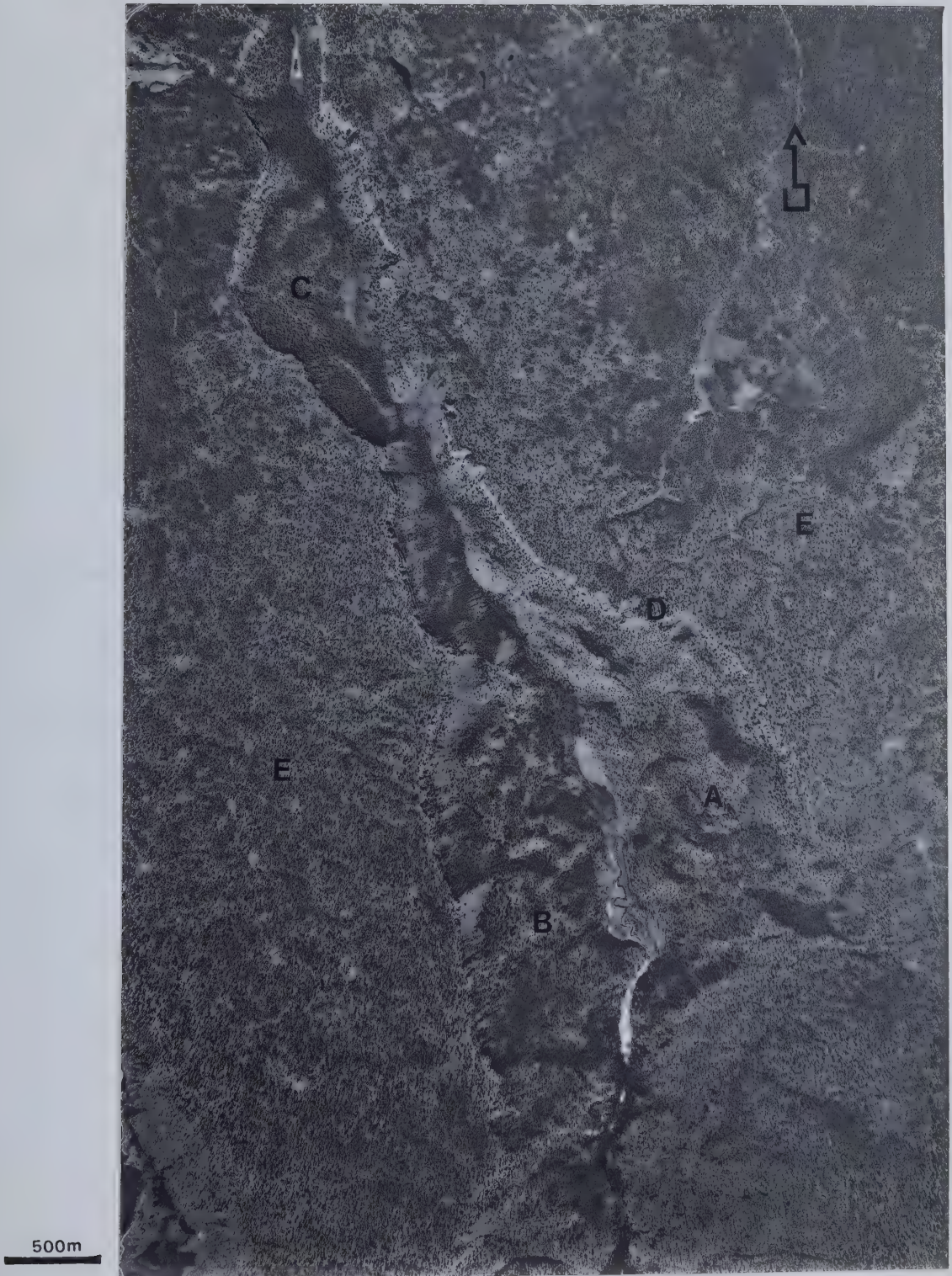
Plate 3.17 Air Photograph of landslides at Chasm Creek (BC air photograph BC 5255-183 exposed July 10, 1967). A = Chasm East; B = Chasm West; C = Chasm North; D = Block currently undergoing movement; E = Fraser Plateau surface.
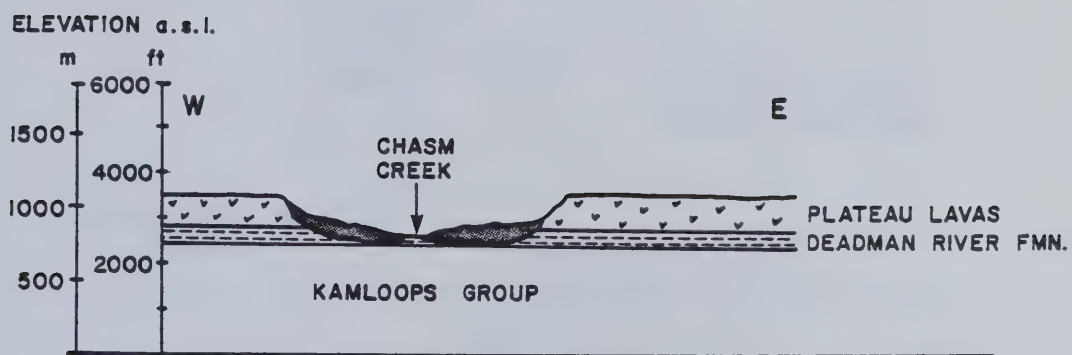
Figure 3.21 Geological cross section of Chasm Creek landslides. Geology after Campbell and Tipper, 1971. Drawn with no vertical exaggeration.
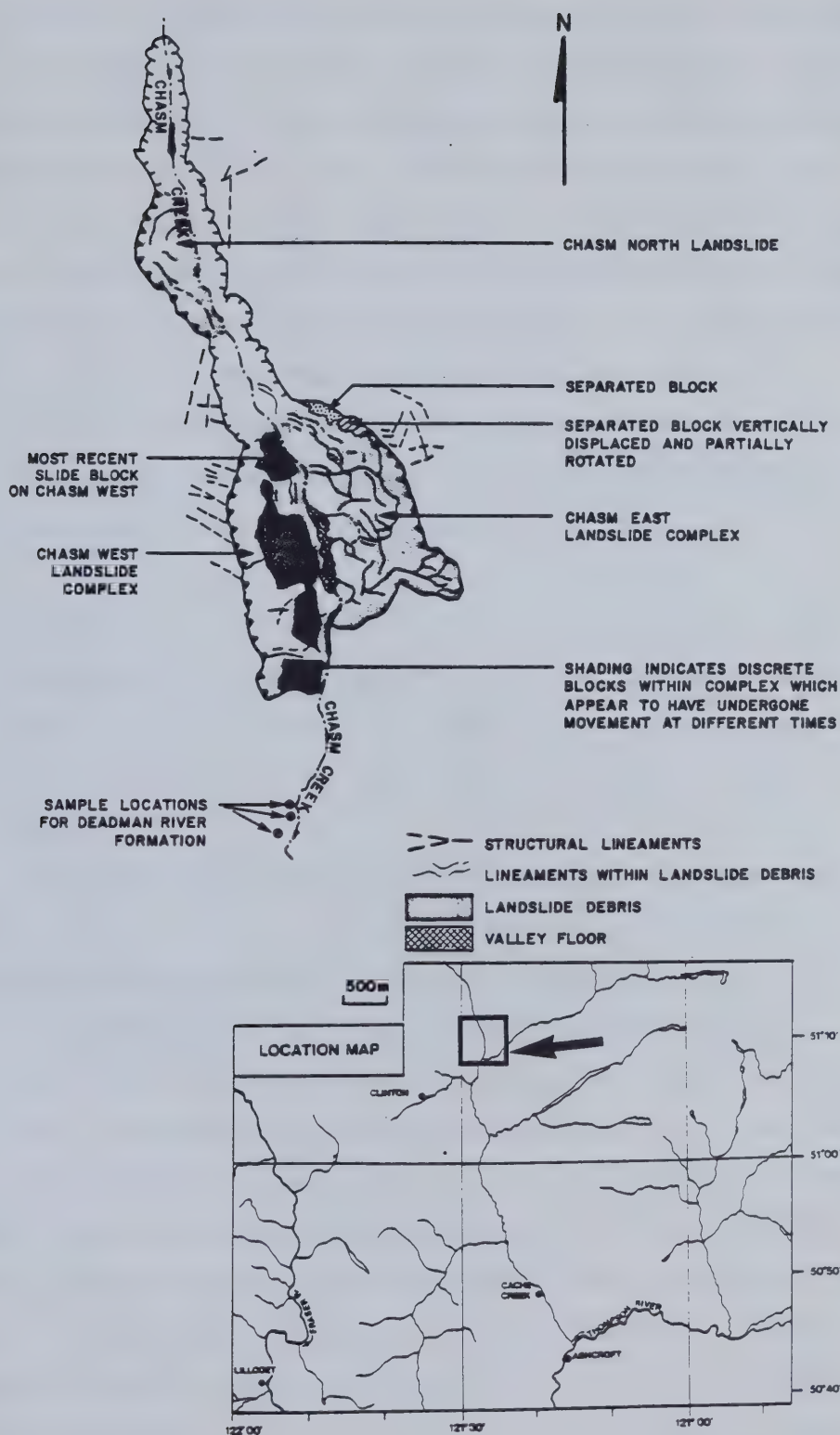
Figure 3.22 Morphology of Chasm Creek landslides (Based on interpretation of B.C. air photograph BC 5255–183).

Each site of instability is the product of multiple failure events. This is best illustrated in the Chasm West complex where each block is well defined. The difference in the apparent freshness of the blocks gives the impression that the most recent block to move is at the north end of the complex. At the north end of Chasm East, block movement is currently taking place. Slight rotation is accompanying extension cracking, and trees on the rotated surface are tilted from the vertical (Plate 3.18). This movement is not taking place in response to basal erosion since Chasm Creek at this point is flowing underground; some other mechanism is thus responsible for movement.

The blocks in the debris are well defined with some exhibiting a well-developed graben behind a debris crest ridge and steep fronted slope (Plates 3.19, 3.20). It is also noted that movement is taking place across the dip.

3.4.3 Leon Creek

The landslides on eastern slopes of the Camelsfoot Range (Plate 3.21) in the vicinity of Leon Creek were first reported by Ryder (1976). They occur in an outlier of Neogene rocks on the west side of the Fraser River at 820 m above sea level. They were inspected in the summer of 1980.

The geology of the area has been described by Dawson (1896) and Trettin (1961). At the landslide sites, basalt flows of the plateau lavas are horizontal and overlie sediments. The basal Neogene unconformity of unknown configuration is developed in rocks of the Spencer Bridge Group, Cache Creek Group and Mt. Lytton Batholith (Fig. 3.22).

Dawson (1896) described a soft yellowish pebbly sandstone which he found in "some places". This led him to suggest that it was locally developed. Later, Trettin (1961) found poorly consolidated sediments in the same area and he included the yellowish sandstone, argillitic sandstone, arenites and conglomerates which contained shaley beds. Trettin reported them to be exposed at an elevation of 1070 m and suggested that less than 30 m of sediments are exposed. Excavations associated with logging road construction (Plate 3.22) have exposed sediments along the base of the landslide areas at an approximate elevation of 1070 m. An inspection of these exposures indicates that failure has taken place in the upper part of these sediments which are overlain by approximately 150 m of plateau lavas. Seepage was also noted at this horizon.

Plate 3.18 Evidence of movement on north block of Chasm East landslide. Note trees out of vertical and slight backward rotation on block surface.

Plate 3.19 View north of Chasm East landslide. Note debris-crest ridge and graben behind it. NB = North block (see Fig. 3.22). Vertical jointing in plateau lava seen in foreground.

Plate 3.20 View to southwest of Chasm West landslide. Note block boundaries and ridges in debris.
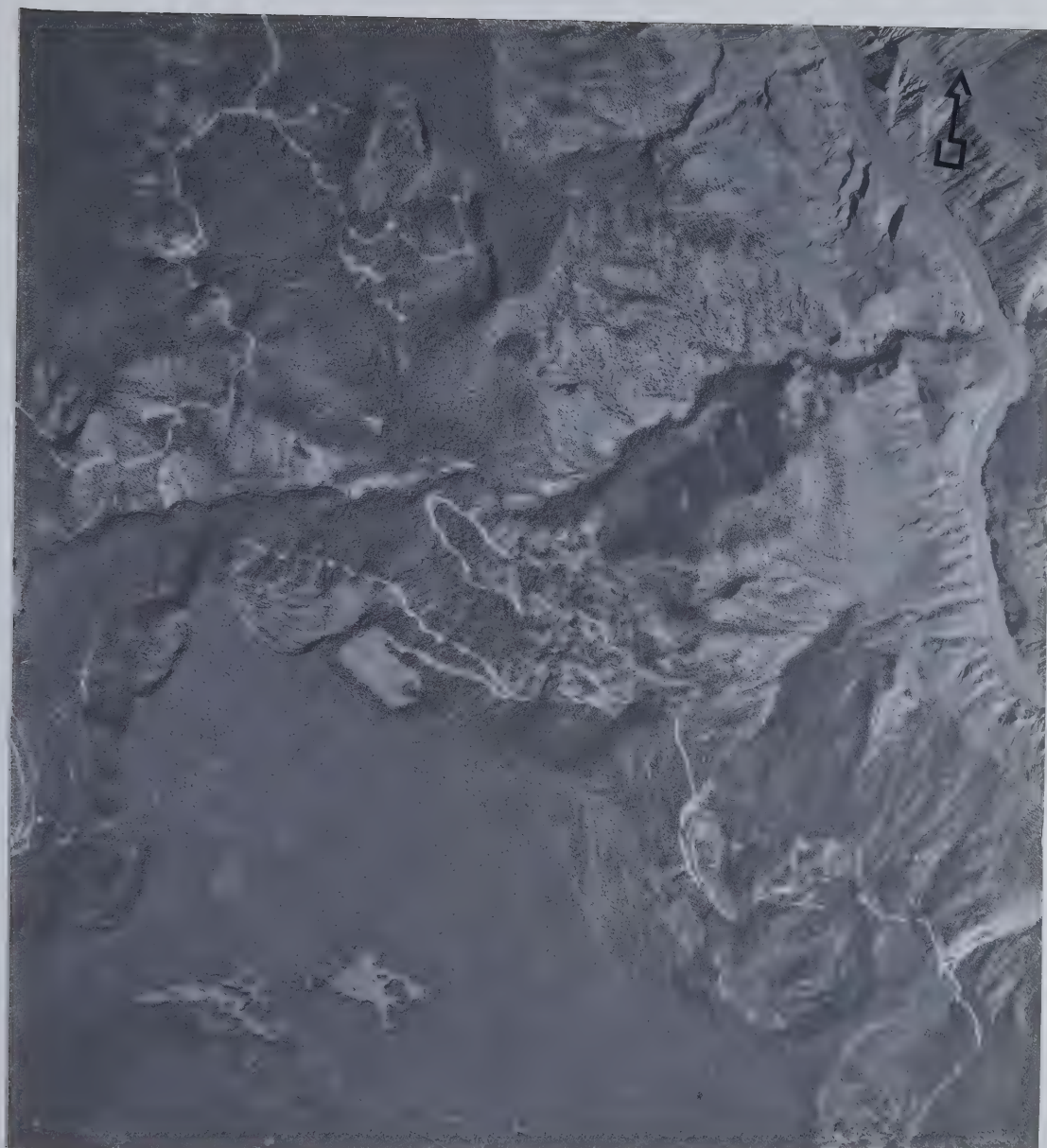
1 km

Plate 3.21 Air photograph of Leon Creek landslides on eastern margin of Camelsfoot
Range (B.C. Air Photograph BC 5742-98 exposed September 8, 1976).
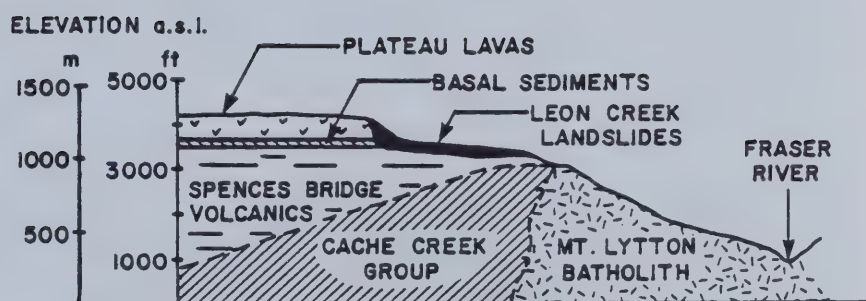
Figure 3.23 Geological cross section of Leon Creek landslides. Geology after Trettin (1961). Drawn with no vertical exaggeration.
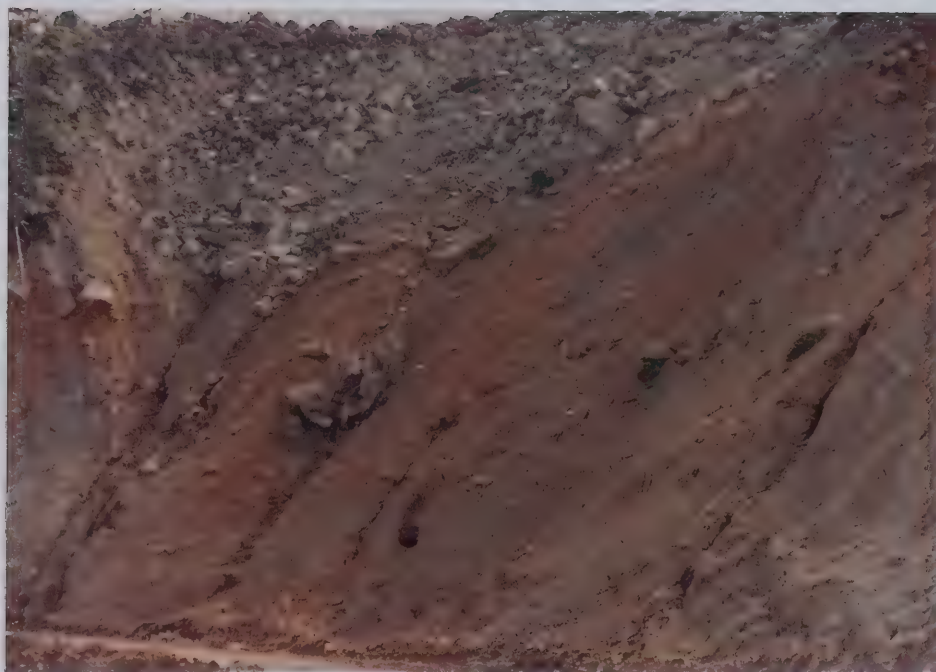
Plate 3.22 Basal shear zone of Leon Creek landslides exposed in logging road cut. Figure is standing at level of yellow tuffaceous sandstone. Note seepage from base of landslide debris.

The landslides exhibit intact blocks in some cases, but generally the blocks have broken up to form debris that resembles a boulder field in which boundaries between former slide blocks remain discernible. The scars of individual slides are arcuate in plan (Fig. 3.24). This may be due to very close joint spacing. Tension cracking behind existing scarps and along unfailed slopes suggests that failure is continuing, i.e., active block separation and supply is taking place at present.

3.4.4 Landslides in the Chilcotin Area

A reconnaissance study of slopes developed in Neogene rocks along the Chilcotin River was undertaken in the summer of 1980. Aerial photographs were examined covering a broad band between Puntzi Lake and Alkali Lake (Fig. 3.2). Landslide sites were identified and a number were inspected in the field.

Only very general bedrock geology maps exist of the Taseko Lakes and Quesnel map-sheets (Tipper, 1959, 1963), and no landslides are marked on the surficial geology maps (Tipper, 1971a, 1971b). Heginbottom (1972) has, however, mapped landslides in Neogene rocks on the Taseko Lakes map-sheet. The stratigraphical framework of slopes in the area is similar to those in other areas examined in Neogene successions, viz. plateau lavas consisting of multiple basalt flow units overlying mechanically weaker sediments and pyroclastics. It is thought that the scattered distribution of failures evident in Figure 3.2 reflects the local accumulation of these weaker strata beneath the lava cap. Aspects of the microstructure of the weaker strata, and shear zones developed in them are discussed in Chapter 5.

The geomorphological conditions for failure, however, whilst being similar to other areas along narrow, steep-sided tributaries of the Chilcotin and the Fraser (at Big Creek, Doc English Gulch, Sword Creek and near Alkali Lake), appear different along the main valley of the Chilcotin River. These landslides have occurred in slopes that are not subject to basal erosion but are buttressed at their toes by benches of glacio-lacustrine deposits. At the Redstone landslide, for example, a shear zone was found exposed in a new road cut high above the valley floor and debris was found deposited on the surface of a glacio-lacustrine bench (Fig. 3.25). Heavy seepage in the road cut suggests that pore pressures were important in determining failure, and that basal erosion was not operative
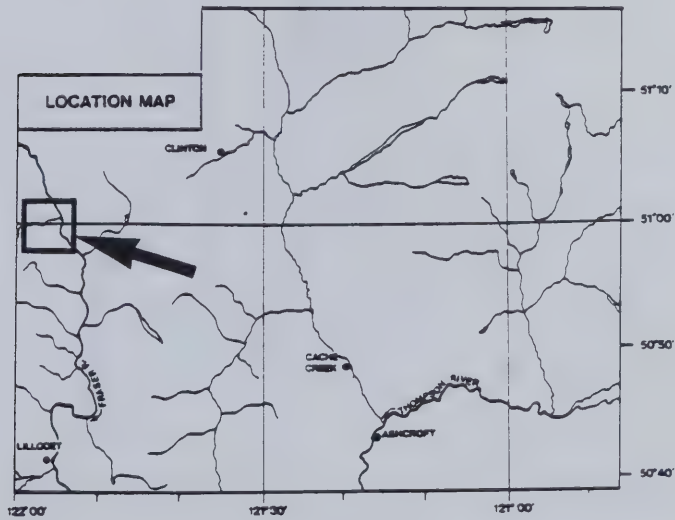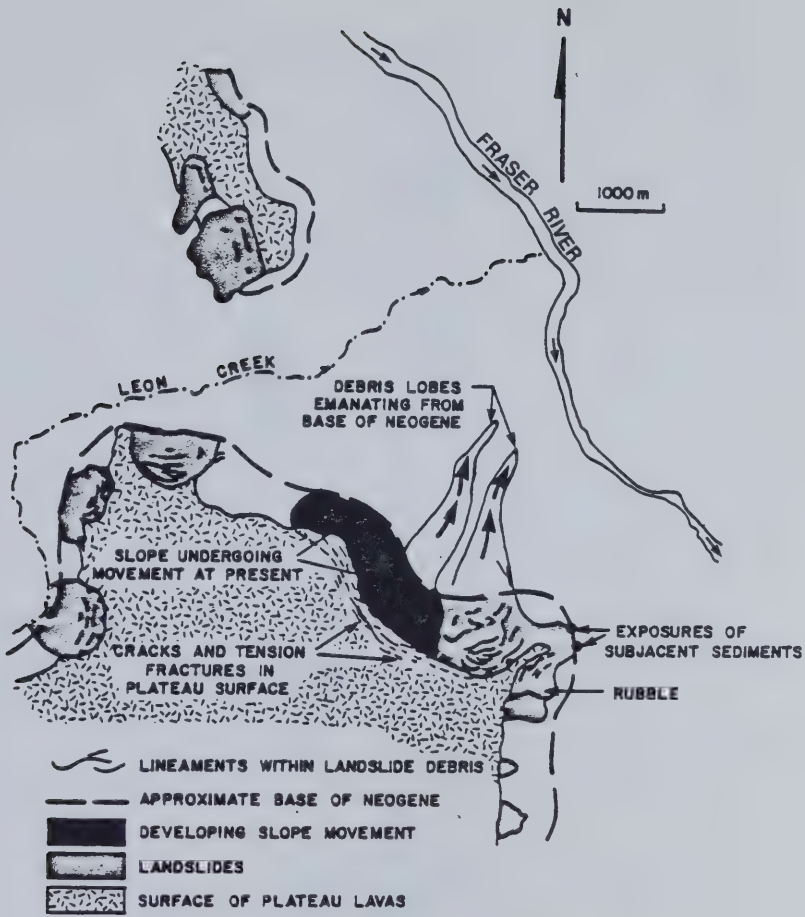
Figure 3.24 Morphology of Leon Creek landslides (Based on interpretation of B.C. air photograph BC 5742-98).
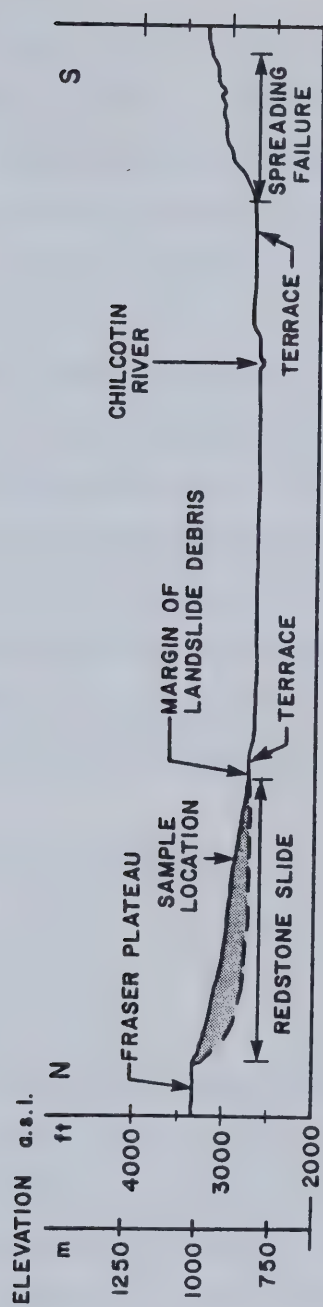
Figure 3.25 Cross section of Chilcotin River valley at Redstone landslide site. Drawn with no vertical exaggeration.

as a contributing factor. A further example is the Anahim's Flat landslide, a cross section of which is seen in Fig. 3.26.

An alternative mechanism of movement could be that of local spreading in response to cap loading. An example of what is interpreted to be a partially developed spreading movement is seen opposite the Redstone landslide (Plate 3.23). Two linear, steep-sided depressions are seen, indicative of vertical and horizontal deformation, and toe bulging is evident. Lateral shear planes are absent, or at least are not obvious on the aerial photograph.

The morphology of most of the landslides indicates that they are block-complexes. In most cases slide blocks are preserved in interlocking ridges, but in other cases the cap has disintegrated to give a deposit similar in morphology to that of block fields. Because of the disintegrated cap, some features are difficult to identify with certainty on aerial photographs, as discussed at the beginning of this chapter. Secondary failures do not seem to be important. Transverse ridges are common in both types of block failures. The absence of structural control is again made evident by the presence of arcuate scars and the absence of lineaments behind the scarps.

3.5 Relationships between Geological Factors and Regional Patterns of Landslide Occurrence

3.5.1 Geomorphological Factors

The majority of landslides examined, both in the Paleogene and Neogene successions, occur on slopes which have been oversteepened by river erosion (meander belt and/or knick-point migration) or by the action of glacial meltwater. The precise role of glacial meltwater in modifying slope geometry during de-glaciation is complex and unknown in detail. It is sufficient to note that most valleys in the Interior Plateau have, at some time during the complex events associated with de-glaciation, acted as conduits for glacial meltwater, so the association may be spurious. The erosion has also resulted in the exposure of mechanically weak pyroclastic and volcaniclastic rocks at the base of slopes where they are present.
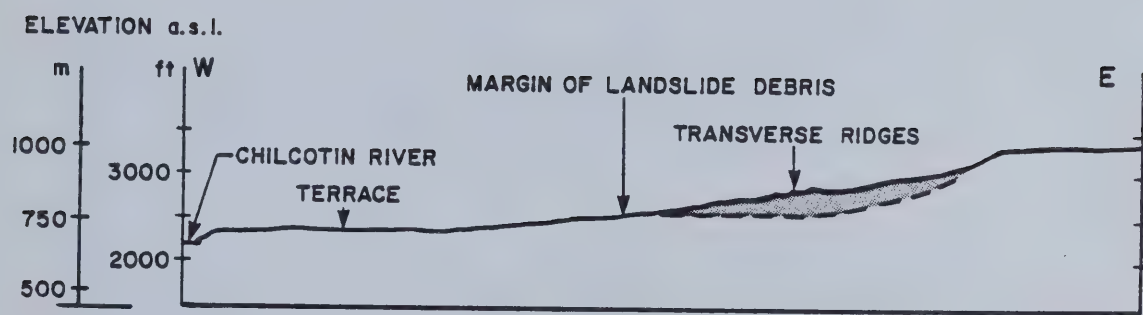
Figure 3.26 Cross section of Anahim's Flat landslide. Drawn with no vertical exaggeration.
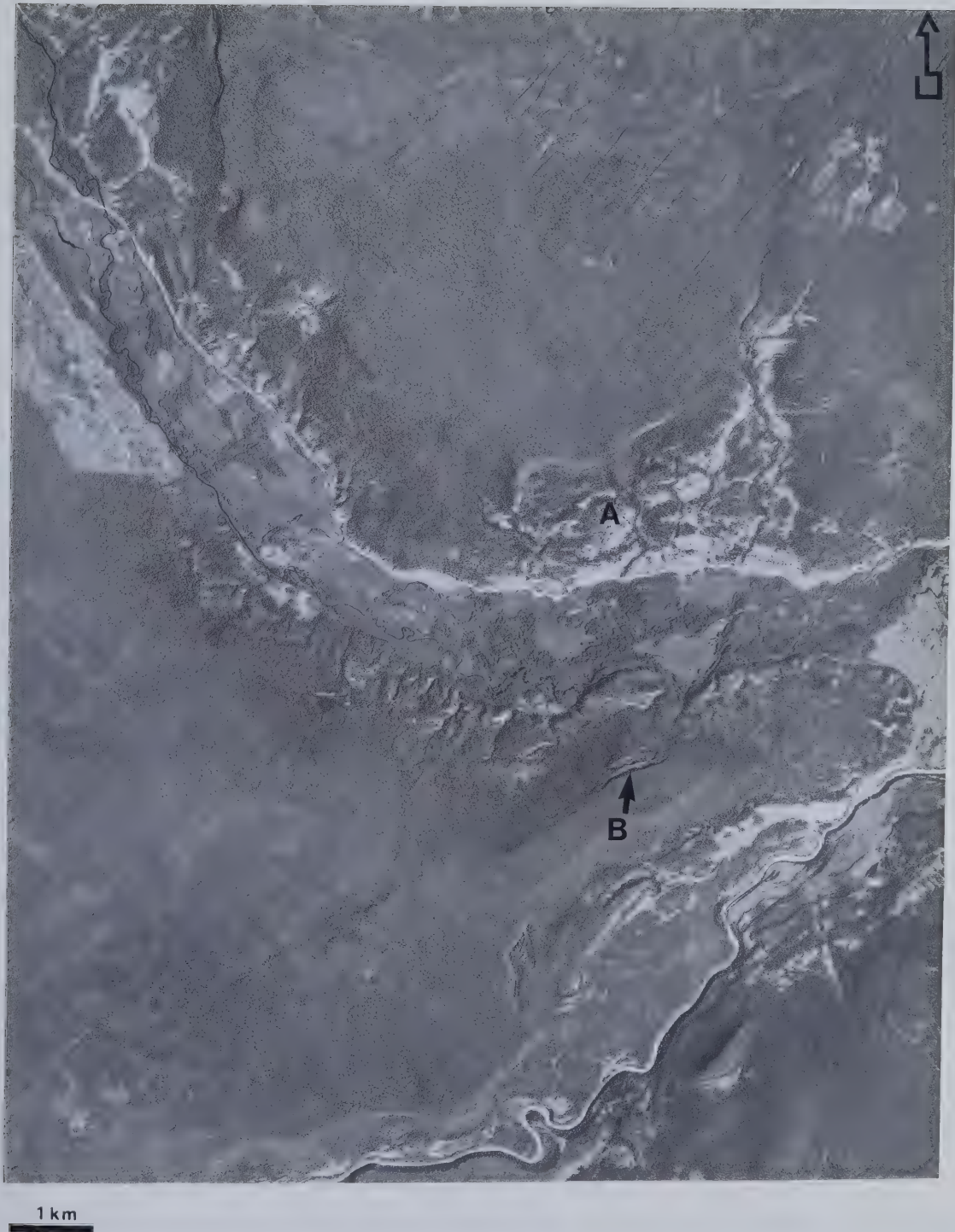
Plate 3.23 Air Photograph of Redstone area, Chilcotin River valley. Note Redstone landslide (A) and spreading movement (B). Other landslides are also marked. (Canada Air Photograph A22415-158).

The location of the basal rupture surface, however, does not always seem to coincide with the slope toe, i.e., the point of erosion or maximum oversteepening, even along valleys identified as oversteepened meltwater channels. This was apparent at Enderby, Deadman River (Criss Creek to Gorge Creek) and in Neogene rocks along the Chilcotin River. In other cases oversteepening does not seem to have been important at any time in slope development (e.g., Buse Hill and Pemberton Hill). In these circumstances a delay between the formation of the slope and movement is inferred, and slope geometry modification may not be considered a factor in landslide occurrence.

The location of the basal rupture surface in relation to the slope toe may also be important in determining the extent of fragmentation experienced by the moving mass. On steep slopes where the basal failure zone is located some way up the slope, the initial block movement moves out and then down, fragmenting in its travel along the plane of separation (cf. Harp *et al.*, 1981). This factor must therefore be considered in addition to stratigraphy and lithology when considering cap behaviour.

The preservation of well-defined blocks in the landslide may also result from topographic constraints on the distance moved by the failing mass. For example, landslides along narrow valleys (e.g., Gorge Creek) show well-defined blocks because travel is impeded by the opposite valley side. In a wider valley (e.g., Pemberton Hill), travel distance is unlimited and thus fragmentation takes place.

3.5.2 Stratigraphical Factors

Not all slopes of similar geometry have been subject to movement. Landslides are found to be localised where mechanically weak layers underlie a competent cap. In all of the landslides examined, in both the Paleogene and Neogene successions, with the exception of the Pemberton Hill complex, the basal part of the rupture zone is located in the sedimentary-pyroclastic assemblage in basal parts of the volcanic succession at a given site. This is based on field examination and the inspection of available geological maps. In certain cases (e.g., Deadman River) a possibility exists that the basal rupture zone was located in the weathered or altered sub-Tertiary surface. However, the surface was only observed in a heavily altered state at one location, and in slopes in which lava flows overlie pre-Tertiary rocks directly, i.e., where the basal sedimentary assemblage is absent,

large landslides do not occur. Landslide shear zones in basal sedimentary–pyroclastic assemblages were noted in the Salmon River (described in detail in the next chapter), Buse Hill, Deadman River, Ducks Meadow, Redstone and Bull Canyon.

Where the basal sedimentary–pyroclastic assemblage is not exposed in high steep slopes, landslides are absent.

Stratigraphical factors are also important in determining the type of landslide occurring at a given site. Complexity in the range of movement events and types appears to be a function of the extent to which the initial failure volume is made up of easily weathered material. For example, slopes involving block movements are made up of dominantly lava flow units with a relatively small thickness of weaker material at its base. This is contrasted with the multiplicity of events which have resulted in a degrading block failure complex where the original slope was mainly made up of volcaniclastic and/or sedimentary material (e.g., Deadman River).

3.5.3 Structural Factors

As noted in Chapter 2, the Paleogene rocks of south central British Columbia have been extensively faulted and slightly folded, whilst the Neogene rocks have been subject to mild warping only and the effect of regional tectonic processes is absent, at least in the study area.

The effect of structural factors is seen with respect to:

(a) *Scarp Plan Geometry*

Structural control on the plan geometry of scarps in Paleogene rocks was well illustrated at a number of landslide sites (e.g., Ducks Meadow, Deadman River and Enderby) where the scarp consists of several linear segments giving rise to a marked headwall and lateral scarps. Based on the interpretation of lineaments on aerial photographs, this was thought to be a result of the existence of persistent systematic discontinuities which may be faults or steeply dipping joint sets that parallel them. In contrast, the plan geometry of Neogene scarps is curved with intersecting linear segments absent. At Leon Creek (Plate 3.2.1), for example, extension fractures above the existing scarp are markedly curved, indicating the absence of persistent systematic discontinuity patterns. This inferred structural homogeneity possibly reflects the random disposition of cooling joints.

(b) *Block Shape and Size*

The existence of regional discontinuity systems arising from tectonic processes in the Paleogene succession gives rise to well-defined large blocks being involved in initial movements. In the Neogene the average block size is very much smaller, and they are more irregular in shape because of the dominance of impersistent, non-systematic cooling joints.

(c) *Direction of Initial Movement*

In the absence of regional discontinuity patterns in the Neogene successions, there is no control on the initial movement direction apart from the slope of the failing slope. However, in Paleogene rocks the orientation of release sets of discontinuities determines the direction of initial movement of landslide blocks. When the blocks begin to move, they are initially contained by the discontinuity sets which correspond to the lateral scarps.

(d) *Faulting Effects in Localising Failures*

In the faulted Paleogene succession, failures end abruptly against faults because of the faulting out of the weak materials at the base of the slope. In addition some Paleogene landslides are contiguous block movements because of the effect of faulting in repeating the weak layer at the base of a slope. Neogene landslides are determined only by the geometry and extent of the basal assemblage.

(e) *Presence of Tectonic Shears*

As discussed in Chapter 4, some weak layers have been further weakened by shear zones developed as a result of tectonic processes. Although tectonic shear zones are not expected to be found in Neogene rocks similar structures due to stress-relief may be present.

3.5.4 Groundwater and Seismicity

(a) *Groundwater:*

The role of groundwater in the occurrence of landslides in the volcanic successions studied cannot be accurately estimated. This is primarily because the present climatic and hydrologic regimes in the area may not reflect those extant at the time of slope movement. The climate of the study areas is dry to semi-arid due to their location in the rain-shadow of the Coast Ranges. Climatic data are given in Table 3.2.

	MEAN TOTAL PRECIPITATION (mm.)	MEAN DAILY AVERAGE TEMP. (°C)	MEAN DAILY MIN. TEMP. (°C)	MEAN DAILY MAX. TEMP. (°C)
THOMPSON				
KAMLOOPS AIRPORT	260.6	8.4	2.4	14.33
FALKLAND	424.4	6.9	0.5	13.33
WESTWOLD	315.7	5.9	-1.0	12.77
ASHCROFT	212.6	8.6	2.5	14.70
CHILCOTIN				
ALEXIS CREEK	418.8	0.3	-7.4	8.00

Table 3.2 Climatic summaries for locations within the study areas. (supplied by the B.C. Ministry of Agriculture.)

Seepage horizons appear to correspond to the footline of some landslides (e.g., Deadman River) and seem to be important in determining the location of some secondary flows (e.g., Bouleau Lake). Further, the role of groundwater systems in developing water pressures and contributing to the formation of diagenetic assemblage zones in the slopes studied has not been evaluated.

(b) *Seismicity:*

Seismic triggers have been important in causing large slope movements in the North American Cordillera (e.g., Hadley, 1978; Mathews and McTaggart, 1978; Mathews, 1979) and seismic forces are also important in causing accelerated pre-landslide movements in a slope.

Data on earthquakes that were felt in the study areas (i.e., with a Mercalli Intensity > II) between 1899 and 1977 inclusive, were provided by the Earth Physics Branch, Energy, Mines and Resources Canada. During this period, 1841 earthquakes were recorded for the Cordilleran region of which 86 could have been felt in the Thompson study area and 91 in the Chilcotin. Epicentres for these events are seen in Fig. 3.28.

In the Thompson study area the maximum acceleration experienced during the 79 years of record is 0.01 g (Maximum Mercalli Intensity = V). Calculations of the return period of various accelerations are given in Table 3.3. A 0.03 g acceleration may be expected to act on slopes in the region with a 200 year return interval.

In the same period the Chilcotin study area experienced a maximum acceleration of 0.02 g (Maximum Mercalli Intensity = V) and a 0.04 g acceleration may be expected to act on the slopes of the region with a 200 year return interval (Table 3.3).

The effect of seismic processes on slope stability is complex. There is no simple correlation between slope movements and epicentral distance (Mathews, 1979), between earthquake magnitude and magnitude of slope movement (Mathews and McTaggart, 1978) or between Intensity and the occurrence of slope movement (Harp et al., 1981). However, the present seismicity of the study areas is characterised by low accelerations which emanate from three sources: high magnitude events along the Pacific margin, intermediate magnitude events along the British Columbia coast and low magnitude events in close proximity to the study areas themselves.
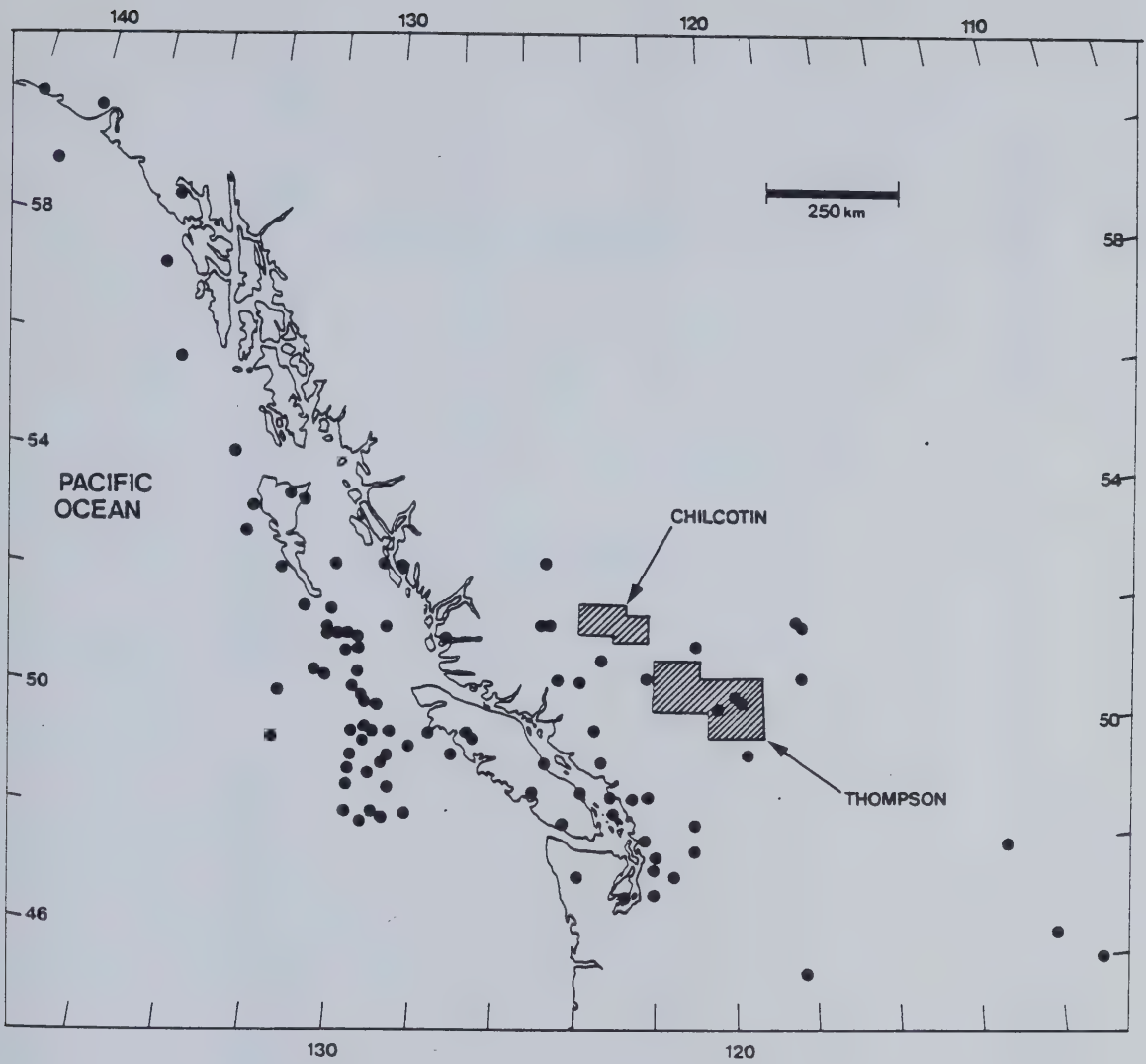
Figure 3.27 Location of epicentres of earthquake events that were felt (i.e., Mercalli Intensity > II) in the study area between 1899 and 1977 inclusive. Data supplied by Earth Physics Branch, Energy, Mines and Resources Canada.

ACCELERATION IN PERCENTAGE GRAVITY (ACC)	MODIFIED MERCALLI INTENSITY (I)	EQUIVALENT RETURN PERIOD (yrs.)
THOMPSON		
0	III	3
1	IV	10
1	V	50
2	V	100
3	VI	200
CHILCOTIN		
0	III	3
1	IV	10
1	V	30
2	V	50
3	VI	100
4	VI	200

Table 3.3 Return periods of various seismic accelerations for the study areas, (supplied by Energy, Mines and Resources Canada).

Three epicentres are located within the Thompson study area and are associated with low magnitude events (M varies between 3.20 and 4.50) in the vicinity of the Louis Creek Fault zone, south of Kamloops Lake. Maximum accelerations were in the order of 0.01 g and Intensity varied between IV and V. These events, however, are not known to be correlated with any slope movements.

4. LANDSLIDES IN THE PALEOGENE ROCKS OF THE SALMON VALLEY

4.1 Introduction

Five large landslides have occurred in Paleogene rocks along a 9 km length of the Upper Salmon Valley, approximately 32 km south-east of Kamloops (Fig. 3.1). The area was selected for detailed investigations since several conditions exist in the valley which were thought to be conducive to a detailed evaluation of the role of geological factors in controlling slope movements in Paleogene rocks. These conditions were;

a. good accessibility to landslide debris and unfailed slopes by public roads, private access roads and trails.

b. the open nature of the forest stands that cover the slopes of the valley.

c. good bedrock exposures.

d. the existence of several well-defined landslides in a small area.

Four of the five landslides (Plate 4.1) were selected for detailed study which had the following objectives:

a. to determine the nature and characteristics of the Paleogene succession within an area of approximately 28 km^2 with emphasis on the location and characteristics of mechanically weak layers (including the sub-Paleogene surface).

b. to determine the structure and attitude of Paleogene rocks in the area with emphasis on those features unfavourable for slope stability.

c. to determine the morphology, kinematics and movement history of each landslide.

d. to determine the relationship between stratigraphical and structural factors and slope movement.

The main field work was carried out in the summer of 1979 and consisted of traverses through landslide debris and around landslide scarps. Ground control was effected using enlargements of aerial photographs and an altimeter. Altimeter readings were corrected using atmospheric pressure readings from a barograph (loaned by the British Columbia Ministry of Agriculture – Kamloops) located in a shed on the Kjellstrup Farm (Plate 4.1). The field work concentrated on the Jupiter Creek and Shell Creek

KEY:A=STEPHEN' LAKE ROAD LANDSLIDE, B=ADELPHI CREEK LANDSLIDE
C=JUPITER CREEK LANDSLIDE, D=SHELL CREEK LANDSLIDE, E=WOODS
LAKE ROAD LANDSLIDE, F=WOODS LAKE, G=JIMMY LAKE.

Plate 4.1 Air Photograph of Salmon Valley landslides (B.C. Air Photograph BC 5377-033).

landslides which were traversed several times in the summer of 1979.

4.2 Previous Geological Observations

The geology of the Upper Salmon Valley within the area studied has been examined by several workers since Dawson (1879) noted the narrow, steep-sided nature of the valley which was "bounded occasionally by high cliffs formed by volcanic breccias" (p. 62). He described basaltic flow units with zeolite amygdales and "interbedded grey ash or mudrock units" (p. 128), noting that the Tertiary rocks rest unconformably on schistose rocks. Dawson made no mention of landslides.

Jones (1959) first mapped the area as part of the Vernon sheet at a scale of 1 : 253,440. Jones' main concern in the valley, shared by subsequent workers, was the so-called Salmon River unconformity which exists in the vicinity of the power line crossing 2.75 km south-west of Twig Creek, between the Palaeozoic Chapperon Group and the Triassic Nicola Group. Investigations of the unconformity are summarised by Read and Okulitch (1977). Okulitch (1979) updated Jones' map with additional detail in the Salmon Valley at a scale of 1 : 250,000 (Fig. 4.1) There is therefore a lack of detailed work on Tertiary rocks within the area studied.

First note of the landslides in the Salmon Valley was made by Fulton (1975).

4.3 Field Characterisation of Rock Masses

The field characterisation of the rock masses making up the slopes of the Salmon Valley involved an evaluation of the mechanical properties of intact rock and an analysis of the discontiniuities which occurred within them.

In order to quantify the mechanical properties of intact rock in field exposures, the classification scheme outlined by Hoek and Bray (1977, p. 99) and ISRM (1978, p.348) was used. The classification is based on the response of the rock to hammer blows and scratching with a knife blade, in the so-called Manual Index Test. This response is correlated with an approximate range of uniaxial compressive strength (q_u).

In addition, the Schmidt Rebound Hammer (Type L) was used to obtain estimates of q_u as described by Barton and Choubey (1977) and ISRM (1978).
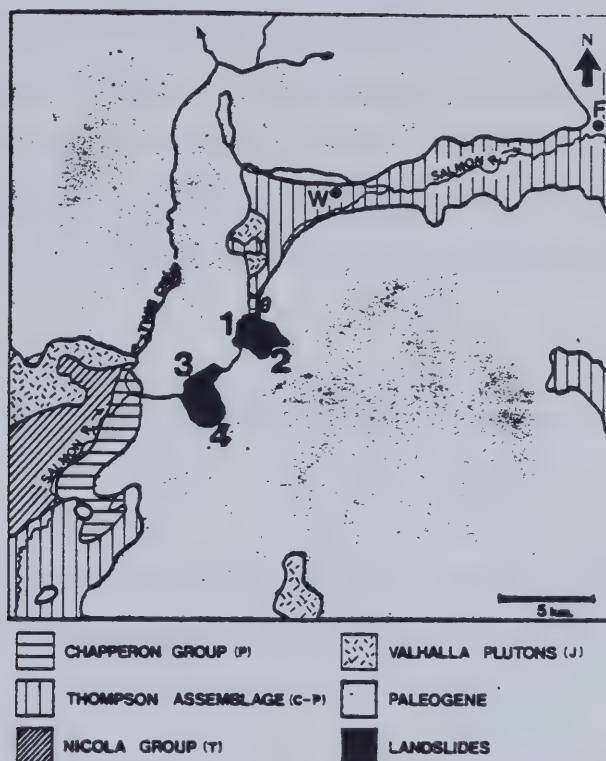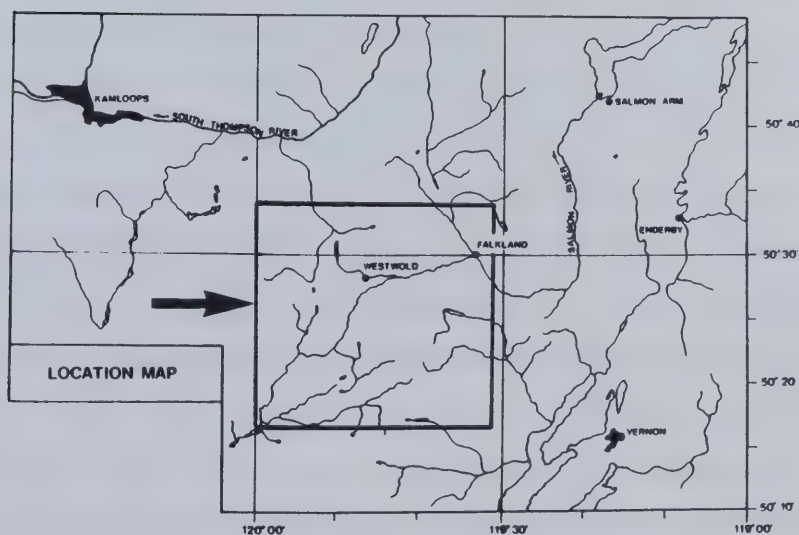
Figure 4.1 Geological setting of the Salmon Valley landslides (modified after Okulitch, 1979).

Discontinuities were described and measured using terms and methods suggested by ISRM (1978). The orientations of discontinuities at each location are represented on the lower hemisphere of a Schmidt Equal Area Net. Pole densities, expressed as a percentage of n points in 1% of the area of the hemisphere, were computed using a program supplied by Professor H.A.K. Charlesworth. The pole densities were contoured by hand.

4.4 The Materials and Characteristics of the Basal Paleogene Surface

4.4.1 Materials

Since the nature of the basal Paleogene surface may be important as a factor in slope movements in the study area, materials making up this surface were examined. They include:

(a) *Chapperon Group:*

The rocks of the Chapperon Group are of Palaeozoic age (Mississippian or older) and consist mainly of chloritic phyllites and schists. They are exposed at several locations in the Salmon Valley (Fig 4.2). The Chapperon Group has been affected by two phases of metamorphism and the schist and phyllites have well-marked, steeply dipping foliation cleavage, as described by Read and Okulitch (1977).

At exposures of the Chapperon Schist near Adelphi Creek and Twig Creek (Fig 4.2), Schmidt Hammer Rebound numbers (R) had mean values of 47.0 and 51.2 respectively. Assuming a rock density of 27 KPa, these values correspond to a value of q_u of about 150 MPa (Deere and Miller, 1966). According to the Qualitative Rock Description (Hoek and Bray, 1977), the Chapperon Schist is Strong Rock (R4).

Discontinuity measurements were made at the two locations noted in Fig 4.2. Joint and cleavage surfaces were clean except for the occasional unweathered mineralised shear. No foliation shears were found. At the Adelphi Creek exposure, pole concentrations representing planes dipping 060/70 and 250/60 were observed (Fig. 4.2). In the exposure near Twig Creek, a small sample size restricts the interpretation of the discontinuity data but suggests a discontinuity set dipping 170/80.

(b) *Valhalla Granite:*
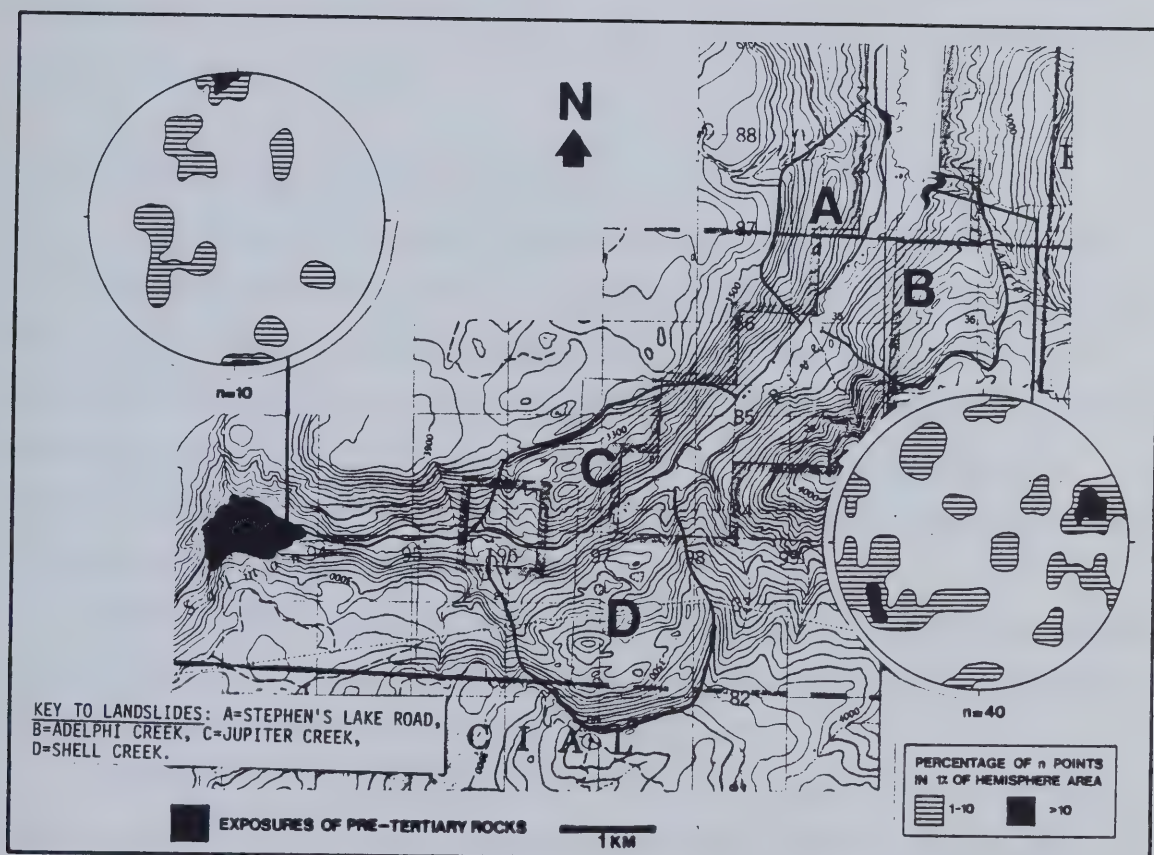
Figure 4.2 Exposures of Pre—Tertiary rocks in the vicinity of the Salmon River landslides. Schmidt nets (lower hemisphere) show pole concentrations of discontinuities.

This is of Jurassic–Cretaceous age and part of the large granite plutons which surround the Salmon River area. It is exposed near the Woods Lake Road just north of Dry Creek (Fig. 4.3.) An exposure of Valhalla Granite was reported by Okulitch (1979) between Twig Creek and Shell Creek but this could not be located in the field.

(c) *Nicola Group:*

These Triassic rocks, consisting of conglomerate overlain by argillite, tuff, feldspathic greywacke and sandstone, is separated from the Chapperon Group by the Salmon River unconformity. It has been affected by one phase of metamorphism and dips generally between 20^0 and 40^0 to the northwest in the vicinity of its only known exposure in the study area, at the unconformity.

4.4.2 Characteristics of the sub-Paleogene Surface

Since borehole information is absent in the study area, the configuration of the sub–Paleogene surface throughout the immediate area of the landslides remains unknown. However, its location has been established at the surface at several places. Near the mouth of Adelphi Creek, it is located at an elevation of 700 m, 46 m above the valley floor. Along the Woods Lake Road, however, 600 m to the northeast, the elevation of the surface is at 1016 m. Detailed mapping (Fig. 4.3) indicates that this configuration is due to normal faulting along the Woods Lake Fault.

East of Adelphi Creek the Chapperon Schist was found to be altered in the vicinity of the Valhalla Granite exposure near Dry Creek. It is probable that the schist is similarly affected wherever it is in contact with the Valhalla Pluton.

The actual contact is exposed only at Twig Creek at an elevation of 775 m, in a steep notch eroded by the creek. The Chapperon schist is overlain directly by basal Tertiary volcaniclastic rocks. The contact forms a brecciated zone about 2 m in thickness and consists of a green micaceous shear matrix enclosing slickensided, rounded, schist fragments (Plate 4.2). Slickensided shear surfaces are present throughout the shear matrix and it appears that movement has been toward the south. The shear breccia is not weathered or altered and appears to be of high shear strength in its present condition. No soft gouge–like seams were observed. Since only a very small exposure of the contact exists, it is not known how extensive this phenomenon at the contact may be. It appears
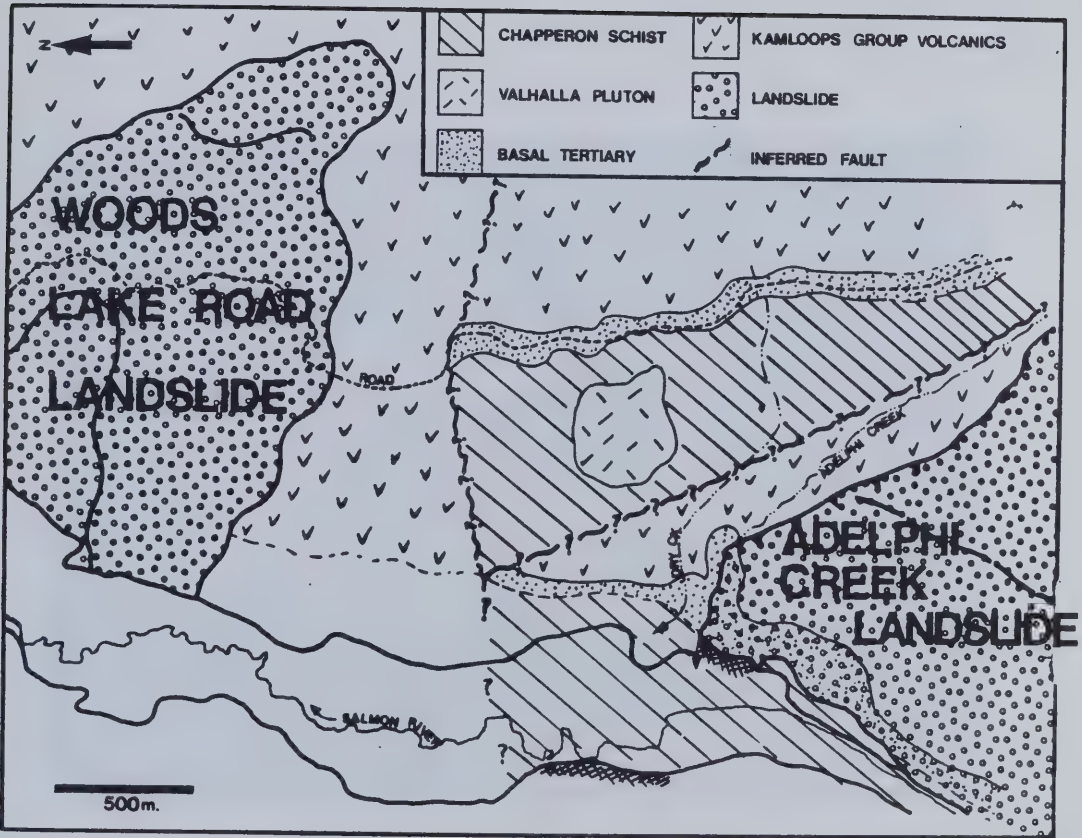
Figure 4.3 Geological map of the eastern margin of Adelphi Creek Landslide. Adelphi Creek is located in Fig. 4.5.

Plate 4.2 Shear breccia in Chapperon Schist at Tertiary unconformity, Twig Creek.

A=Chapperon Schist, B=Paleogene Twig Creek Tuff.

unrelated to any present landsliding and the attitude of the overlying Tertiary rocks
suggests one of three origins:

  a.   localised penecontemporaneous landsliding during accumulation of Tertiary
        volcaniclastic rocks, known to be a common process in the filling of Tertiary
        basins in the Thompson Plateau (cf. Chapter 2);

  b.   local low—angle normal faulting;

  c.   part of a decollement surface associated with a metamorphic core complex
        such as that described by Davis *et al.* (1980) in south—east California and
        western Arizona, and by Read (1980) in the Frenchman's Cap area.

       It may be noted that the Twig Creek Shear Zone is one of several low—angle
structural features observed in the basal 195m of the Tertiary rocks in the study area,
which are discussed in detail below.

       Within the immediate area of the landslides no pre—Tertiary rocks have been
located, with the exception of the exposure at the foot of the Adelphi Creek landslide (Fig.
4.3)

4.5 The Paleogene Succession

       An initial step in evaluating the relationship between geological factors and slope
movement was to establish a stratigraphical sequence in the study area. The Paleogene
succession is a complex series of interbedded lava flows with associated flow top
breccias, massively bedded volcanic breccias of various origins, pyroclastic rocks and
tuffaceous sediments.

       A composite succession was established from scattered exposures. Whilst good
exposures occur in steep wall—like slopes at Adelphi Creek Bluffs (Plate 4.3) and in the
scarps of landslides, these are inaccessible. Other slopes contain good exposures of lava
flows and breccias but many covered intervals are present particularly in the lower part of
the succession. Thus only a composite, generalised succession was established.

       550 m of the succession is exposed at Adelphi Creek Bluffs. This was mapped by
plane table and telescopic alidade from a station on the opposite side of the valley in a
manner similar to that described by Compton (1962, p. 172). The method was considered
accurate for the purpose of establishing a general succession, although descriptions of

Plate 4.3 View to the east toward Adelphi Creek landslide (A) and Adelphi Creek Bluffs (B).
Note slopes between Adelphi Creek Bluffs and Cain Creek (C) are not affected to slope
movement.

the individual units were limited to gross lithology and colour.

Data on rock mass properties were obtained by traverses of slopes containing rocks at various levels in the succession.

On this basis a fourfold subdivision of the succession was possible (Fig. 4.4), consisting of the Basal Beds, Brown Beds, Red Beds and Salmon Beds.

The Basal Beds constitute the lower 195 m of the succession. They exhibit wide lithological variation within the study area. At the base of the Basal Beds, there occurs a series of interbedded fragmental volcaniclastic rocks collectively termed the Twig Creek Tuff (Plate 4.4). They overly the shear breccia described above and contain angular clasts of the Chapperon Schist. Similar materials outcrop in a limited exposure between Adelphi Creek and Dry Creek and are found in the rupture zone of the Adelphi Creek landslide described below (Plate 4.23). These are overlain by a series of basalt flows interlayered with grey andesitic lavas, which are in turn overlain by basaltic flows interlayered with volcanic breccias. Above these beds is a brown tuff– tuff breccia termed the Salmon River Tuff (Plate 4.5), which appears to be limited in distribution and variable in thickness. It is exposed in the area of Shell Creek, and at the base of the Shell Creek and Jupiter Creek landslides. This unit was not found exposed west or east of Shell Creek but may be concealed beneath covered intervals. The Salmon River Tuff is underlain by a brick red tuff (the Red Tuff) which is up to 3m. thick. The distribution of Paleogene volcaniclastics in the Salmon Valley is given in relationship to the landslides in Fig. 4.5.

Whole–rock K–Ar dating was carried out by the British Columbia Ministry of Mines and Petroleum Resources on two basalt flows. The basalt above the Twig Creek Tuff (the Basal Basalt) gave an age of 49.3±1.7 Ma, while a basalt just below the tuff breccia at a road cut at the margin of Jupiter Creek landslide gave an age of 48.6±1.7 Ma (Fig 4.4).

As seen in Plates 4.4 and 4.5, the Twig Creek and Salmon River Tuffs have undergone a form of alteration similar to spheroidal weathering. The rocks are crumbly in exposure and are generally brown in colour. Fresh unweathered tuff is generally blue. Fresh unweathered tuff 4 m above the Chapperon schist at Twig Creek gave a mean Schmidt Hammer Rebound number of 27.4 and rated R2 in rock quality The Rebound number suggests a value of q_u = 22 Mpa for the intact Twig Creek Tuff. According to Hoek and Bray (1977), it is classified as very weak rock. Generally, exposures were too

Composite Stratigraphical Section of Kamloops Group
Volcanic Rocks in the Salmon River Valley, S.W. of Westwold

SALMON BEDS	Thick, massive breccia beds with occasional lava flows and minor interbeds of tuffaceous material. Vertical joints marked in places form steep upper scarps of Adelphi Creek and Shell Creek Slides. Dykes noted in Adelphi Creek bluff rocks are salmon-pink in color.
RED BEDS	Upper red beds; thick massive breccia beds with some lava flows, - brown-red in color.
	Lower red beds; lava flows with minor breccia interbeds brown-red in color. Thick tuffaceous sediments occur at base in places, pink-yellow in color.
BROWN BEDS	Dominantly massive brown breccia beds with occasional lava flows and minor tuffaceous sediments and arkosic sandstones.
BASAL BEDS	Andesitic and basaltic lava flows with occasional breccias.

WEAK LAYER
SRT
TC
U/C

PRE—TERTIARY *(see Text)*

*NOTE: LOCATION OF K-Ar DATES ARE AT A (49.3 ± 1.7 Ma) and B (48.6 ± 1.7 Ma).

TC = TWIG CREEK TUFF   SRT = SALMON RIVER TUFF

Figure 4.4 Composite stratigraphical section of Paleogene rocks (Kamloops Group) in the Salmon Valley, south-west of Westwold.
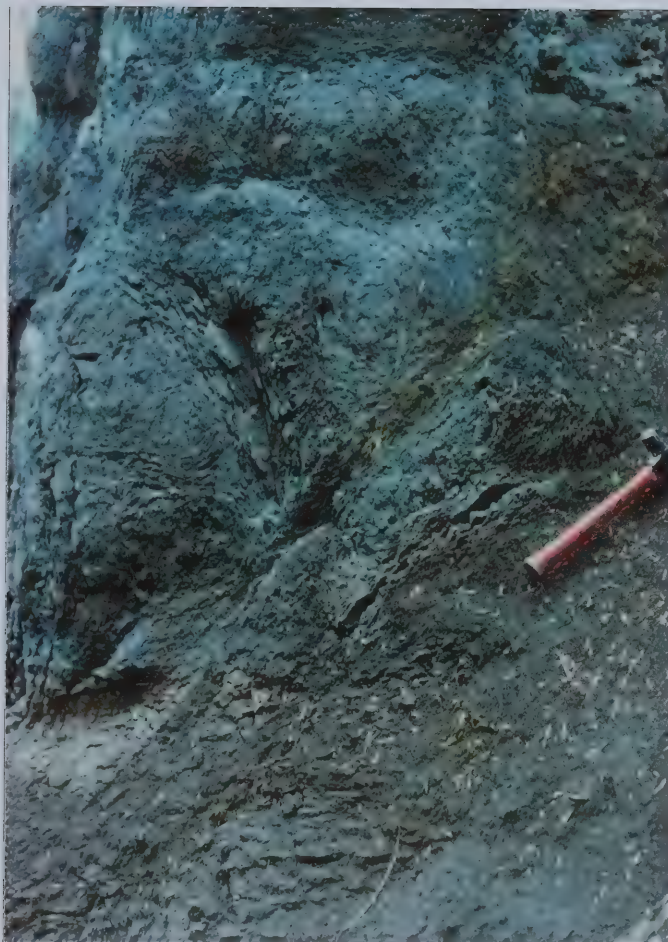
Plate 4.4 Typical exposure of Twig Creek Tuff at Twig Creek. Note spheroidal-type weathering or alteration.

Plate 4.5 Salmon River Tuff-Tuff Breccia exposed at the west margin of the Jupiter Creek landslide. Note filled discontinuities, spheroidal-type alteration or weathering and basaltic blocks (B).
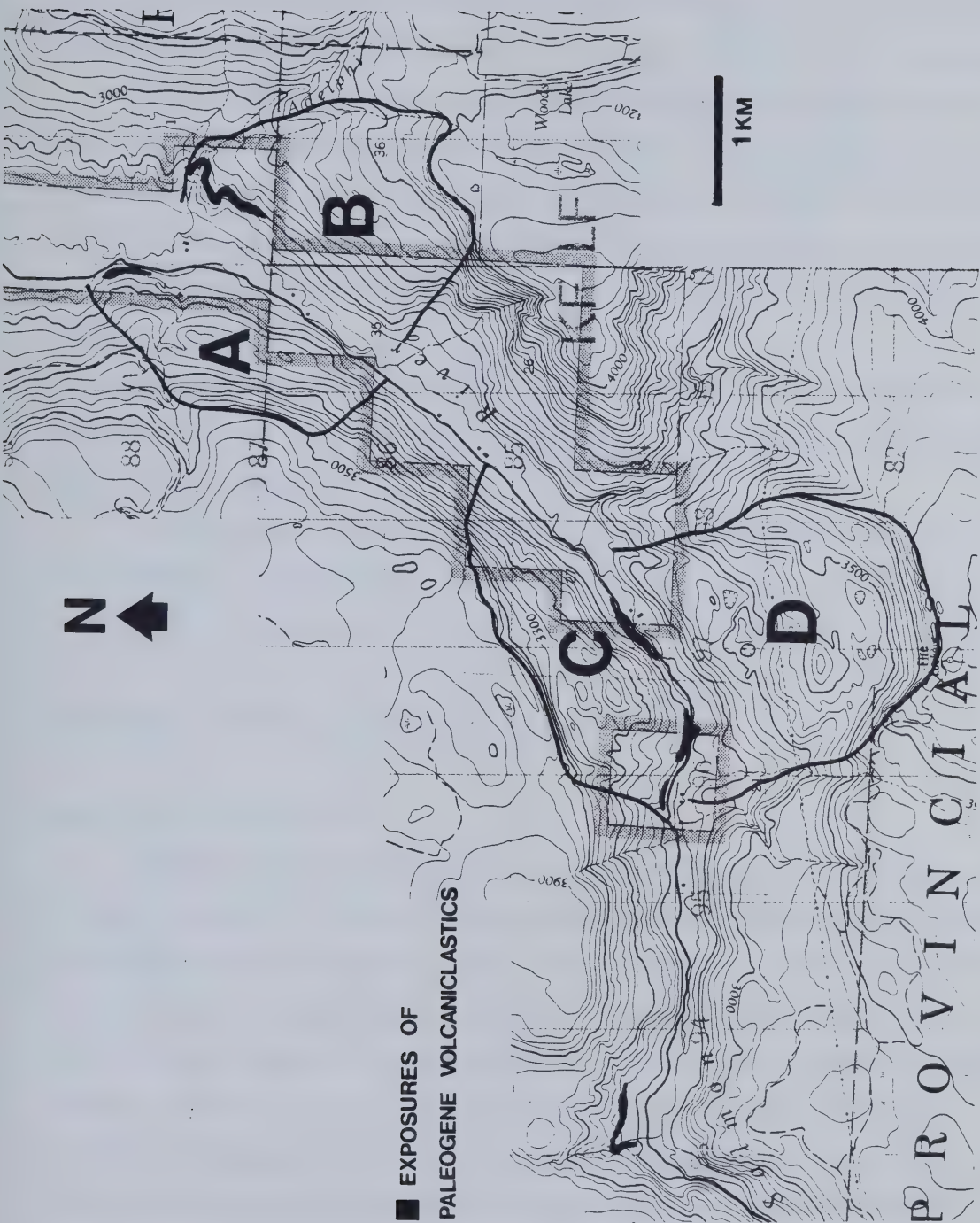
Figure 4.5 Exposures of Paleogene volcaniclastics in relation to the landslides in the Salmon Valley.

soft for the Schmidt Hammer to rebound. No Rebound Numbers were obtained for the Salmon River Tuff because of this factor which suggests values of q_u less than 15.0 MPa.

Basalts and breccias within the Basal Beds are resistant materials and commonly form prominent topographic features. Rebound numbers for basalt vary from 33.6 for highly amygdaloidal basalt to 51.2 for hard vesicular basalt. Rebound numbers of between 26 and 30 were obtained for volcanic breccias. These rebound numbers indicate values of q_u equal to 35 MPa (Moderately Weak Rock) for the breccias and >100 MPa for the basalts (Strong Rock)

The overlying Brown, Red and Salmon Beds are a series of flows and volcanic breccias and do not contain mechanically weak rock except for a thin tuffaceous unit at the top of Brown Beds (Fig. 4.4)

In summary, therefore, the Paleogene succession in the Salmon River Valley is characterised by a complex series of interlayered lava flows and volcanic breccias and the occurrence of two mechanically weak volcaniclastic zones within 120 m of its base.

4.6 Structure of the Paleogene Rock Mass

4.6.1 Lineaments and Faults

Persistent sub—parallel linear features are very marked on aerial photographs of the study area (Plate 4.1). These are interpreted as structural lineaments and are common in other parts of the Thompson Plateau (e.g., Schau, 1968; Ewing, 1981a). Some are known to be faults, whilst others are thought to be persistent joint systems related to faults (cf. Fookes, 1966). As discussed in detail below, these gross structural features are important in defining the lateral margins of the landslides in the Salmon Valley and morphological zones within them. The trend of these features is generally between 015° and 050° and their linear traces suggest vertical to steeply dipping planar structures.

Field observations indicate that the vertical separation on some faults are in the order of 320 m. Ewing (1981a) has commented on the complexity of faulting processes and fault zone morphology in the Paleogene rocks of the Thompson Plateau. Splaying and secondary shearing can be observed in the lineament patterns in Figure 4.6.
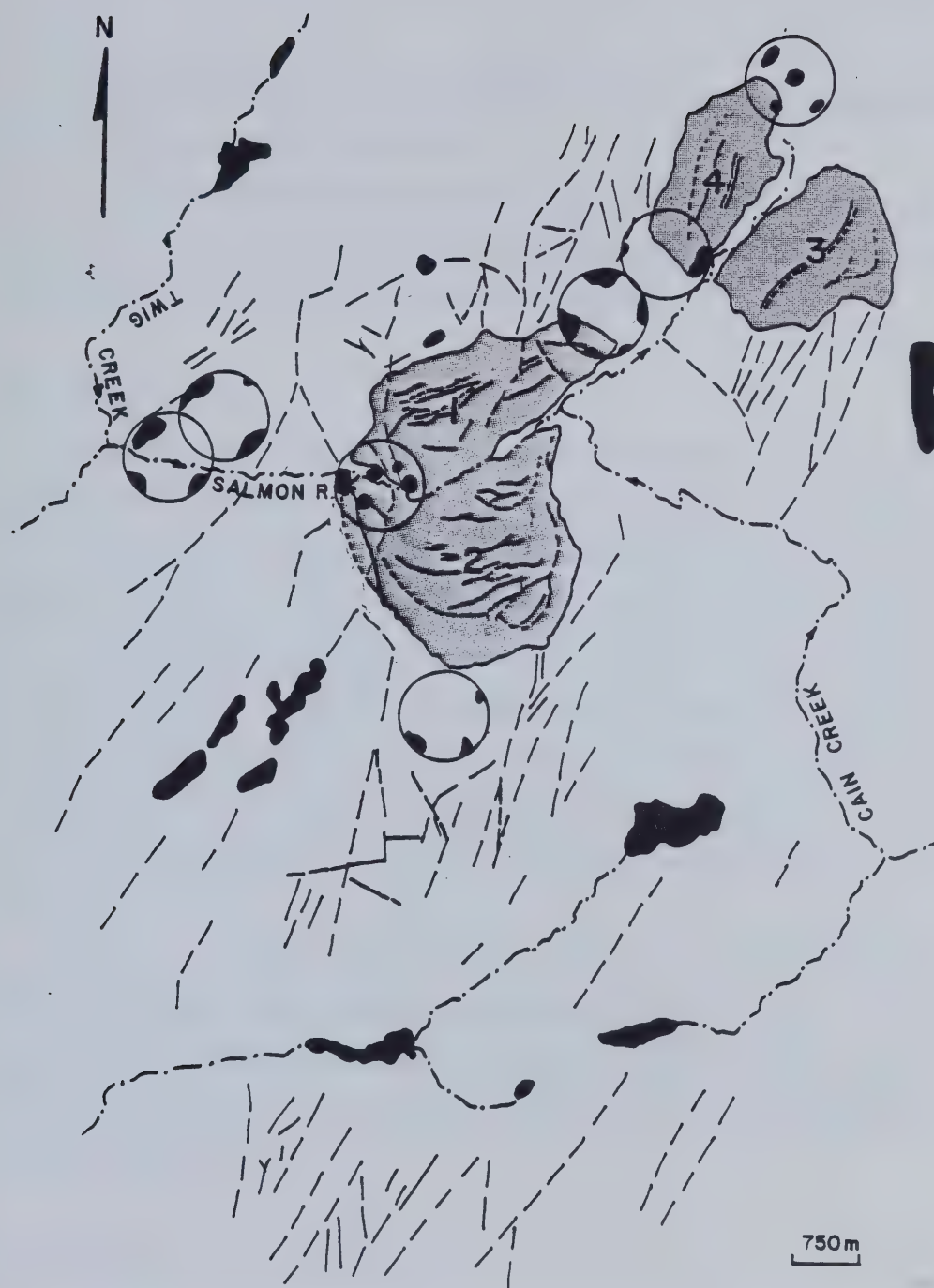
1   JUPITER CREEK LANDSLIDE

2   SHELL CREEK LANDSLIDE

3   ADELPHI CREEK LANDSLIDE

4   STEPHEN'S LAKE ROAD LANDSLIDE

Figure 4.6 Structural lineaments evident on air photograph BC 5377-33 and pole

concentrations from discontinuity surveys in the vicinity of the Salmon River landslides.

Very few fault zones are exposed in the slopes of the area. Generally, inferred fault zones are gullies filled with regolith.

Curvilinear lineament traces are observed around the scarps of some of the landslides. Whilst initially they were thought to be stress-relief features, they appear to form part of the regional structural framework (Fig. 4.6).

4.6.2 Discontinuities

Joint surveys were carried out around the margins of the landslides where accessible outcrop allowed. The volcanic breccias tend to be massively bedded and exhibit vertical to near-vertical persistent curved joints with apertures up to .1 m. Joint spacing is in excess of 10 m. The joints may be related to stress-relief. Flow rocks are also massively bedded and exhibit dominantly vertical joints. Columnar jointing is not observed in any of the flows. Both lava and breccia unit boundaries are irregular (Plate 4.6). Joint spacing was observed to vary from .10 cm to a limit of .1 m. The aperture of open joints varied from 0.5 cm to 20 cm. In bedded volcaniclastic rocks, joints and thin shear zones are closely spaced (≤1 m) and are often filled by gouge or calcite veins as discussed below.

In Figure 4.6 the pole concentrations of discontinuities in Paleogene rocks are presented in relation to the lineaments discussed above. It is seen that, in most cases, the concentrations represent discontinuities parallel to the lineaments in the vicinity of the field survey location, suggesting that the meso-fabric of the rock mass is related to the regional macro-fabric.

4.6.3 Attitudes

The effect of faulting is to divide the Paleogene rocks into fault blocks which have varied orientations. Similar structural patterns in Paleogene rocks of the Southern Interior have been noted by Campbell and Tipper (1971) and Ewing (1979). Figure 4.7A gives attitude measurements obtained both by direct measurement of bedding planes in volcaniclastic rocks and lava flow surfaces, and indirect measurements of general dips in inaccessible scarps and cliffs by a method outlined by Wallace (1950) and Phillips (1971, p. 15-17). The indirect method was checked several times by direct measurement and the

Plate 4.6 Exposures of lava flows and breccias (Upper Red Beds) in the scarp of the Jupiter Creek landslide. Note irregular nature of unit boundaries and predominance of vertical jointing.
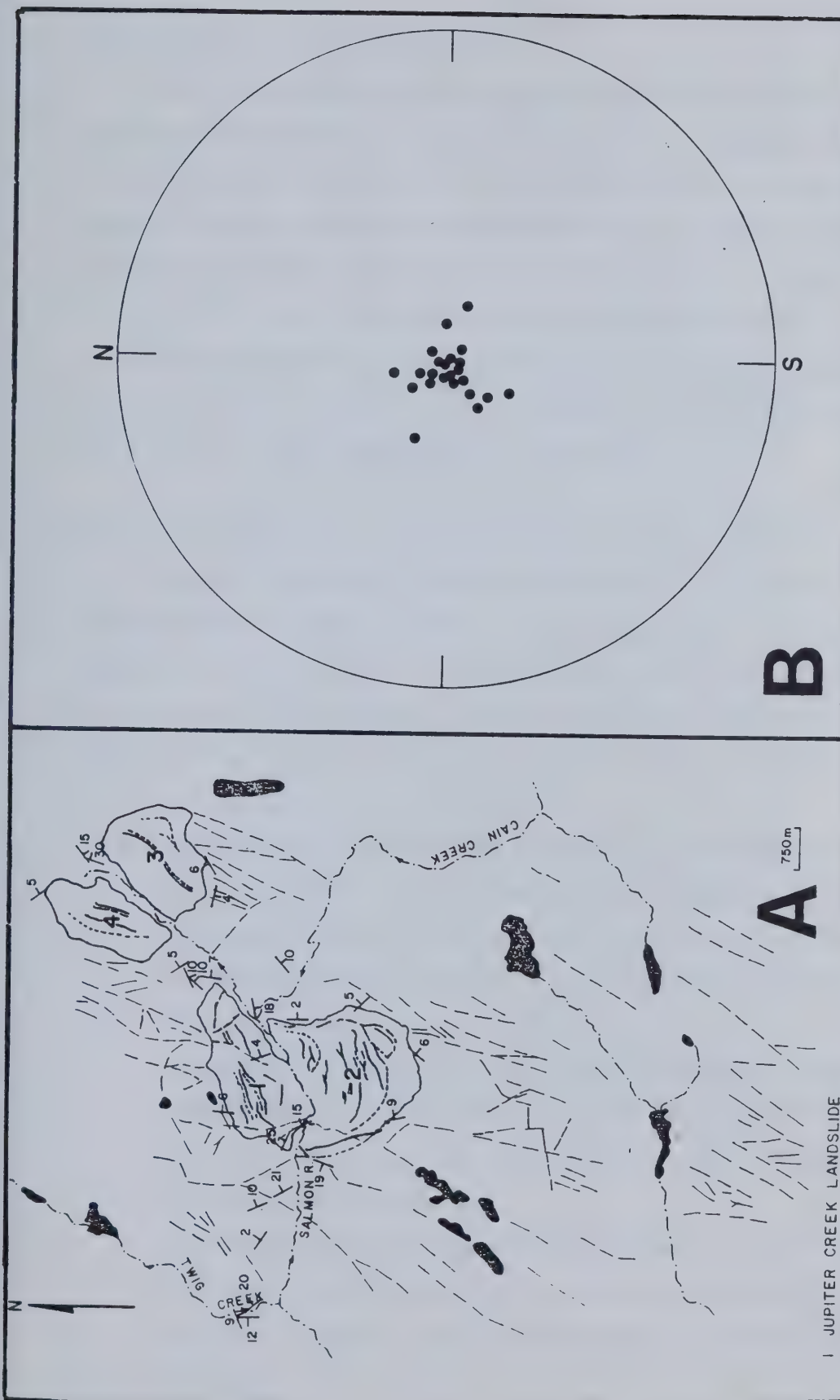
Figure 4.7 A=Attitude measurements in Paleogene rocks in the vicinity of the Salmon River landslides. B=Dispersion of poles to bedding and unit surfaces (Wulff Net – lower hemisphere).

1 JUPITER CREEK LANDSLIDE

2 SHELL CREEK LANDSLIDE

3 ADELPHI CREEK LANDSLIDE

4 STEPHEN'S LAKE ROAD LANDSLIDE

differences were found to be insignificant.

With reference to Figure 4.7A, the dips of units within the study area show an erratic areal pattern with abrupt changes of attitude over small distances (*e.g.*, in the vicinity of Cain Creek and the western margin of Shell Creek landslide). There also appears to be a variation in attitude with stratigraphical position within the succession (*e.g.*, at Adelphi Creek Bluffs). The range of dips measured is between 30^0 and 2^0, and Figure 4.7B shows the dispersion of poles to bedding and unit boundaries in the study area.

The variation in attitudes may be partly explained by variations in original depositional attitudes but may also reflect the irregular "jostling" experienced during the faulting process. Folding was not observed in outcrops.

4.6.4 Structural Disturbance in the Twig Creek and Salmon River Tuffs

Exposures in the tuffs of the Basal Beds commonly show the effects of structural disturbance both within slope movement areas and outside them. Whilst Holocene landslide movement accounts for some of the examples of structural disturbance, others may be the result of processes such as those discussed above with respect to the Twig Creek shear zone, viz. tectonic processes or landsliding during accumulation in the Tertiary.

These features consist of:

a.   small-scale normal faulting with calcareous gouge infilling along the shear
      planes (Plate 4.7) In other cases these have been filled by calcite veins.
      Displacement on these faults varies up to 20 cm and spacing varies between
      0.5 and 0.75 m. Slickensides are common in the thin gouge and along the
      margins of calcite veins .

b.   irregularities in attitude and abrupt changes of dip across low-angle
      discontinuities. This is observed at exposures along the Salmon River in the
      vicinity of Shell Creek and is interpreted to be the result of the Shell Creek
      landslide movement (Plate 4.8).

c.   bedding plane shears consisting of thin calcareous gouge up to 20 cm wide,
      with gouge boundaries showing well-marked slickensides parallel to the dip
      direction. These were observed at the margins of the Jupiter Creek landslide
      (Plate 4.9).

Plate 4.7 Small scale normal faulting with gouge in Salmon River Tuff at western margin of Jupiter Creek landslide.

Plate 4.8 Irregularities in attitude in the Salmon River Tuff at the base of the Shell Creek landslide.

4.7 Landslide Morphology, Kinematics and Relations to Stratigraphy and Structure

Four of the landslides in the Salmon Valley were selected for detailed study. Morphological data on these movements are provided in Table 4.1.

4.7.1 The Jupiter Creek Landslide

The Jupiter Creek landslide is a complex slope movement of the contiguous block movement type, involving an area of 2 km^2 along a valley length of 2.85 km (Plate 4.10 and 4.11). The estimated volume of the slope movement is in the order of 2.0 X 10^{8}m^3.

(a) Morphology

A contour map and slope profiles of the landslide and adjacent slopes are found in Fig. 4.8. Included in Fig. 4.8 is a reconstucted pre-movement slope profile. This was based on extending the contours from the slope adjacent to the contours into the slope area affected by movement. The morphology of the Jupiter Creek landslide as interpreted from aerial photographs and field traverses is seen in Figure 4.9. Four morphological zones have been distinguished in the landslide debris.

(i) *Zone 1:*

This marginal area has been tentatively interpreted as part of the landslide on the basis of the presence of transverse depressions on the pronounced rib that marks the western boundary of the main movement (Plate 4.10). These depressions continue laterally into the main movement zone to the east and across the zone to its western boundary. Exposures of the Salmon River Tuff at the base of the zone do not show evidence of brecciation due to slope movement, which is inferred to be limited in scale.

(ii) *Zone 2:*

This zone has undergone the greatest amount of movement and is also termed the main movement zone within the landslide complex. Movement has been mainly by lateral extension and vertical displacement, resulting in an almost vertical head scarp about 150 m in height. The scarp is made up of easterly dipping volcanic breccias and lava flows which exhibit persistent vertical open joints with apertures varying from 0.5 m to 2.0 m (Plate 4.6). These joints are persistent through beds of varying lithologies and are thought to control the geometry of blocks within the graben below. The graben is well marked and the debris within it consists of interlocking almond-shaped rock masses defined by an

Plate 4.9 Bedding plane shear zone in Salmon River Tuff at west margin of the Jupiter Creek landslide.

LANDSLIDE	AREA (km^2)	WIDTH ALONG VALLEY SLOPE BASE (km)	ESTIMATED VOLUME (m^3)	MOVEMENT DIRECTION	DIP OF BASAL PLANE[1]	BASAL STRATIGRAPHIC UNIT
JUPITER CREEK	2.00	2.85	2×10^8	145	+2	SRT[2]
SHELL CREEK	4.10	2.00	8×10^8	350	-1	SRT/TWIG
ADELPHI CREEK	2.62	2.00	4×10^8	310	+2-4	TWIG
STEPHEN'S LAKE R.	1.25	1.75	1×10^8	105	+6	TWIG

[2]SRT = SALMON RIVER TUFF

[1]DIP OF BASAL SURFACE IN DIRECTION OF MOVEMENT (MINUS VALUE DENOTES DIP DIRECTION OPPOSITE TO MOVEMENT DIRECTION)

Table 4.1 Summary of landslide geometry for Salmon River landslides.
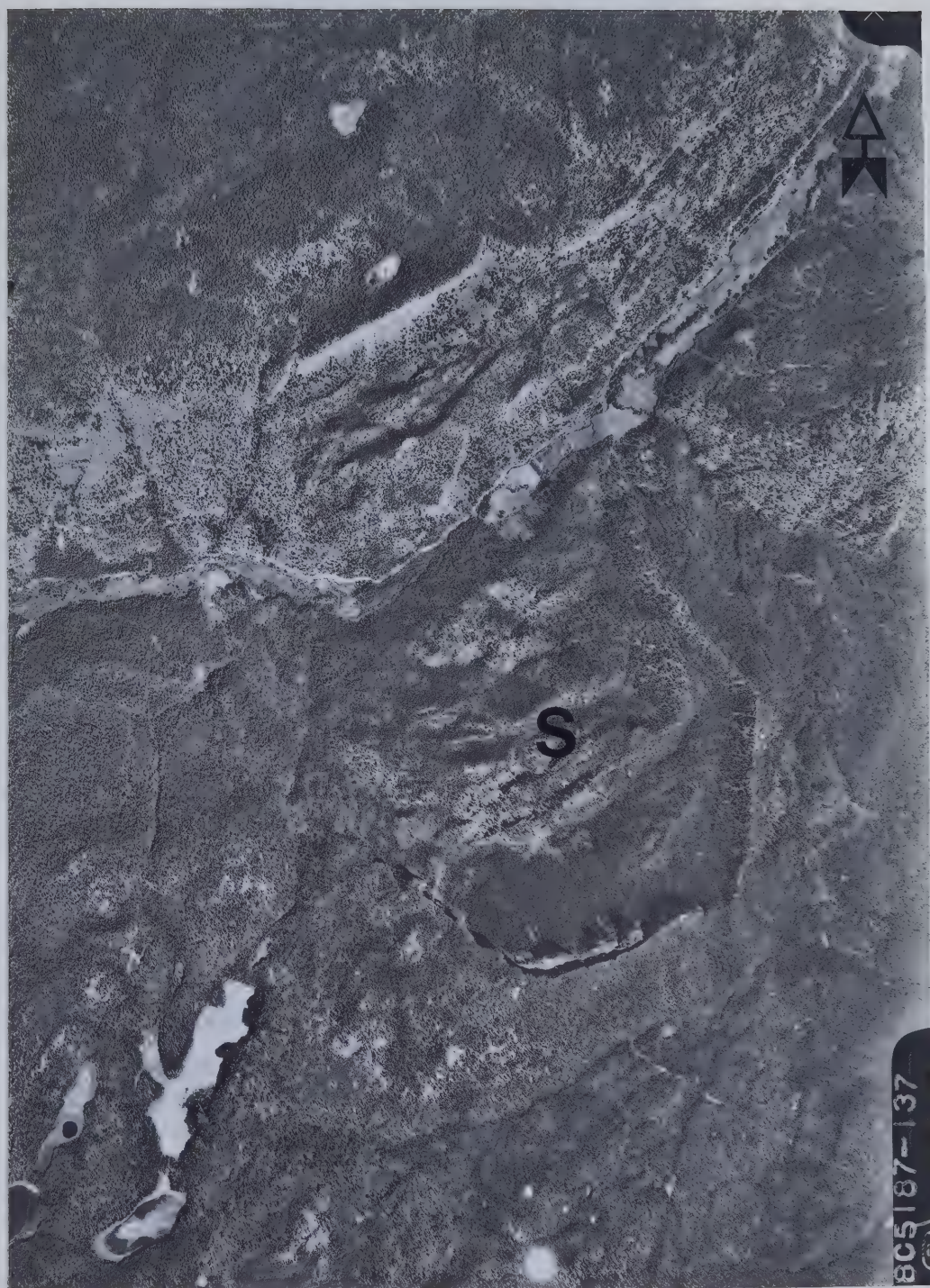
1 KM

Plate 4.10 Aerial photograph of Jupiter Creek landslide (BC 5187–137). Note also the Shell Creek landslide (S).
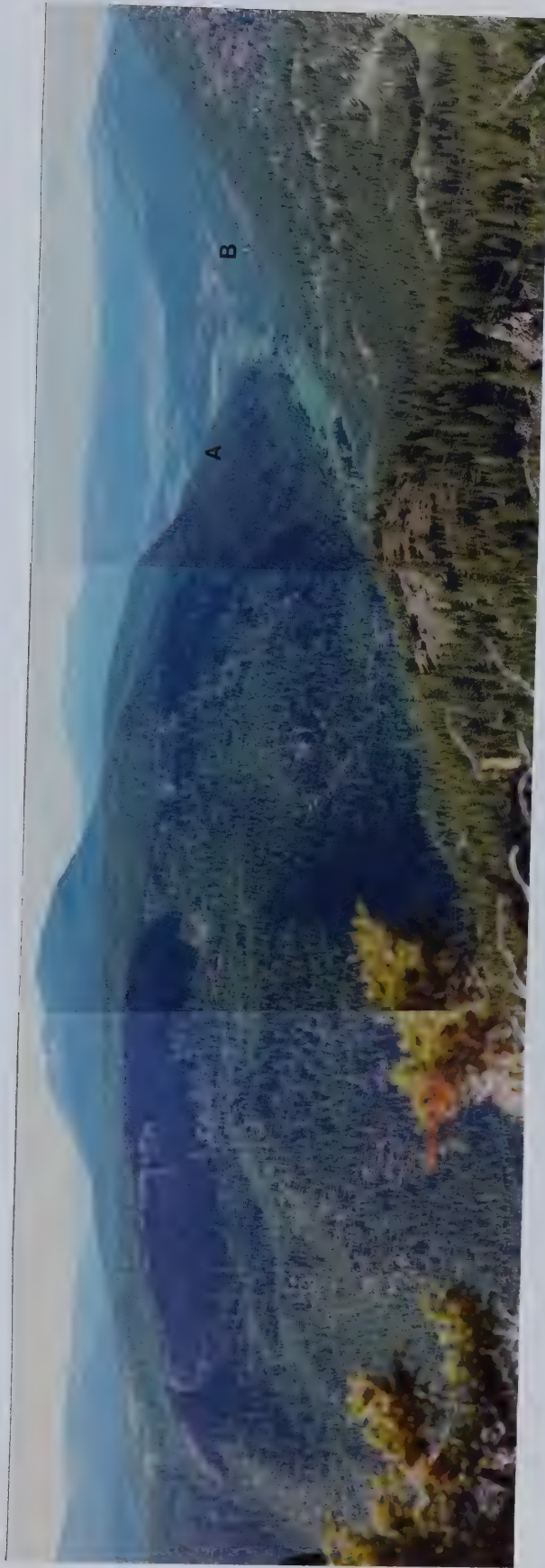
Plate 4.11 Jupiter Creek landslide from the Shell Creek landslide scarp (view to the north).

A=Stephen's Lake Road Landslide, B=Adelphi Creek Landslide.
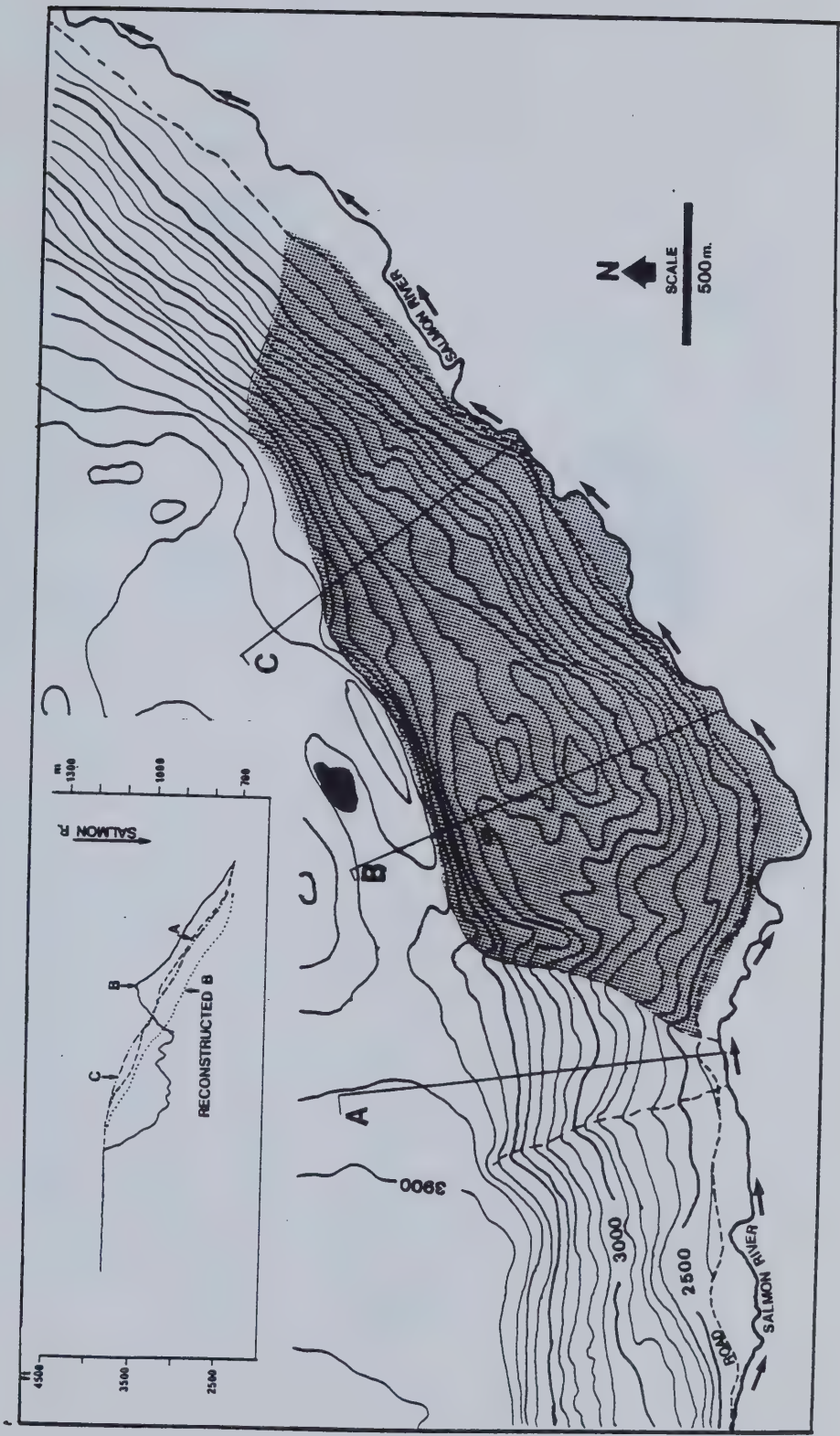
Figure 4.8 Map and slope profiles of Jupiter Creek landslide.
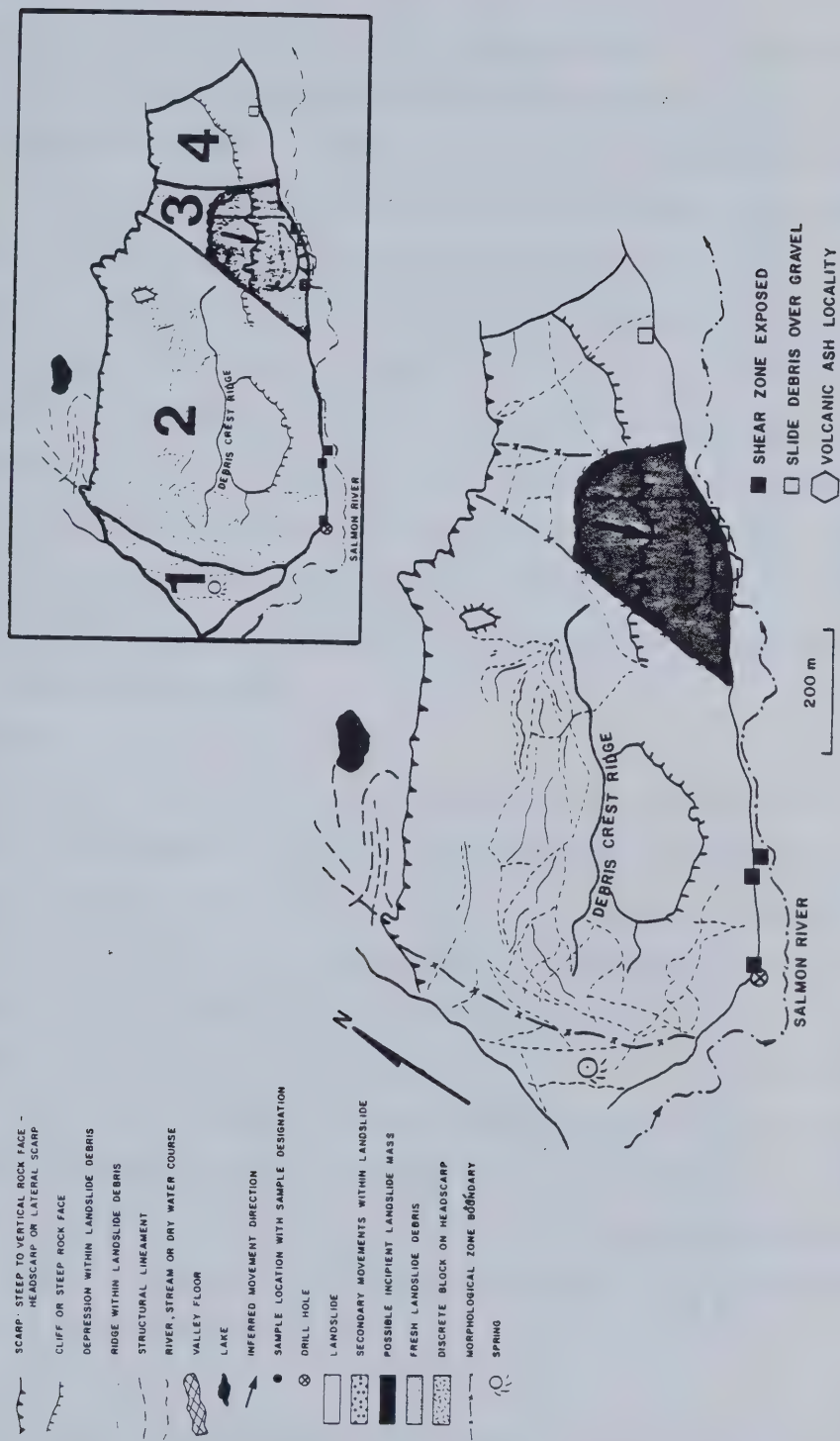
Figure 4.9 Morphology of Jupiter Creek landslide interpreted from air photographs and field traverses. Inset map shows morphological zones discussed in text.

interconnecting network of steep-sided depressions (Plate 4.12A) In traverses through the graben, the maximum relative relief observed was 60 m. The crest of each block is sharply defined and exposures along these ridges indicate that the strata within them are horizontal, suggesting that no rotation has taken place in the movement, (Plate 4.12B).

The graben is terminated by a very steep reverse slope with a maximum relative relief of 113 m, which marks the boundary of the debris crest ridge and the main body of the debris. This consists of a large unfragmented block about 200 m long (parallel to movement) and 600 m wide (transverse to movement), the summit of which is at an elevation of 1033 m and the base at 717 m. The main block has undergone a lateral movement in the order of 250 m to form the graben, whilst undergoing an unknown vertical displacement. The front of the block is marked by a 35° debris slope. at the foot of which occurs an exposure of the sheár zone described below. A cross section of Zone 2 is given in Figure 4.8 together with an approximate reconstruction of the pre-movement slope profile.

(iii) *Zone 3:*

This zone is separated from the main movement zone by a diffuse area in which the graben and debris crest ridge die out, (Plate 4.10 and Figure 4.9). It is bounded by two lineaments, thought to be fault traces, which trend 3° and 327° respectively (Figure 4.9) The faults converge into the slope, thus forming a release set of discontinuities along which movement is currently taking place. Evidence for present movement was observed at elevation 950 m, 240 m above the valley floor, and consisted of a transverse depression about 4.5 m in depth. Trees on both sides of the depression showed evidence of movement during their growth, being tilted out of the vertical (Plate 4.13) It is thought that a block, outlined in Figure 4.9, is gradually moving outwards and forming a graben behind it, since other transverse depressions are noted upslope beneath a vertical scarp. A cross section of Zone 3 is found in Fig. 4.8.

(iv) *Movement Zone 4:*

The east marginal zone has undergone less lateral movement than Zone 3. Linear transverse depressions do exist, however, but are not as well marked. The boundary of the zone and the eastern margin of landslide area is marked by a possible fault.

(b) Relationship to Stratigraphy and Structure

A - VIEW FROM THE SCARP OF THE JUPITER CREEK LANDSLIDE INTO GRABEN. NOTE SHARP RIDGES AND DEEP LINEAR DEPRESSIONS BETWEEN RIDGES. A=SUMMIT OF DEBRIS CREST RIDGE; B=PILLAR PHOTOGRAPHED IN PLATE 4.12B.

B - PILLAR WITHIN GRABEN. NOTE LACK OF ROTATION OF ORIGINAL BEDDING WITHIN THE PILLAR.

Plate 4.12 Features of the graben, Jupiter Creek landslide.

Plate 4.13 Disturbance of tree cover by slope movement in Zone 3 of Jupiter Creek
landslide 240m above the valley floor. Figure is standing in centre of transverse
depression.

On the basis of field exposures, it is concluded that the basal rupture zone is located in the Salmon River Tuff. Exposures of these rocks are found at the base of Zone 1 and are cut by the main movement. In addition, highly disturbed exposures of the tuff are found at the base of Zone 2. A diamond drill hole at the base of Zone 2 penetrated highly fractured basalt for a depth of 29.5 m below river level.

The attitude of the beds forming the rock slopes which experienced movement is variable (Fig. 4.7). Overall true dip is 089/6. The main movement direction is 145° which, if the overall true dip is applied to the basal rupture zone, implies that movement is taking place obliquely across the bedding on a plane, or zone, dipping out of the slope at an apparent dip of 2°. Given the variability of dip measurements around the landslide site, the apparent dip of this surface could vary between 0° and 5°.

In the absence of normal faulting, the tuff breccia would dip beneath the valley floor and would not daylight in the slope east of Zone 2. Tentative reconstruction of the geology of the Jupiter Creek slope suggests that the effect of normal faulting is to ensure that the tuff is continuously exposed along the foot of the slope, resulting in slope movement along a substantial length of slope (Fig. 4.10).

In Figure 4.11, the Jupiter Creek landslide can be seen in relation to the lineament pattern discussed above. It is seen that the western and eastern margins are coincident with persistent linear features which correspond to faults. The boundaries of the movement zones are also determined by faults (Fig. 4.9).

The relationship between mesostructural fabric and the morphology of the landslide is less clear (Fig 4.12). Analysis of discontinuities measured in the Salmon River Tuff at the foot of Zone 2 yields three pole concentrations. Two are steeply–dipping joints and normal faults (090/90 and 060/270) related to the regional structural trend, while the third is a group of clay–filled shear planes dipping out of the slope at 120–140/20.

The western margin of the landslide and the eastern boundary of Zone 2 parallels joint sets 1 and 2, which parallel the lineaments noted in Figure 4.11.

Joint surveys of unfailed slopes at the eastern margin of the Jupiter Creek landslide exhibit a more complex pattern of pole concentrations. In addition to the north–trending joint set, stress–relief joints that parallel the valley side are also evident as
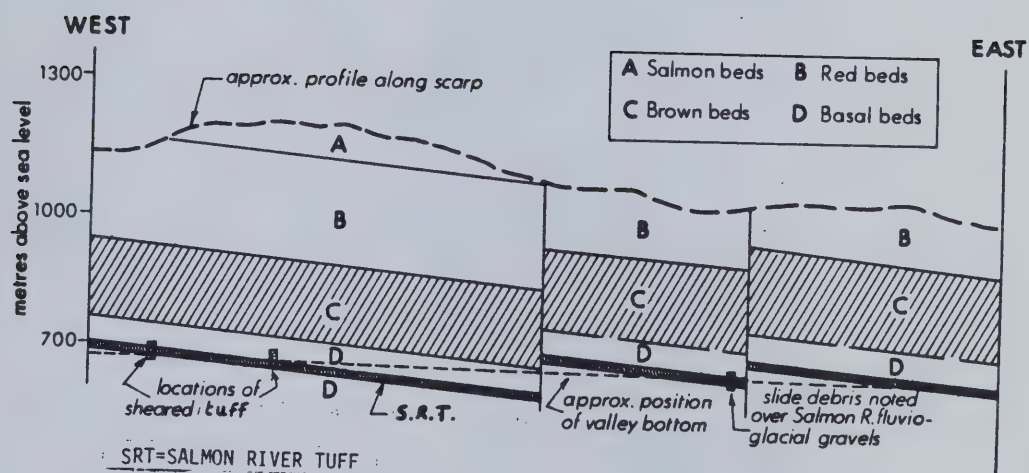
Figure 4.10 Inferred stratigraphical relations across the pre−movement slope, Jupiter Creek landslide.
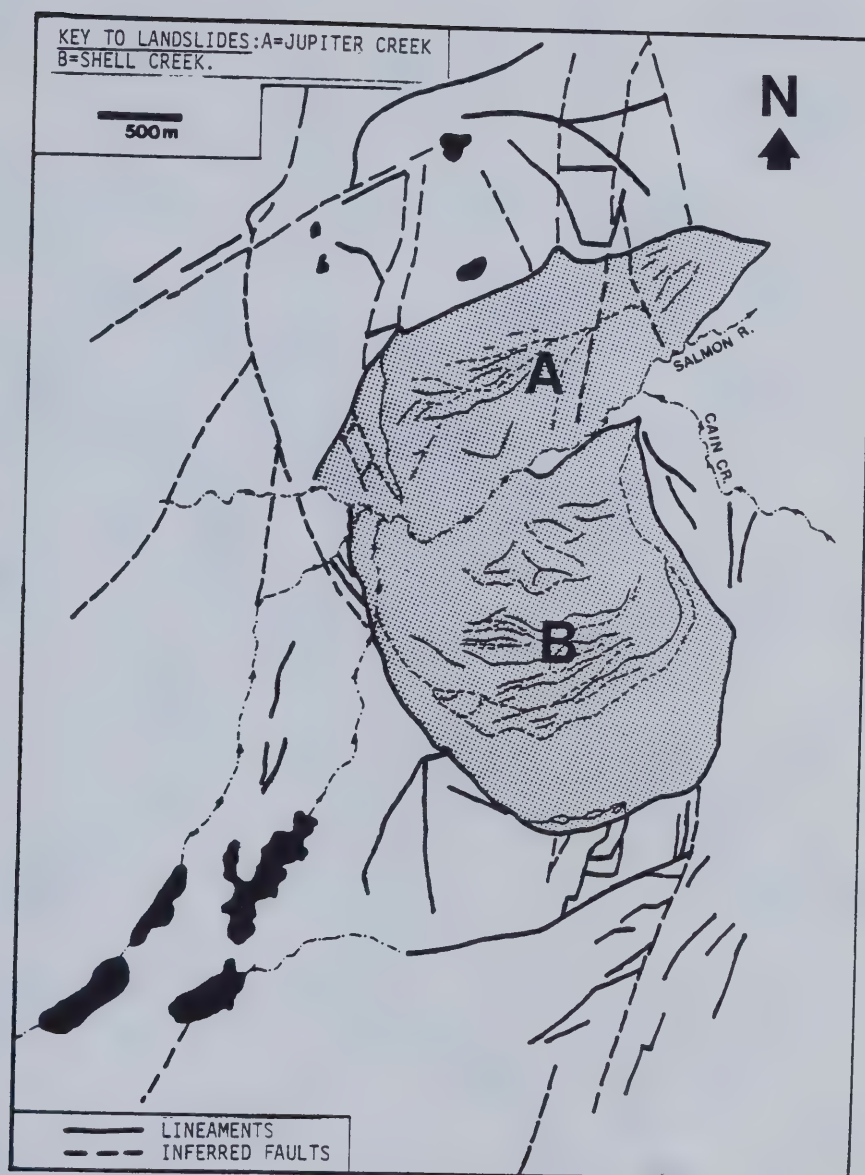
Figure 4.11 Relationship of Jupiter Creek and Shell Creek landslides to macrostructural elements in Paleogene rocks, Salmon Valley, as observed on B.C. air photograph BC 5187-137 and field traverses.
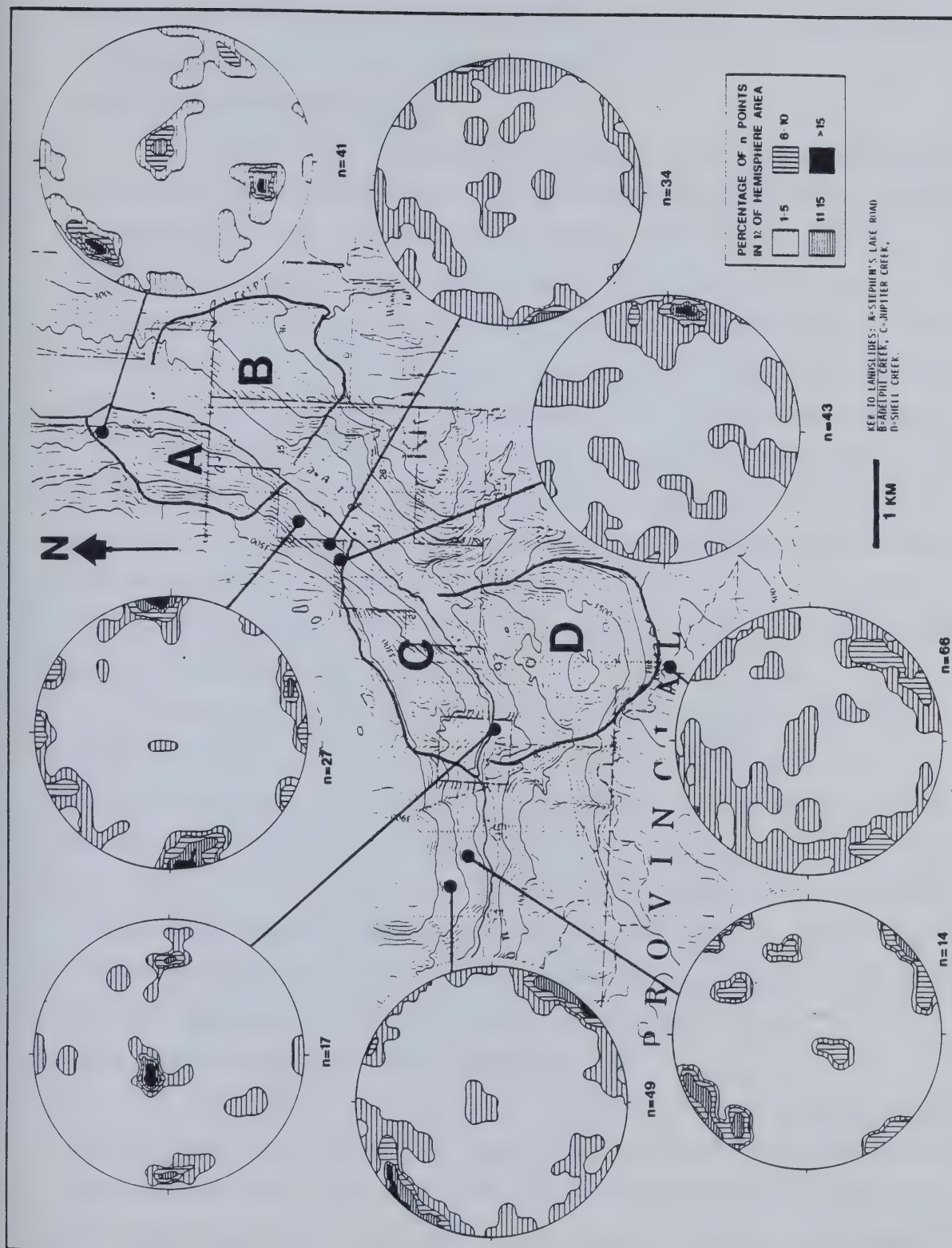
Figure 4.12 Relationship of Jupiter Creek and Shell creek landslides to mesostructural elements (Schmidt nets—lower hemisphere) in Paleogene rocks, Salmon Valley.

well as are other minor concentrations. Movements in Zones 3 and 4 are parallel to the main lineaments and joints evident in Figs. 4.11 and 4.12.

(c) Kinematics and Movement History

Based on the interpretation of debris morphology, the Jupiter Creek landslide has involved differential extensional and vertical movements along a basal shear zone located in the Salmon River Tuff. Movement direction within the morphologic zones has been controlled in large part by the orientation of near vertical discontinuities. During movement in zone 2, a slight easterly rotation of the debris has taken place in plan which may reflect the effect of the true dip of the rupture surface (089,6) to the east. Rotation toward the true dip direction is seen in the other landslides of the Salmon River Valley.

The presence of landslide debris on top of fluvial or fluvioglacial gravels at several locations at the foot of the movement (Fig. 4.9 and Plate 4.14) indicates that the slope movement took place some time after the valley was formed. The main movement within the landslide appears to be related to the effect of renewed erosion resulting from the Shell Creek landslide which displaced the Salmon River to the northwest side of the valley, thus undercutting the Jupiter Creek slope.

It is evident that movement has taken place at different times throughout the history of the Jupiter Creek landslide. Within the frontal debris slope, pod-like accumulations of white silt deposits are found. These were first thought to be volcanic ash deposits. However, only two locations yielded sufficient shards for analysis and these were located in debris at the foot of Zone 3 (Fig. 4.9). Analysis by N.Catto showed them to be reworked Mazama Ash deposited approximately 6640 years B.P. (Clague, 1981). The disposition of the deposits indicates that the ash layer was disrupted by movement in this Zone, suggesting that movement has taken place since 6640 years B.P.

(d) The Macrostructure of the Jupiter Creek Shear Zone

The rupture zone of the Jupiter Creek landslide is exposed along the base of Zone 2 in several roadside exposures (Plate 4.15A) The exposure consists of highly fragmented calcareous shear matrix of brecciated Salmon River Tuff with disoriented inclusions of pyroclasts and larger fragments of unbroken rock up to 1m in diameter. These larger fragments appear to have been rounded by the movement.

Plate 4.14 Jupiter Creek landslide debris overlying gravels at base of Zone 3.

A1 - DEGRADED SALMON RIVER TUFF. NOTE LARGER FRAGMENT
OF MATERIAL ENCLOSED IN SHEAR MATRIX. VERTICAL
SLICKENSIDES ARE SEEN AT V.

A2 - CLOSE UP OF AREA OUTLINED IN A1. FRAGMENT-
SHEAR MATRIX BOUNDARY.

B - PLANAR SHEAR SURFACE WITHIN SHEAR MATRIX.

Plate 4.15 Rupture zone of Jupiter Creek landslide.

Steeply dipping, discontinuous closely spaced non–planar surfaces up to 20 cm long occur throughout the shear matrix and dip into the slope, opposite to the direction of movement. Some are curved around the inclusions (Fig. 4.13) suggestive of flowage but also may reflect the presence of non–uniform shear strength within the shear zone (cf. Lupini *et al.* 1981). Superimposed on this fabric are sub–horizontal, persistent shear surfaces, (Plate 4.15B), indicative of a later phase of movement. In detail, these consist of a highly friable shear matrix approximately 1 cm in thickness bounded by slickensided clay surfaces oriented parallel to the direction of movement.

A comparison of the undisturbed tuff with the sheared tuff under the reflected light microscope indicates that there has been a general disturbance of the fabric of the intact material. It is evident from the thickness and characteristics of the shear breccia that movement has not taken place along structural elements such as bedding planes and joints, but that within the height of the exposure it has involved the shearing of intact Salmon River Tuff.

4.7.2 The Shell Creek Landslide

The Shell Creek landslide is a massive slope movement of great complexity, located opposite the Jupiter Creek landslide (Plate 4.16). The landslide is 2050 m wide at its widest point and approximately 2000 m long from headscarp to foot, affecting a slope with a maximum height of 730 m. The movement covers an area of 4.1 km^2 and the volume of the debris may approach 1×10^9 m^3.

(a) Morphology

A contour map and slope profiles of the landslide and adjacent slopes are found in Fig. 4.14. Pre–movement slopes were reconstructed as explained in section 4.7.1. A profile based on an altimeter traverse of the landslide debris is shown in Fig. 4.15. As shown in Figure 4.16, the landslide can be divided into three distinct areas on the basis of aerial photograph interpretation and field observation.

Zone 1-Head and Lateral scarps:

Zone 1 consists of the head and lateral scarps, associated debris slopes and the lateral margins consisting of linear segments (Fig 4.16). The headscarp is a high wall–like rock slope trending 251°, along parts of which several detached slide blocks are found. They
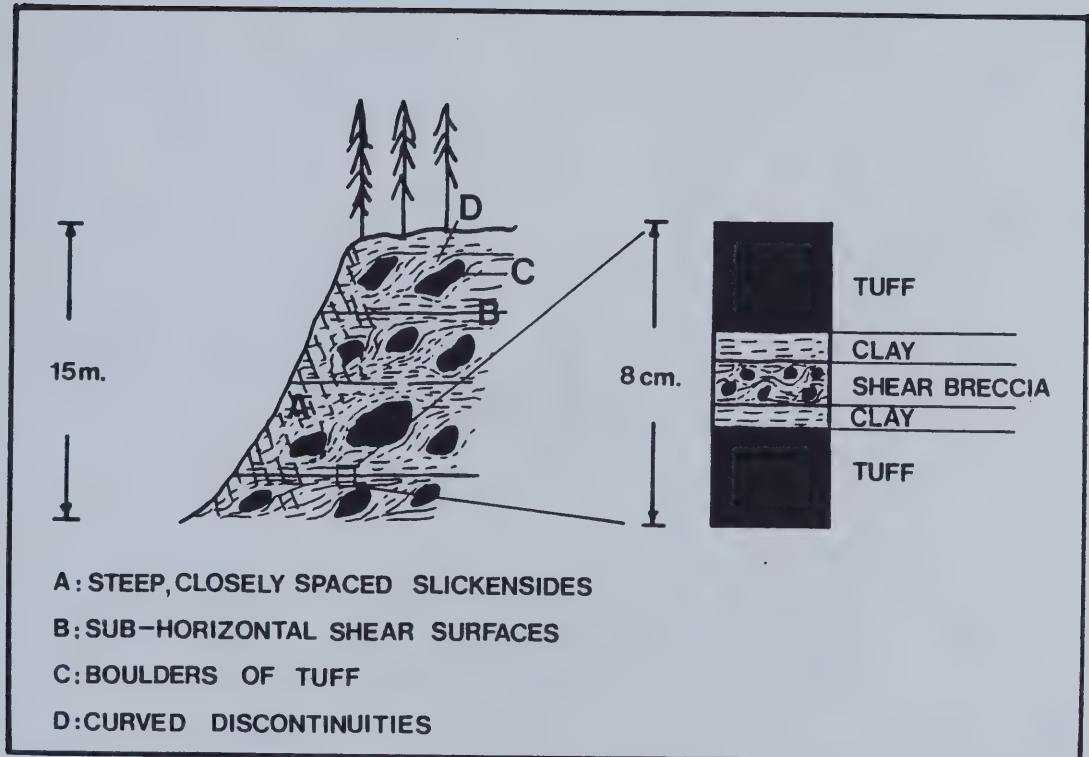
Figure 4.13 Sketch of structural elements of shear zone, Jupiter Creek landslide.

500 M
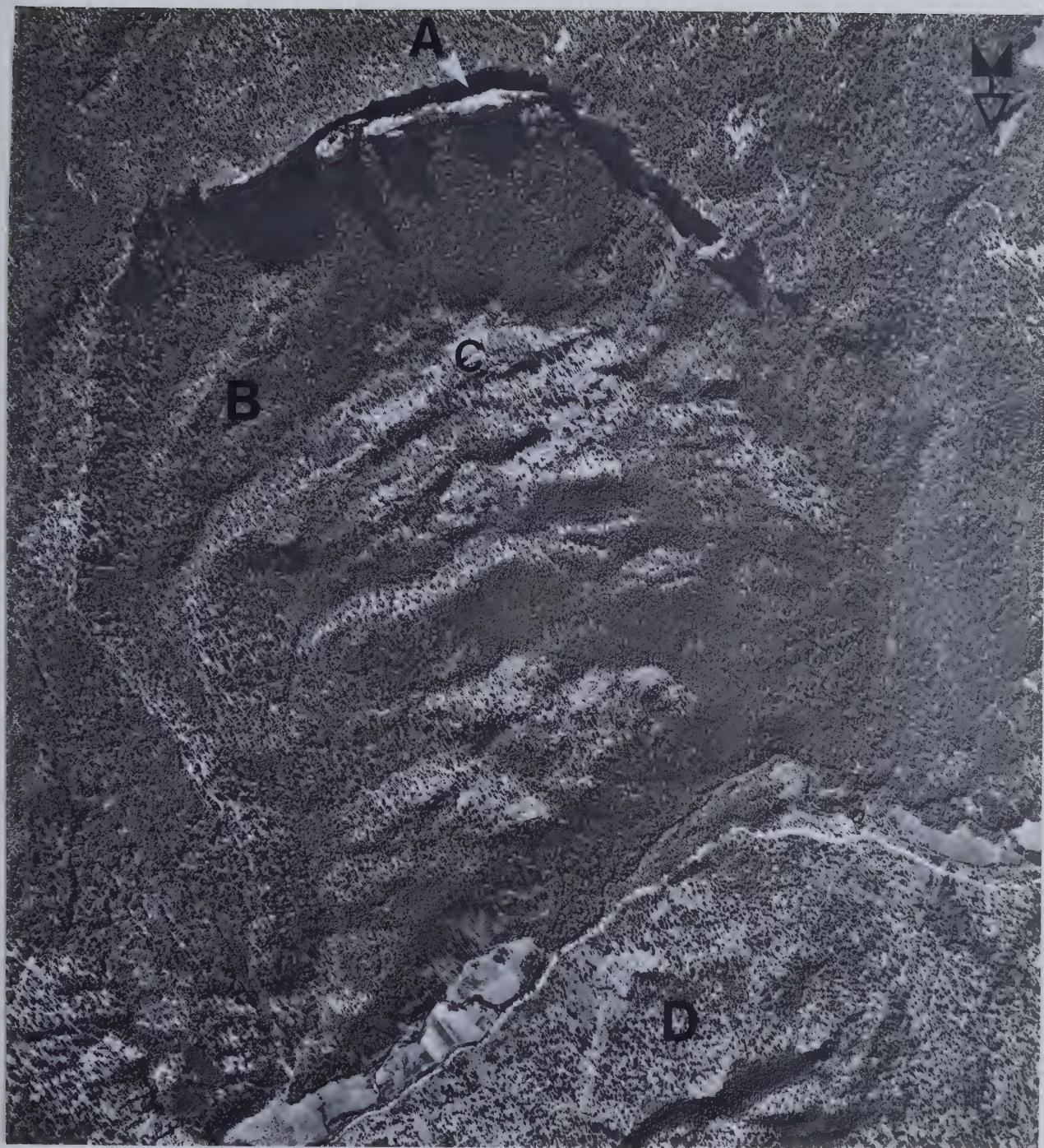
KEY : A=GRABEN AT HEADSCARP, B=SLUMP BLOCK ON EAST LATERAL SCARP, C=THE JUMBLES, D=JUPITER CREEK LANDSLIDE.

Plate 4.16 Aerial photograph of Shell Creek landslide (BC 4409-134).
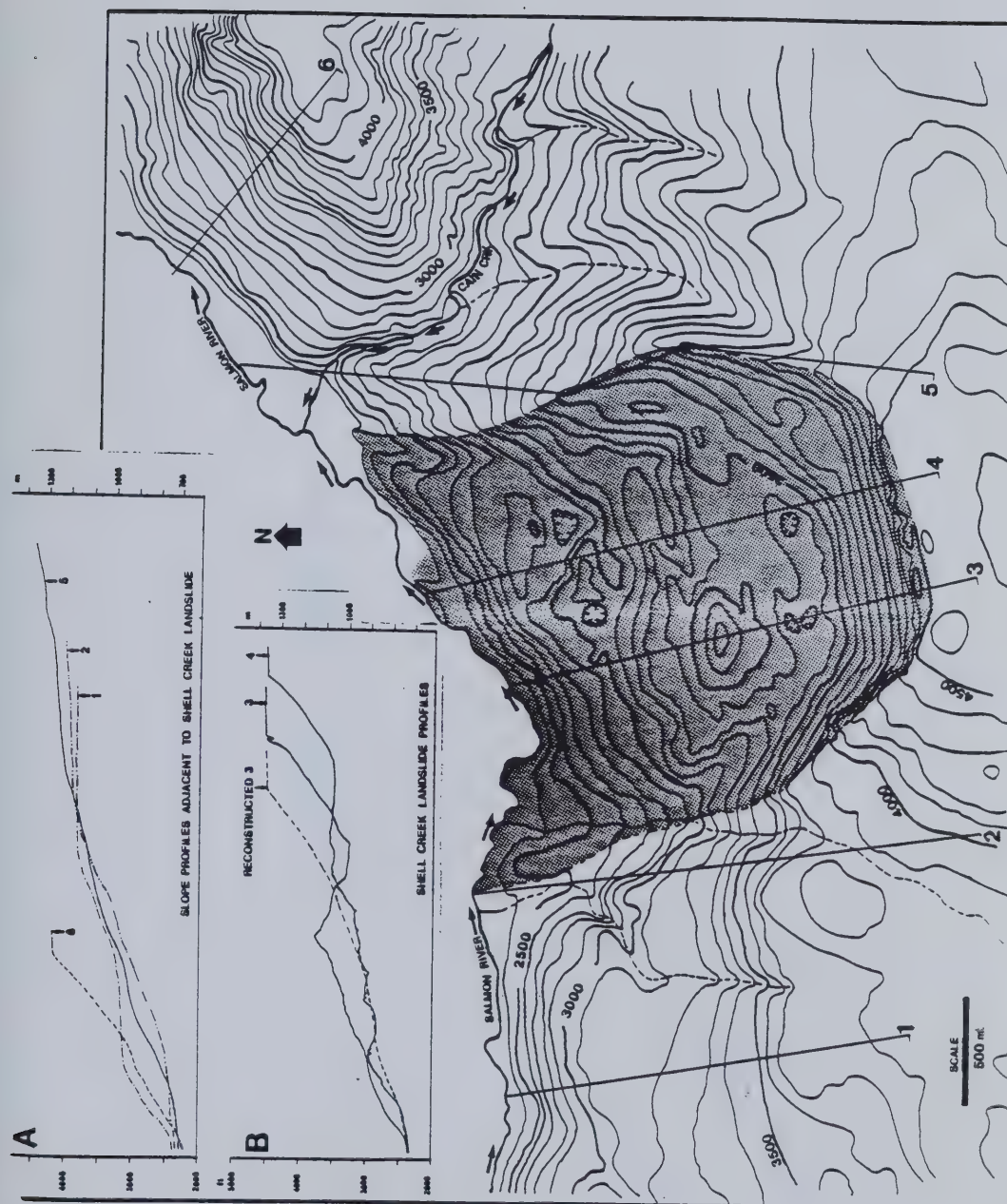
Figure 4.14 Contour map and slope profiles of the Shell Creek landslide and adjacent slopes.
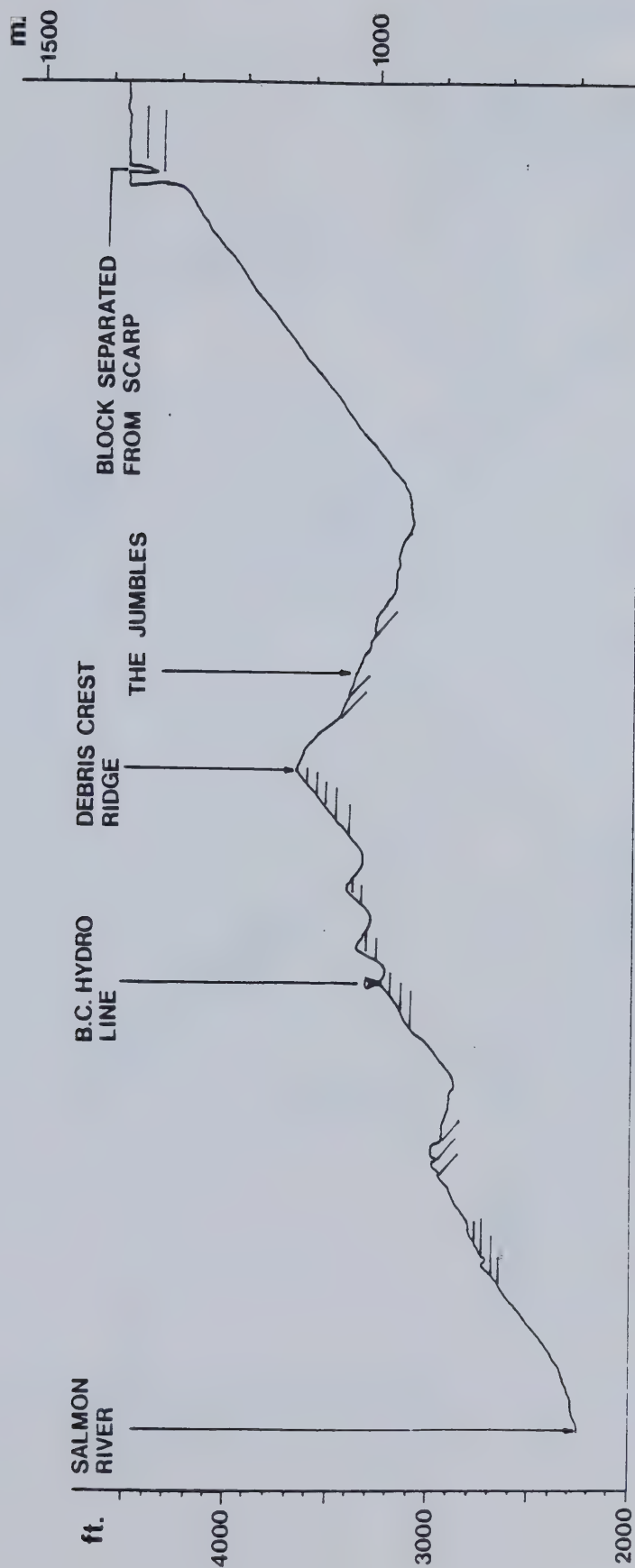
Figure 4.15 Profile of the Shell Creek landslide based on an altimeter traverse of the debris. Lines beneath the profile line suggest attitudes of strata encountered in traverse.
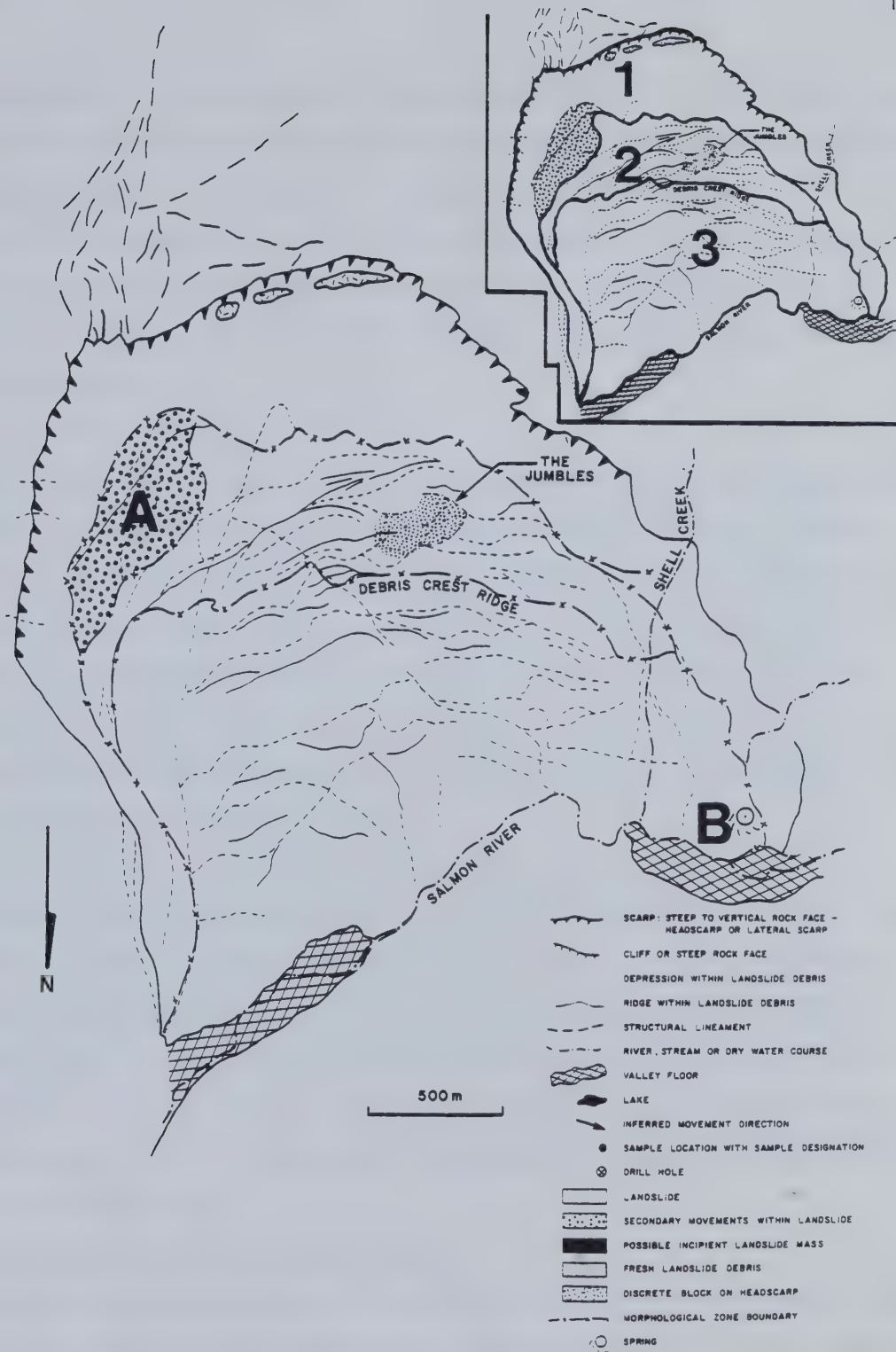
Figure 4.16 Morphology of Shell Creek landslide based on interpretation of air photograph BC 4409-134. A=slump blocks on east lateral scarp, B=spring. Inset shows morphologic zones.

are separated from the headscarp by a graben feature (Plate 4.17). The east lateral scarp is also linear and well-defined, although not steep and wall-like. Secondary movement has taken place (Fig. 4.16) on the east lateral scarp where a marked rotational slide block is noted. Below an elevation of 1180 m, the east lateral margin trends 145°. The west lateral scarp is a nearly vertical precipitous wall trending 139° (Plate 4.18), but below elevation 1060 m the west lateral margin is diffuse, possibly reflecting a pre-movement gully or small valley.

Zone 2-Debris behind Debris Crest Ridge:

Zone 2 consists of the landslide debris behind the debris crest ridge and exhibits rugged irregular topography (Plate 4.19). The sharp ridge and hollow topography reflect the presence of interlocking almond-shaped ridges and steep-sided, flat-topped blocks in which the beds generally show little or no rotation. Ridge spacing is in the order of 90 m and the intervening hollows are up to 35 m deep. At what was termed "The Jumbles", steep scarp-facing, smooth surfaces were found, which may indicate under-thrusting in the debris (Plate 4.20), and backward rotation was also observed due to "bunching" behind "The Knob" (Fig. 4.15 and 4.16, Plate 4.19).

Zone 3-Debris in front of the Debris Crest Ridge:

The area consists of much larger blocks (Fig. 4.16) with much deeper and wider intervening hollows indicative of greater distension (Plate 4.21). Ridge spacing is in the order of 200 m and only local rotation or piling up is observed. Blocks are less common in the western part of Zone 3. Some of the block boundaries are precipitous and appear to be structurally controlled. Locally, rockfall and toppling take place on these boundaries. The lower margin of Zone 3 is a steep, heavily vegetated debris slope that slopes at 35° down to the Salmon River, (Fig. 4.15).

(b) Relationship to Stratigraphy and Structure

An attempt was made to reconstruct the geology of the pre-movement slope by traverse around the landslide. The reconstruction is complicated by two factors. First, normal faults traverse the slide and have resulted in uncertain vertical displacements of beds within the slope. Second, an anomalous exposure of Salmon River Tuff between the elevations of 884 m and 760 m was found along Shell Creek. This thickness is not exposed elsewhere. Sheared Salmon River Tuff was found near the western margin of
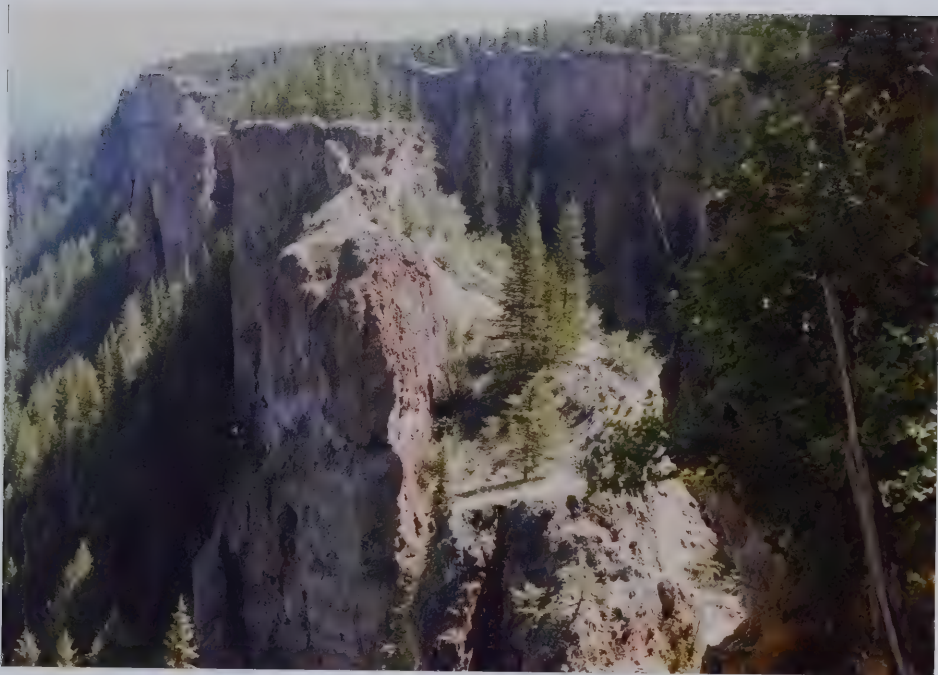
Plate 4.17 Blocks and graben feature at headscarp, Shell Creek landslide. View to the east.

Plate 4.18 West lateral scarp of Shell Creek landslide. Note high wall-like nature of scarp and persistent vertical joints. View to the west.

Plate 4.19 View westward, from east lateral scarp, into Zone 2, Shell Creek landslide. J= The Jumbles, K=The Knob.

Plate 4.20 Scarp facing surface, suggesting underthrusting, at The Jumbles, Shell Creek landslide.

KEY ; A=SLUMP BLOCK ON EAST LATERAL SCARP. B=EAST LATERAL
SCARP. NOTE ABSENCE OF HIGH WALL-LIKE ROCK SLOPES.
C=HIGH WALL-LIKE ROCK SLOPE OF WEST LATERAL SCARP.
D=HEAD SCARP WITH BLOCKS SEPARATED FROM HEAD OF
SLIDE BY GRABEN AND TENSION CRACKING.
DASHED LINE IS DEBRIS CREST RIDGE.

Plate 4.21 Shell Creek landslide from the scarp of Jupiter Creek landslide. Note Jupiter

Creek landslide in foreground and transmission towers circled for scale.

the Shell Creek landslide along the Salmon River (Plate 4.8). Faulting has displaced rocks in the eastern part of the pre-movement slope upward, and in this part of the landslide the rupture zone may involve the Twig Creek volcaniclastics or the sub-Paleogene surface. In the absence of suitable exposure, however, the relation between the rupture zone location and stratigraphy remains uncertain. The inferred stratigraphical relations presented in Figure 4.17 are, therefore, tentative only.

The overall true dip of the beds around the margins of the landslide was calculated to be 092/9. Given that the initial movement direction in the landslide was 350°, shearing took place in beds with an average apparent dip of 1° into the slope. Given the variability of dips around the scarp this apparent dip could vary between 0° and 5° into the slope in a direction opposite to movement.

In Figure 4.11 the location of the Shell Creek landslide can be seen in relation to the lineaments discussed in Section 4.6. The landslide occurs between two well-defined lineaments which are inferred to be faults and which define the east lateral scarp and part of the west lateral margin.

A lack of accessible exposure has limited the amount of joint survey work undertaken but in Figure 4.12, pole concentrations are given for an outcrop behind the headscarp. Two joint sets are represented by these concentrations, the first being a series of near vertical joints dipping between 85° and 90° with a strike of 144°, and the second dipping at 70° with a strike of 248°. The strike of these joint sets approximates the orientation of the west lateral scarp and main headscarp, respectively (Fig 4.12).

(c) Kinematics and Movement History

The direction of movement within the debris was inferred from the orientation of block boundaries (Fig. 4.18). Initial movements were perpendicular to the headscarp followed by secondary movements along the lateral scarps (Fig 4.18). Slight rotation of slide blocks in the horizontal plane took place towards the direction of true regional dip. A complex and multiple movement therefore took place. The western part of zone 3 did not undergo as much distension as the east side. As can be seen in Fig. 4.14, profiles down each side of the landslide are dissimilar. Greater movement occurred on the east side which probably resulted in the secondary scarp movement noted in Fig. 4.16. This increased movement may have resulted from an initial movement phase or a later re-activation.
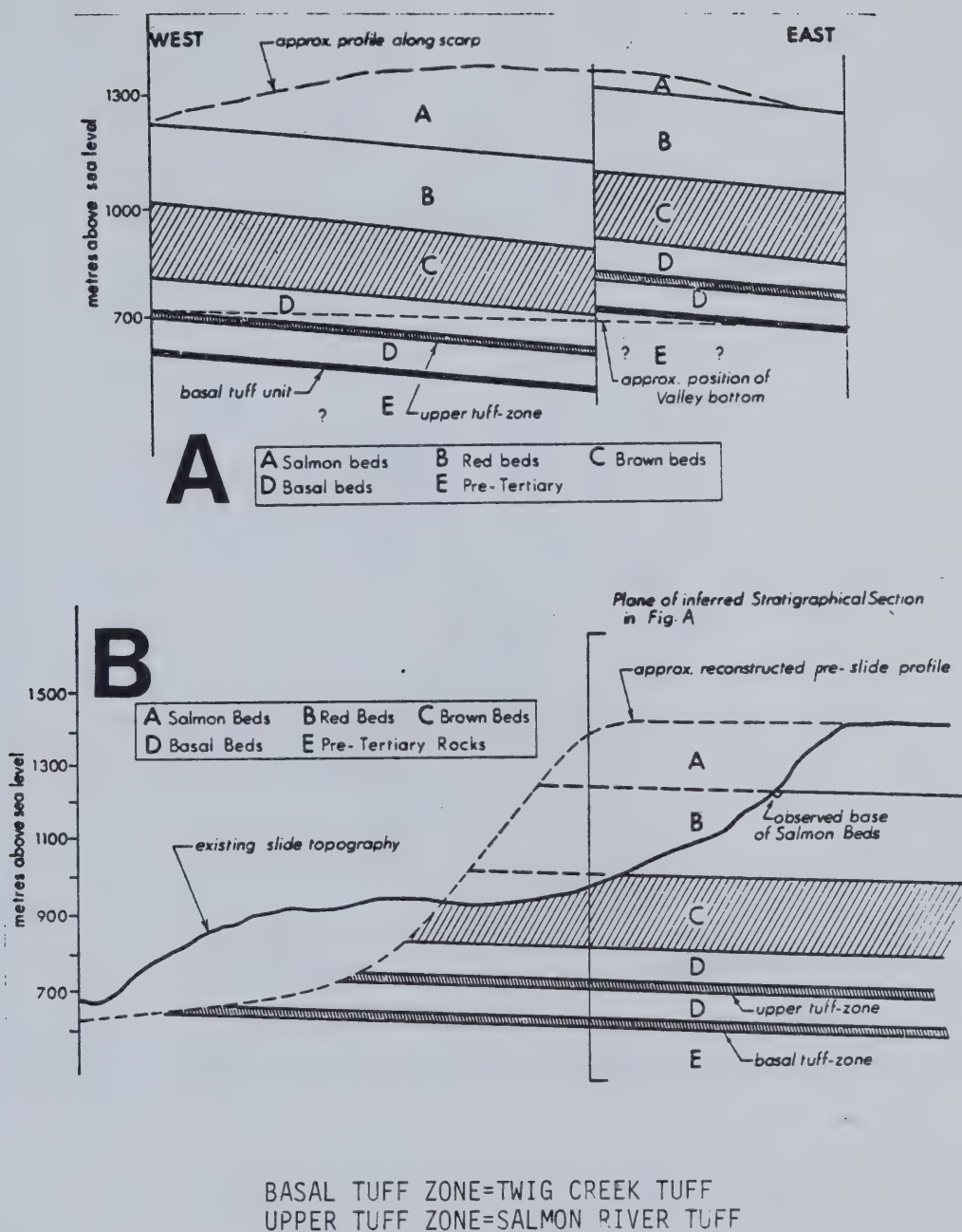
Figure 4.17 Inferred geological cross sections of the pre−movement slope. Shell Creek landslide.   A=Transverse to movement, B=Parallel to movement.
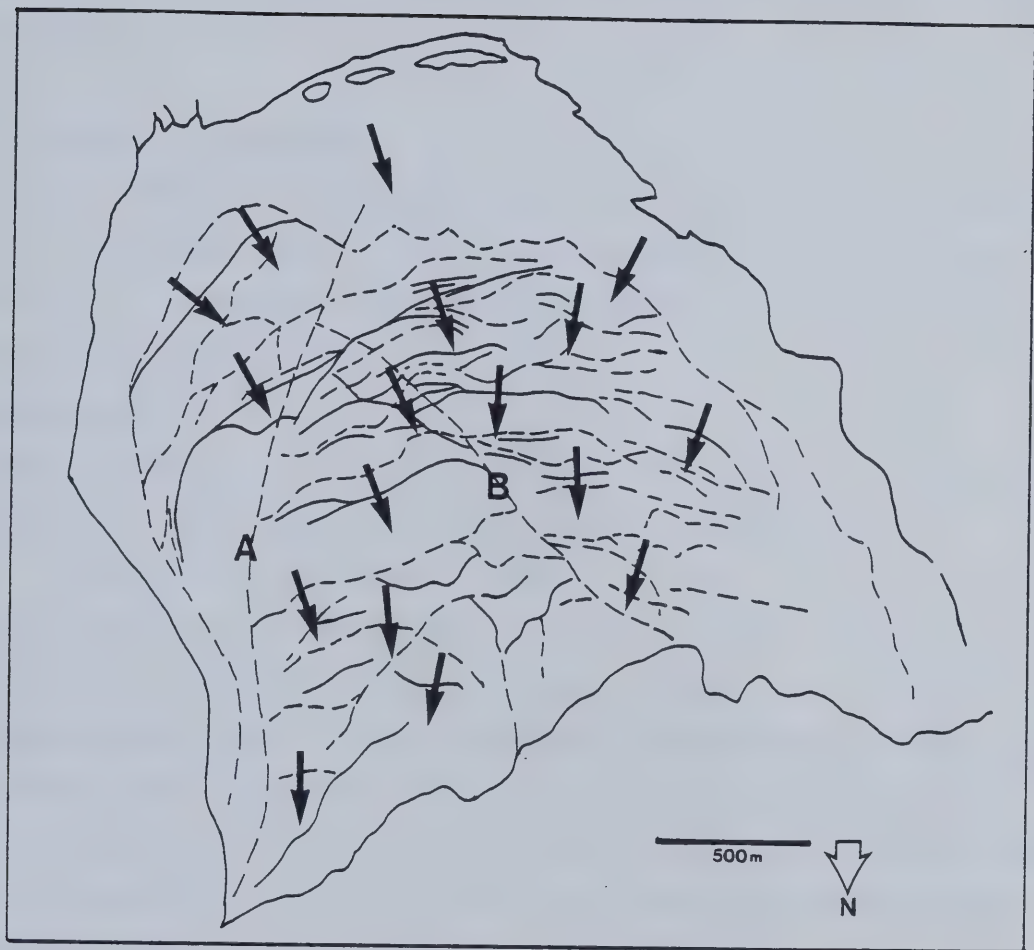
Figure 4.18 Inferred movement direction within the Shell Creek landslide debris. A and B are lineaments within the debris discussed in the text.

Lineaments within the debris (A and B in Fig. 4.18) are suggestive of preserved fault lines within the debris or lateral shear planes related to recent movement. However, no movement has been detected on the B.C. Hydro transmission line which traverses the debris since its construction in the early 1970s. The debris is heavily vegetated and extensive organic soil development in parts of the debris suggests a substantial age for the Shell Creek landslide.

4.7.3 Adelphi Creek Landslide

The Adelphi Creek landslide (Plate 4.22) is a simple massive movement located 8.5 km southwest of Westwold. The landslide involves an area of 2.62 km^2 along a valley length of 2 km. The volume of the landslide, which affects a slope with a maximum height of 550 m, is approximately 9.6×10^8 m^3

(a) Morphology

A contour map and a cross section of the landslide are shown in Fig. 4.19. As can be seen in Figure 4.20, the landslide can be divided into three morphological zones.

Zone 1-Head and lateral scarps and associated debris slopes.

As can be seen in Plate 4.22 and Figure 4.20 the scarp is compound in nature. The west lateral scarp is wall-like, trending 320^0. The headscarp is segmented and embayed by erosion along discontinuities. The east lateral scarp is not well defined and exhibits few exposures. Below elevation 900 m it becomes indistinct and merges with surficial deposits which results in the north-eastern boundary being difficult to distinguish, both on aerial photographs and in the field. The linear nature of the east lateral scarp suggests structural control.

Area 2: Area behind the Debris Crest Ridge

This is similar in morphology to the graben in the Shell Creek and Jupiter Creek landslides, consisting of interlocking almond-shaped ridges and blocks, and the beds within the blocks show no rotation. Although steep-walled block boundaries were traversed, the topography of this part of the landslide is much more subdued when compared to the other landslides discussed, due to infilling of hollows by organic soil and pebbly surficial materials. The debris crest ridge is prominent and a marked linear reverse slope is noted (Plate 4.22).

500 M

Plate 4.22 Aerial Photograph of Adelphi Creek Landslide (A) and Adelphi Creek Bluffs (B) (B.C. Air Photograph BC7675-171).
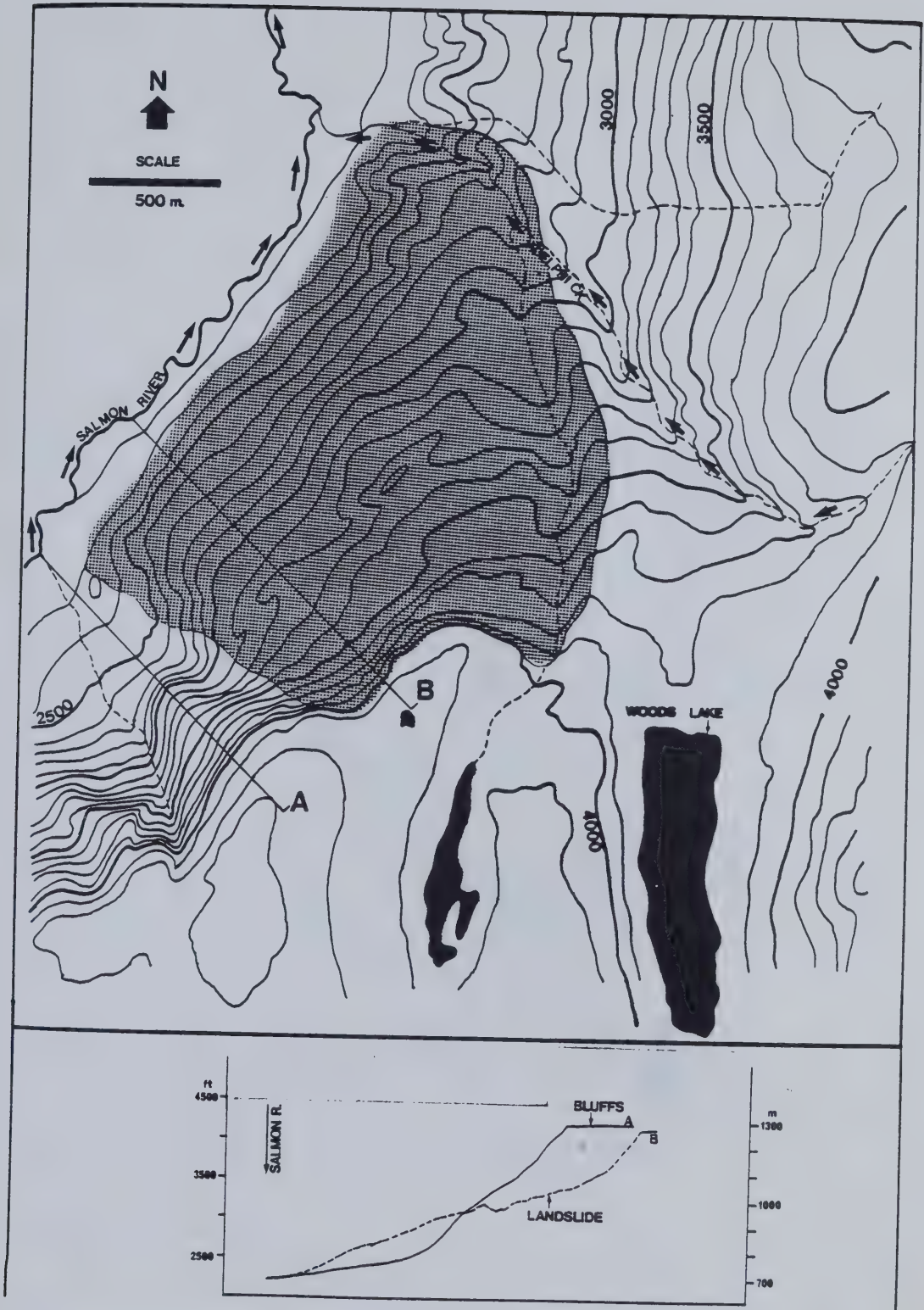
Figure 4.19 Contour map and slope profiles of Adelphi Creek Bluffs and Adelphi Creek Landslide.
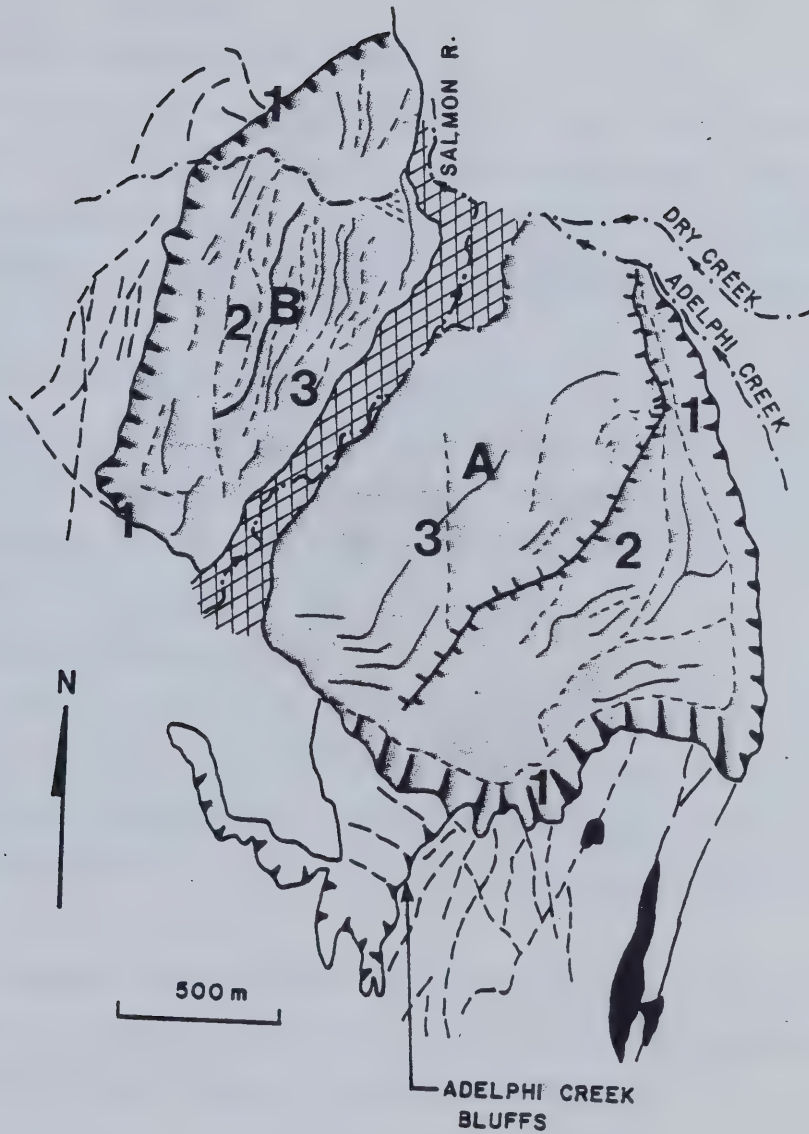
Figure 4.20 Morphology of Adelphi Creek (A) and Stephen's Lake Road (B) landslides based on B.C. Air Photograph BC 1352-112

Zone 3: Area beyond the Debris Crest Ridge

This consists of subdued, ridged topography. The cover of surficial materials becomes important below an elevation of 86.1 m. These include pebbly diamictons and varved glacio-lacustrine silt. At the southwest extremity of the landslide, low fluvial terraces abut against the foot of the debris.

(b) Relationship to Stratigraphy and Structure

The lower part of this landslide has an extensive road network with road-cut exposures. Highly disturbed, sheared Twig Creek Tuff equivalents, named the Hummingbird Tuff, containing Chapperon schist fragments are found at various locations throughout the debris in these exposures and it is concluded that this represents the exposed rupture zone (Plate 4.23).

Remote dip measurements on scarp exposures give an overall true dip of rocks in the landslide area of 277/5 which results in the apparent dip of $2°-4°$ in the direction of movement ($3.12°$). Discontinuity surveys were only possible in Palaeozoic Chapperon schists exposed at the base of the landslide (Fig.4.3), and an absence of discontinuity sets unfavourable for slope stability is noted in these rocks.

(c) Kinematics and Movement History

The well preserved linear debris crest ridge indicates that the slide mass had unusual coherence, and perhaps indicates one phase of movement along a basal shear plane. This is also reflected in the smaller number of slide blocks and ridges within the debris. Movement was dominantly extensional and gave rise to the well-marked graben noted in Plates 4.22 and 4.26.

The extensive cover of surficial deposits in the lower part of the landslide and the presence of river terraces at its foot indicate that movement may have taken place prior to the deposition of these late glacial – early post-glacial deposits.

4.7.4 Adelphi Creek Bluffs

The high steep face at the southwest margin of the Adelphi Creek landslide (Plate 4.22) was termed Adelphi Creek Bluffs. During traverses around the Bluffs and on the upland surface behind, indications that the slope has undergone limited movement were observed. These indications included the existence of tension cracks over 3 m wide at the

Plate 4.23 Exposed shear zone of Adelphi Creek landslide. Note Hummingbird Tuff which
contains Chapperon Schist fragments (H) and fluvioglacial boulders (F).

crest of the Bluffs (Plate 4.24) , the existence of a series of steps down from the plateau level to the edge of the Bluffs, indicating that differential vertical movement had taken place (Plate 4.22), and limited downslope displacement of less than 10 m along discontinuities between blocks on the Bluffs (Plate 4.25). Based on this evidence, the slope was considered to be in limiting equilibrium.

As mentioned in Section 4.5, the stratigraphy of the Bluffs was established by indirect means from the opposite side of the valley, using a plane table and telescopic alidade. The stratigraphy (Fig. 4.21) indicates that both the Twig Creek and Salmon River Tuffs are exposed near the base of the slope. A basal shear surface (or zone) within either of the tuffs dipping toward the valley at between 2° and 4° is suggested.

The moved mass has an area of approximately 0.94 km^2 and appears to be defined by linear fracture traces, evident on aerial photographs , that trend 025 and 320 (Fig. 4.22). The limited movement in the rock mass is due in part to the berm effect of the Adelphi Creek landslide debris in the northeast part of the rock mass (Fig. 4.22).

It is concluded that this berm effect, together with the lateral forces at the southwest margin of the rock mass, accounts for the limited movement exhibited in the Bluffs. It is probable that the movement was a response to the Adelphi Creek landslide event.

4.7.5 Stephen's Lake Road Landslide

This is the smallest of the Salmon River landslides (Plates 4.26 and 4.27) investigated, having an area of 1.25 km^2 along a valley length of 1.75 km. The landslide involves a volume of approximately 2 x 10^8 m^3. It is located opposite the Adelphi Creek landslide.

(a) Morphology

A contour map and cross section of the landslide can be found in Fig. 4.23. As shown in Figure 4.21 the landslide can be divided into three morphological zones.

Zone 1: Headscarp and Landslide Margins

The headscarp of this slide is bi-linear, the two segments trending 0.15° and 050°. It is breached by a small creek. Behind the headscarp several linear depressions have been observed; these represent tension cracks (Plate 4.26). There is an absence of lateral

Plate 4.24 Tension crack at the crest of Adelphi Creek Bluffs.

Plate 4.25 Downslope displacement (arrowed) along discontinuity at Adelphi Creek Bluffs.
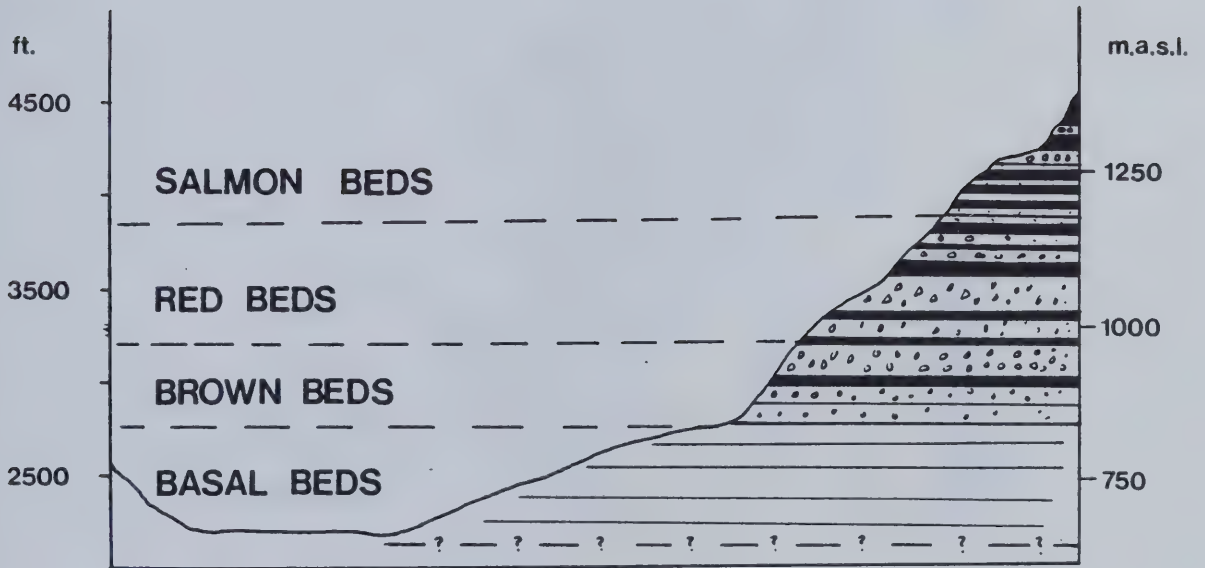
Figure 4.21 Stratigraphy of Adelphi Creek Bluffs obtained by telescopic alidade and plane table from opposite side of valley. Drawn with no vertical exaggeration.
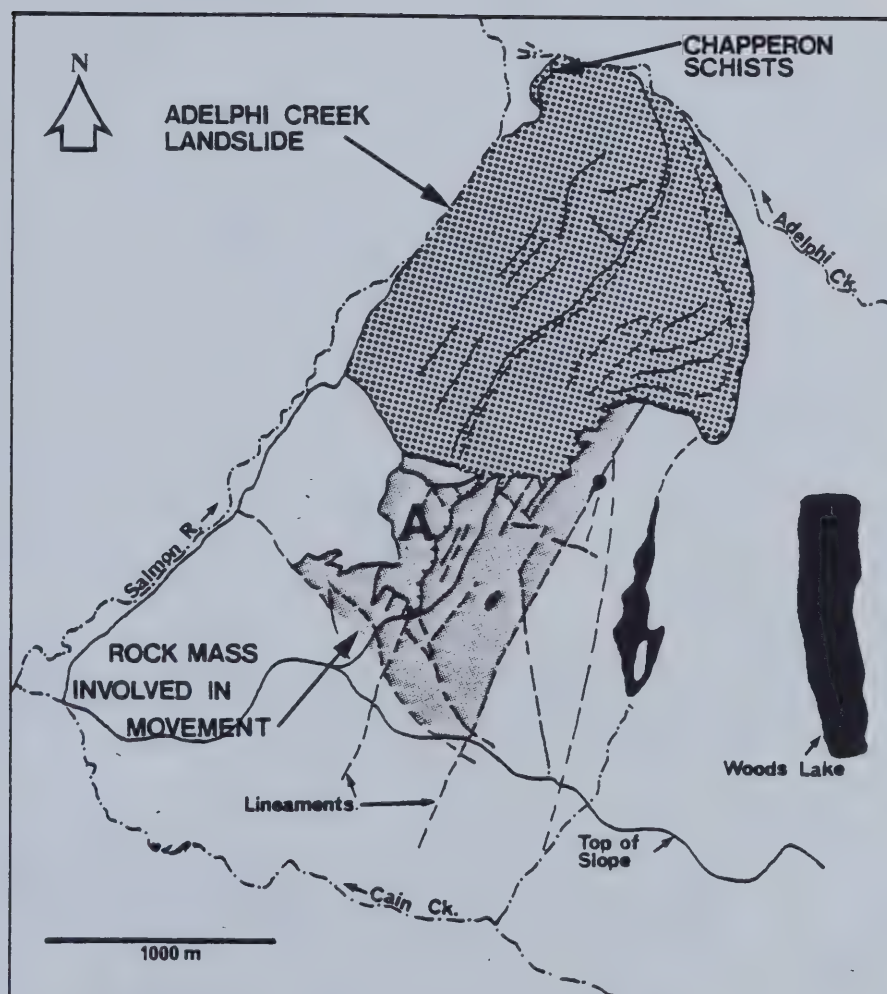
Figure 4.22 Map of Adelphi Creek Bluffs area, showing inferred extent of rock mass involved in movement. Note fracture traces. Based on air photograph BC 5187-168.

1 KM

Plate 4.26 Air photograph of Adelphi Creek landslide (A) and Stephen's Lake Road landslide (S). Note also Woods Lake (W) and Jupiter Creek landslide (J). (BC5 187–168).

Plate 4.27 View to the north of Stephen's Lake Road landslide.
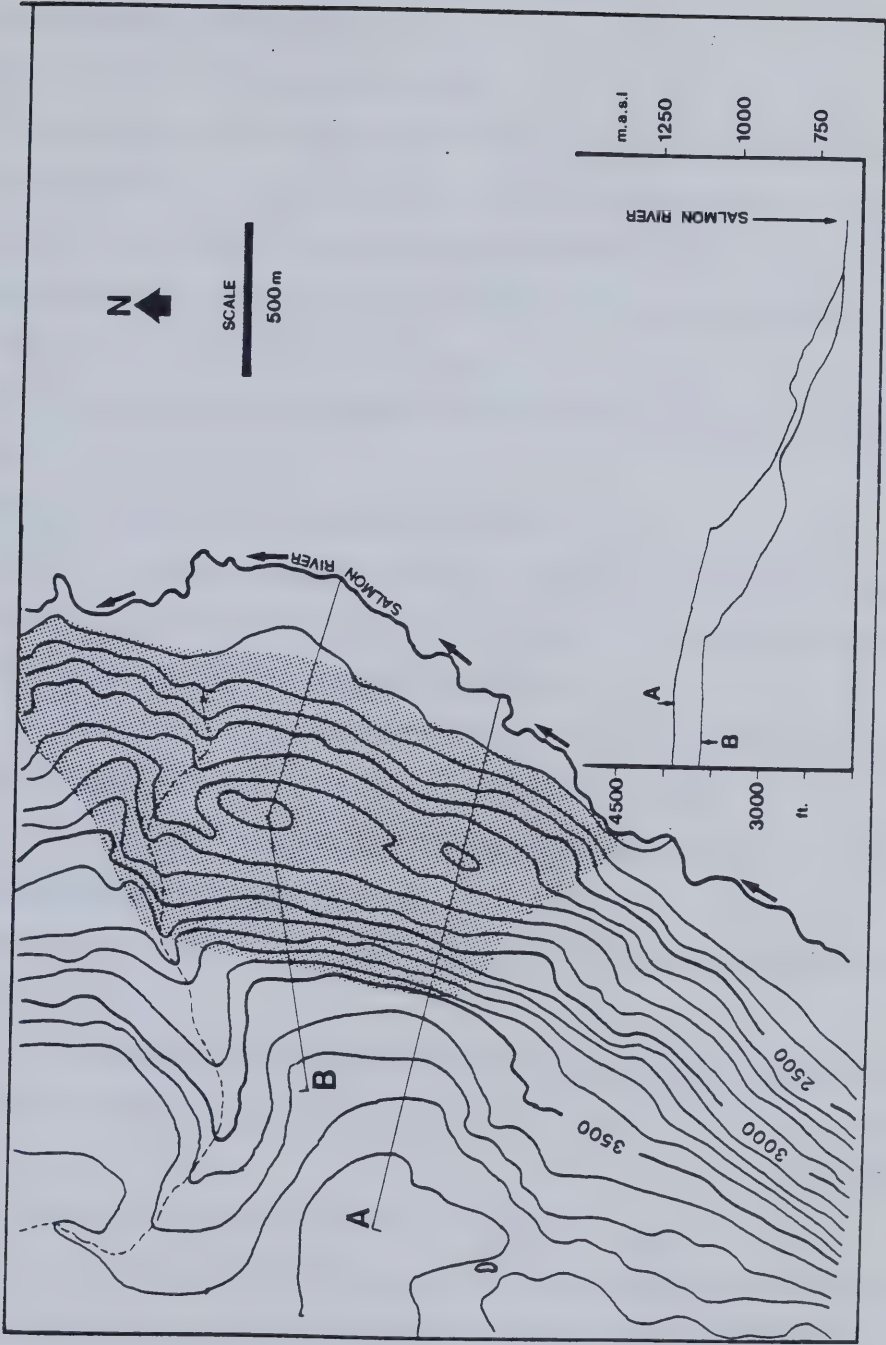
Figure 4.23 Contour map and slope profile of Stephen's Lake Road landslide.

scarps. The northeast margin of the landslide is diffuse but the southwest margin is clearly distinguishable. It is linear and corresponds to the southwest margin of the Adelphi Creek landslide, trending 320^0.

Zone 2: Behind the Debris Crest Ridge

This resembles Zone 2 in the Adelphi Creek slide and exhibits similar interlocking slide blocks and ridges separated by an interconnected system of hollows and depressions. Again, as compared to the Jupiter Creek and Shell Creek landslides, the topography is subdued due to an extensive cover of organic soil and pebbly diamicton.

Zone 3: Beyond the Debris Crest Ridge

Similar subdued ridges and hollows merge with surficial deposits at lower elevations (Plate 4.26).

(b) Relationship to Stratigraphy and Structure

Movement is thought to have taken place in the basal tuffs as at the Adelphi Creek landslide. This conclusion is based on the exposure of Chapperon schist and basal basalt at the northeast margins of the landslide debris.

The mean true dip of beds in the landslide area is $135^0/8^0$, yielding an apparent dip into the valley of 6^0 along a direction of movement of 092^0.

Lack of accessible exposures precluded detailed structural mapping.

(c) Kinematics and Movement History

The movement appears to be dominantly translational along a basal surface. No rotation is seen in the debris.

Slide debris overlies fluvioglacial gravels at the foot of the slide, suggesting an early post-glacial date for the landslide.

4.7.6 Discussion on Salmon River Landslides

Four large block type-landslides have been examined in a structurally complex Paleogene volcanic succession in the Salmon Valley. The succession is dominated by inter-bedded basaltic lava flows and thick volcanic breccias. Two weak volcaniclastic layers occur within 120 m of the base of the succession and landsliding has occurred where these strata were exposed at the base of the pre-movement slopes. The estimated volume of each of the landslides exceeds 2.0×10^8 m³.

The landslides show a similarity in morphology characterised by :

a.　high, near vertical head and lateral scarps;

b.　the presence of a graben in the debris at the foot of the scarp consisting of interlocking ridges and blocks separated by steep sided depressions up to 60 m deep.

c.　a debris crest ridge which marked the downslope boundary of the graben;

d.　a frontal zone of distended blocks downslope of the debris crest ridge which is either terminated by a steep debris slope, as in the case of the Shell Creek and Jupiter Creek landslides, or a gentler slope which blends into surficial deposits at the foot of the debris as at the Adelphi Creek and Stephen's Lake Road landslides.

A reconstruction of the kinematics of the Jupiter Creek and Shell Creek landslides, based on observations of debris morphology and reconstructed profiles is given in Fig. 4.24. It is noted that the frontal blocks were subject to dominantly horizontal movement and that the debris crest ridge was located on the face of the pre-movement slopes.

Results of geological mapping indicate that the basal shear surface or rupture zone is located in one of two weak volcaniclastic layers (the Twig Creek and Salmon River Tuffs), which as mentioned above, occur near the base of the succession. These rocks show a high degree of alteration and structural disturbance and contain filled discontinuities and pre-sheared surfaces. The steep back surface is located in the overlying cap of lavas and breccias.

The effect of stratigraphy on slope stability is seen in the field slope stability chart in Fig. 4.25. In the absence of a tuff layer at the slope base , high, steep slopes may exist that show no evidence of slope movement, whereas landslides have only taken place where tuff layers have been present. The position of the Adelphi Creek Bluffs slope, where evidence of movement has been observed, is noted.

The morphology of the block movements and the fact that they exhibit little or no rotation suggests a strongly bi-linear rupture surface consisting of a sub-horizontal basal shear surface, or rupture zone, and a steep back surface. The morphologies of the landslides are therefore compatible with either a translational sliding or spreading slope movement mechanism.

A – APPROXIMATE RECONSTRUCTED PRE-MOVEMENT PROFILE ALONG PROFILE B IN FIG. 4.8 AND PROFILE 3 IN FIG. 4.14. INITIAL SLOPE MOVEMENT IN SHELL CREEK LANDSLIDE TAKES PLACE.

B – SHELL CREEK LANDSLIDE TAKES PLACE. NOTE POSITION OF DEBRIS CREST RIDGE.

C – EROSION OF HATCHED AREA TAKES PLACE,UNDERCUTTING JUPITER CREEK SLOPE , AND RESULTING IN INITIAL MOVEMENT OF JUPITER CREEK LANDSLIDE.

D – JUPITER CREEK LANDSLIDE TAKES PLACE. NOTE POSITION OF DEBRIS CREST RIDGE.

E – EROSION OF HATCHED AREA RESULTING IN EXISTING PROFILE

Figure 4.24 Reconstruction of the kinematics of the Jupiter Creek and Shell Creek landslides.
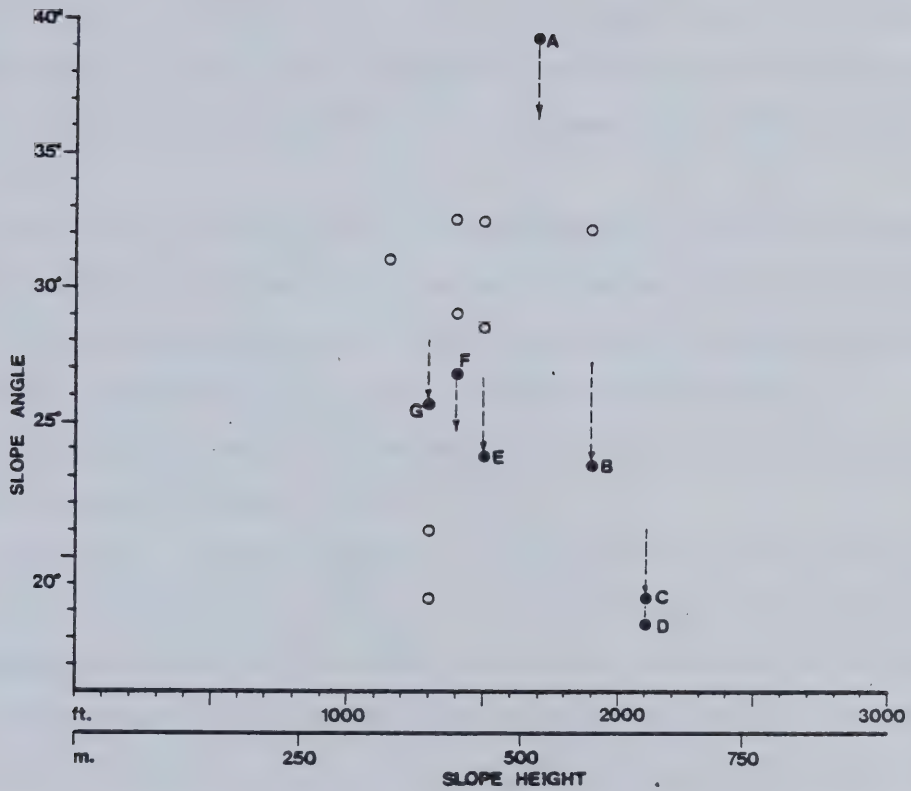
Figure 4.25 Field slope stabilty chart for slopes in the Salmon Valley, between Twig and Adelphi Creeks.

If translational sliding has taken place, movement has taken place obliquely across bedding planes at some angle to the direction of true dip on surfaces which have an apparent dip varying between 6° out of the slope and 1° into the slope. The surfaces were assumed to vary within 5° of the horizontal.

The evidence for spreading is seen in the exposed rupture zone of the Jupiter Creek landslide where the Salmon River Tuff is highly fragmented and structurally degraded (Plate 4.15, Figure 4.13). This evidence indicates that movement has not taken place along discontinuities in the tuff and that movement has involved the rupture of intact rock material.

The direction of initial movement and landslide plan geometry are controlled by the orientation of structural elements within the cap, viz. near vertical faults and associated joints. Both the Shell Ceek and Jupiter Creek landslides show that slight rotation in the debris toward the direction of true dip accompanied slope movement.

The geological controls on slope movement in the Salmon Valley are shown in schematic fashion in Fig. 4.26, (cf. Fig. 2.3).

The history of slope development in the Salmon Valley remains unknown. The relationship between surficial deposits and debris at the Adelphi Creek and Stephen's Lake Road landslides indicates a late glacial age for these slope movements. Shell Creek and Jupiter Creek landslide debris overlies surficial deposits and a later age is suggested. The occurrence of first-time slope movement in the Salmon Valley shows, therefore, a wide distribution in post-glacial time and it would appear that some of the slope movements were not an immediate response to slope geometry changes in late-glacial or early post-glacial time but were delayed failures related to the operation of an unidentified time-dependent process subsequent to final valley formation. A tentative model of post-glacial slope development in the valley is given in Fig. 4.27.

Evidence of current movement was observed in Zone 3 of the Jupiter Creek landslide. At Adelphi Creek Bluffs a rock mass, approximately 0.94 km^2 in area, has undergone limited slope movement in the past without developing into a full scale landslide.

The question of future movement at Adelphi Creek Bluffs together with the possible re-activation of undercut landslide debris (cf. Fig. 4.24) at the Shell Creek and Jupiter Creek landslides deserves further attention.

A : LATERAL SHEAR SURFACES CONTROLLED BY
    NEAR VERTICAL FAULTS
B : BASAL RUPTURE SURFACE WITHIN WEAK TUFFS
C : LANDSLIDE MASS
D : HEADSCARP CONTROLLED BY NEAR VERTICAL
    JOINTS OR FAULT
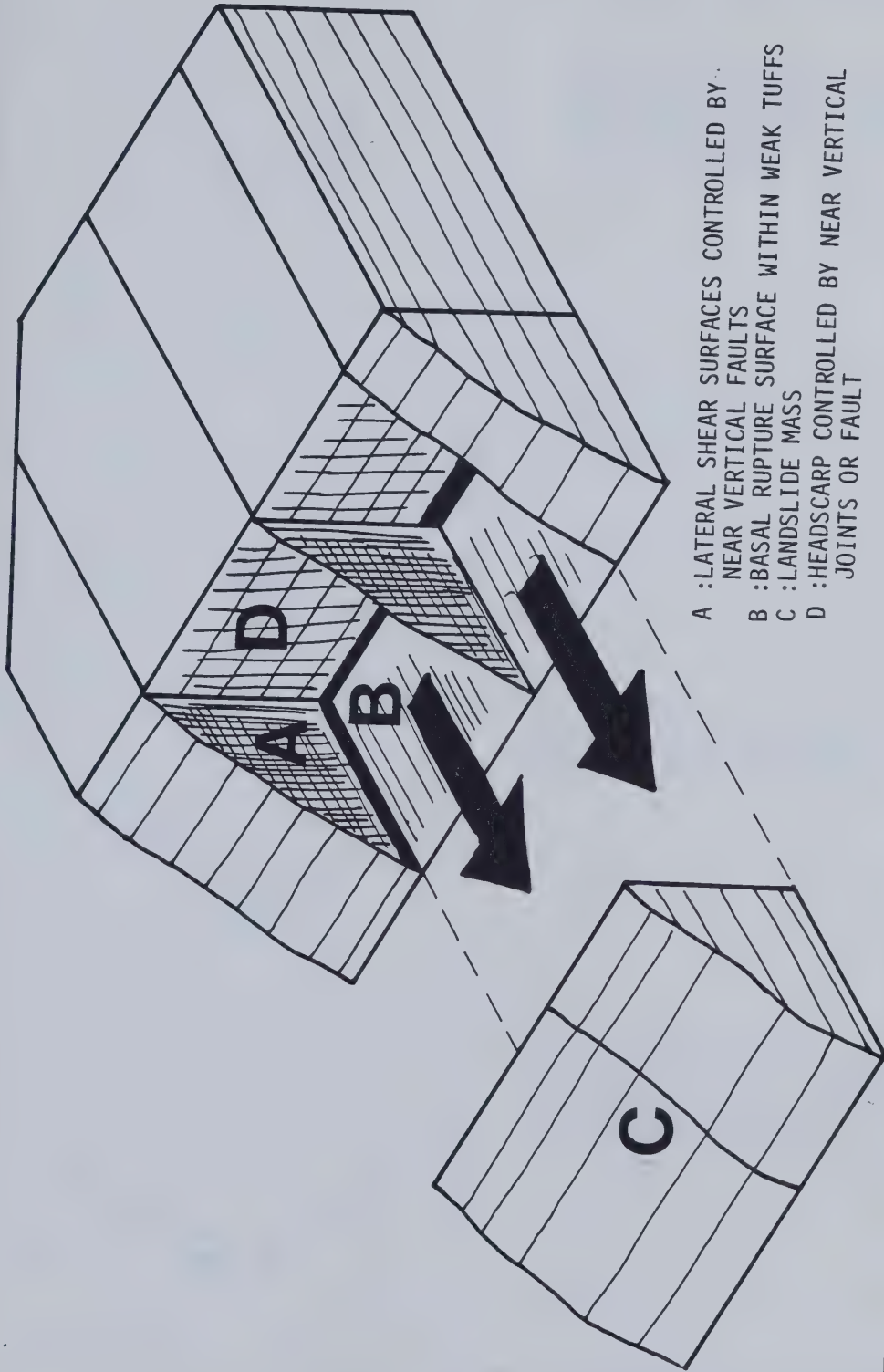
Figure 4.26 Schematic block diagram of geological controls on slope movement in the Salmon Valley.

INITIAL POST-GLACIAL OVER-
DEEPENING. POSSIBLE OCCURRENCE OF
ADELPHI CREEK AND STEPHEN'S LAKE
ROAD LANDSLIDES.

INITIAL POST-GLACIAL
AGGRADATION.

OCCURRENCE OF SHELL CREEK AND
JUPITER CREEK LANDSLIDES.

SECOND POST-GLACIAL OVERDEEPENING
TO CURRENT THALWEG. EXPOSURE OF
DEBRIS-GRAVEL CONTACTS.
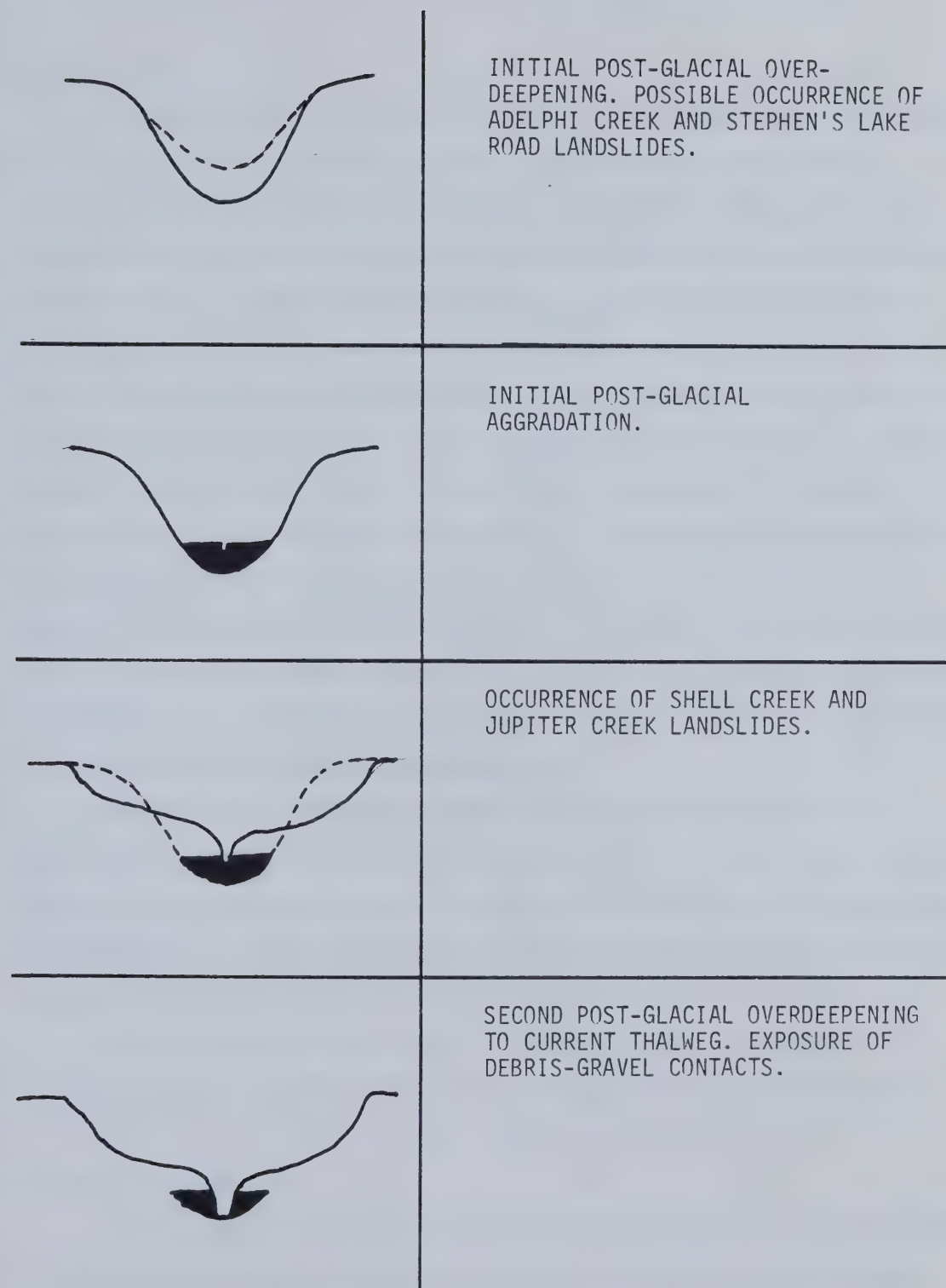
Figure 4.27 Model of post−glacial slope development in the Salmon Valley.

5. MICROSTRUCTURE OF VOLCANICLASTIC MATERIALS

5.1 Introduction

Investigations reviewed in chapter 1, summarised on a regional basis in Chapter 3 and detailed for the Salmon River in Chapter 4, indicated that in layered volcanic successions slope movements were generally localised where a weak pyroclastic or sedimentary layer underlies a resistant cap consisting of lava flows and breccias. Further, all three levels of investigation suggested that slope movements frequently occurred independently of larger structural relations, i.e., through or across weak beds and rarely down dip or along other discontinuities known to exist in basal weak layers. Observations in Chapter 4 on exposed rupture zones also indicated that with respect to the landslides studied in the Salmon Valley, movement has involved the degradation of intact rock material and the production of thick shear breccias. It was on this basis that a study was undertaken of the microstructure of intact rock material, from undisturbed ground adjacent to landslides, material from landslide rupture zones, and from landslide debris in order to ascertain those elements of microstructure that might contribute to weaknesses in the intact rock. In the following chapter these findings are related to the engineering behavior of selected samples of volcaniclastic rock.

Microstructure is defined by Mitchell (1976) as the fabric, composition and inter-particle forces that contribute to the behaviour of a soil (or rock) that cannot be seen by the naked eye. Fabric is defined as the arrangement of particles, particle groups and pore spaces in a soil, whilst composition is defined as the nature and mineralogy of the constituent particles (Mitchell, 1976).

This chapter presents the results of an analysis of the microstructure of volcaniclastic rocks associated with selected landslides described in Chapters 3 and 4.

5.2 Materials Examined

Twenty samples were selected for microstructural investigation; these consisted of Paleogene volcaniclastic rocks from the Salmon and Deadman Rivers and Neogene volcaniclastic materials from exposures along Gorge Creek, Chasm Creek and the Chilcotin River.

The volcaniclastic material was grouped with respect to fabric disturbance as follows;

1. Fabric undisturbed and intact (I), in which the material is taken from blocks that are undisturbed directly adjacent to a landslide or from a stratigraphic unit interpreted to be an important weak layer. In some cases blocks were taken from landslide shear zones but the disposition of slickensides along discontinuities indicated that the fabric was intact and undisturbed by movement (e.g., Redstone).

2. Fabric Sheared (S), in which the material is taken from the shear breccia of a basal rupture zone (e.g., Bull Canyon, Jupiter Creek).

3. Fabric Remolded (R), in which the material was taken from flow debris (e.g., Deadman River).

Sample locations in relation to landslide sites are given in Fig. 5.1 for the Salmon Valley, Fig 5.2 for the Deadman Valley and Fig. 5.3 for Chasm Creek and the Chilcotin River. Sample descriptions, fabric group and the microstructural investigation carried out are found in Tables 5.1, 5.2, and 5.3.

5.3 Methods

The microstructure of the volcaniclastic materials was examined by low powered reflected light microscope, polarising microscope and by the Scanning Electron Microscope (SEM) (see Tables 5.1, 5.2 and 5.3). Samples for the SEM consisted of freshly broken chips of material which were freeze dried before being cemented onto stubs. In the case of slickensides from shear zone exposures, the surface was not freshly broken so as to allow direct observation of the shear surfaces. Samples were sputter coated with gold prior to examination.

The detailed objectives of this phase of the investigation were as follows:

1. To establish grain-matrix relationships and identify their components at various sections within the material.

2. To locate and identify clay particles and assemblages.

3. To describe the characteristics and location of voids within intact fabrics.

4. To ascertain the effect of slope movement on microstructure as deduced from samples collected from exposed rupture zones and landslide debris.
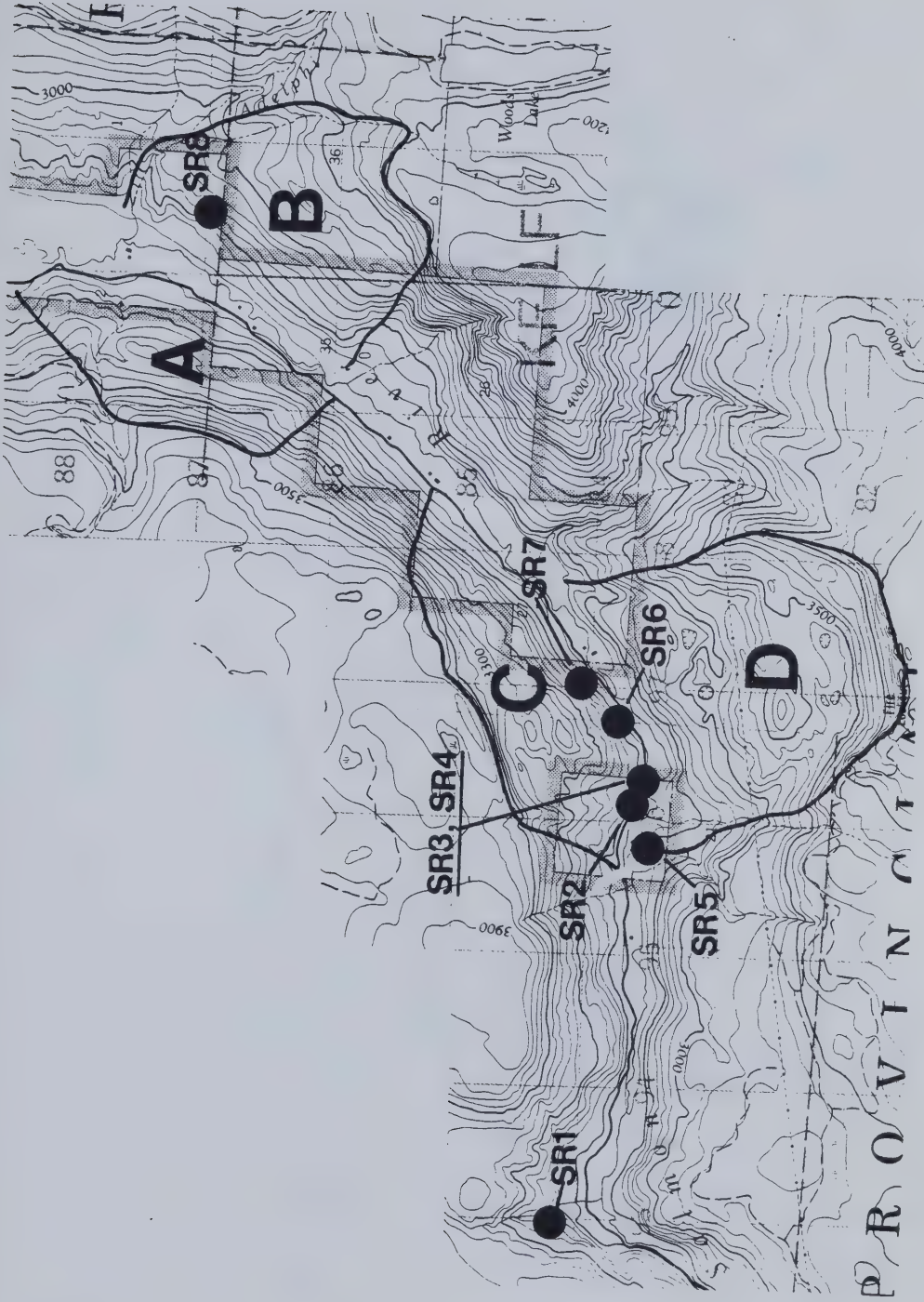
Figure 5.1 Microstructure sample locations in the Salmon Valley. Landslides are Stephen's Lake Road (A), Adelphi Creek (B), Jupiter Creek (C), Shell Creek (D).
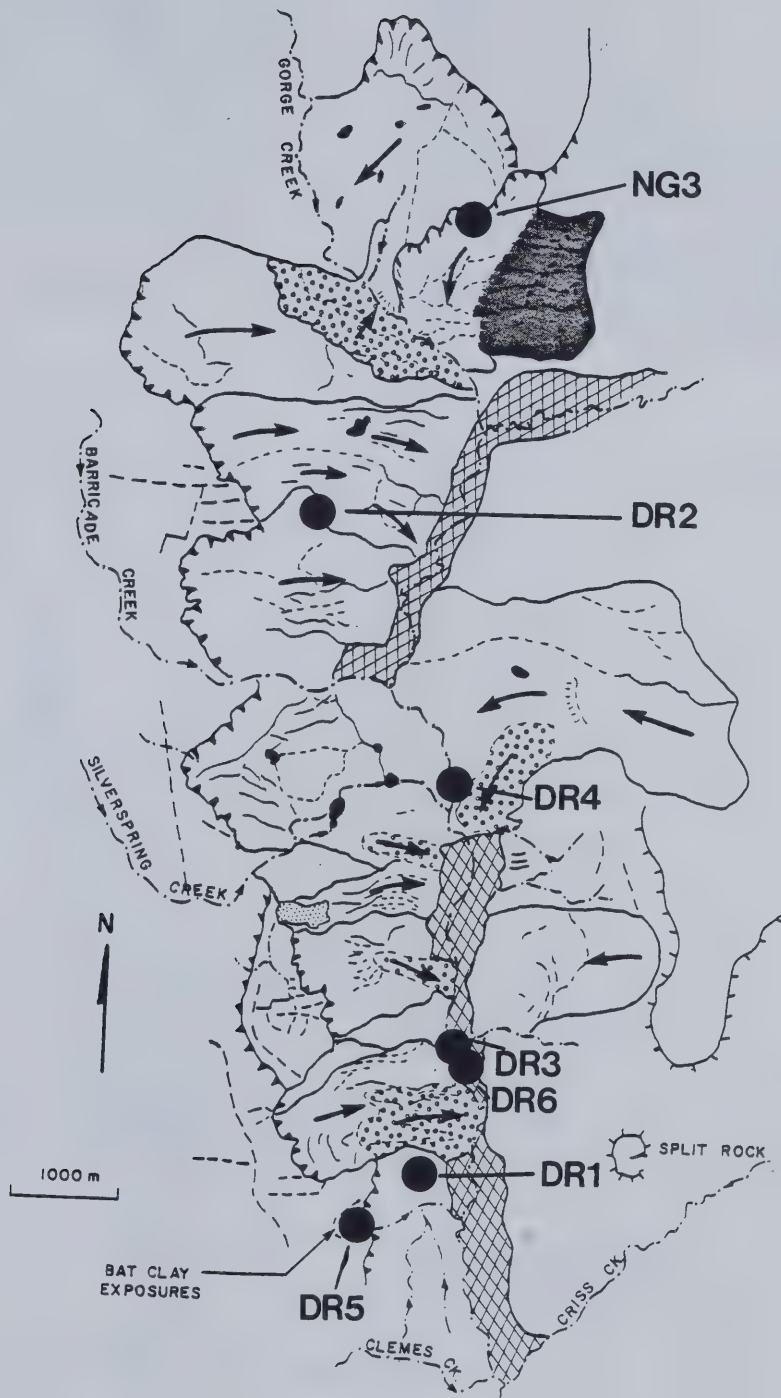
Figure 5.2 Microstructure sample locations in the Deadman Valley.
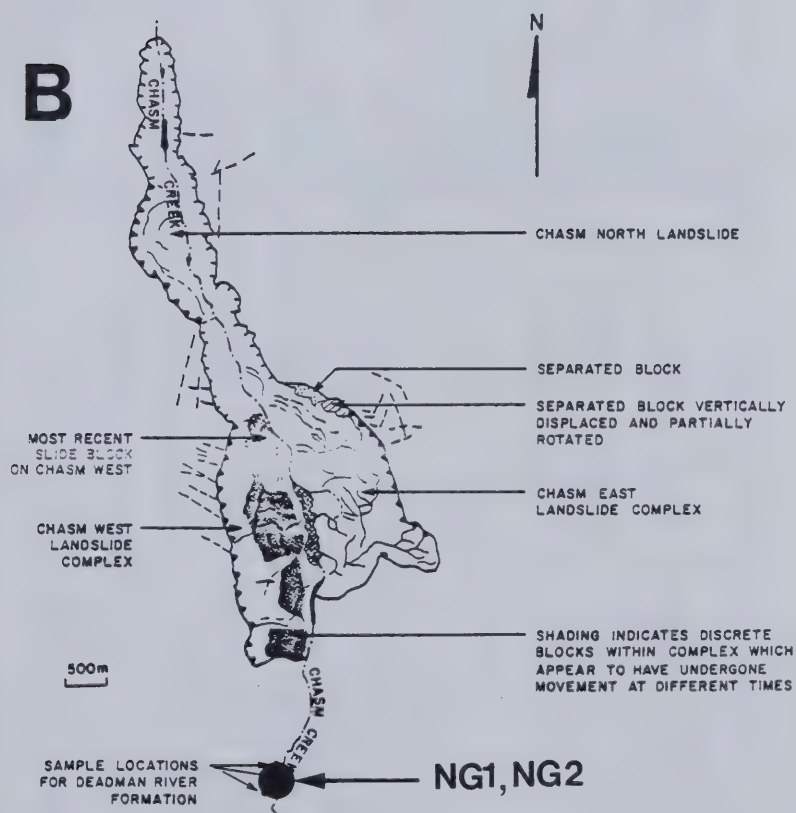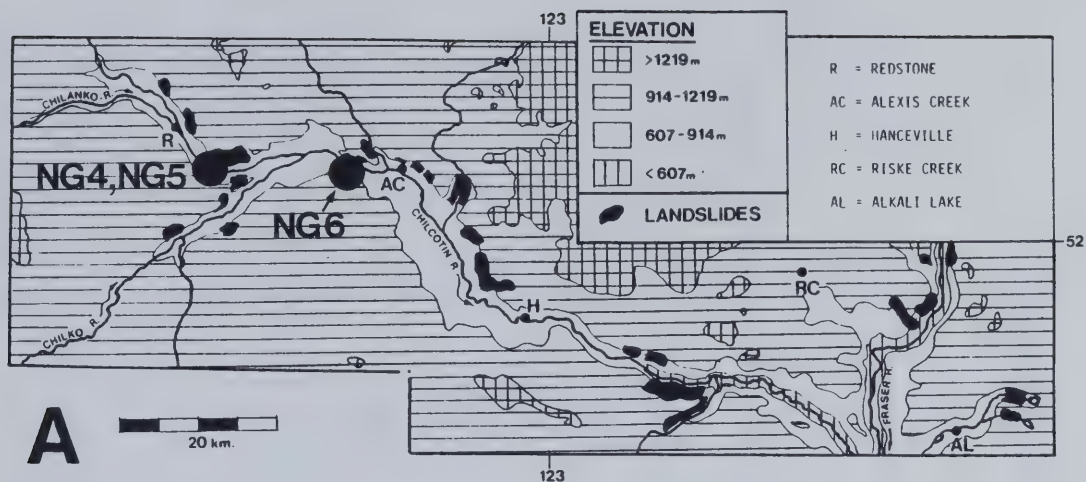
Figure 5.3 Neogene microstructure sample locations in the Chilcotin Study Area (A) and Chasm Creek area (B).

	SAMPLE LOCATION	SAMPLE DESCRIPTION	FIELD DESIGNATION	Fabric Type[a]	Thin Section	SEM
SR1	River exposure 0.5 km upstream on Twig Creek	Blue grey tuff 5m above Tertiary unconformity	----------	I	x	x
SR2	Road cut at west margin of Jupiter Creek landslide	Red tuff-tuff breccia	----------	I	x	x
SR3	Road cut at west margin of Jupiter Creek landslide	Brown tuff-tuff breccia, weathered Salmon River Tuff.	----------	I	x	x
SR4	Road cut at west margin of Jupiter Creek landslide	Blue grey tuff-tuff breccia, unweathered Salmon River Tuff	20A5	I	x	x
SR5	River exposure at base of Shell Creek landslide	Weathered,sheared Salmon River Tuff	23A2	S		x
SR6	Road cut at base of Jupiter Creek landslide	Sheared brown Salmon River Tuff	11L2	S		x
SR7	Road cut at base of Jupiter Creek landslide	Sheared brown Salmon River Tuff	11L3	S		x
SR8	Logging road cut within Adelphi Creek landslide	Sheared brown tuff-tuff breccia (Hummingbird Tuff)	20A3	S		x

[a] FABRIC TYPE: I=INTACT, S=SHEARED

Table 5.1 Sample descriptions and microstructural investigations carried out – Paleogene material from Salmon River locations.

	SAMPLE LOCATION	SAMPLE DESCRIPTION	FIELD DESIGNATION	FABRIC TYPE[a]	THIN SECTION	SEM
DR1	Road cut near south margin of landslide 1	Yellow cloddy clay	16L2	I		X
DR2	Road cut on Hi-Hium road on landslide 4	Yellow gritty clay	28L4	R		X
DR3	Road cut in landslide 1	Yellow gritty clay from landslide debris	16L6	R		X
DR4	River exposure along Deadman River at base of landslide 3	Brown slickensided clay	17L3	S		X
DR5	Hillside exposure south of landslide 1	Yellow cloddy clay- the Bat Clay	16L3	I		X
DR6	Road cut through landslide 1	Intact block of grey clay	15G1	I		X

[a]FABRIC TYPE: I=INTACT, R=REMOULDED, S=SHEARED.

Table 5.2 Sample descriptions and microstructural investigations carried out – Paleogene material from Deadman Valley locations.

	SAMPLE LOCATION	SAMPLE DESCRIPTION	FIELD DESIGNATION	Fabric Type[a]	Thin Section	SEM
NG1	River exposure on Chasm Creek, south of landslides	White to buff tuff	29L3C	I	x	x
NG2	River exposure on Chasm Creek, south of landslides.	White to buff tuff-tuff breccia	29L3B	I	x	x
NG3	Road cut on Gorge Creek road, beneath plateau basalts.	Yellow tuff	28L2	I		x
NG4	Road cut through Redstone slide	Slickensided white to buff clay	23L1C	I		x
NG5	Road cut through Redstone slide	Slickensided finely laminated brown clay	23L1B	I		x
NG6	Road cut at base of Bull Canyon slide	Slickensided yellow clay	23L3	S		x

[a]FABRIC TYPE=I-INTACT, S-SHEARED

Table 5.3 Sample descriptions and microstructural investigations carried out – Neogene material from Gorge Creek, Chasm Creek, and the Chilcotin Valley.

The microfabric observed in the SEM was described according to the scheme of Collins and McGown (1973) where possible. This scheme is in general use in the field (e.g., Mitchell, 1976). Clay particles were generally identified on the basis of morphology and on some occasions by an X–ray energy – dispersive analyser attached to the SEM. The morphology of clays is well illustrated in Borst and Keller (1969), Boher and Hughes (1971) and Wilson and Pittman (1977), sources which were used to aid in the morphological identification of clay particles.

Discussions and SEM photographs of the microstructure of volcaniclastic materials are found in Almon *et. al.* (1976), Surdam and Boles (1979), Stanley and Benson (1979), Davies *et al.* (1979), Khoury and Eberl (1979), Ratterman and Surdam (1981) and Walton *et al.* (1981). Descriptions of volcanic ash morphology with SEM photographs, are reviewed by Walker and Croasdale (1971), Heiken (1972, 1974). These sources aided substantially in the interpretation of SEM images.

X–ray diffraction (XRD) analysis was carried out on clay fractions ($< 2\mu$) from the 20 samples. Initial disaggregation was carried out by hammer blows. Successive disaggregation and dispersion was then carried out by ultrasonic methods, and the suspension centrifuged to separate out the clay particles, which were freeze dried. An oriented mount was produced by sucking the clay particles on to a porous ceramic disc. The sample was saturated with Ca^{2+} cations and subjected to XRD analysis using Co K alpha radiation at a scan speed of 1° 2–theta per minute. The same disc was then glycolated using ethylene glycol and subjected to a second XRD analysis.

The resultant diffractograms were analysed for the major clay mineral groups and were interpreted using the methods suggested by Carroll (1970), Thorez (1976) and Brindley and Brown (1980). The criteria for the major clay mineral groups were as follows:

1. *Smectite:* In Ca–saturated samples, a peak at 15 Å (001) which swells to one at approximately 17 A on glycolation. Higher order reflections after glycolation are very marked.

2. *Kaolinite:* A reflection at approximately 7 Å (001) unaffected by glycolation.

3. *Illite:* A (001) reflection at 10 Å unaffected by glycolation.

4. *Chlorite:* A (001) reflection at 14 Å unaffected by glycolation.

Some uncertainty may exist with a mixture of kaolinite and iron-rich chlorites. In this case the (001) and (003) reflections of the chlorite may be weak or absent (Thorez, 1976). The 7 Å peak may therefore be the (001) reflection of kaolinite or the (002) reflection of chlorite. This was thought to be significant only in the case of SR1, the Twig Creek sample, as discussed below.

A semi-quantitative method of estimating the proportions of clay minerals based on relative peak heights was used to estimate the relative amounts of each clay mineral in the clay fraction of each sample. This method is to be interpreted as an index only, and it is in use at the Alberta Research Council. A similar method was used by Locker (1973) and is outlined in Table 5.4. It is emphasised that estimates of clay mineral proportions using this semi-quantitative method may be in error by up to 5-10%.

Attention was also given to the presence of non-clay minerals in the clay fraction with emphasis on quartz, feldspar, calcite and zeolites. Identification of these minerals on the diffractogram was made on the basis of criteria outlined in Brindley and Brown (1980).

5.4 Microstructural Domains in Volcaniclastic Rocks

In discussing microstructural observations it is important to establish the relative scale dealt with, for example, when examining a thin section beneath a polarising microscope. This is particularly the case when analysing the microstructure of a complex fragmental system such as is found in volcaniclastic rocks. The structure of this group of rocks is a response to the primary pyroclastic and epiclastic processes active in initial deposition, secondary processes such as diagenetic or hydrothermal alteration, and a tertiary group of processes which might consist of shearing, weathering or post-alteration solution. The macro-structure of such rocks may be viewed as a hierarchical multi-grain system, which contains different grain and matrix relationships at different scales. In this discussion we may define the matrix as those particles smaller than the dominant grain size. Further, fabrics are classified as matrix supported or grain supported, a factor which strongly influences geotechnical behavior (Marsal, 1965 ; Lupini *et al*. 1981).

Initially, a macrostructural multi-grain system may be defined in which the macrofabric domains correspond to air-fall pyroclastic rock types (Fig. 5.4). It is within

Table 5.4 Semi-quantitative method of computing clay mineral percentage using the Peak Height Method (after Alberta Research Council)

Calculate the form factors:

The 10Å mineral (illite) is the internal standard and has a form factor value of 1.000.

For the other minerals:

$$17\text{Å} = \frac{\text{height of } 17\text{Å peak}}{4 \times \text{height of } 10\text{Å peak}}$$

$$14\text{Å} = \frac{\text{height of } 14\text{Å peak}}{3 \times \text{height of } 10\text{Å peak}}$$

$$7\text{Å} = \frac{\text{height of } 7\text{Å peak}}{2.5 \times \text{height of } 10\text{Å peak}}$$

Sum the form factor values and calculate percentages

Example

Peak	Form Factor	% of Total Clay	
10Å	1.000	$\frac{1.000}{2.500}$ =	40
17Å	.250	$\frac{.250}{2.500}$ =	10
14Å	.750	$\frac{.750}{2.500}$ =	30
7A	.500	$\frac{.500}{2.500}$ =	20
	2.500		100
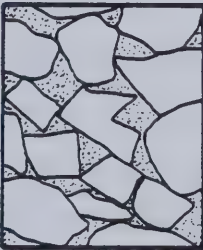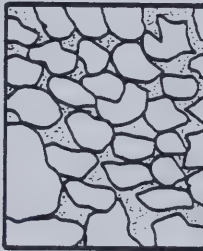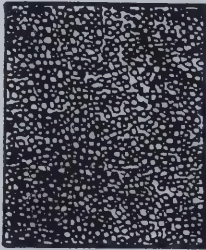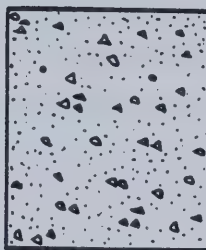
SCALE OF DRAWINGS	1:10	1:2	1:1
GRAIN SUPPORTED	100 mm	20 mm	10 mm
MATRIX SUPPORTED	100 mm	20 mm	10 mm
ROCK NAME	BRECCIA or AGGLOMERATE	LAPILLI TUFF	TUFF
GRAINS	BLOCKS (> 64 mm)	LAPILLI (64 mm <> 2 mm)	ASH (2 mm <> 0.0625 mm)
MATRIX	LAPILLI, ASH DUST	ASH DUST	DUST

Figure 5.4 Hierarchical multi-grain systems in air-fall pyroclastic rocks. Size classification and nomenclature are those proposed by Schmid (1980)

these macrofabric domains that investigations of microfabric take place. With respect to tuffs, which are the most numerous volcaniclastic rock studied in this investigation, additional microfabric domains may be distinguished corresponding roughly to the scales investigated when using the polarising microscope and the Scanning Electron Microscope. An example of a microstructural model of grain—matrix relations is given in Fig. 5.5 for an analysis of the Twig Creek tuff discussed in the following section. In Fig. 5.5 Domain A corresponds to the smallest macro—structural domain in Fig 5.4 at a scale of 1:1.

The three domains identified in Fig. 5.5 are used as a framework to describe the microstructure of volcaniclastic materials discussed below.

5.5 Clay Mineralogy

5.5.1 Paleogene Volcaniclastics - Salmon River

The glycolated diffractograms for the intact and sheared Salmon River samples are seen in Figs. 5.6 and 5.7, respectively. The relative amounts of major clay minerals in the clay fraction calculated by the semi—quantitative method are seen in Table 5.5.

The clay mineralogy in all samples is seen to be dominated by smectite clays as is evident in the intense, sharp peaks at 17 Å and the well marked higher order reflections. The estimated proportion of smectites varies between 78% and 98% (Table 5.5). No other clay mineral is significant, with the exception of kaolinite in sample SR1. The only non—clay mineral to give significant reflections is potassic feldspar. No distinction can be made between the fabric groups on the basis of the results of the XRD analysis. It is also noted that weathered and unweathered samples of Salmon River Tuff show essentially the same diffraction pattern.

5.5.2 Paleogene Volcaniclastics - Deadman River

The diffractograms of 6 glycolated samples are shown in Figs. 5.8 and 5.9 and the relative amounts of major clay minerals in the clay fraction in Table 5.6.

As in the Salmon River materials all the diffractograms are dominated by an intense sharp peak at 17 Å and very well marked higher order reflections indicative of smectite. In a grey sample of clay, (DR6), from the debris of landslide 1, a significant

HAND SPECIMEN –
LOW POWER MICROSCOPE
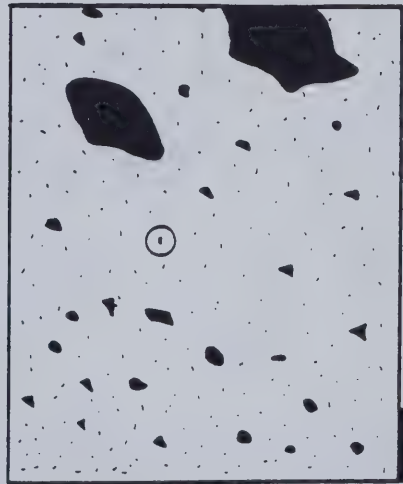
POLARIZING MICROSCOPE

SCANNING
ELECTRON MICROSCOPE

Scale → 1:1

1:026

1:0.001

10,000 μ

500 μ

20 μ

Domain → A

B

C

NOTE: CIRCLED AREAS IN A AND B REPRESENT AREAS IN LARGER SCALE MICROSTRUCTURAL DOMAIN.
MICROFABRIC OF DOMAIN B IS TRACED FROM PLATE 5.1

Figure 5.5 Hierarchical microstructure model of grain–matrix relations in Twig Creek Tuff.
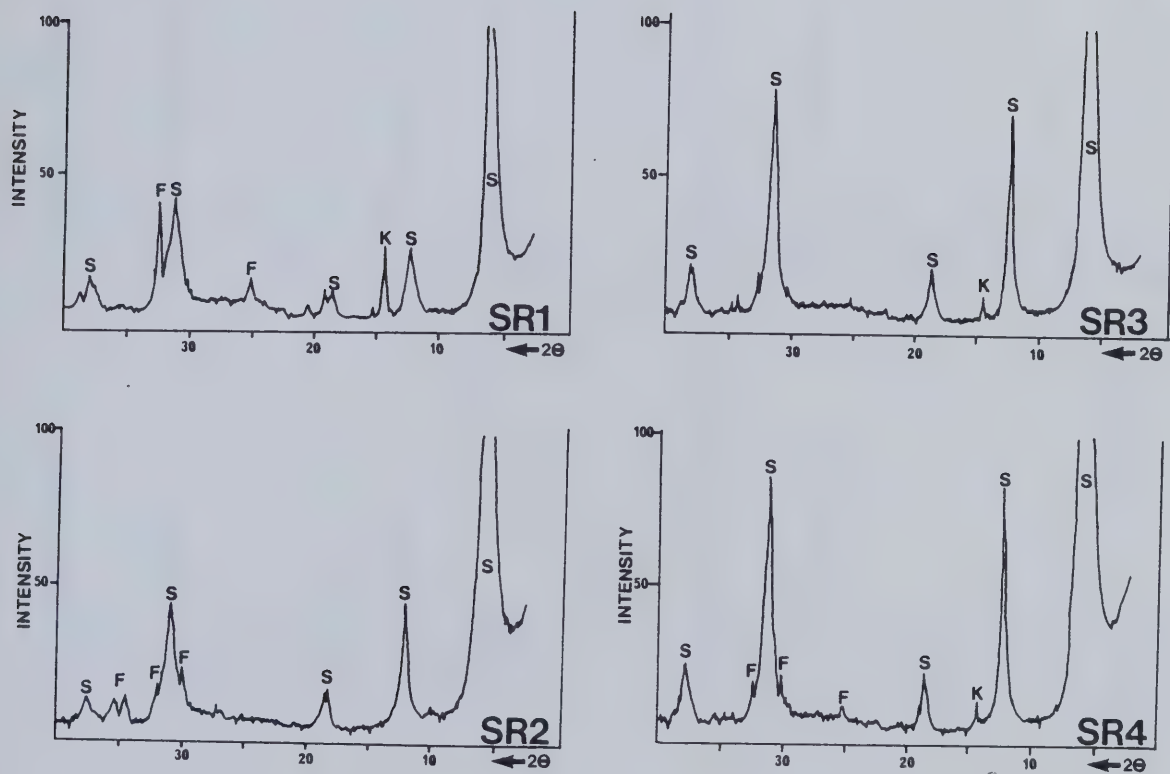
Figure 5.6 Diffractograms for clay fraction of intact Paleogene volcaniclastic material from the Salmon Valley (Glycolated). S=Smectite, I=Illite, K=Kaolinite, F=Feldspar.
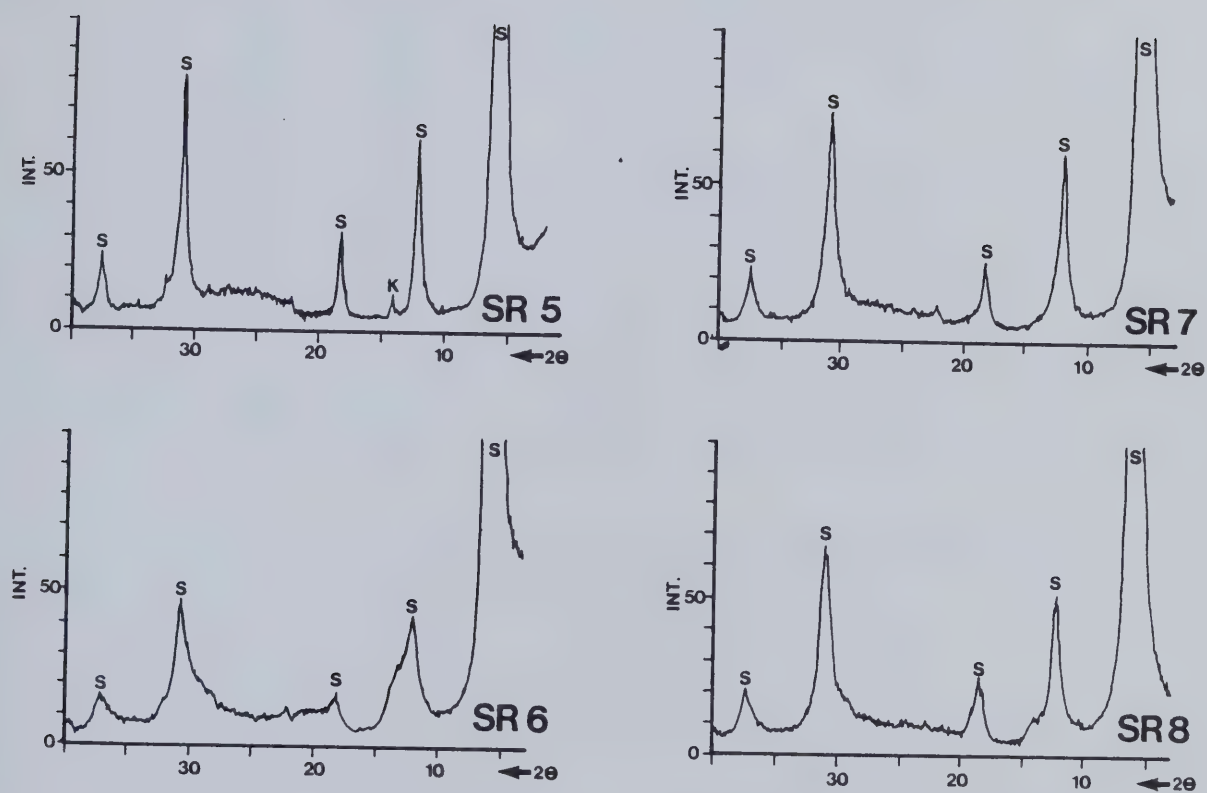
Figure 5.7 Diffractograms for clay fraction of sheared Paleogene volcaniclastic material from the Salmon Valley (Glycolated). S=Smectite, I=Illite, K=Kaolinite, F=Feldspar.

Table 5.5 Relative amounts of major clay minerals in clay fraction of the Salmon River samples . .

	% SMECTITE	%CHLORITE	% ILLITE	%KAOLINITE
SR1	78.0	----	5.0	16.0
SR2	94.0	----	4.0	1.0
SR3	96.0	----	1.0	2.0
SR4	92.0	----	4.0	3.0
SR5	98.0	----	1.0	1.0
SR6	91.0	----	3.0	6.0
SR7	97.0	----	1.0	2.0
SR8	91.0	----	3.0	6.0

amount of illite is present. SEM observations detailed below indicate this was mica (Plate 5.9).

The amount of smectite varied between 88% and 99% (Table 5.6). The only significant reflections obtained for non–clay minerals were those of potassic feldspar which was present in all samples. No distinction can be made between the three fabric groups on the basis of the diffractograms.

5.5.3 Neogene Samples

A more diverse clay mineralogy is indicated in the 6 diffractograms in the glycolated Neogene samples in Figs. 5.10 and 5.11 and in the relative amounts of clay minerals present in Table 5.7.

Tuff from beneath the plateau lavas at Gorge Creek (NG3) has a diffractogram similar to older pyroclastic material in the main Deadman Valley. The diffractogram is dominated by intense, sharp smectite peaks at 17 Å and feldspar reflections are also present. In tuffs from Chasm Creek (NG1, NG2), whilst the smectite peak is sharp and well defined higher order peaks are not as well defined, as those observed on the Paleogene diffractograms. Small amounts of illite and kaolinite are also present in the Chasm Creek samples.

Volcaniclastic materials from beneath plateau lavas along the Chilcotin River (NG4, NG5) show a more heterogeneous assemblage of clay minerals and this is thought to reflect the detrital origin of these materials. Diatomaceous clay from the Redstone landslide (NG4), for example shows a dominance of illite whilst NG5 shows a significant presence of kaolinite.

The results of the X–ray diffraction analysis are summarised in the triangular diagram in Fig. 5.12.

5.6 Microstructure of Undisturbed Paleogene Volcaniclastics – Salmon River
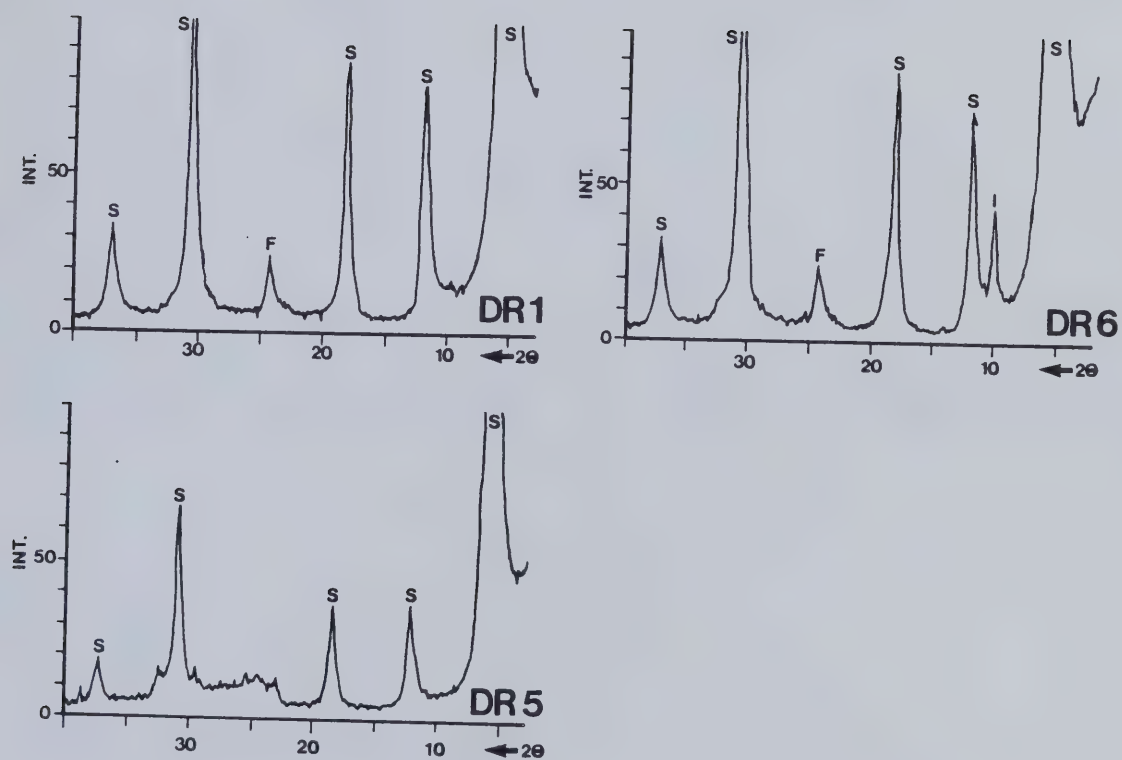
Figure 5.8 Diffractograms for the clay fraction of intact Paleogene volcaniclastic material from the Deadman Valley (Glycolated). S=Smectite, I=Illite, K=Kaolinite, F=Feldspar.
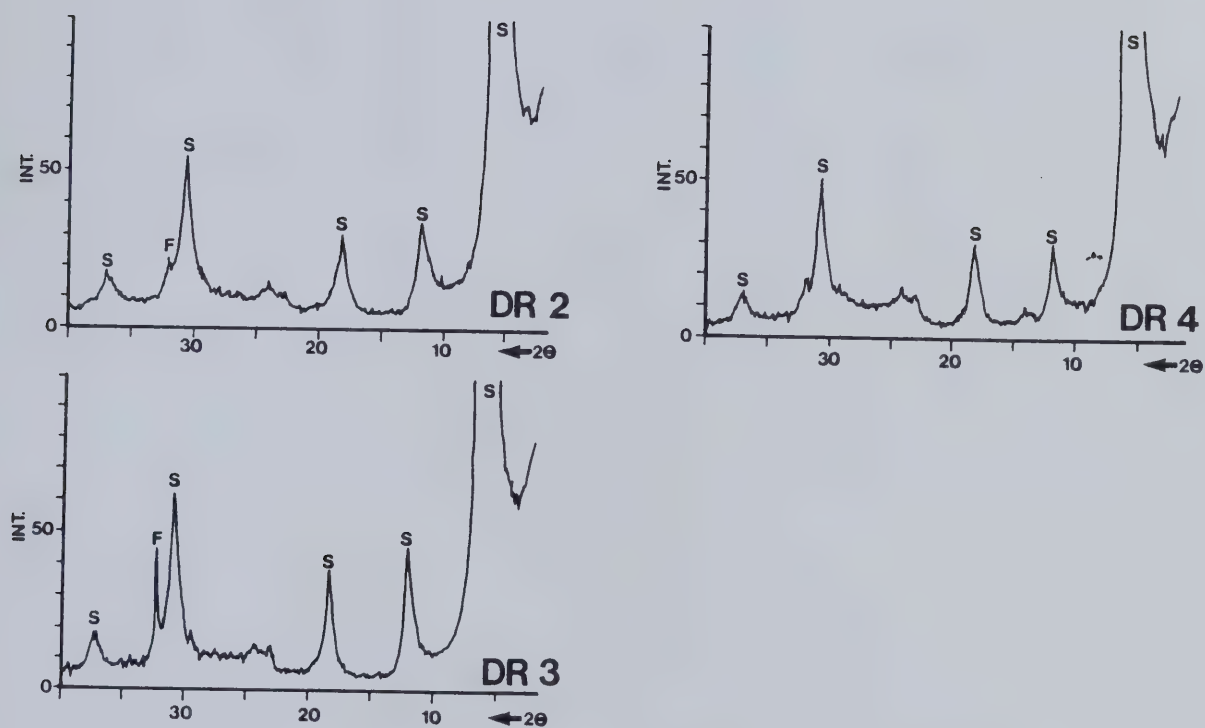
Figure 5.9 Diffractograms for the clay fraction of sheared and remoulded Paleogene material from the Deadman Valley (Glycolated).   S=Smectite, I=Illite, K=Kaolinite, F=Feldspar.

Table 5.6 Relative amounts of major clay minerals in the clay fraction of the Deadman River samples

	%SMECTITE	%CHLORITE	% ILLITE	%KAOLINITE
DR1	98.0	----	2.0	----
DR2	89.0	----	10.0	2.0
DR3	99.0	----	1.0	----
DR4	91.0	----	6.0	3.0
DR5	96.0	----	3.0	1.0
DR6	88.0	----	12.0	----
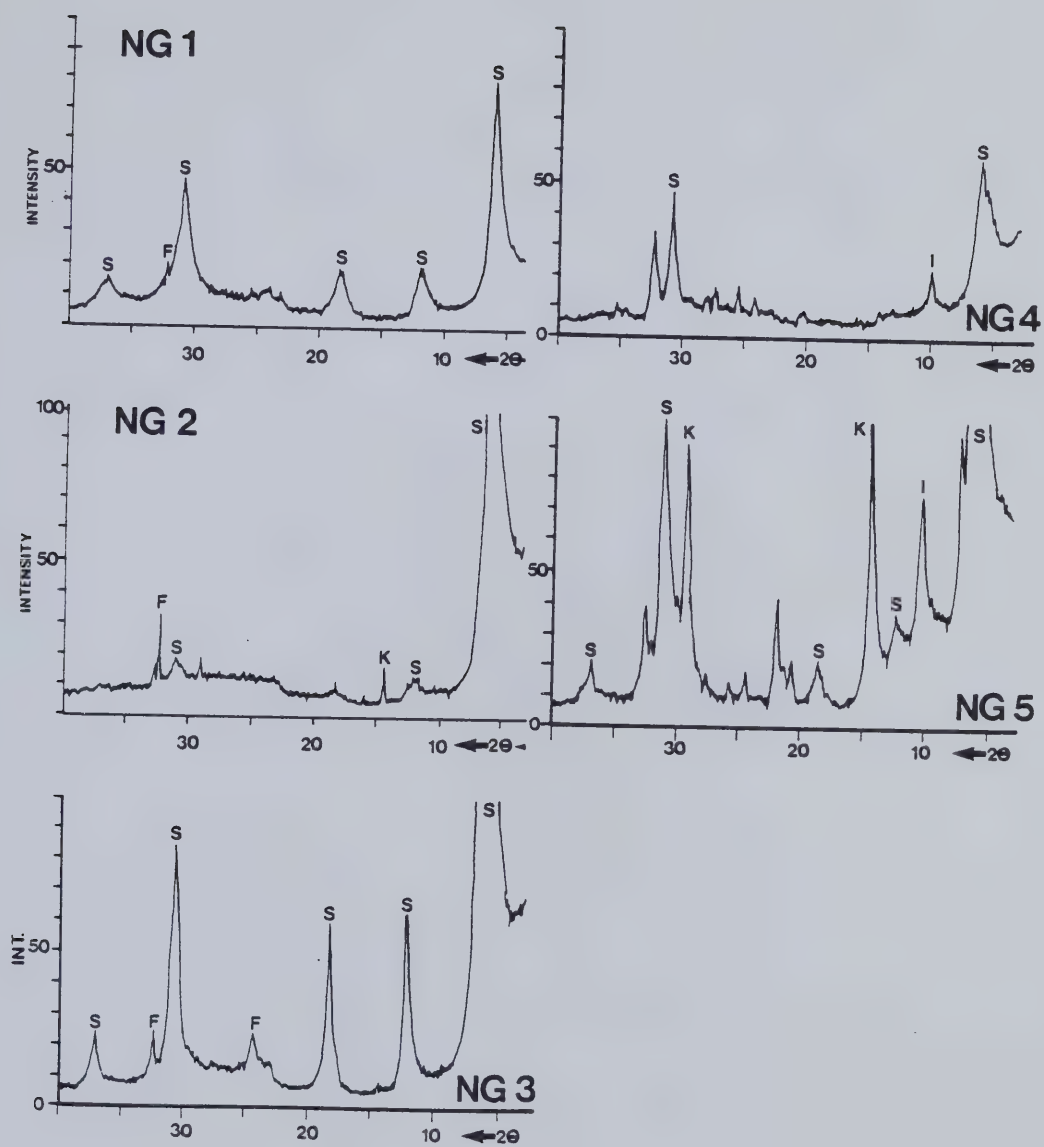
Figure 5.10 Diffractograms for the clay fraction of intact Neogene volcaniclastic material (Glycolated). S=Smectite, I=Illite, K=Kaolinite, F=Feldspar.
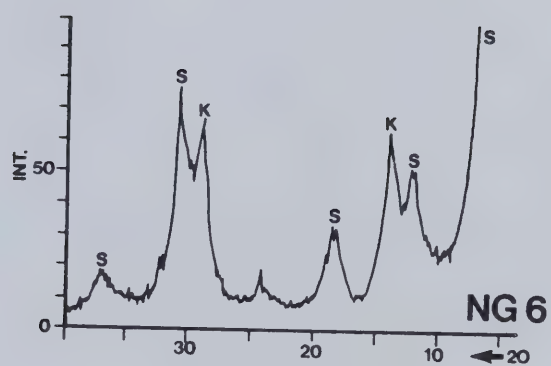
Figure 5.11 Diffractogram for the clay fraction of sheared Neogene volcaniclastic material (Glycolated). S=Smectite, I=Illite, K=Kaolinite, F=Feldspar.

Table 5.7 Relative amounts of major clay minerals in the clay fraction of Neogene volcaniclastic materials.

	% SMECTITE	%CHLORITE	% ILLITE	%KAOLINITE
NG1	81.0	----	15.0	4.0
NG2	81.0	----	7.0	11.0
NG3	99.0	----	1.0	1.0
NG4	37.0	----	55.0	8.0
NG5	34.0	12.0	30.0	24.0
NG6	73.0	----	6.0	21.0
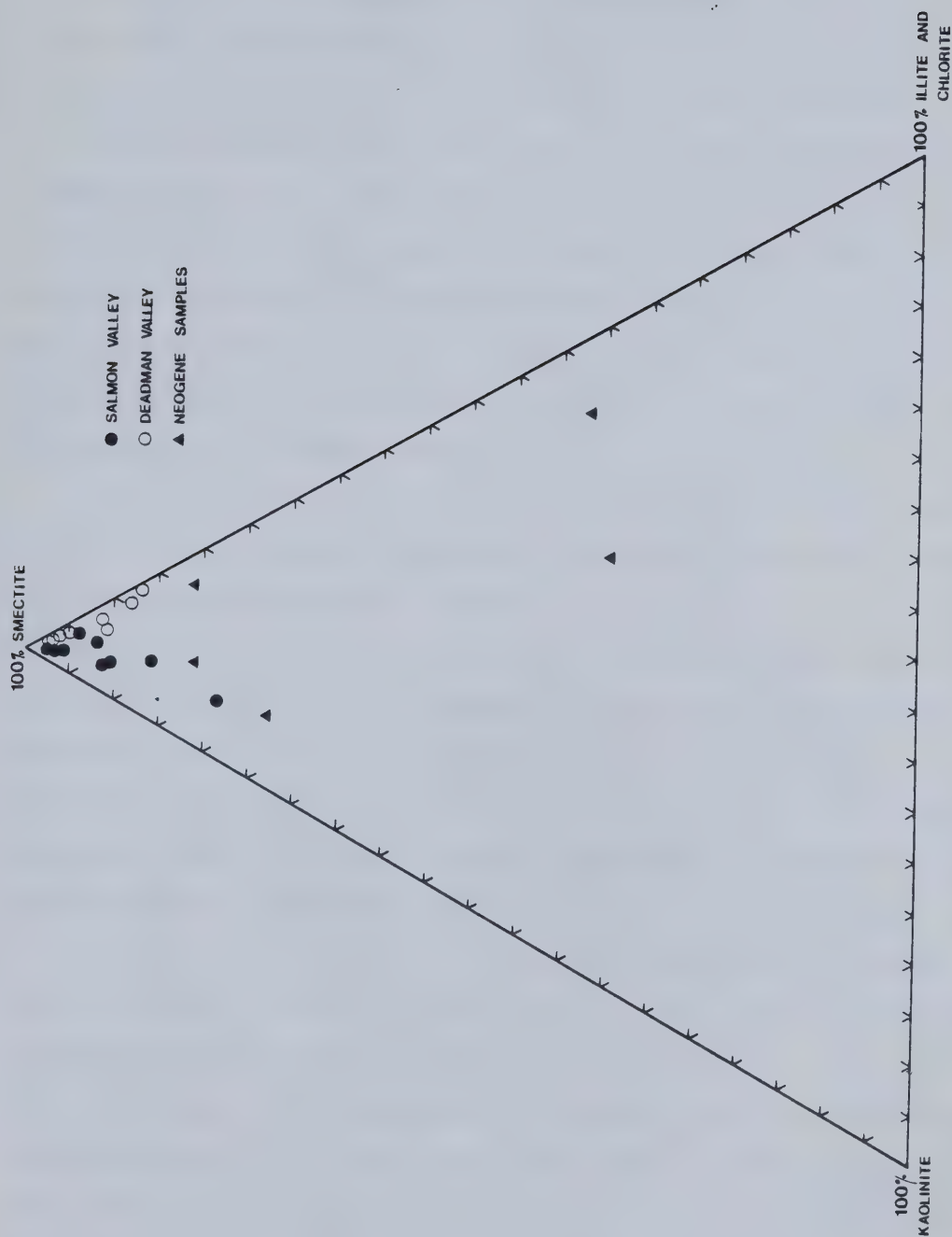
Figure 5.12 Triangular diagram showing estimated clay mineral ratios for the volcaniclastic materials examined. Percentages based on semi-quantitative method discussed in text.

5.6.1 SR1 - Twig Creek Tuff

The grain system in the Twig Creek Tuff contains a number of components and includes angular clasts of Palaeozoic chloritic schist as well as angular quartz fragments up to 30 mm long. Grains smaller than 20 mm appear to be angular black pyroclastic fragments of basalt. The grains occur in a matrix which has two major components: a brown amorphous material with a resinous lustre, which is so soft that it can be easily indented with the point of a steel needle, and scattered patches of a white microcrystalline mineral which can easily be scraped with a needle and does not react with HCl. It occurs as a void filling and as cement around larger grains. Calcium carbonate is present, however, in small amounts. It is noted that the brown resinous material formed clay films on prepared shear surfaces during direct shear tests on the Twig Creek Tuff. At the natural scale the tuff is matrix supported.

In thin section (Plate 5.1) grains are noted up to 600 micrometres in size. These consist of vesicular, embayed volcanic rock fragments and crystal euhedra. Euhedra are partially corroded and fractured. The grains occur in a matrix that contains smaller rock fragments between 100 and 200 micrometres in length, fragments of broken euhedra and microlites. However, the matrix is dominated by an amorphous microcrystalline groundmass which is isotropic to faintly anisotropic under crossed nicols. This is interpreted to be volcanic glass dust which is mostly altered to clay. There is evidence of ghosts of particles within the matrix making the delimitation of grain matrix borders very difficult (Plate 5.1). At the scale of the thin sections, the tuff is matrix supported.

In the SEM, as seen in Plate 5.2, the matrix is dominated by clay particles showing edge-to-edge (EE) and edge-to-face (EF) contacts. Matrix components also include euhedral particles between 5 micrometres and 10 micrometres in length. Intra-assemblage and inter-assemblage pore space appears to be considerable and some trans-assemblage pores are seen. Larger voids resemble irregular cavities. Into some of these cavities elongate needle-shaped crystals up to 40 micrometres long have grown. Sand size grains up to 200 micrometres in diameter clearly show clay coatings in which the clay platelets are attached perpendicularly to the grain surface (Plate 5.2). A chemical precipitate, probably calcium carbonate, also coats some grains. Unidentified tabular fibrous particles up to 20 micrometres thick are also observed. Clay particles are thought
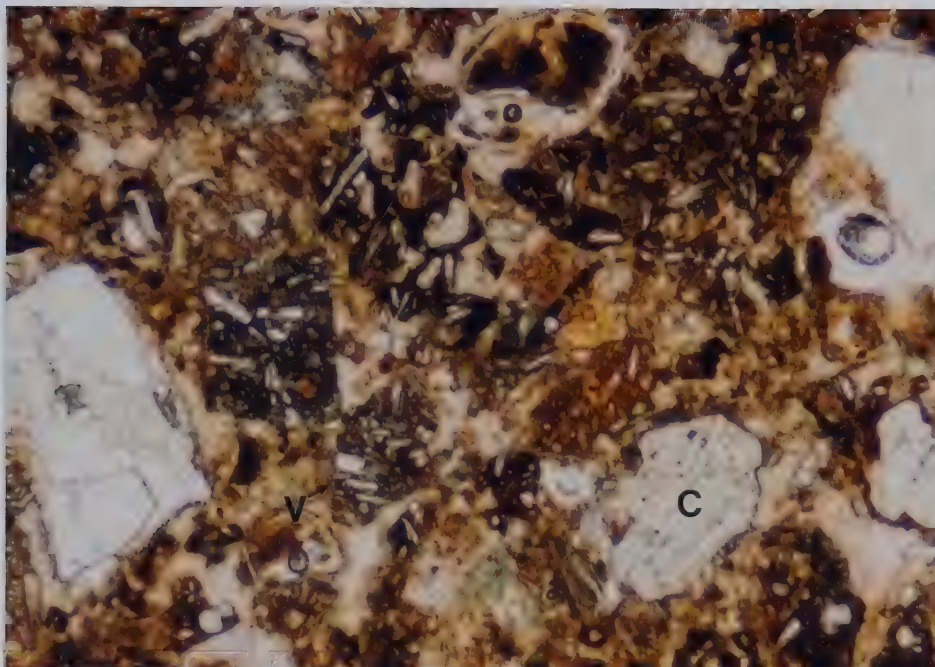
A. PLANE POLARISED LIGHT. NOTE CORRODED CRYSTAL EUHEDRA (C) AND ANGULAR FRAGMENTS OF VOLCANIC ROCK (V) SOME OF WHICH EXHIBIT PRONOUNCED EMBAYMENTS AND VESICLES. MATRIX CONSISTS OF SMALLER LITHIC FRAGMENTS, GLASS, AND CLAY (MAINLY MONTMORILLONITE).
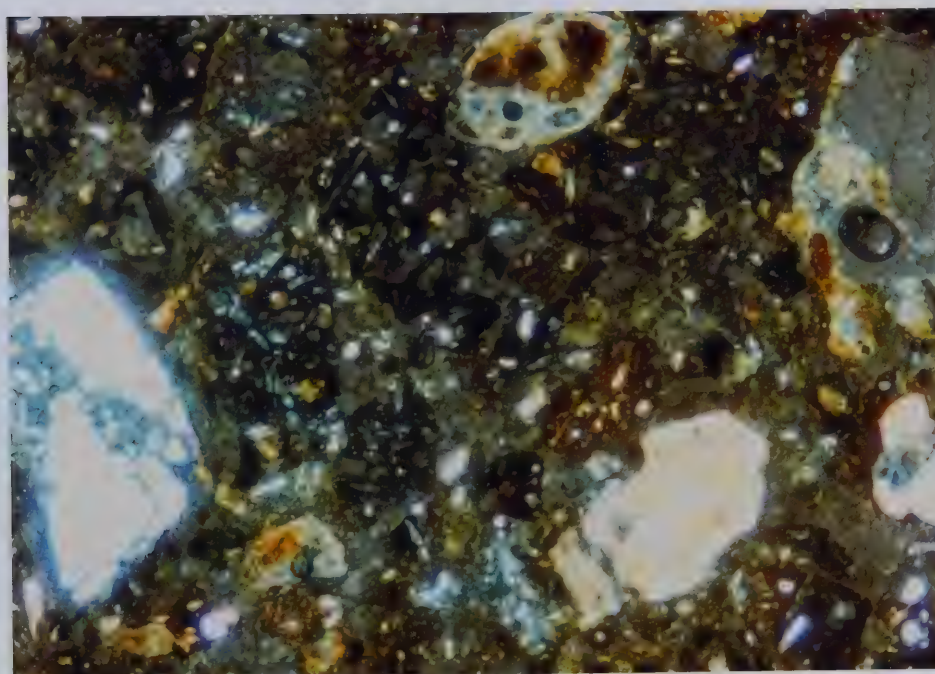
B. CROSS-POLARS. BLUE GREY AREA OF MATRIX CORRESPONDS TO DISTRIBUTION OF AMORPHOUS GLASS AND CLAY.

500 μ

Plate 5.1 Photomicrographs of intact Twig Creek Tuff (SR1).

B. ENLARGEMENT OF AREA OUTLINED IN A.
   A=INTERPARTICLE PORE SPACE IN MONTMORILLONITE
   ASSEMBLAGE. B=INTRA-ASSEMBLAGE PORES.
   C=INTER-ASSEMBLAGE PORES. D=TRANS-ASSEMBLAGE
   PORES. E=KAOLINITE.
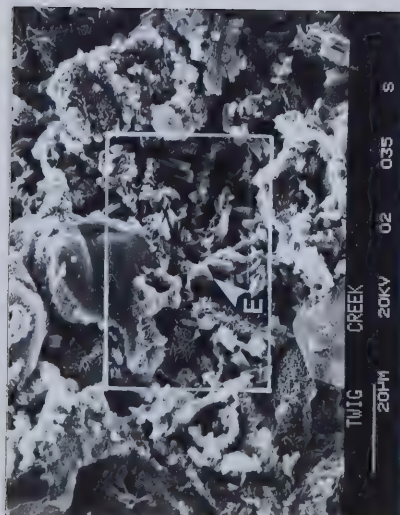
A. NOTE OPEN MICROSTRUCTURE OF TWIG CREEK
   TUFF AND GRAIN-MATRIX RELATIONS. E=EUHEDRA
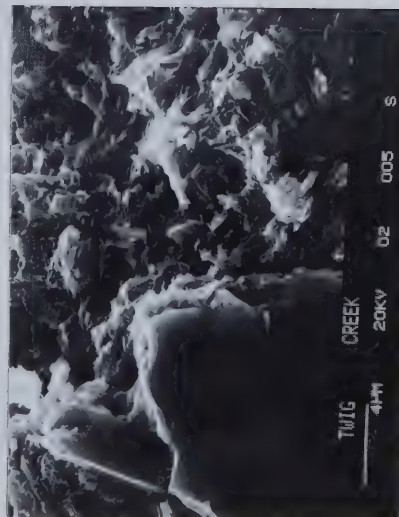
C. GRAIN-MATRIX CONTACT. NOTE PREDOMINANCE OF
   MONTMORILLONITE IN MATRIX.

Plate 5.2 SEM micrographs of intact Twig Creek Tuff (SR1).

to be dominantly montmorillonite both on the basis of XRD results and their morphology. They occur as an important element in the matrix and as grain coatings in an open fabric which is matrix supported.

5.6.2 SR2 - Red Tuff

The Red Tuff consists of pumiceous fragments up to 5 mm in size. These grains tend to be irregular in shape with many vesicles. Large euhedra which include plagioclase feldspar up to 2 mm long are also a component in the grain system in Domain A. The grains are set in a soft red microcrystalline matrix which has a resinous lustre. In this respect it is similar in appearance to the matrix of the Salmon River Tuff and the Twig Creek Tuff, and it is the same red clayey material that forms the slickensided films on sheared pre-cut surfaces during shear tests described in the following chapter. A hard white mineral, a form of silica, fills some embayments and vesicles and also occurs as irregular pods and cement throughout the rock. In Domain A the tuff is matrix supported and individual grains are easily dislodged from the matrix with a steel needle.

Under the polarising microscope, the fabric in Domain B is dominated by large pyroclastic fragments of volcanic rock containing laths and other crystal shapes (Plate 5.3). The large grains are up to 1 mm long and show irregular outlines and many vesicles. The grains appear to be cemented by a clear mineral which is thought to be opal since it is isotropic and white (Plate 5.3.). The material appears to have replaced the matrix where it occurs. The same white isotropic silica occurs as vesicle fillings. Some grains are euhedra, many of which are broken and corroded. The matrix consists of an isotropic microcrystalline amorphous material which is brown-orange under plane-polarised light and dark grey under crossed nicols. It also contains smaller rock fragments, fragments of euhedra and microlites. In Domain B the material is grain supported and the grains are partially cemented by isotropic silica.

In Domain C (Plate 5.4) the matrix is dominated by montmorillonite particles and a fibrous mineral thought to be a zeolite. Euhedral crystals of secondary minerals up to 100 micrometres long are elements in the grain system together with both rounded and highly fragmented grains up to 500 micrometres in diameter. Some of these grains are quartz. Frothy montmorillonite coatings occur on some grains and are smeared in places.
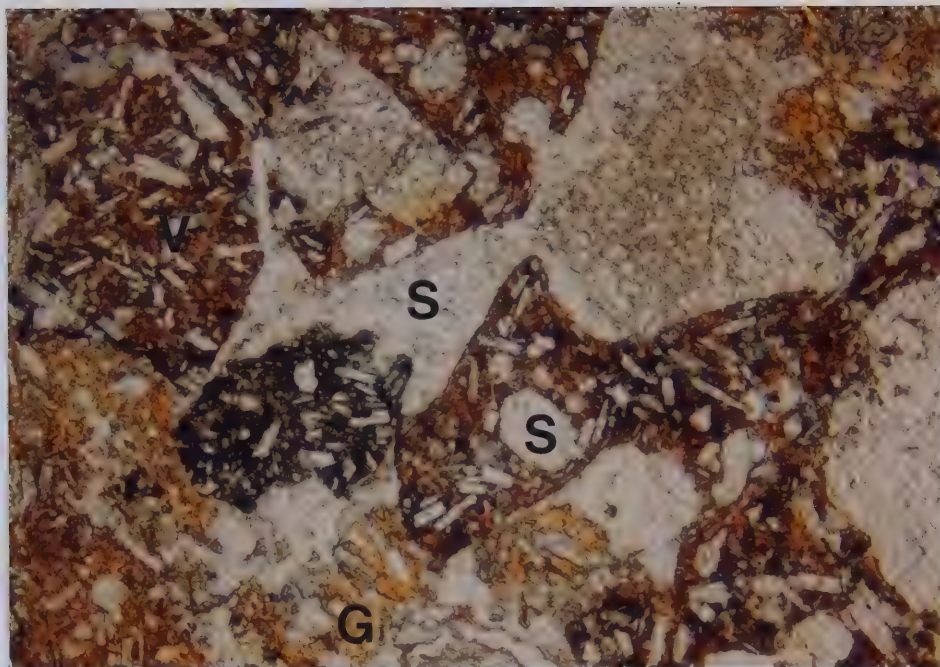
PLANE POLARISED LIGHT. NOTE FRAGMENTS OF
VOLCANIC ROCK (V), GLASS AT MATRIX SITES (G),
AND PRESENCE OF ISOTROPIC DIAGENETIC SILICA AS
CEMENT AND VESICLE FILLINGS (S). FOR FURTHER
DESCRIPTION SEE TEXT.

500 μ

Plate 5.3 Photomicrographs of intact Red Tuff (SR2).
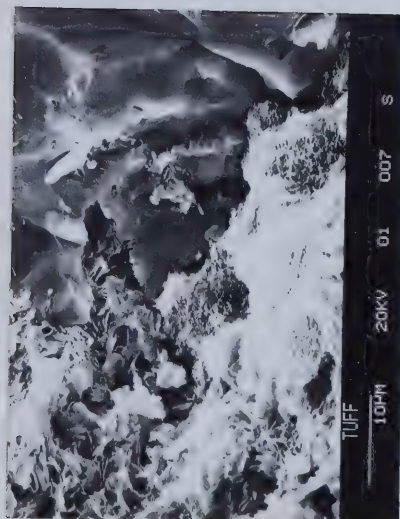
A. GRAIN-MATRIX BOUNDARY. CLAY MATRIX DOMINANTLY MONTMORILLONITE. GRAIN IS PYROCLASTIC FRAGMENT (EMBAYED QUARTZ?) THE SURFACE OF WHICH IS PITTED AND TUBED.

B. ENLARGEMENT OF EMBAYMENT SHOWN IN A ILLUSTRATING CHARACTERISTICS OF INTER- AND INTRA-ASSEMBLAGE PORE SPACE. CLAY IS MONTMORILLONITE. NOTE ETCHING.

C. MATRIX (DOMINANTLY MONTMORILLONITE PARTICLES) SHOWING EXAMPLES OF INTER-PARTICLE (P) AND INTER-ASSEMBLAGE (A) PORE SPACE.
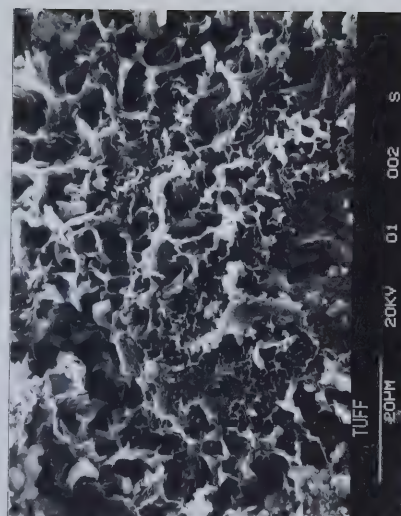
D. FROTHY MONTMORILLONITE GRAIN COATING. NOTE SWISS CHEESE TEXTURE.

Plate 5.4 SEM micrographs of intact Red Tuff (SR2).

Contorted aggregates of montmorillonite indicate the growth of secondary fibrous minerals following the formation of the clay. Montmorillonite appears to be the result of replacement of pyroclastic fragments. Inter-assemblage pores are not so marked as in SR1 and individual assemblages are not so well defined within the matrix. The tuff is matrix supported in Domain C.

5.6.3 SR3, SR4: Salmon River Tuff

In Domain A the Salmon River Tuff is very similar to the Twig Creek Tuff with the exception that fragments of Palaeozoic chloritic schist are absent. The grains are of 2 types; angular black aphanitic basaltic fragments and angular reddish-brown scoriaceous pyroclastic fragments. Grains vary is size from .1 mm to .10 mm but are generally in the range 1 mm - 3 mm. In field exposures large blocks of basaltic lava about 35 cm long were observed. Grains are set in a soft brown resinous matrix from which the grains are easily dislodged by the point of a steel needle. This is the case even for the freshest sample examined. Local disaggregation results from applying dilute HCl indicating that the matrix is locally rich in carbonates. As reported in the previous chapter calcareous clays are common as discontinuity fillings in outcrops of the Salmon River Tuff.

As can be seen in Plate 5.5, the microfabric in Domain B is very complex as a result of undergoing alteration probably by deuteric fluids. Grains are dominated by much-embayed, vesicular pyroclastic fragments some of which appear to have undergone almost complete alteration giving rise to ghost textures. Reticulate veins of calcite traverse the material. Calcite is also present as a grain replacement and void filling in characteristic cauliflower-like masses. Zeolites are also present as void fillings. The fabric in Domain B is matrix supported. The matrix consists of submicroscopic masses of amorphous material much of which is clay. Some zeolitic component is also present (Plate 5.5) as well as microlites and euhedra fragments.

In the SEM microphotograph in Plate 5.6, pyroclastic particles of all shapes with vesicles and tubes are noted. These particles make up the grain component of Domain C in the Salmon River Tuff and are up to 400 u in diameter. Bubble replacement textures are common and are illustrated in Fig. 5.17. Most clay particles are montmorillonite and are in edge-to-edge and edge-to-face contact. Montmorillonite also occurs as grain coatings.
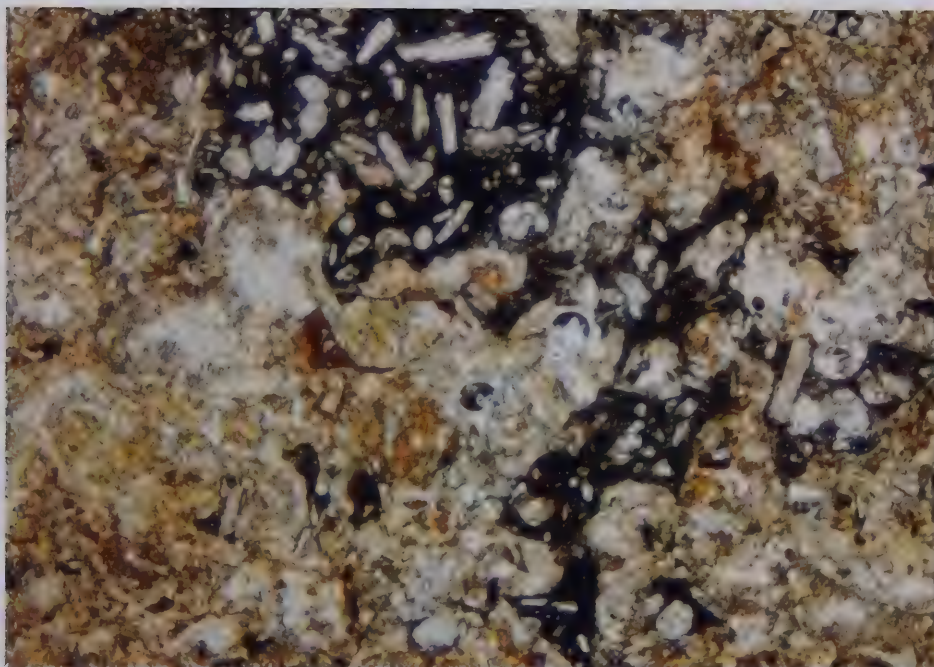
A. PLANE POLARISED LIGHT. NOTE EMBAYED, VESICULAR LITHIC PYROCLASTIC FRAGMENTS. GLASS SHARDS AND DUST IN ADDITION TO CLAY MAKE UP MATRIX.
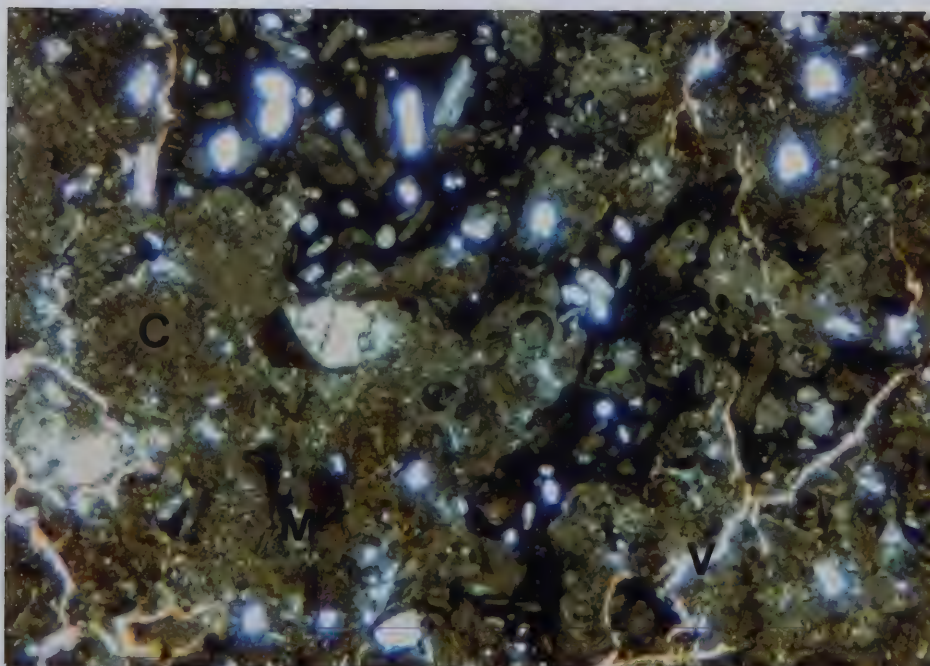
B. CROSS-POLARS. NOTE RETICULATE VEINS OF CALCITE (V), AMORPHOUS AREAS OF CLAY (C), FRAGMENTAL MATRIX (M), AND IRREGULAR OUTLINE OF LITHIC PYROCLASTIC FRAGMENTS.

|⊢—————————————⊣500 μ

Plate 5.5 Photomicrographs of unweathered Salmon River Tuff (SR3,SR4).
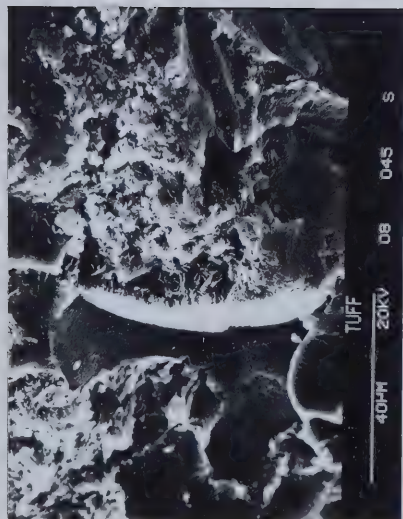
A. EXAMPLE OF GLASS BUBBLE REPLACEMENT IN
SALMON RIVER TUFF. INSIDE OF BUBBLE FILLED
WITH MONTMORILLONITE WITH MINOR KAOLINITE.
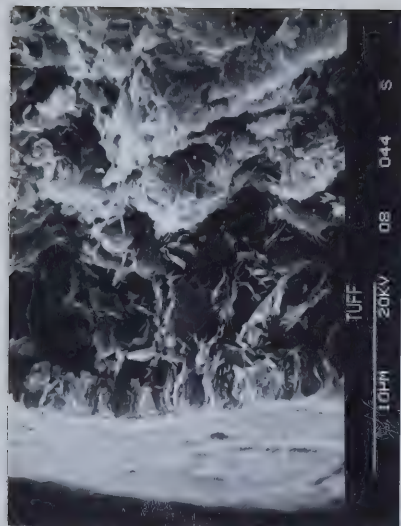
B. CLOSE UP OF BUBBLE WALL IN A. BUBBLE WALL
REPLACED BY MONTMORILLONITE. NOTE SURFACE PITS
RETAINED ON REPLACEMENT SURFACE.

C. REPLACEMENT FEATURE SHOWING MONTMORILLONITE
AND RELICT SURFACE ON GLASS BUBBLE.
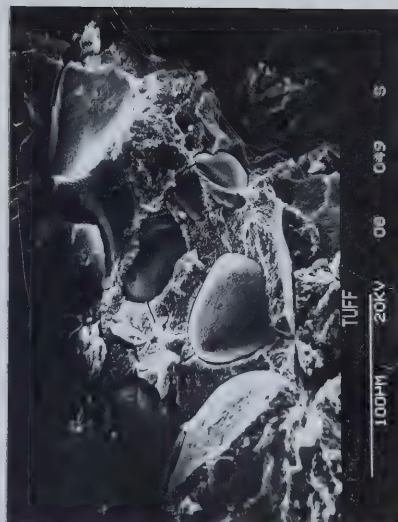
D. MATRIX-SUPPORTED NATURE OF SALMON RIVER TUFF.
MATRIX IS DOMINANTLY MONTMORILLONITE.

Plate 5.6 SEM micrographs of unweathered Salmon River Tuff (SR4)

Some grains are opalescent and are probably isotropic silica. Several euhedral crystals of a fibrous mineral are noted. Silt-size glass bubbles up to about 50 micrometres in diameter are observed throughout the fabric and the shells are replaced by montmorillonite. Some are also filled by montmorillonite. Montmorillonite is therefore present in matrix sites, and grain replacements and as grain coatings.

Intergrain and inter-assemblage pores are variable in size. Large trans-assemblage pores up to 30 μ in diameter also occur in a matrix-supported fabric.

5.7 Microstructure of Undisturbed Paleogene Volcaniclastics - Deadman River

Remoulded smectite-rich clays are commonly found in the landslide debris of the Deadman River Valley between Clemes Creek and Gorge Creek. Undisturbed clays, i.e., clays not having been remoulded by slope movement, are found in slope exposures south of the main landslide area and also as large blocks within landslide debris exposed in road cuts through the toe areas of the landslide. In both cases, surface exposures were samples and the extent to which these clays have been altered, or perhaps produced, by weathering processes is not known. As mentioned in Chapter 3, the precipitous walls of the head and lateral scarps of the landslides did not permit in-situ rock samples to be collected. Because of the extremely friable nature of the clays, thin sections were not prepared.

5.7.1 DR1: Yellow Clay - Cache Creek Road

DR1 is an extremely slick gritty, yellow, cloddy, clay dominated by smectite clay minerals. In the SEM grains in the initial fabric appear to have been interlocking euhedra of feldspar varying between 20 and 40 micrometres in length (Plate 5.7). These have undergone partial replacement by montmorillonite. The matrix is composed only of montmorillonite particles. This clay is interpreted to be an altered crystal tuff.

Voids are not extensive and assemblages are not well defined. Although the clay is grain-supported much of the grains have undergone the replacement by montmorillonite, effectively producing a matrix supported microfabric. This illustrates the effect of alteration processess in highly alterable volcaniclastic materials in changing grain-matrix relationships.
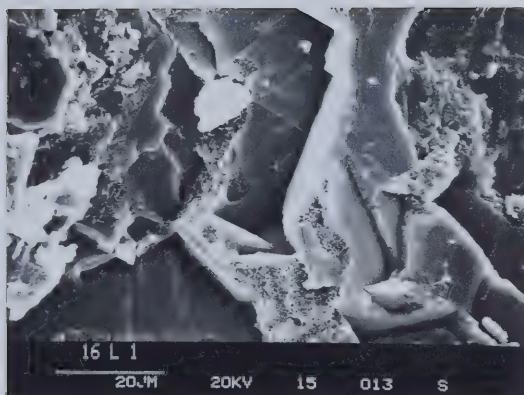
NOTE; INTERLOCKING EUHEDRA OF FELDSPAR UNDER-
GOING REPLACEMENT BY MONTMORILLONITE.

Plate 5.7 SEM micrographs of DR1

5.7.2 DR5 : Bat Clay

The fabric of the Bat Clay (Plate 5.8) collected from a hillslope exposure is dominated by montmorillonite clay particles which occur at matrix sites and as grain replacements. Grains consist of partially replaced euhedra and amorphous particles which are probably quartz. The shape of the amorphous particles varies from angular to rounded; these particles average about 10 μ in size. Irregular voids occur throughout the sample. Void spaces are noted at the trans-assemblage scale and may be up to 20 μ in width. Intra-assemblage pores are also marked. Inter-particle voids, up to 5 micrometres in width, are common throughout the fabric and appear to have been enlarged by solution processes. Montmorillonite also acts as a grain coating in the microfabric which is matrix supported.

5.7.3 DR6: Grey Clay

The sample of grey clay was collected from a fresh undisturbed block contained within the debris of landslide 1 exposed in a road cut at its toe. It is grey in colour and appeared to have a high mica content. This is reflected in the results of the XRD analysis discussed below. In the SEM (Plate 5.9) mica particles up to 100 micrometres wide were observed to be an important element in the grain component of the microfabric in Domain C. Other grains consist of angular amorphous pyroclastic particles up to 200 micrometres in length. The matrix is dominated by montmorillonite but grain fragments are also present. As seen in Plate 5.9, the clay is matrix-supported. Voids are not as pervasive as was found to be the case in the Bat Clay. Interparticle voids up to 5 micrometres in width occurred, some inter-assemblage voids are also noted. Grains do not appear to be replaced by montmorillonite.

5.8 Microstructure of Undisturbed Neogene Volcaniclastic Materials

Undisturbed samples of a variety of Neogene volcaniclastic materials were collected from exposures at Gorge Creek, Chasm Creek and the Chilcotin River. The materials are from the basal volcaniclastic assemblage of the Neogene volcanic succession as discussed in Chapter 2.
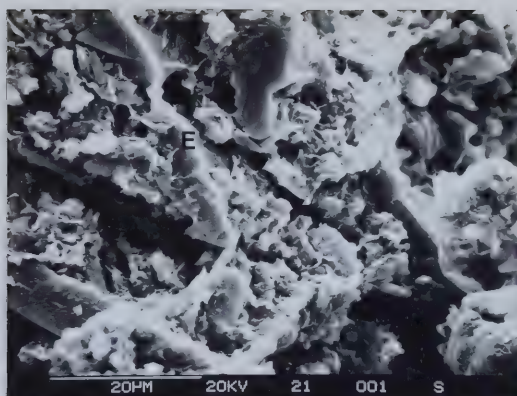
A. NOTE NATURE OF TRANS-ASSEMBLAGE PORES.
   GRAINS CONSIST OF PARTIALLY REPLACED
   EUHEDRA (E) AND MATRIX DOMINATED BY
   MONTMORILLONITE .
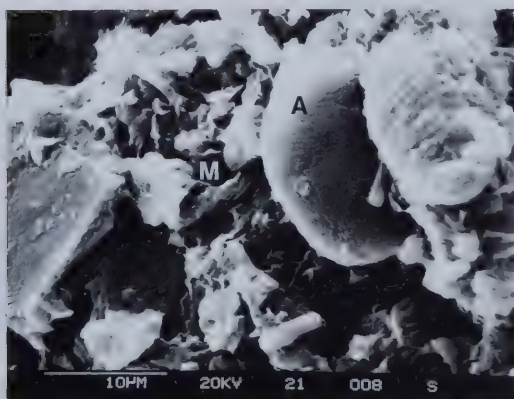
B. AMORPHOUS GRAIN (A) IN A MONTMORILLONITE
   MATRIX (M). NOTE CHARACTERISTICS OF INTRA-
   ASSEMBLAGE PORE SPACE.

Plate 5.8 SEM micrograph of DR5
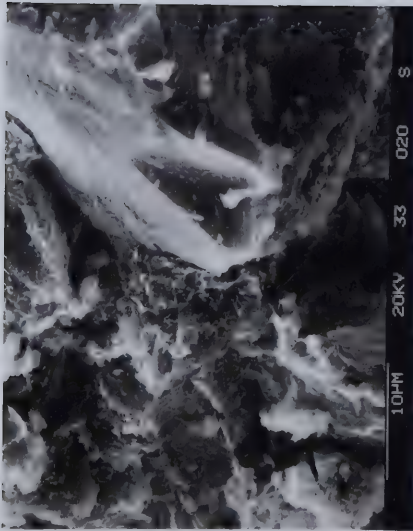
A. GRAIN-MATRIX RELATIONSHIPS IN DR6. NOTE MATRIX-SUPPORTED NATURE OF MICROFABRIC. MATRIX IS DOMINATED BY MONTMORILLONITE.
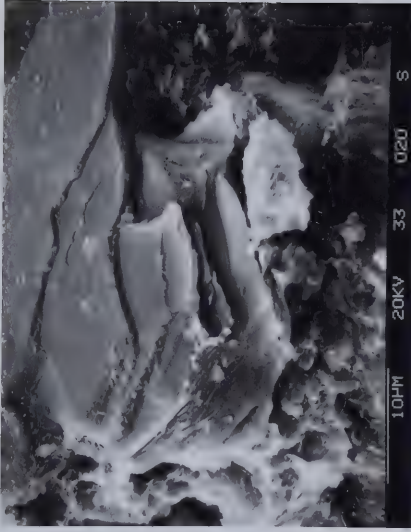
B. MICA GRAIN IN MONTMORILLONITE MATRIX

C. NOTE DISTORTION OF MONTMORILLONITE PARTICLES AROUND BASE OF GRAIN AND PRESENCE OF GRAIN FRAGMENTS.

Plate 5.9 SEM micrographs of DR6

5.8.1 NG1: Chasm Tuff C

The sample was collected from the same location in Chasm Creek as Tuff B described above. It is white fine grained tuff in which the matrix in Domain A is submicroscopic. Grains scattered throughout the material consist of crystal fragments, mainly quartz, less than 1 mm in diameter. The occasional lithic fragment less than 1 mm in diameter is also seen. The matrix is soft, being easily indented with a steel needle and the grains can be picked out of the matrix with little effort. Specks of magnetite are also seen throughout the matrix. The material is matrix-supported in Domain A.

In thin section (Plate 5.10) the grain component of the matrix-supported microfabric is seen to consist of several elements. It includes isolated lithic fragments up to 200 micrometres in size, fragments of opaque minerals, crystal fragments of feldspar and quartz up to 300 micrometres in size and isotropic glass particles up to 500 micrometres in length. The glass particles are shard-like in shape and also include frothy, vesicular particles (Plate 5.10). The matrix consists of amorphous glass dust which is partially altered to clay, as well as smaller fragments of rock and minerals.

The microfabric in Domain C is shown in SEM photographs in Plate 5.11 Grains observed in this domain are mainly glass shards and bubbles, some of which show the egg-shell characteristics noted in the Gorge Creek Tuff (NG3) described below. Many of the glass particles have been replaced totally or partially by montmorillonite. The matrix consists of montmorillonite. The microfabric is characterised by extensive pores at all scales. Large trans-assemblage voids occur up to 20 micrometres in diameter, and tubular inter-assemblage pores up to 4 micrometres in diameter give the montmorillonite matrix a swiss-cheese texture.

5.8.2 NG2: Chasm Tuff B

The tuff is white to buff in colour and in Domain A fragments up to 2 mm in diameter make up the grain component. The fragments are dominantly clear angular particles of quartz which are in the 0.5 mm to 2 mm size range. Other grains are angular lithic fragments up to 2 mm in length and crystal euhedra. The matrix is submicroscopic but is speckled by fragments of mafic materials and magnetite. The matrix is surprisingly resistant to the point of a steel needle and the quartz fragments could not be pried from
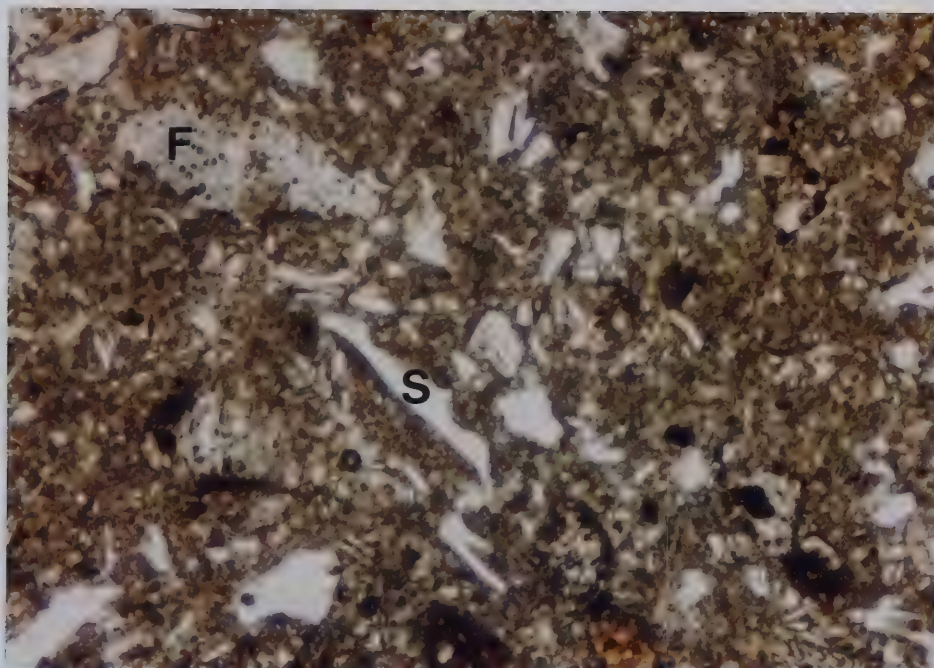
A. PLANE POLARISED LIGHT. GRAIN COMPONENTS DOMINATED BY GLASS SHARDS (S) SOME OF WHICH ARE FROTHY (F).

⊢————————⊣500 μ
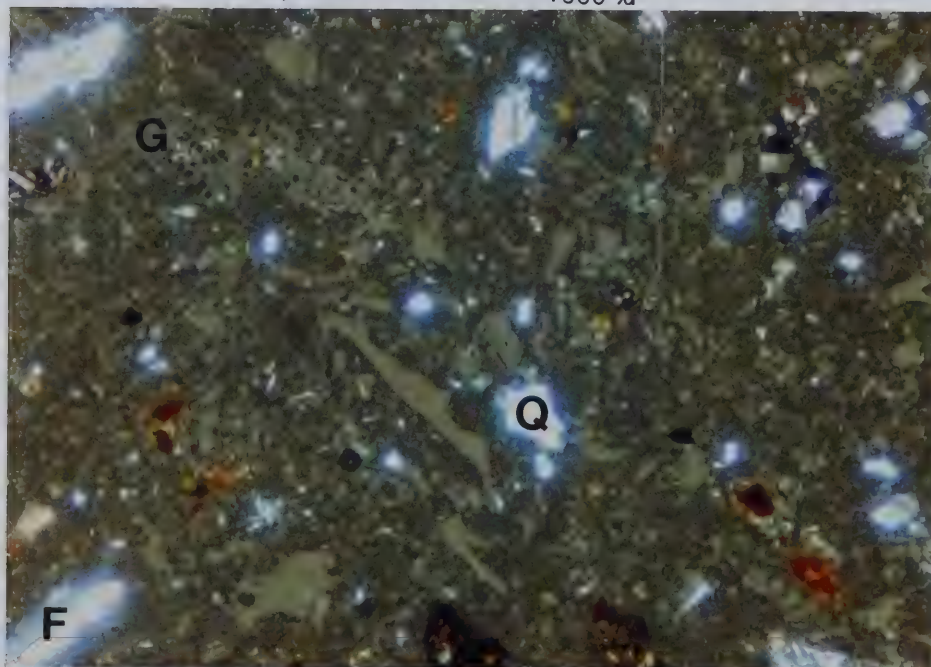
B. CROSS POLARS. NOTE FROTHY VESICULAR GLASS PARTICLES (G), FRAGMENTS OF FELDSPAR (F) AND QUARTZ (Q). MATRIX IS AMORPHOUS AND IS DOMINANTLY GLASS DUST PARTIALLY ALTERED TO CLAY.

Plate 5.10 Photomicrograph of intact Neogene tuff, Chasm Creek (NG1).

A. SPHEROIDAL AND SHARD-LIKE GLASS PARTICLES WITH WISPY FLAKES OF MONTMORILLONITE. GLASS PARTICLES ARE HOLLOW. NOTE INTER-PARTICLE PORE SPACE.

B. SWISS-CHEESE TEXTURE OF MONTMORILLONITE IN MATRIX. LARGE TUBULAR INTER-ASSEMBLAGE PORES ARE NOTED.

C. NOTE INTER-PARTICLE AND INTER-ASSEMBLAGE PORE SPACE AND PARTIAL REPLACEMENT OF GLASS SHARD IN LOWER RIGHT.
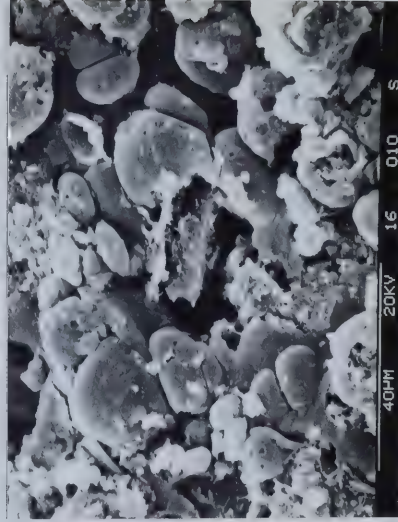
D. SPHEROIDAL GLASS BUBBLES WHICH APPEAR TO BE HOLLOW. NOTE INTER-PARTICLE PORE SPACE AND LARGE TRANS-ASSEMBLAGE PORES.

Plate 5.11 SEM micrographs of intact Neogene tuff, Chasm Creek (NG1)

the matrix with ease.

In thin section (Plate 5.12) the grain component is dominated by angular crystal fragments up to 400 micrometres in length. These are dominantly quartz but feldspar is also present . The grains are set in a submicroscopic matrix which is a mottled brown in plane polarised light and is mainly isotropic under crossed nicols. The matrix is thought to be altered glass dust with small lithic and crystal fragments, including much quartz. In Plate 5.13 an enlargement is shown of the matrix between a vesicular glass particle and a felspar grain. Both particles have undergone considerable alteration to clay. The nature of the matrix is also shown and it is noted that the alteration to clay is spatially discontinuous. In Domain B the tuff is matrix supported.

In Domain C, SEM micrographs (Plate 5.14) show a matrix—supported microfabric in which the grains consist of vesicular glass fragments with considerable intra—particle pore space. Glass particles show the effect of airbourne transport surface (Plate 5.14) and show partial replacement by montmorillonite. The matrix is dominated by montmorillonite which also occurs as grain coatings. The microfabric is typified by extensive inter— and intra—assemblage pores.

5.8.3 NG3: Gorge Creek Tuff

A yellow tuff—clay was collected from a road cut above Gorge Creek in the Deadman River valley. A Neogene age was assigned to the material because of its proximity to the base of the plateau lavas at the site and also on the basis of a K/Ar date reported from the vicinity by Mathews (1964) which indicated a Mio—Pliocene age.

It is a fine grained material although occasional quartz fragments and brown—red vesicular pyroclasts are noted in the microfabric in Domain A.

In Domain C the grain component of the microfabric is dominated by oddly shaped glass fragments (Plate 5.15) up to 60 micrometres in length and partially broken or altered euhedra up to 100 μ in length. Some glass particles resemble egg shells and are hollow. Others show classic bubble—wall replacement and infilling by montmorillonite. The microfabric is dominated by inter—particle pore space and is grain supported only in the sense that former grains are in contact. As can be seen in Plate 5.15 the majority of the grains have been replaced by montmorillonite effectively changing the fabric to a
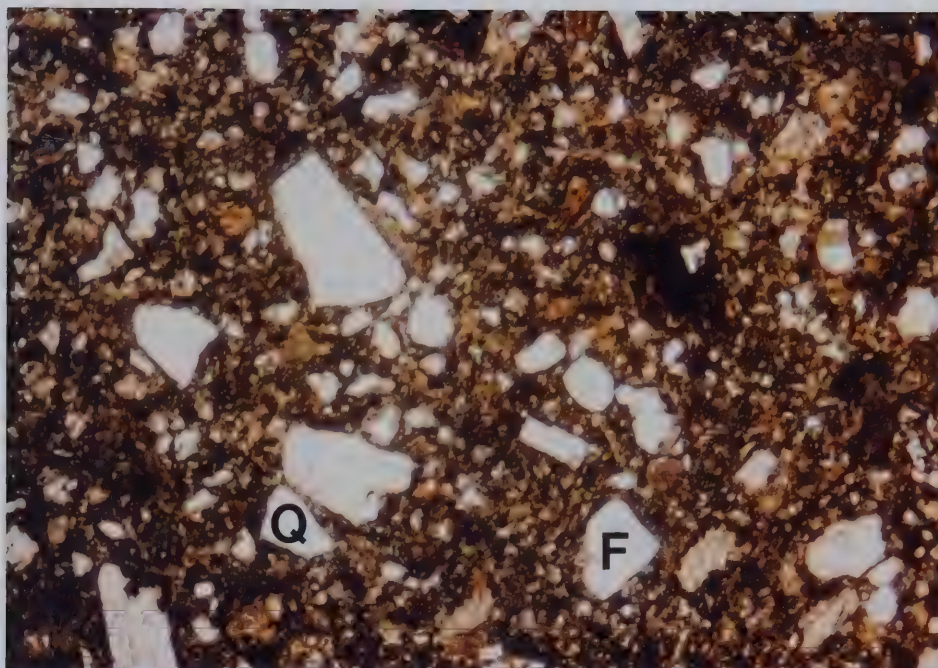
A. PLANE POLARISED LIGHT. GRAIN COMPONENT DOMINATED BY ANGULAR
CRYSTAL FRAGMENTS INCLUDING QUARTZ (Q) AND FELDSPAR (F).

⊢————————⊣500 μ
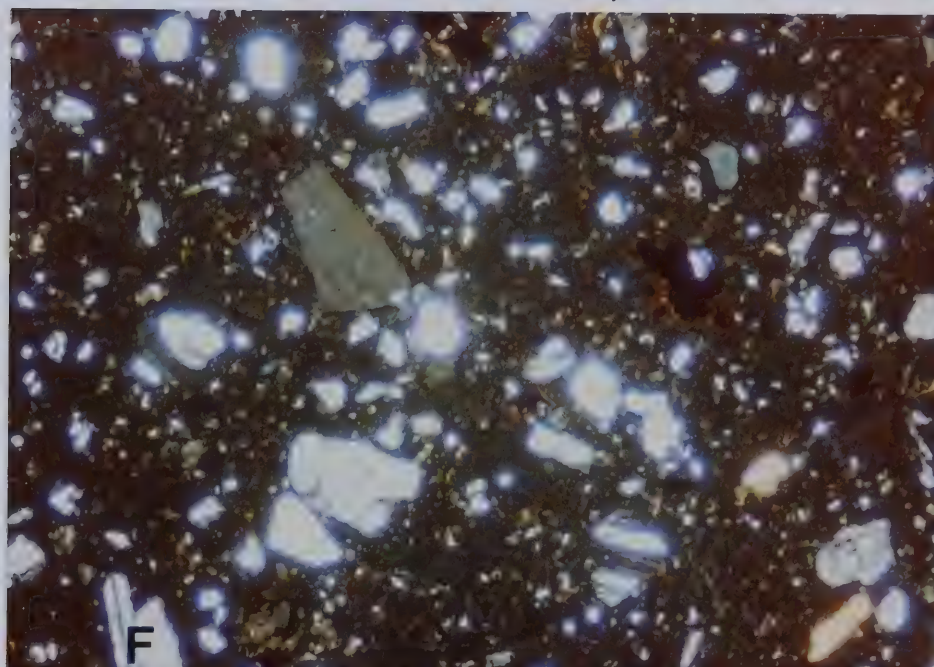
B. CROSS POLARS. NOTE FELDSPAR FRAGMENTS (F) AND MOTTLED NATURE
OF MATRIX OF GLASS DUST PARTIALLY ALTERED TO CLAY. LITHIC
AND CRYSTAL FRAGMENTS ARE ALSO SEEN.

Plate 5.12 Photomicrographs of intact Neogene tuff, Chasm Creek (NG2)
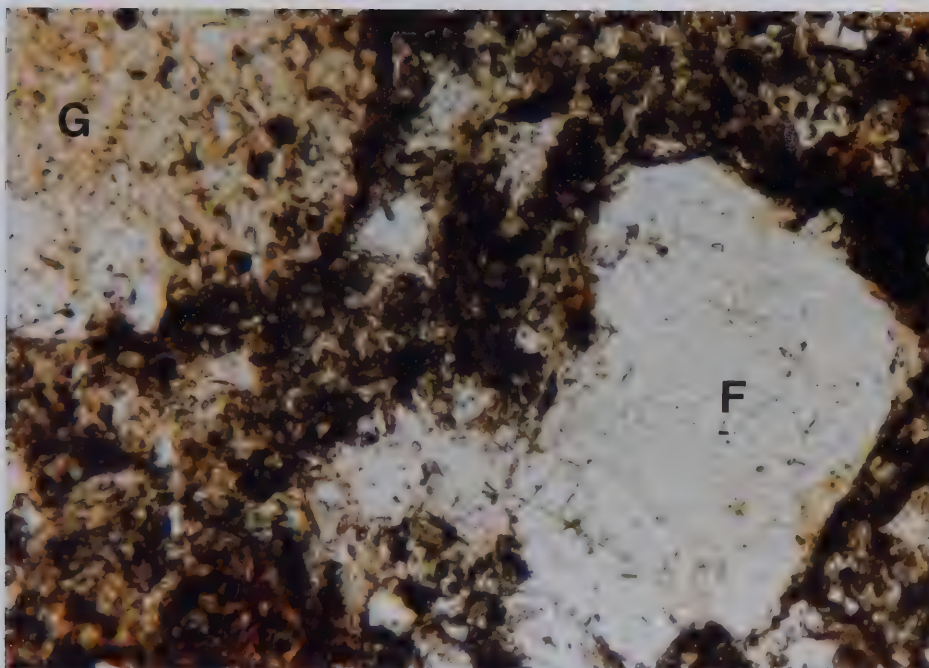
A. PLANE POLARISED LIGHT. GRAINS ARE VESICULAR FROTHY GLASS
FRAGMENTS (G) AND FELSPAR (F). NOTE MOTTLED APPEARANCE OF
MATRIX.

⊢————————⊣100 μ
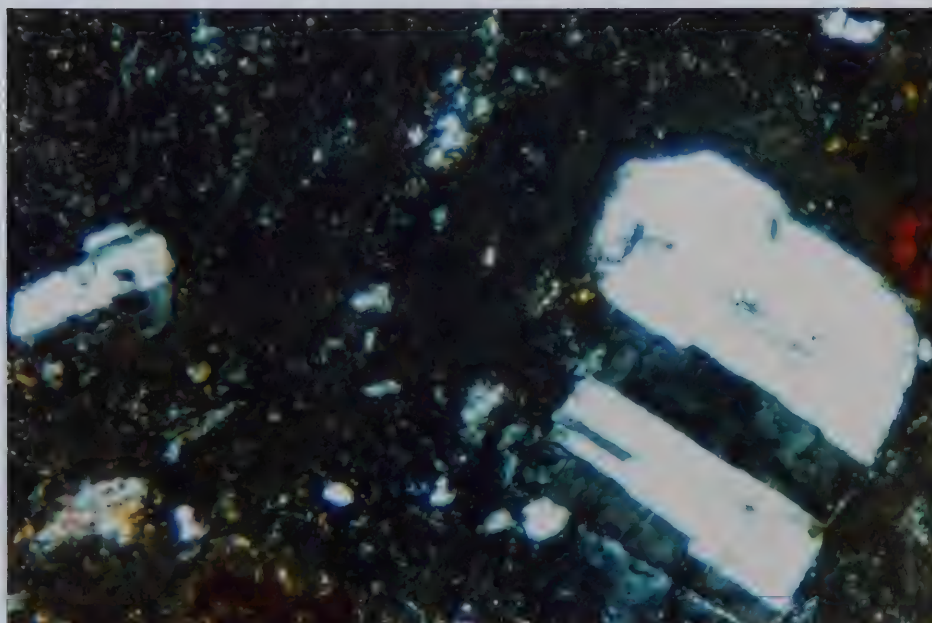
B. CROSS POLARS. NOTE FELDSPAR FRAGMENT ENCLOSED IN GLASS PARTICLE.
ALTERED AREAS OF GLASS DUST MATRIX ARE DARK BROWN. GREY
COLLOFORM TEXTURE APPEARS TO BE GLASS.

Plate 5.13 Photomicrograph of grain-matrix relationship in intact Neogene tuff,

Chasm Creek (NG2).

A. VESICULAR PYROCLASTIC FRAGMENTS SET IN MONTMORILLONITE MATRIX. NOTE INTRA-PARTICLE PORE SPACE.

B. GLASS PARTICLE PARTIALLY REPLACED BY MONTMORILLONITE ALONG JAGGED ALTERATION FRONT.

C. GLASS FRAGMENT SHOWING EFFECTS OF AIRBORNE TRANSPORT. NOTE MONTMORILLONITE GRAIN COATING.

D. VESICULAR PYROCLAST WITH PARTIAL INFILLING OF INTRA-PARTICLE PORE SPACE BY MONTMORILLONITE. NOTE TRANS-ASSEMBLAGE PORES.

Plate 5.14 SEM micrographs of intact Neogene tuff, Chasm Creek (NG2)

243
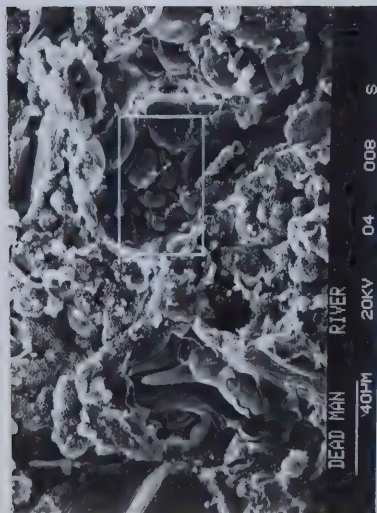
A. NOTE VOLCANIC GLASS PARTICLE MORPHOLOGY IN
MATRIX SYSTEM. GRAIN COATINGS OF
MONTMORILLONITE ARE SEEN AND THE OPEN NATURE
OF THE MATRIX MICROFABRIC DOMINATED BY INTER-
PARTICLE PORE SPACES.

B. ENLARGEMENT OF AREA OUTLINED IN A. HOLES AT
A AND B INDICATE VOLCANIC GLASS PARTICLES ARE
HOLLOW. LACEY STRING OF MONTMORILLONITE IS
SEEN.
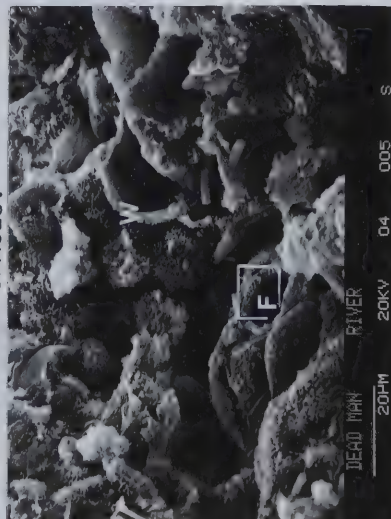
C. MATRIX DOMINATED BY REPLACED GLASS PARTICLES
BUBBLE WALL REMNANTS, SHARD SPLINTERS.
MONTMORILLONITE OCCURS AS WALL REPLACEMENT (W),
BUBBLE FILLING (F), AND AS PARTICLE COATING.
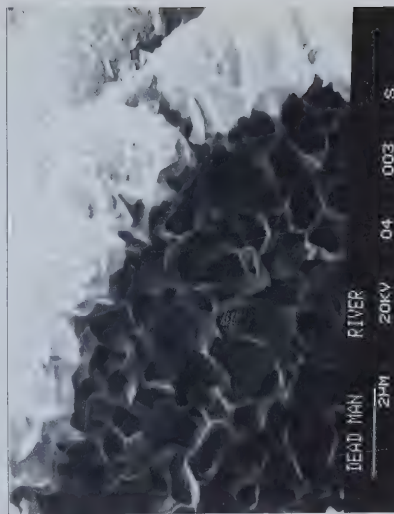
D. ENLARGEMENT OF AREA OUTLINED IN A. NOTE
DIFFERENCE IN INTER-PARTICLE PORE SPACE
IN WALL REPLACEMENT AND FILLING MONTMORILLONITE.

Plate 5.15 SEM micrographs of intact Neogene tuff, Gorge Creek (NG3)

matrix-supported one. Many grains have montmorillonite coatings.

5.8.4 NG4: Redstone Clay B

This brown finely laminated clay, with slickensided joint surfaces, was collected from the shear zone of the Redstone landslide discussed in Chapter 3. It is lacustrine in origin and in SEM photographs (Plate 5.16) a more typical detrital clay microstructure is observed (cf. Barden, 1972). Although the sediment is of detrital origin there is a significant proportion of pyroclastic grains in the microfabric.

The grain component of the microfabric in Domain 3 consists of angular amorphous fragments up to 20 micrometres in length which are probably pyroclastic in origin. In addition euhedra of pyroclastic origin can be seen. The matrix consists of a variety of clay mineral particles including kaolinite, montmorillonite and illite. Pore space at all scales is common throughout the matrix-supported microfabric as seen in Plate 5.16. It is noted that indications of the operation of secondary processes (e.g., corroded or replaced grains) are not present in the material.

5.8.5 NG5: Redstone Clay C

A light brown to buff clay was collected from above Clay B at the Redstone landslide. The grains are the skeletal remains of diatoms which occur up to 40 micrometres in diameter. The siliceous shell of the diatom has considerable intraparticle pore space (Plate 5.17). The diatoms are preserved in a matrix of smaller diatom fragments and clay particles which include montmorillonite, kaolinite and illite. The diatomaceous clay has a lacustrine origin and is matrix supported. Pore characteristics in the microfabric of Domain 3 is seen in Plate 5.17.

5.9 Microstructure of Sheared and Remolded Volcaniclastic Materials

Samples with a disturbed microfabric were collected from shear zones of landslides and debris of flow-type landslides which had undergone remoulding during flow movements. The objective of the exercise was to examine the effect of shearing and remoulding on fabric particularly with respect to void characteristics and grain-matrix relationships.
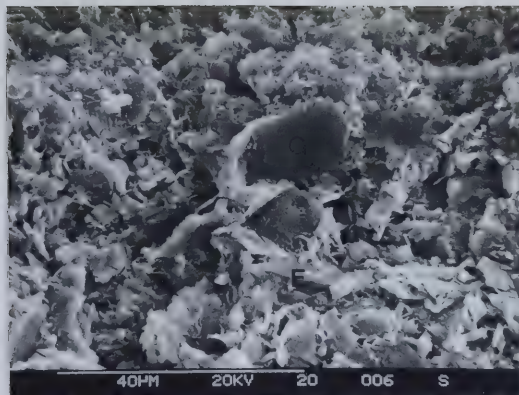
A. NOTE GRAINS (G) IN CLAY MATRIX AND FRAGMENTS OF
   EUHEDRAL CRYSTALS (E). INTER-ASSEMBLAGE AND
   TRANS-ASSEMBLAGE PORE SPACES LESS WELL
   DEFINED.
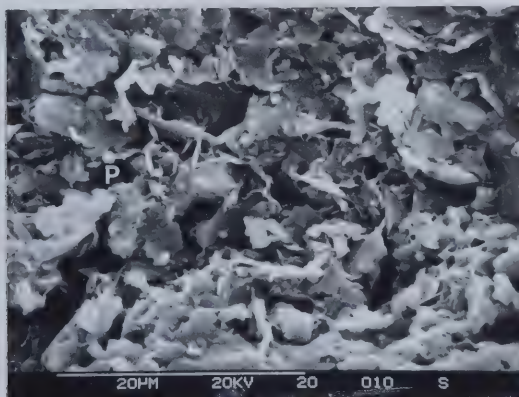
B. INTER-PARTICLE PORE SPACE WELL MARKED AT P.
   NOTE ARRANGEMENT OF CLAY AND SILT SIZE PARTICLES.

Plate 5.16 SEM micrograph of NG4
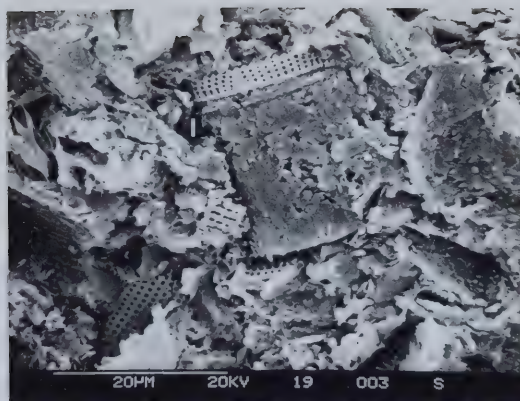
A. DIATOM DEBRIS AND CLAY PARTICLES IN MATRIX. NOTE
   LARGE INTER-ASSEMBLAGE PORE SPACES (I).
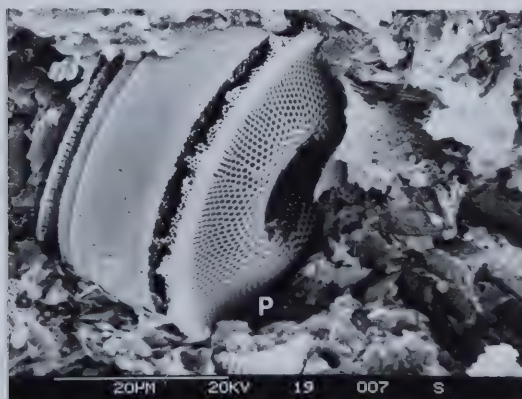
B. DIATOM SHOWING INTRA-PARTICLE PORE SPACE. NOTE
   INTERPARTICLE (P) PORE SPACE IN MATRIX.

Plate 5.17 SEM micrograph of NG5

The effect of shearing, remoulding and flowage on the microfabric of soils has been investigated in detail by a number of workers. Using the polarising microscope, Weymouth and Williamson (1953), Mitchell (1956), and Morgenstern and Tchalenko (1967) examined the change in microfabric which resulted from flowage, remoulding and shearing respectively. In work which utilised the Transmission and Scanning Electron Microscope the effect of remoulding and shearing on microfabric has been analysed by Pusch (1970), Foster and De (1971), McKeyes and Young (1971), Bennett *et. al.* (1981) and Lupini *et. al.* (1981).

5.9.1 SR8: Hummingbird Tuff, Adelphi Creek Landslide

Planar slickensided surfaces and wispy aggregates are found throughout the material (Plate 5.18) which was collected from the basal shear zone of the Adelphi Creek landslide. Shear surfaces consist of montmorillonite and involved the matrix of Domain C. A result of the shearing is that more particles in the matrix have face–to–face contacts and inter–particle and inter–assemblage pore spaces are reduced.

5.9.2 SR5: Salmon River Tuff, Shell Creek Landslide

Slickensided surfaces consisting of matrix montmorillonite are observed throughout the microfabric (Plate 5.19).

5.9.3 SR6, SR7: Salmon River Tuff, Jupiter Creek Landslide

Slickensided surfaces developed in matrix montmorillonite are observed in the SEM micrographs in Plate 5.20. The fabric shows a lack of aggregation when compared to the undisturbed samples. Face–to–face contact in the montmorillonite matrix is more common and bonding of clay particles occurs. Plate 5.20 illustrates angular grains up to 15 micrometres in diameter which are coated with montmorillonite. These grains appear to be fragmented pyroclasts.
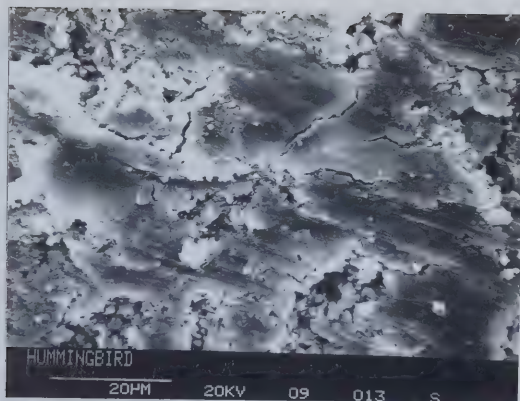
A. SLICKENSIDED SHEAR SURFACE.
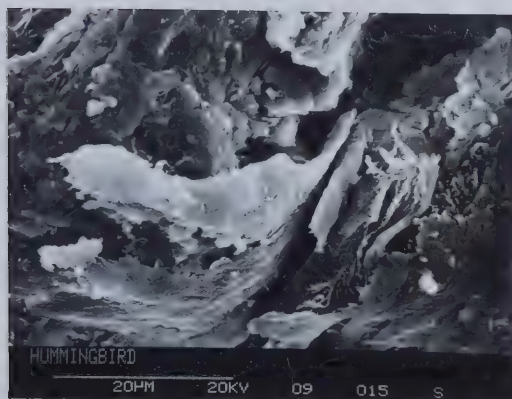
B. WISPS OF CLAY INDICATING MICROSTRUCTURE
DISTURBANCE IN DOMAIN C.

Plate 5.18 SEM micrographs of sheared Hummingbird Tuff (SR8)

A. CLOSELY PACKED MONTMORILLONITE PARTICLES.

B. SLICKENSIDED SHEAR SURFACE.
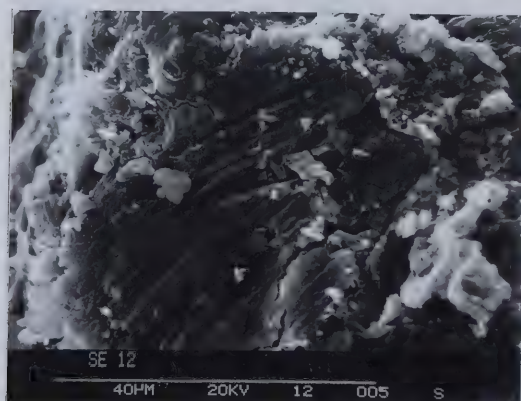
Plate 5.19 SEM micrographs of sheared Salmon River Tuff, Shell Creek landslide.

A. SHEAR SURFACE SHOWING SLICKENSIDES AND
   FLATTENED CLAY PARTICLES.

B. MONTMORILLONITE MATRIX SHOWING FACE-TO-FACE
   BANDING.

Plate 5.20 SEM micrographs of sheared Salmon River Tuff, Jupiter Creek landslide

5.9.4 DR4: Brown Clay

SEM photographs (Plate 5.21) of clay collected from a shear zone at the toe of landslide 3 show concentration of clay particles into wavy, tightly packed seams about 30 micrometres thick. Plate 5.21B is a view perpendicular to a slickensided shear surface and very fine multidirectional striations are seen. Deeper grooves indicative of uneven ploughing are noted in Plate 5.21C. In Plate 5.21D unidentified thin rectangular particles about 20 micrometres long are oriented parallel to the direction of sliding and give the impression of being stacked up. This is interpreted as being the result of re-orientation during sliding.

5.9.5 DR2: Hi-Hium Clay

In both remolded Deadman Valley clays there are no marked slickensides indicative of movement (Plate 5.22). A disruption of the fabric is suggested, however, and pore spaces are more extensive than intact materials. The pyroclastic grains sit in a montmorillonite matrix in which no obvious re-orientation has taken place.

5.9.6 DR3: Yellow Clay - Landslide 1

This sample is a yellow clay taken from landslide debris and had been subject to remoulding during flow. As with DR2, an absence of slickensides is noted. The microfabric is grain supported in places, as can be seen in Plate 5.23, suggesting that microfabric disturbance has taken place.

5.9.7 NG6: Bull Canyon Clay

A yellow-buff clay was taken from the exposed shear zone of the Bull Canyon landslide along the Chilcotin River. Highly oriented planar slickensides at a variety of scales are observed in SEM photographs (Plate 5.24). There are indications of directional changes at different scales and uneven ploughing (Plate 5.24). Definite layering and face-to-face alignment can be observed in bands of clay particles.

B. SLICKENSIDED SHEAR SURFACE.

C. PREFERRED ORIENTATION OF RECTANGULAR PARTICLES
   ON SHEAR SURFACE.

A. CONCENTRATION OF MONTMORILLONITE PARTICLES
   INTO WAVY, TIGHTLY PACKED SEAM.

Plate 5.21 SEM micrographs of sheared clay from shear zone of landslide 3

Deadman River valley (DR4)
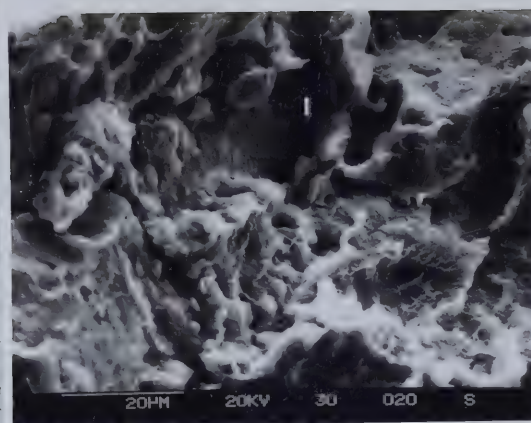
A. MONTMORILLONITE MATRIX. NOTE INTER-ASSEMBLAGE
PORE SPACE (I).
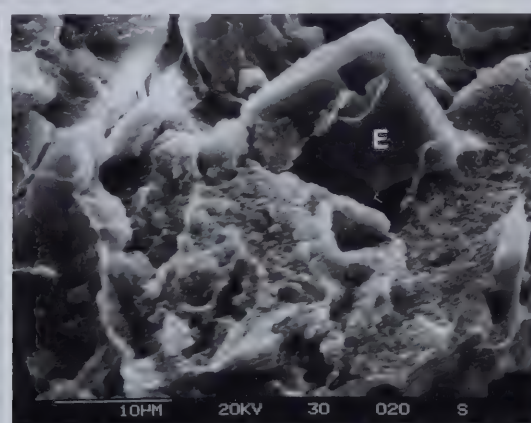
B. EUHEDRAL GRAIN (E) SET IN MONTMORILLONITE
MATRIX.

Plate 5.22 SEM micrographs of DR2
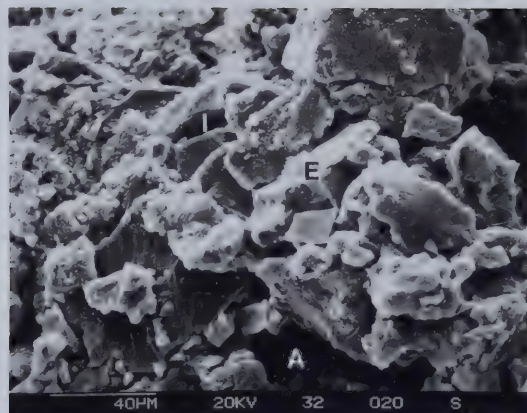
A. REGION OF GRAIN SUPPORT PROBABLY RESULTING
   FROM REMOULDING PROCESSES. NOTE FRAGMENTS
   OF EUHEDRAL GRAINS (E), INTER-PARTICLE (I),
   AND INTER-ASSEMBLAGE PORE SPACE (A).

B. MONTMORILLONITE MATRIX.

Plate 5.23 SEM micrographs of DR3
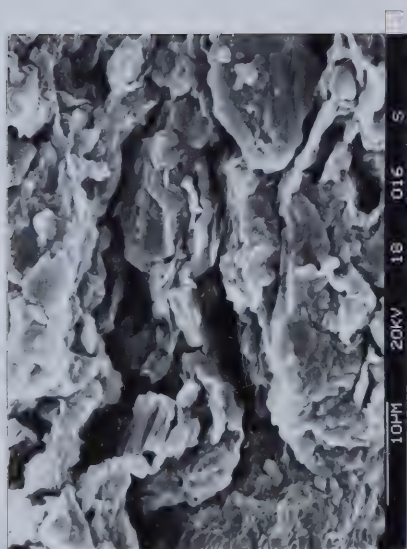
A. LAYERING OF CLAY PARTICLES PARALLEL TO THE DIRECTION OF MOVEMENT.
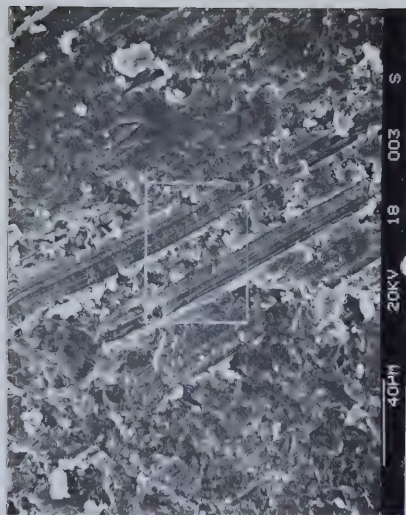
B. SLICKENSIDED SHEAR SURFACE. NOTE UNEVEN PLOUGHING.
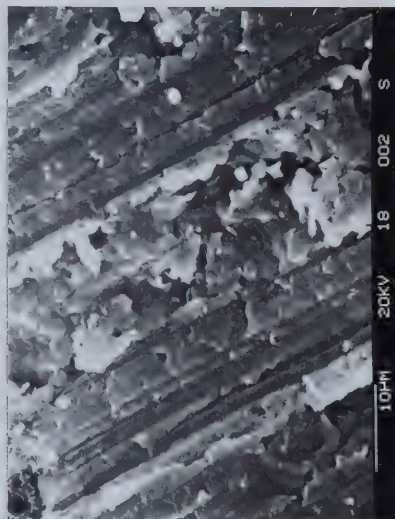
C. CLOSE-UP OF REGION OUTLINED IN B. NOTE FLATTENED AND ALIGNED CLAY PARTICLES.

Plate 5.24 SEM micrographs of sheared Neogene clay (NG6)

5.10 Discussion and Conclusions on the Microstructure of Volcaniclastic Rocks

The microstructure of the Tertiary volcaniclastic rocks examined here is a complex response to the initial processes of deposition, secondary processes of alteration and tertiary processes of weathering, remolding and shearing. With respect to the microstructure of undisturbed materials, a hierarchical multi-grain system was established in which 3 microstructural domains were established (Fig. 5.5).

Grain-matrix relationships were established for each domain and the microfabric was generally found to be matrix-supported at all scales. An important exception was the Paleogene Red Tuff from the Salmon Valley which was found to be grain-supported in Domain B (Plate 5.3).

In Domain A the grains are in excess of 500 micrometres in size (ash or medium to coarse sand) and consisted of lithic pyroclastic fragments. These fragments were generally vesicular but some were aphanitic. Again, important exceptions were noted (e.g., Chasm B-NG2) in which quartz particles made up a substantial portion of the grains in this domain. The matrix appeared to be a soft amorphous resinous material in Paleogene pyroclastic rocks whilst in the Neogene samples examined it tended to be powder-like.

Grains in Domain B are defined in the size range 500 micrometres to 75 micrometres, i.e., in the medium to fine sand/fine ash range. As in Domain A grains tend to be lithic fragments many of which are vesicular or amygdaloidal (Plates 5.1, 5.5). In Neogene rocks they also include frothy glass fragments (Plates 5.10, 5.13). An important element in the grain component of the microstructure in Domain B is the occurrence of euhedra of feldspar (Plates 5.5, 5.13) and fragments of quartz (Plate 5.12) and other silicon oxides. The matrix is a microcrystalline amorphous material which varies in colour in plane polarised light from white to orange to brown to dark brown. Within this material which contains pyroclastic dust much of which is altered to clay, are smaller lithic and crystal fragments.

In Domain C grains consist of silt size volcanic dust ($\leq$ 75 micrometres > 2 micrometres) which are fragments of minerals (e.g., mica), euhedra (Plate 5.7) and lithic materials. In Paleogene rocks no glass fragments were directly observed, all having been replaced by montmorillonite (e.g., Plate 5.6). However, in Neogene material glass fragments make up a substantial proportion of the grain in this domain (e.g., Plates 5.11,

5.15). The matrix in both types of materials is dominated by clay minerals.

X-ray diffraction and analysis of the < 2 micrometre portion of these volcaniclastic materials (i.e., matrix materials in Domain C) showed the clay mineralogy to be dominated by smectite clays (Fig. 5.12). Other clays were important in the Neogene volcaniclastic sediment collected from the Redstone landslide. Feldspar was the only non-clay mineral to give significant reflections on the diffractograms.

Based on SEM observations, the smectite is in the form of montmorillonite which appears to result from diagenesis. The evidence for the diagenetic origin as opposed to an allogenic origin includes the delicate form of the clay particles, their location with respect to replacement sites, and their presence as grain coatings. In the Salmon River Tuff (SR3, SR4) it is also possible that deuteric alteration may have contributed to the formation of the clays (cf. Plate 5.5).

The montmorillonite originates from the alteration of volcanic glass and feldspar crystals as well as being precipitated from groundwater. Plates 5.6, 5.11 and 5.15 show volcanic glass replacement structures whilst in Plates 5.7 and 5.8 feldspar crystals are shown partially replaced by montmorillonite. Lace-like trails of montmorillonite (Plate 5.15) and grain coatings (Plate 5.2) are evidence of direct precipitation from groundwater. Diagenetic silica has contributed to intergranular cement in the case of the Red Tuff as mentioned above.

The formation of diagenetic montmorillonite has important geotechnical consequences. Montmorillonite has formed at grain as well as matrix sites. The cohesion and frictional components of matrix shear strength would be expected to be reduced in all domains in material which has undergone diagenesis. In addition the cohesion of the grain-matrix contact is also reduced. Grain coatings and limited replacement of glass and feldspar within lithic fragments, evident from embayed and etched grain boundaries, would be expected to reduce the frictional resistance and compressive strength of the grains, respectively.

The microstructure of volcaniclastic materials is also characterised by a very open, porous microfabric characterised by large inter-assemblage pores. This aspect of the microstructure is evident in most of the SEM micrographs.

Two volcaniclastic sediments from the Redstone landslide area show significant differences in microstructure when compared to the pyroclastic materials. In the clay mineralogy the percentage of non-smectite clays in the clay fraction, calculated by the semi-quantitative method referred to in Section 5.3, is significantly higher than other materials studied (Fig. 5.10), reflecting the contribution of clay from other sources. These materials are detrital in origin having been deposited in a lacustrine environment. The remainder of the samples studied were of airfall pyroclastic origin.

Differences in microfabric were noted in disturbed samples. The formation of slickensides in the matrix of Domain C (Plates 5.20, 5.24), banding of clay particles (Plates 5.21, 5.24) and the disturbance of the microstructure (Plate 5.20) were noted in samples from shear zones whilst remolded landslide debris exhibited an increase in pore sizes (Plate 5.23).

Differences between the Paleogene and Neogene materials have been referred to in the discussion above. Diagenetic alteration appears more complete in the Paleogene materials and is manifested by the absence of volcanic glass particles which have been completely replaced by montmorillonite.

6. GEOTECHNICAL PROPERTIES OF VOLCANICLASTIC ROCKS

6.1 Introduction

A laboratory programme was carried out on selected volcaniclastic materials. The basis of sample selection was the role of these materials in slope movements in the Salmon Valley and at Chasm Creek which are analysed in the following chapter. The geotechnical behaviour of selected samples was characterised by a variety of engineering classification tests, estimates of the uniaxial compressive strength of the intact rock material (q_u) together with the ultimate shear strengths of artificially prepared surfaces. The objectives of the laboratory programme were to investigate the relationship between microstructure and the geotechnical behaviour of those samples selected, and to provide parameters for the analysis of movement mechanisms in Chapter 7. The laboratory work carried out is summarised in Table 6.1. It may be noted that attempts to disaggregate sufficient of the selected volcaniclastic materials for grain-size analyses proved unsuccessful.

The laboratory programme was carried out under several constraints which resulted from the character of the materials under examination. As discussed in the previous chapter, the material was either disturbed or undisturbed. Both types of material are friable due to surface weathering processes or alteration, and it was difficult to collect block samples that did not exhibit cracking of some magnitude. An effort was made to collect fresh samples by taking blocks from as deep within the slope as was possible but even these were found to crack during transport by backpack and vehicle. This aspect of the intact material involved considerable waste in sample preparation and limited the range of tests that could be carried out.

It is noted that the geotechnical properties of pyroclastic and volcaniclastic rocks are not widely reported in the literature and lists of rock properties in textbooks and manuals frequently omit reference to this group of materials.

Table 6.1 Laboratory tests carried out on volcaniclastic materials.

	Density	Adsorption I	Slake Durability	Point Load	Direct Shear
SR1 Twig Creek Tuff	X	X	X	X	X
SR2 Red Tuff	X	X	X	X	X
SR3 Weathered Salmon River Tuff	X				
SR4 Unweathered Salmon River Tuff	X	X	X	X	X
SR10 Purple Volcanic Breccia	X	X		X	
SR11 Red Volcanic Breccia	X	X		X	
NG1 Chasm C Tuff	X	X	X	X	X
NG2 Chasm B Tuff	X	X	X	X	X
NG3 Gorge Creek Tuff	X	X	X	X	
NG4 Redstone C clay	X		X		
NG5 Redstone B clay	X		X		

6.2 Dry Bulk Density, Porosity and Absorption Index

The dry bulk density, γ_d, was established by the water displacement method outlined in Gyenge (1977) and ISRM (1979). In this method a fragment of rock is oven-dried, weighed, coated with wax, weighed again and immersed in a measuring cylinder. The volume of water displaced is measured and corrected for the volume of the wax coating and γ_d is calculated by dividing the oven-dry weight by the corrected volume of water displaced.

The results are given in Table 6.2 and it is seen that the Paleogene pyroclastics are approximately 20% denser than Neogene materials. Table 6.3 shows the values of for other Tertiary pyroclastic and volcaniclastic rocks reported in the literature and comparable values for γ_d are seen.

No porosity measurements were made directly but an estimate of porosity, n, was made from Equation 6.1 in which γ_w is the density of water and G_s is the specific gravity of the particles making up the material.

$$\gamma_d = G\,(1-n)\,\gamma_w \qquad\qquad 6.1$$

In this estimate G_s was assumed to be 2.5 (cf. Keller's (1960) estimate of G_s for tuff at the Nevada Test Site) since it reflects the vesiculated nature of some constituent particles. The void ratios were also calculated from this estimate of n and the results are found in Table 6.2. Estimated porosities vary between 10.7% and 43.2% reflecting the values of γ_d being intermediate between soils and the more common rocks.

The dry density and porosity measurements reported here result from the complex interaction of initial depositional density, diagenetic processes and loading history. Values of initial depositional densities for airfall tuff from Hekla (Thorarisson, 1967) and Mount St. Helens (Sarna-Wojicki et. al 1981) range from 9 KN/m^3 to 17.8 KN/m^3. These values are estimated for tuffs that have undergone compaction over periods of up to 1000 years since depostion, and the range in these values overlaps the range of the Tertiary rocks examined here. Low valus of γ_d reflect the loose structure produced by rapid airfall deposition from a dense ash cloud and are comparable to those of loess.

Pore-space reduction is expected to have taken place within a short time of depostion by the chemical precipitation of clay minerals (Almon et. al. 1976; Davies et. al.

Table 6.2 Dry bulk density and estimated porosity of intact volcaniclastic rocks.

SAMPLE	DRY DENSITY (KN/m) $-\gamma_d$	POROSITY[1] (%) - n	VOID RATIO[1] - e
SR1	21.47	12.3	0.14
SR2	21.86	10.7	0.12
SR3	21.92	9.2	0.12
SR10	17.85	27.0	0.37
SR11	20.71	15.3	0.18
NG1	18.63	24.2	0.32
NG2	14.90	39.1	0.64
NG3	14.90	39.1	0.64
NG4	13.98	43.2	0.76
NG5	15.98	34.8	0.53

[1] ASSUMES G_s OF PARTICLES = 2.5 gms./cc

Table 6.3 Data on comparable Tertiary rock types from literature sources.

SOURCE	ROCK TYPE	γ_d (KN/m³)	e	n
a	Bedded Tuff	14.70	.634	38.8
a	Bedded Tuff	13.43	.690	40.2
a	Friable Tuff	14.70	.633	35.5
a	Welded Tuff	21.37	.164	14.1
b	Tuffs and Tuffites	17.00	-	-
c	Welded Tuff	14.37	-	-
d	Decomposed Tuff	12.75	1.235	55.2
d	Decomposed Tuff	17.44	.639	38.9
e	Basalt	26.7-28.12	-	-

Sources ; a-Keller (1960), b-Heitfeld et al. (1980),
            c-Morland and Hastings (1973),
            d-Corns and Nesbitt (1967), e-Deere and
            Miller (1966).

1979). Davies *et. al.* (1979) show a 20% decrease in porosity in Tertiary volcaniclastic compared to equivalent contemporary deposits due to the production of authigenic montmorillonite and other minerals. Comparison with data from the Hekla and Mount St. Helens deposit suggests a pore space reduction of the same magnitude for the Paleogene and Neogene rocks studied here. This porosity may also be modified by the dissolution of pyroclastic material, or the dissolution of authigenic materials as discussed in Chapter 5. The fact that pores may be of hybrid origin (Schmidt and McDonald, 1979) was noted in scanning electron micrographs in the previous chapter.

The effect of loading history is also of importance since both Paleogene and Neogene rocks come from basal locations in their respective volcanic successions. The presence of such highly porous materials at the base of volcanic successions does suggest that the effect of consolidation of these deposits has been reversed in relatively recent geological time and that this process may have contributed to the landslides that mark their location.

For selected samples, an estimate of porosity was also made by the quick absorption test (ISRM, 1979) based upon the Weathering Index of Hamrol (1961). The test measures the Absorption Index (AI) which is defined as the mass of water contained in a rock sample after a 1 hr. period of immersion as a percentage of its original oven-dry mass. The index has been found to be correlated with porosity and such properties as degree of alteration (Hamrol, 1961), where porosity is a product of weathering or alteration processes. It also can be correlated with shear strength (Rocha, 1964) and unconfined compressive strength (Serafim, 1964) due to porosity and mineralogical changes that are a response to alteration processes. Values of the absorption index (AI) determined on a number of rocks are seen in Table 6.4.

Difficulty is found in applying this test to pyroclastic rocks because some samples slake completely when immersed in water for one hour (e.g. NG3). In addition, porosities in pyroclastic rocks are high due to factors other than weathering or alteration (i.e., initial depositional density, vesicular particles). For example, a Paleogene vesicular welded breccia from the Salmon River yielded AI = 18, a value in excess of the value of AI = 15, which, according to Rocha (1964), corresponds to a residual soil state in which the rock is completely diseggregated.

Table 6.4 Values of the Absorption Index (AI) obtained in the quick absorption test.

SR1.........12.0

SR2.........10.0

SR3.........12.0

SR10........18.0

SR11.........7.5

NG1.........14.5

NG2.........17.3

NG3.........SLAKED

The relationship between estimated porosity and AI is seen in Fig. 6.1 and considerable scatter is seen in the plot.

6.3 Slake Durability

The water deterioration characteristics of 8 intact samples were established using the Slake Durability test. Other samples were too friable to be tested using this method. An estimation of the water deterioration characteristics of the material is important in estimating the role of long term strength changes (softening) and changes of slope stability with time (Morgenstern and Eigenbrod, 1974). The standard apparatus and method, recommended by Franklin and Chandra (1972) and ISRM (1979), were used. In this test ten lumps of material weighing approximately 500 g are subjected to two cycles of 6 hours drying and 10 minutes of tumbling and wetting. Distilled water was used in the test. The Slake Durability Index (SDI) is the ratio of the oven–dry weight of rock remaining in the drum after the 2 cycles of slaking to the initial oven dry weight expressed as a percentage.

The Slake Durability Test is a measure of the ease with which water can enter the rock, the reaction of the fabric to the ingress of water (e.g., solution of cement, hydration, destruction of interparticle bonds) and the resistance of the rock material to this reaction in the form of intergranular strength (i.e., water sensitive cohesion). Franklin and Chandra (1972) found that the results of the Slake Durability test closely correlate with in–situ weathering performance. It was anticipated that the SDI would reflect the presence of swelling clay particles and the degree to which interconnected voids transmitted water to the swelling clay sites. The results are seen in Table 6.5.

Whilst useful relative data were produced by the Slake Durability Test, viz. the Paleogene material exhibited less tendency to deteriorate in contact with water than Neogene material, the method produced misleading absolute results. For example, NG3, a Neogene tuff from Gorge Creek slaked completely within an hour when soaked for the absorption test and yet was estimated to be of medium slake durability in this test with SDI = 64.1%. It is of interest to note the remarks of Goodman (1976) that the Slake Durability test is unsuitable for swelling materials as the clay near the surface of the lumps swells to occlude exterior pores thereby limiting access to the interior of the specimens. It is therefore concluded that the dynamic slake test is unsuitable for establishing the water
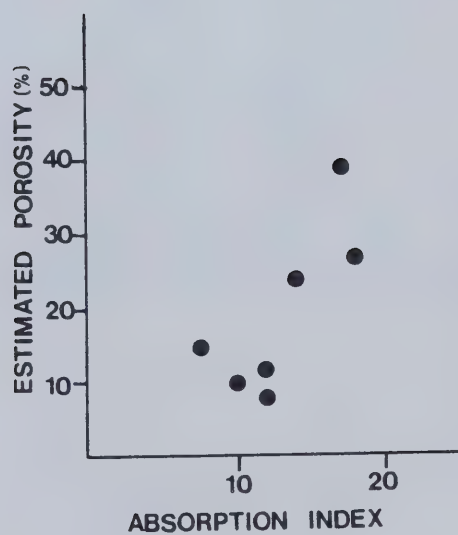
Figure 6.1 Relationship between porosity and Absorption Index.

Table 6.5 Results of Slake Durability Tests.

SAMPLE	SDI	SLAKING CLASSIFICATION[1]
SR1	96.4	EXTREMELY HIGH
SR2	98.0	EXTREMELY HIGH
SR4	92.1	VERY HIGH
NG1	72.7	MEDIUM
NG2	91.0	VERY HIGH
NG3	64.1	MEDIUM
NG4	79.8	HIGH
NG5	74.7	MEDIUM

SDI = SLAKE DURABILITY INDEX
[1]ACCORDING TO FRANKLIN AND CHANDRA (1972).

deterioration characteristics of the group of materials under examination.

The relationship between porosity and SDI is seen in Fig. 6.2. A nomalously high slake durability in relation to porosity is exhibited by NG2 and NG4 probably reflecting the problem of occluded pores as well as the fact that both of these materials have a high degree of intra-particle pore space in the form of vesiculated glass particles and diatom skeletons, respectively.

6.4 Point Load Strength and Estimated Uniaxial Compressive Strength (q_u)

Point load tests were conducted on materials involved in slope movements in the Salmon Valley and Chasm Creek. In addition, pyroclastic breccias and tuff from the Salmon Valley and Gorge Creek were tested to provide comparative data. Details of the test may be found in Broch and Franklin (1972) and Bieniawski (1974). As discussed by these authors, an approximation to the uniaxial compressive strength (q) may be obtained by the test. It is particularly useful in estimating the q_u of highly weathered, altered or friable rock as are the rocks considered here (cf. Fookes *et. al.*, 1971; Raphael and Goodman, 1979). Due to the lack of availability of samples, the effects of water content on the value of the Point Load Strength could not be evaluated.

Irregular lumps of rock were obtained from large blocks which had been air dried. Irregular lump tests were then carried out according to the procedures followed by Broch and Franklin (1972). The following exceptions, however, were made to the procedure due to the availability of materials and their friable nature;

(a) Values of the Shape Factor (S) defined as the ratios of the largest diameter to the shortest diameter, ranged from 1.18 to 3.3 in the tests carried out. Broch and Franklin (1972) recommend a maximum shape factor of 1.4 for the irregular lump test. However, the failure load (P) was found to be insensitive to the value of S over the range encountered in this study and is not thought to affect the value of P obtained.

(b) Broch and Franklin (1972) also recommend 20 as the minimum number of irregular lumps that should be tested. However, during the preparation of the irregular lumps from the larger blocks using a hammer and chisel, much of the block was reduced to a highly fragmented crumbly mass, mitigating against the testing of the recommended minimum number.
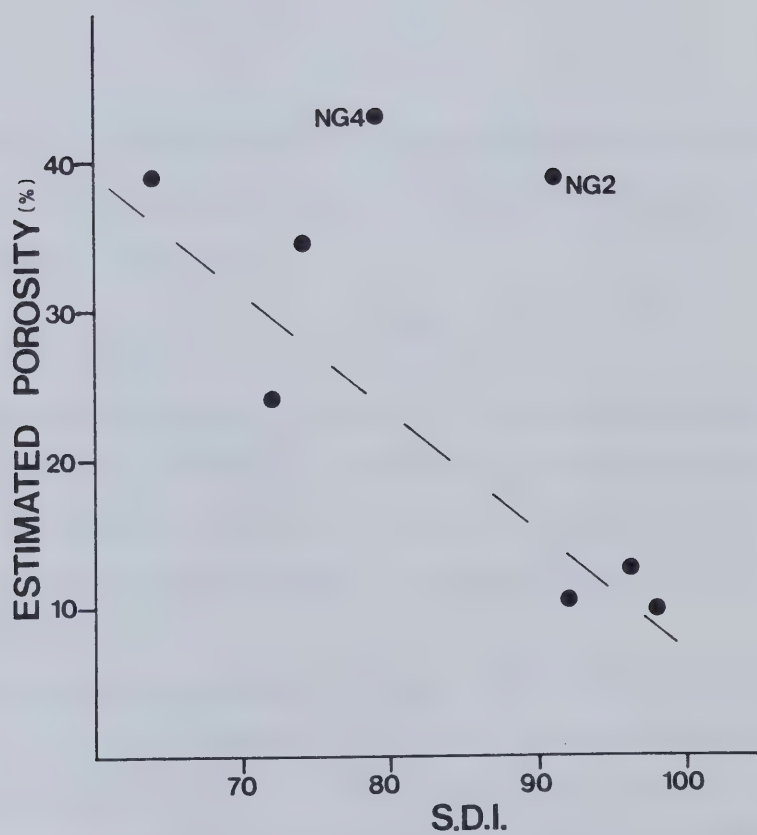
Figure 6.2 Relationship between estimated porosity and Slake Durability Index (SDI).

The lumps were placed between the conical platens of the point load apparatus and the separation of the platens (D) measured. The platens were then driven toward each other by hydraulic jack and the load at which the rock lump failed (P) was measured on a dial gauge.

The values of P were corrected for size effects (Broch and Franklin, 1972). In cases where the corrected value was below 300 KN/m³ the corrected value was estimated.

To obtain the Point Load Strength of the rock (I_s), following Broch and Franklin (1972),

$$I_s = P/D^2 \qquad\qquad 6.2$$

The Point Load Strength Index of the rock is the median value of I_s and the results are presented in Table 6.6. An approximation to the unconfined compressive strength (q_u) of the rock may be obtained by

$$q_u = 24 \, (I_s)_{50} \qquad\qquad 6.3$$

Values of q_u obtained by Equation 6.3 are shown in Table 6.6; these estimates are thought to be within 15% of the q_u of the intact rock substance in the air dry state. Values of q_u varied between 4.70 MPa and 13.48 MPa. Under the Geomechanics Classification Scheme of Bienawaski (1978) they are considered to be very low strength (1–5 MPa) or low strength (5–25 MPa).

Interrelationships between the estimated q_u and the other geotechnical parameters are illustrated in Fig. 6.4. The dependence of q_u on porosity is seen Fig 6.4A and reflects similar results by Fookes et al. (1971). The process by which porosity changes take place after valley excavation and the development of groundwater flow systems, therefore becomes important in controlling the threshold value of q_u . q_u is also seen to be related to the Absorption Index (Fig. 6.3A). The limiting value of AI suggested by Rocha (1964) is not applicable to volcaniclastic rocks since a value of AI > 15 would imply q_u =0 which is not found to be the case. The relationship with SDI is not clear, reflecting the problem in the interpretation of the SDI results. At values of q_u below 7MPa, there is a steep decline in SDI with q_u , but above this value there is no relationship.

SAMPLE DESIGNATION	NUMBER OF FRAGMENTS TESTED	POINT LOAD INDEX (MPa)	q_u (MPa)	GC^1
SR1	12	0.31	7.44	L
SR2	8	0.41	9.93	L
SR4	15	0.19	4.70	VL
SR10	5	0.26	6.45	L
SR11	6	0.56	13.48	L
NG1	13	0.20	4.82	VL
NG2	14	0.27	6.60	L
NG3	10	0.21	4.96	VL

[1]GC = Geomechanics Classification of Bieniawski (1979):L=Low Strength, VL=Very Low Strength.

Table 6.6 Results of Point Load Tests and estimates of uniaxial compressive strength (q_u)
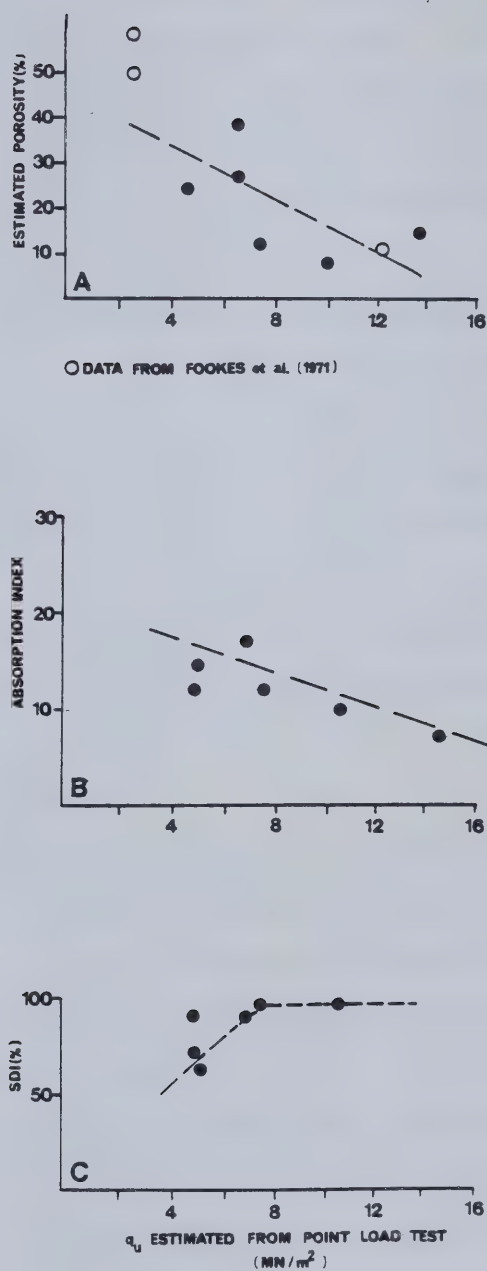
Figure 6.3 Interrelationships between q_u estimated from the point load test and other geotechnical parameters. q_u is the abcissa in each of the diagrams.

6.5 Direct Shear Tests

Direct shear tests were carried out on four pyroclastic rocks and on material from the shear zone of the Jupiter Creek landslide. The samples were selected because they were associated with the landslides analysed in Chapter 7. The tests provide lower-bound shear strength data for the analysis of the translational sliding movement mechanism in which it is assumed that sliding takes place along pre-sheared surfaces in the volcaniclastic rocks. These data are in the form of ultimate angles of shear resistance of flat saw-cut surfaces which were found by Krahn and Morgenstern (1979) to give the best approximation to the ultimate shear resistance of a flexural slip surface in material from the Frank Slide. Residual shear strength data were for disaggregated Salmon River Tuff and fragmented material from the Jupiter Creek landslide shear zone.

Four rocks were tested in a 5.1 cm. x 5.1 cm high capacity shear box Samples were cut by saw and sanded to fit the box. Prior to placement an artificial shear surface was prepared by diamond saw cut. Before shearing, the shear box was flooded for 24 hours with distilled water. Examination of the rock blocks after the test confirmed that the shear surface was wet when sheared. Test data were recorded directly on a Hewlett-Packard XYY recorder. In all of the tests, a thin, slickensided film of clay developed on the shear surface.

Several difficulties were encountered in sample preparation and testing. In cutting the samples to fit the shear box, much of the rock fractured making it impossible to prepare a large number of samples. In the testing process, samples in the shear box were frequently ruined by degradation around the edges during the movement of the shear box. This degradation resulted in the decision to restrict the travel distance of the shear box which avoided excessive cracking around the edges of the sample. Examination of load-displacement curves indicated, however, that ϕ'_{ult} was obtained.

The ultimate shear strength envelopes are presented in Figs. 6.4, 6.5, 6.6, and 6.7.

The Salmon River Tuff from intact and sheared exposures was too friable to test in the high capacity shear box; this tuff was tested in a conventional 6 cm. x 6 cm. Wykeham-Farrance shear box. The intact Salmon River Tuff was disaggregated using a mechanical pestle and fragments passing the #4 sieve were placed wet in layers and then consolidated. Only a limited range of normal pressures was possible with the
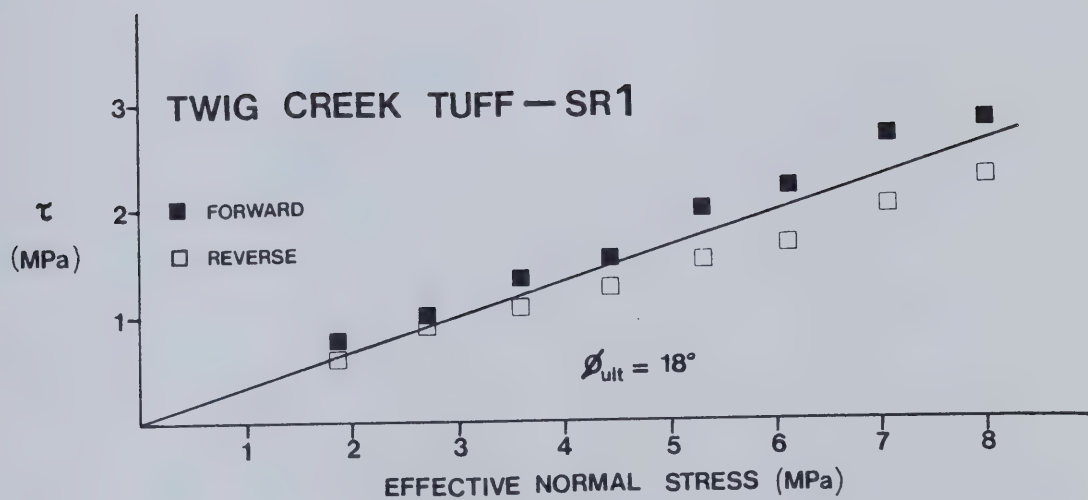
Figure 6.4 Ultimate shear strength envelope for the Twig Creek Tuff (SR1).
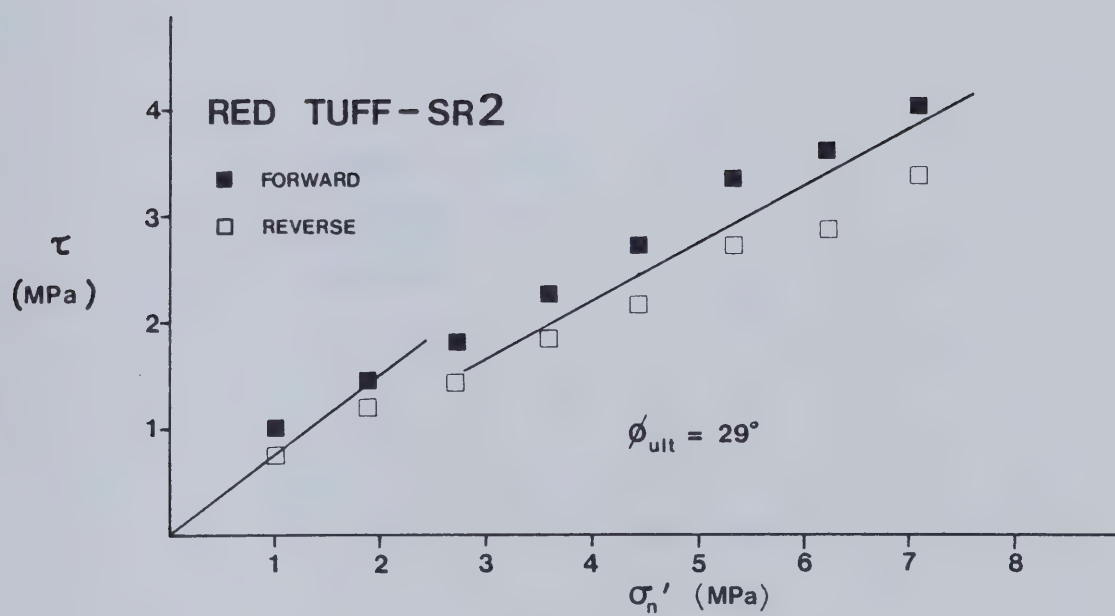
Figure 6.5 Ultimate shear strength envelope for the Red Tuff (SR2).
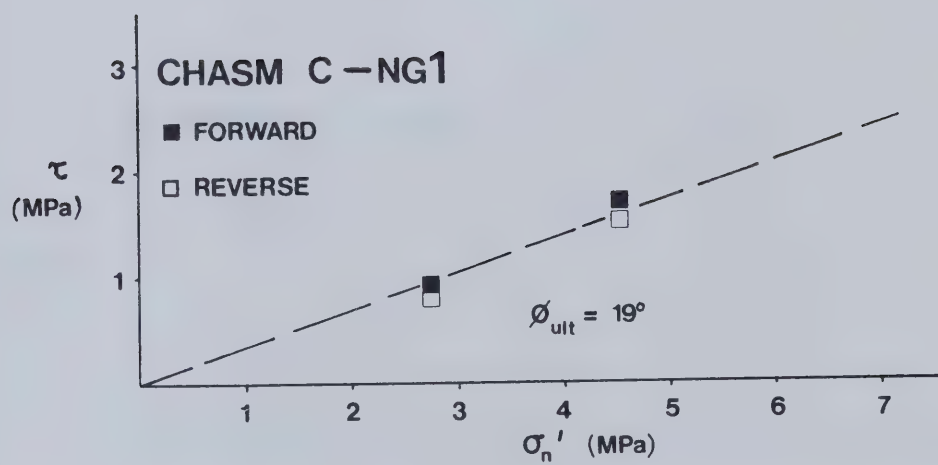
Figure 6.6 Ultimate shear strength envelope for Neogene tuff (NG1), Chasm Creek.
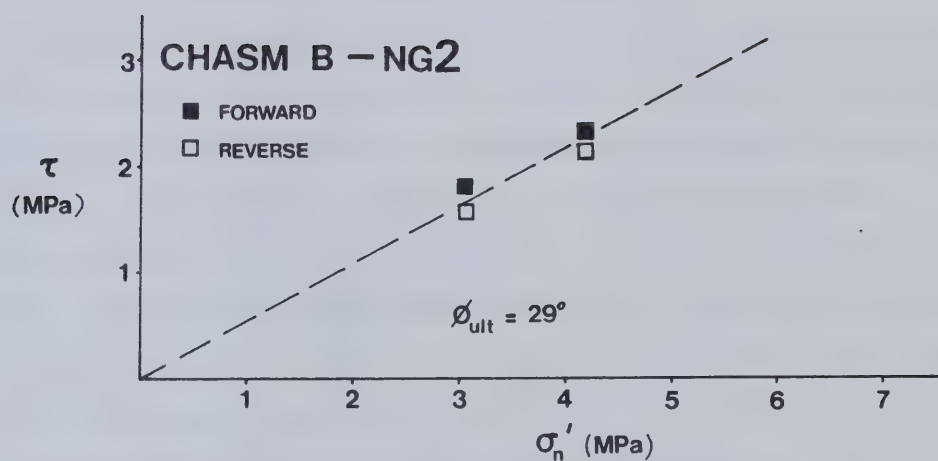
Figure 6.7 Ultimate shear strength envelope for Neogene tuff (NG2), Chasm Creek.

Wykeham–Farrance apparatus. Material from the Jupiter Creek shear zone was prepared and placed in the a same way. Data from the tests were recorded through a Datalogger. Residual shear strength envelopes are found in Fig 6.8.

6.6 Relationship between Microstructure and Geotechnical Properties

The low dry densities and associated high porosities obtained in this part of the investigation reflect the observations detailed in the previous chapter on the nature of extensive pore space in microstructural Domain 3. The porosities indicate a material transitional between soil (e.g., loess, glacio–lacustrine silt) and the more common igneous, sedimentary and metamorphic rock types. In this respect the materials examined here are similar to Chalk.

The problem in the interpretation of the Slake Durability results reflects the extensive presence of montmorillonite at grain and matrix sites.

Volcaniclastic materials are characterised by low uniaxial compressive strength (q_u). This is a response to the presence of montmorillonite within the matrix and at grain replacement sites and the high porosity of intact samples. In the case of the Salmon River Tuff (SR4), a contributory factor in reducing q_u is the presence of calcite–filled microcracks (Plate 5.5). The Red Tuff (SR2) exhibited a comparatively high value of q_u due to the patchy occurrence of authigenic silica at matrix sites. The presence of swelling clays in these materials would result in q_u being particularly sensitive to water content.

The ultimate angles of shear resistance measured on artificially prepared shear surfaces were more difficult to interpret in relation to miocrostructure. The low angles obtained for the Twig Creek Tuff (18^0) and NG1 (19^0) reflected the presence of montmorillonite at grain and matrix replacement sites. As mentioned above, clay films formed on the shear surfaces during the tests. The higher values of ϕ'_{ult} found in the Red Tuff (**29**^{o}) and NG2 (**29**^{o}) were a response to the presence of silica in matrix sites in the former and numerous quartz grains in the latter (Plate 5.12), although clay films formed on the shear surfaces during the tests.

The volcaniclastic materials examined here are thought to constitute the basal rupture zones of the Salmon River and Chasm Creek landslides. They are characterised by low dry density (13.98 – 21.92 KN/m³) , high porosity (9 – 43.3%), low compressive
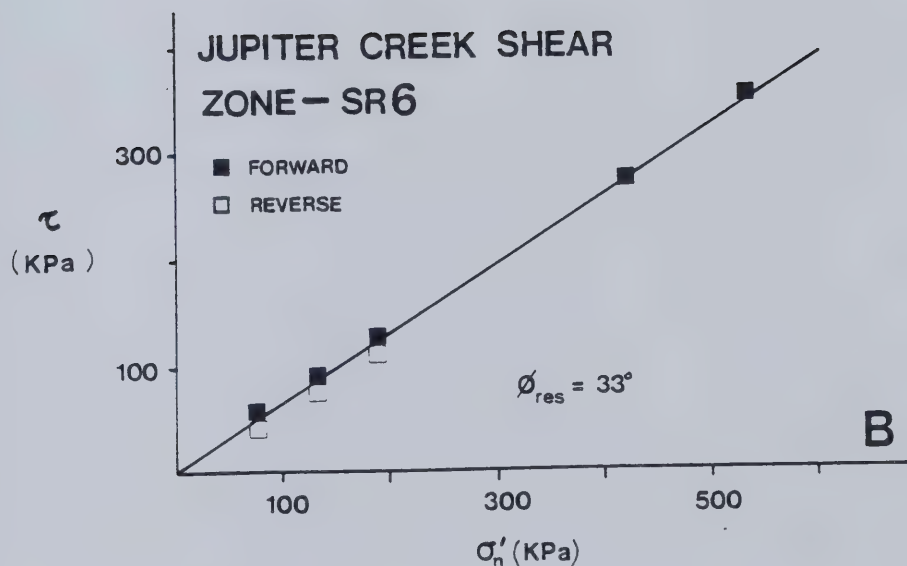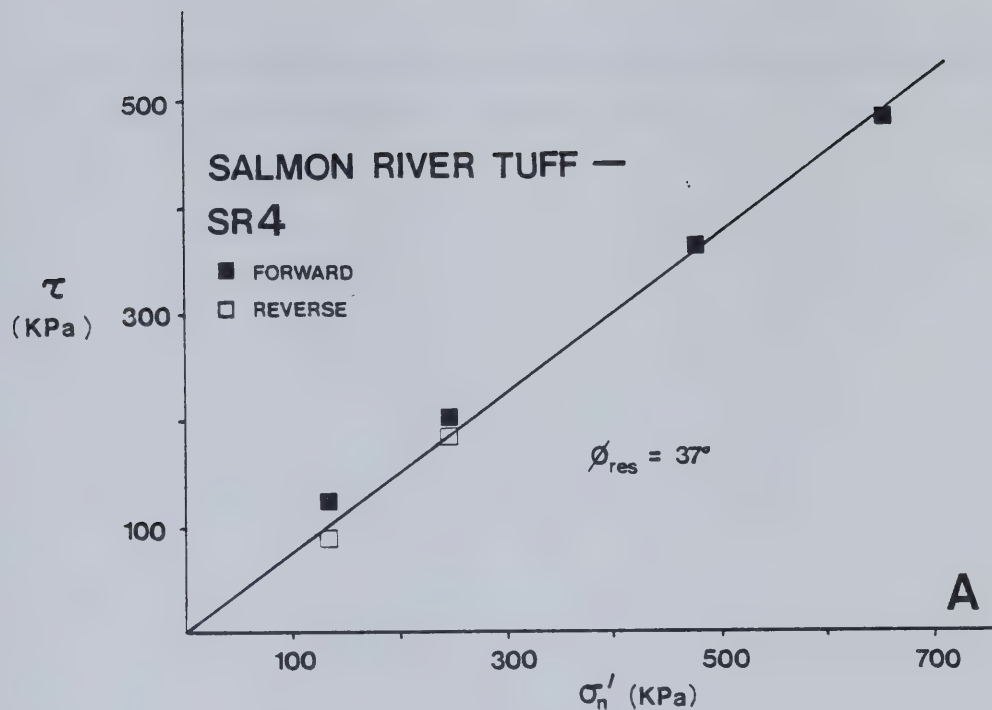
Figure 6.8 Residual shear strength envelopes for Salmon River Tuff. A=Disaggregated Salmon River Tuff (SR4), B=Salmon River Tuff from the Jupiter Creek shear zone (SR6).

strength (<13.5 MPa) and ,dependent on the presence of authigenic or pyroclastic silica, they exhibit low angles of ultimate shear resistance ($\leq 20^0$).

7. ANALYSIS OF MOVEMENT MECHANISMS

7.1 Introduction

A first-order evaluation of movement mechanisms was carried out with respect to the Jupiter Creek and Shell Creek landslides in Paleogene rocks and the Chasm West landslide in Neogene rocks. Adelphi Creek Bluffs was analysed as an example of a slope which, on the basis of field evidence, is in limiting equilibrium. The objective was to evaluate two models of movement mechanisms given the knowledge of geology, morphology of landslides and shear zones, and the properties of materials discussed in previous chapters.

Constraints which limit the evaluation of landslide mechanisms include lack of knowledge on the sub-surface macrostructure of the rock masses involved in movement, in-situ stresses, and uncertainty concerning the groundwater conditions either at the time of slope movement or in the present environment. A further constraint lies in the effect of secondary movements in modifying landslide morphology and the great scale and complexity of the movements examined. The analyses presented here are those of initial movement conditions.

Two models were applied to the slopes mentioned above in order to explore whether the movements were due to translational sliding or spreading as defined by Varnes (1978). The two models are considered to be end points of a spectrum of possible movement mechanisms which may have occurred in these slopes.

In the translational sliding model, the failure surface is assumed to be bi-linear and to consist of a steep back surface which passes through the cap and a sub-horizontal basal shear surface located in the weak volcaniclastic layer at the slope base. These surfaces are assumed to be controlled by discontinuities in the slope which include joints and faults in the cap and bedding plane surfaces or flexural slip planes in the weak subjacent volcaniclastic layer.

According to Varnes (1978), spreading movements involve the lateral extension of the cap as a result of the plastic flow or liquefaction of the weaker subjacent material. The failure usually starts in a local area within the weak layer , then develops into a general progressive failure. Spreading movements require the failure and structural degradation

of the intact rock substance, and take place independently of existing discontinuities in the spreading layer.

7.2 Analysis of Translational Sliding Model

7.2.1 Methods and Assumptions

The translational sliding model was examined by a limit equilibrium method through the use of a simple wedge analysis (Morgenstern and Sangrey 1978; Lutton and Banks, 1970; Lamb *et al.* 1981). In this approximate procedure, the potential sliding mass is divided into a number of wedges and the equilibrium of each wedge is considered in turn, satisfying the conditions of horizontal and vertical equilibrium only. It was performed by graphical means and the forces used in the analysis are noted in Fig. 7.1.

The analysis is sensitive to the direction of the force transmitted across the boundary of the two wedges, as seen in Fig. 7.1 (cf. Seed and Sultan, 1967; Sultan and Seed, 1967). In this analysis, δ is assumed equal to zero and thus conservative values of the factor of safety (F) are to be expected (Morgenstern and Sangrey, 1978). According to Lutton and Banks (1970), the assumption of $\delta = 0$ in the wedge analysis produced values of F which are 10-20% lower than those produced by more refined slope stability methods. Wedge analyses by the same authors on trial slopes in limiting equilibrium at the Panama Canal showed the value of F to be 5-6% lower when more rigorous solutions indicated F=1.0. Thus, in the analyses below, the strength parameters obtained for F=1 may be high by 5-6% which is considered adequate for a first order approximation to movement mechanisms.

A further conservative assumption involves the use of a horizontal phreatic surface within the slopes. This assumption was made for simplicity but it may also reflect more accurately the geometry of the surface in a slope consisting of sub-horizontal layers of varying permeability.

The first part of the analysis was conducted to establish the ultimate angle of shear resistance required (ϕ'_{req}) for the slopes to be in limiting equilibrium, i.e., F=1.0, where F is defined as the Factor of Safety (Fig. 7.1). The analysis considered a variety of shear surface and water table configurations.

DEFINITIONS

(SUBSCRIPT a DENOTES ACTIVE WEDGE, p DENOTES PASSIVE WEDGE)

W = WEIGHT OF WEDGE
U = RESULTANT WATER PRESSURE ACTING ON BASE OF WEDGE
N = EFFECTIVE NORMAL FORCE TO BASE
S = SHEAR FORCE ACTING ALONG BASE OF WEDGE
α = INCLINATION OF BASE OF PASSIVE WEDGE
θ = INCLINATION OF BASE OF ACTIVE WEDGE
P_w = RESULTANT WATER PRESSURE AT INTERFACE
P_a = EFFECTIVE FORCE AT INTERFACE
δ = INCLINATION OF P_a TO HORIZONTAL

(AFTER MORGENSTERN , 1978)

Figure 7.1 Diagram of forces used in the wedge analysis.

The second part consisted of a comparison between ϕ'_{req}. and the results of the shear testing discussed in the previous chapter. The analysis assumes the existence of pre-existing shear surfaces parallel to bedding planes in the volcaniclastic layers which may have resulted from tectonic or stress relief processes. Based on field observations in Chapter 4, this assumption is considered reasonable.

Figure 7.2 shows the slope geometries, groundwater conditions, and failure surfaces which were analysed. The generalised pre-movement slope geometries in Fig. 7.2 were based on the detailed reconstructed slope profiles in Chapters 3 and 4.

The geometries of the failure surfaces in Fig. 7.2 were best estimates based on landslide morphology, estimated retrogression and field observations of discontinuities and block boundaries. However in some cases, e.g., Jupiter Creek 2, observations on block boundaries and the implied dip of the back surface are not consistent with the discontinuity patterns observed in the cap. The precise nature of the surfaces must remain unknown without detailed subsurface exploration (cf. Chapter 4). The back surface was assumed to be determined by pre-existing discontinuities within the cap, and ϕ'_{basic} was assumed to equal 35^0 which is considered a realistic value for basalt and breccia, (cf. Barton and Choubey, 1977). The basal shear surface was assumed to be located in the volcaniclastic layers which exist at the slope base. The volcaniclastic layer was initially assumed to be horizontal but, where field evidence had indicated a dip ±5^0 to the horizontal, a second analysis with a dipping basal surface was carried out. As would be expected, the results of the analysis were found to be sensitive to the tension crack assumptions used. A mid-slope location is favoured for the boundary of the two wedges since, as discussed in Chapter 4, the boundary is preserved in the debris in the form of the debris-crest ridge.

7.2.2 Results

The results of the wedge analyses are summarised in Table 7.1. In evaluating the results, the value of the residual friction angle of the Salmon River Tuff may be considered. The difference between the residual angle of shear resistance of cohesionless material (ϕ'_{res}.) and the ultimate angle of shear resistance of rock discontinuities (ϕ'_{ult}.) has been discussed by Krahn and Morgenstern (1979). It is thought
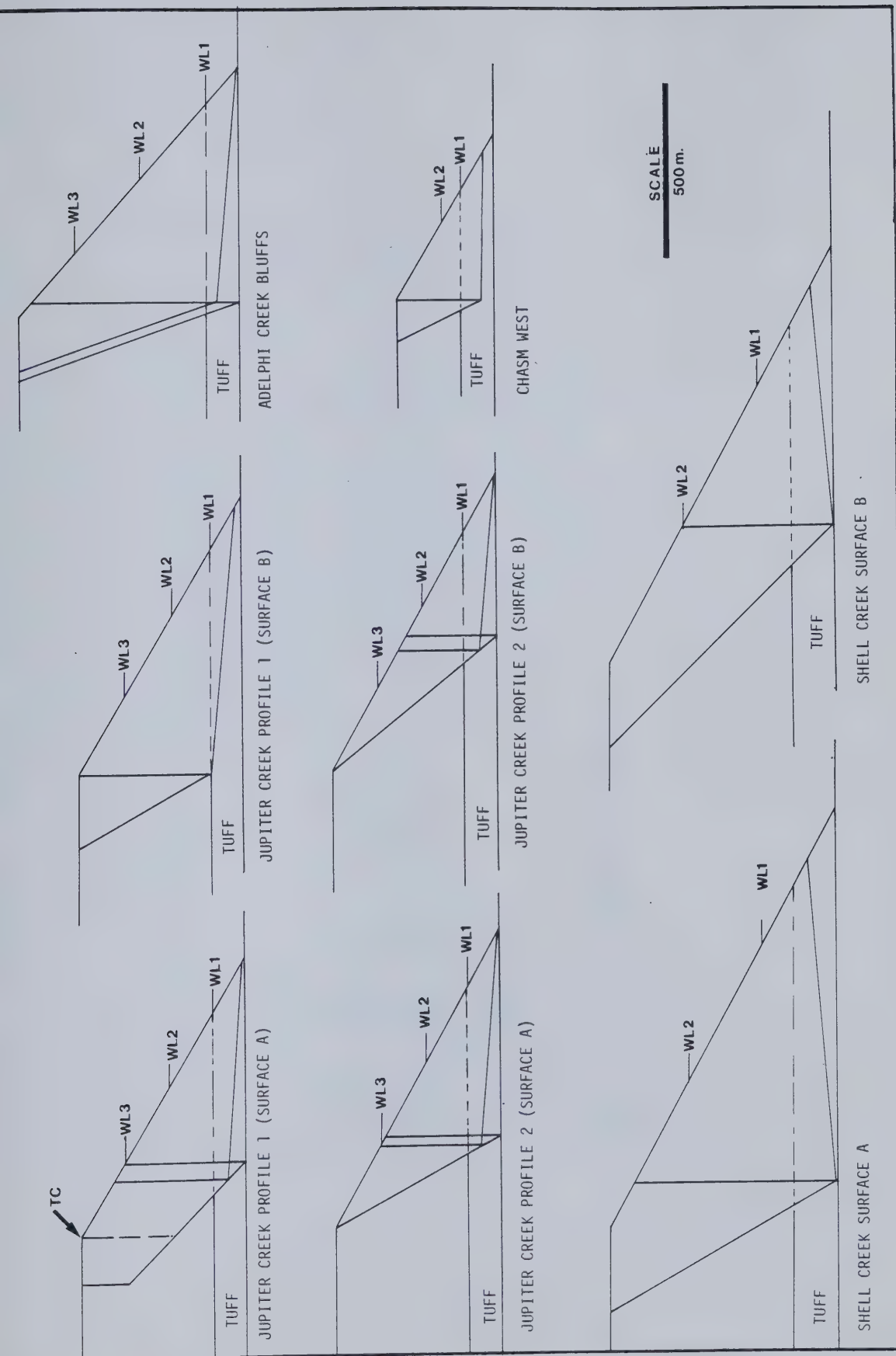
Figure 7.2 Generalised slope geometries, groundwater surfaces, and shear surfaces analysed in the translational sliding model.

287

SLOPE ANALYSED	ANGLE OF SHEAR RESISTANCE REQUIRED FOR EQUILIBRIUM							
	DRY		WL1		WL2		WL3	
	$\alpha=0$	$\alpha=5$	$\alpha=0$	$\alpha=5$	$\alpha=0$	$\alpha=5$	$\alpha=0$	$\alpha=5$
JUPITER CREEK PROF. 1 SURFACE A	9.4	12.5	12.2	14.0	19.4	18.0	29.2	27.0
JUPITER CREEK PROF. 2 SURFACE B	0	5.0	4.6	8.0	19.0	21.0	20.1	24.0
JUPITER CREEK PROF. 1 SURFACE A	11.2	14.5	14.3	16.0	21.8	21.0	29.4	30.0
JUPITER CREEK PROF. 2 SURFACE B	13.4	15.5	18.6	18.5	29.8	28.0	30.7	32.0
SHELL CREEK SURFACE A[a]	9.7	6.5	13.5	10.0	21.4	20.0	--	--
SHELL CREEK SURFACE B[a]	7.2	2.5	9.7	6.0	13.1	9.0	26.0	24.0
ADELPHI CREEK BLUFFS	12.8	15.5	14.7	17.5	21.3	22.5	31.1	32.0
CHASM WEST	9.1	--	11.5	--	15.8	--	--	--

[a]SHELL CREEK ANALYSIS CARRIED OUT WITH $\alpha=-5$ (INTO SLOPE) AND NOT $\alpha=+5$ (OUT OF SLOPE)

Table 7.1 Results of wedge analyses

that the values of ϕ'_{res} obtained for disaggregated Salmon River Tuff overestimate the value of ϕ'_{ult} which may pertain for a pre-sheared surface in the same material. In the shear tests on disaggregated material no smooth shear surface was formed and the sample behaved like a granular mass. It is assumed in the discussion below, in the absence of a value of ϕ'_{ult} for the Salmon River Tuff that its value is comparable to the Twig Creek Tuff.

It may also be noted that in Figures 7.3, 7.4, 7.5, and 7.6 which summarise the results of the stability analysis below, the average shear and normal effective stresses represented are those calculated for the passive wedge only.

(a) Jupiter Creek Profiles 1 (JC1) and 2 (JC2): JC1 was drawn through Zone 2 and JC1 through Zone 3 which, as noted in Chapter 4, exhibits evidence of current movement. The results are summarised in Fig. 7.3. Both analyses give comparable results.

With respect to profile JCI, with $\alpha = 0$, values of ϕ'_{req} varied from 9° for a dry slope, to 29° for a horizontal phreatic surface 335 m above the present valley floor (WL 3 in Fig. 7.2). For $\alpha = 5°$, ϕ'_{req} varied between 12.5° and 27.0° for the same phreatic conditions, approaching the estimated value of ϕ'_{ult} at a water level approximately 213 m above the valley floor (WL 2 in Fig. 7.2). JC2 yields $\phi'_{req} = 11°$ for a dry slope with $\alpha = 0$ and 29° for the maximum elevation of the phreatic surface considered. These values increase to 14.5° and 30° respectively for $\alpha = 5$.

ϕ'_{req} is very sensitive to the assumption of water-filled tension cracks existing in the slope face. This is general for all the slopes analysed and it will suffice to illustrate this sensitivity with reference to profile JC1 (Fig. 7.3). In an otherwise dry slope, with a water filled tension crack at a location marked in Fig. 7.3, and $\alpha = 0$, ϕ'_{req} increases from 9° to 16°. With the phreatic surface at 91m (WL 1), ϕ'_{req} increases from 12° to 20°, (Fig. 3).

As seen in Fig. 7.3, the average shear stresses at the base of the passive block exceeds the existing shear strength in the Salmon River Tuff either at a water level approximately 213 m above the valley floor, or at lower water levels with water filling a tension crack above the phreatic surface. The possible combinations of both tension crack and phreatic surface assumptions are too numerous to evaluate.
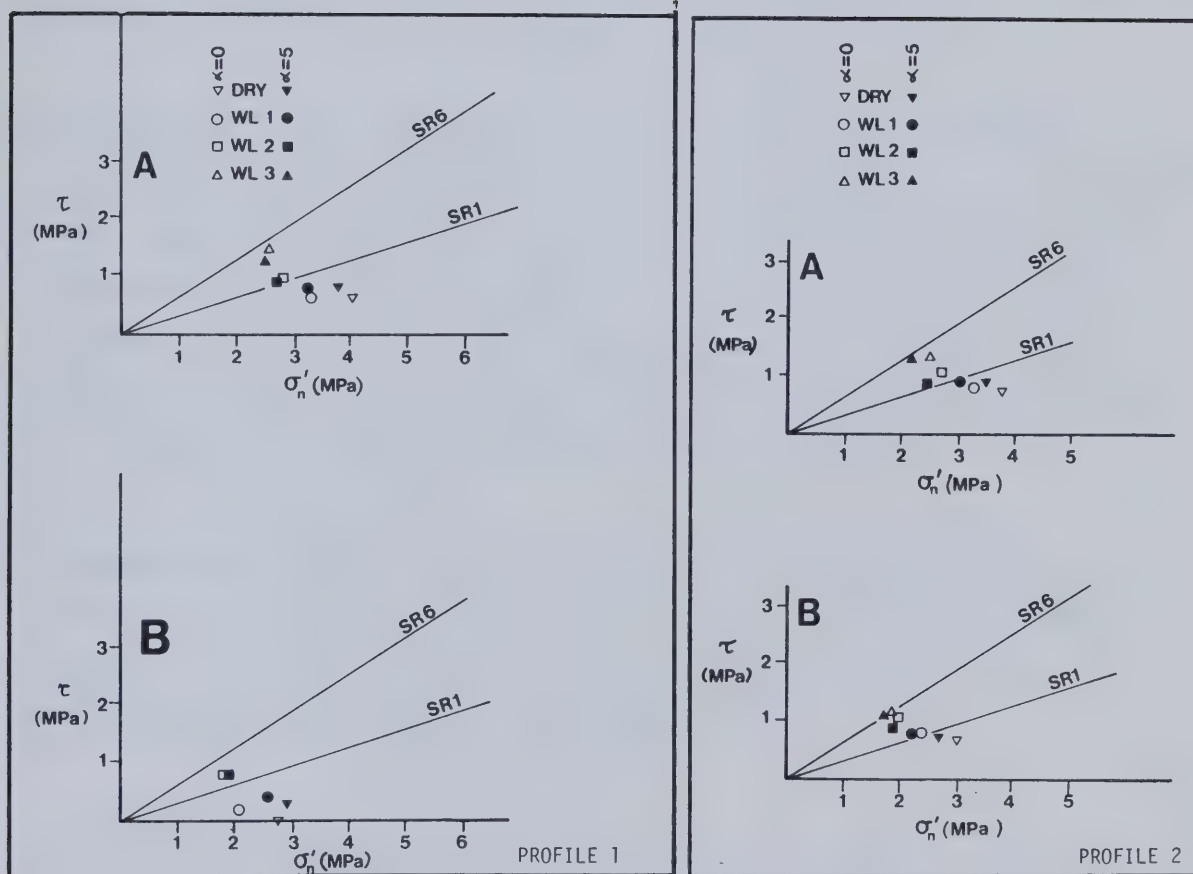
Figure 7.3 Results of wedge analysis of the Jupiter Creek landslide.

NOTE:

1. RESULTS OF WEDGE ANALYSIS ARE PRESENTED AS POINTS
   REPRESENTING THE AVERAGE EFFECTIVE NORMAL STRESS
   AND THE AVERAGE SHEAR STRESS ON THE BASE OF THE
   PASSIVE WEDGE.

2. SR1 AND SR6 REPRESENT STRENGTH ENVELOPES FOR TWIG
   CREEK TUFF AND SALMON RIVER TUFF FROM THE JUPITER
   CREEK LANDSLIDE SHEAR ZONE AS DISCUSSED IN CHAPTER 6.

(b)Shell Creek Landslide: For the reconstructed slope geometry and failure surfaces (Fig. 7.4), lower values of ϕ'_{req}. are required (Table 7.1). ϕ'_{req}. varied between $7°$, for a dry slope, and $26°$ with a water level 335 m (WL2) above the valley floor for $\alpha = 0$. For a basal surface dipping into the slope ($\alpha = -5°$) these values varied from $3°$ to 25. Assumptions regarding a water filled tension crack at the slope crest (fig. 7.4) increased the ϕ'_{req}. to $18°$ with a phreatic surface 213 m (WL1) above the valley floor ($\alpha = 0$). This value decreases to $16°$ with $\alpha = -5°$. The relationship between average shear stresses and average normal effective stresses at the base of the passive block is seen in Fig. 7.4.

(c)Adelphi Creek Bluffs: On the basis of morphological evidence noted in Chapter 4, the slopes at Adelphi Creek Bluffs were assumed to be in limiting equilibrium. This is reflected in the results of the wedge analyses in Table 7.1 and Fig. 7.5. Limiting equilibrium is almost predicted with $\alpha = 5°$ in a dry slope. Where $\alpha = 0$, a water level only 9.1 m (WL1) above the valley floor will result in movement in the absence of any berm effects. This water level is to be compared with the estimate of the existing water level in the slope of 65 m. In both these analyses no water-filled tension cracks were assumed.

(d)Chasm Creek West: The results of the wedge analysis are presented in Table 7.1 and Figure 7.6. Assuming the absence of water-filled tension cracks, limiting equilibrium is only approached when the water level is 185 m (WL2) above the valley floor. Stratigraphic evidence indicated the value of $\alpha = 0$.

7.2.3 Discussion

Using a very simple wedge analysis, first order approximations to initial movement conditions have been obtained in the Salmon Valley and Chasm Creek landslides. The results of all the Salmon Valley analyses are summarised in Fig. 7.7. The conditions were obtained using what are thought to be reasonable assumptions concerning the existence of pre-sheared material in the volcaniclastic strata at the base of the slopes (i.e., the use of ϕ'_{ult}.), shear surface geometry, and elevations of the phreatic surface.

Whilst the outcome appears reasonable, several constraints limit the interpretation of the results;
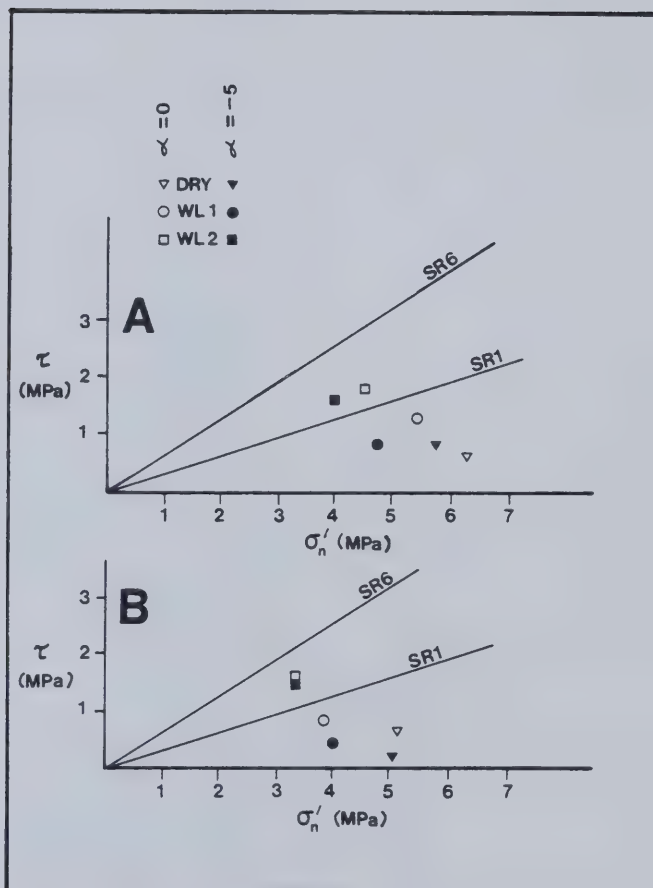
Figure 7.4 Results of wedge analysis of the Shell Creek landslide.
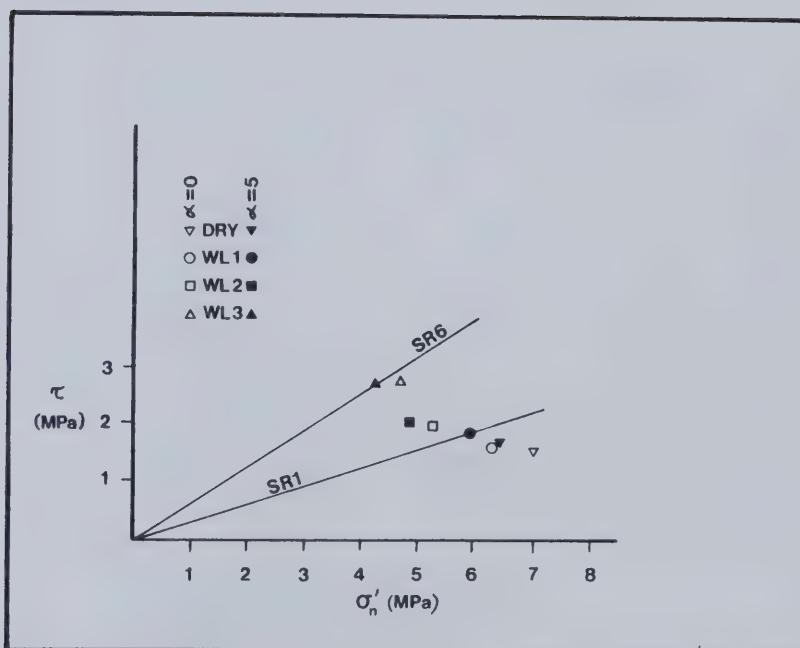
NOTE:

1. RESULTS OF WEDGE ANALYSIS ARE PRESENTED AS POINTS
   REPRESENTING THE AVERAGE EFFECTIVE NORMAL STRESS
   AND THE AVERAGE SHEAR STRESS ON THE BASE OF THE
   PASSIVE WEDGE.

2. SR1 AND SR6 REPRESENT STRENGTH ENVELOPES FOR TWIG
   CREEK TUFF AND SALMON RIVER TUFF FROM THE JUPITER
   CREEK LANDSLIDE SHEAR ZONE AS DISCUSSED IN CHAPTER 6.

Figure 7.5 Results of wedge analysis of Adelphi Creek Bluffs
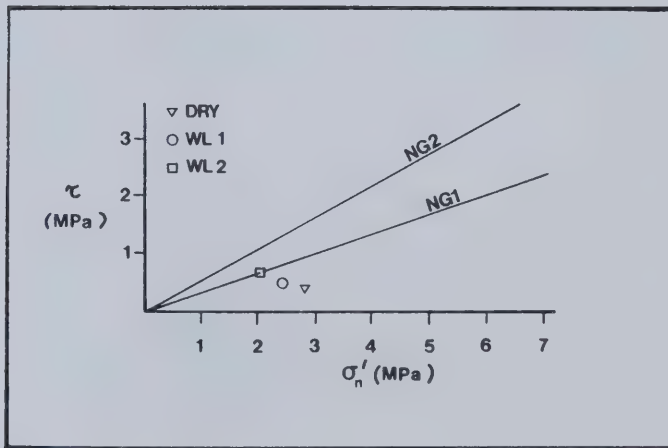
NOTE:

1. RESULTS OF WEDGE ANALYSIS ARE PRESENTED AS POINTS
    REPRESENTING THE AVERAGE EFFECTIVE NORMAL STRESS
    AND THE AVERAGE SHEAR STRESS ON THE BASE OF THE
    PASSIVE WEDGE.

2. NG1 AND NG2 REPRESENT STRENGTH ENVELOPES FOR
    NEOGENE VOLCANICLASTIC MATERIAL FROM CHASM CREEK
    AS DISCUSSED IN CHAPTER 6.

Figure 7.6 Results of the wedge analysis for the Chasm Creek West landslide.
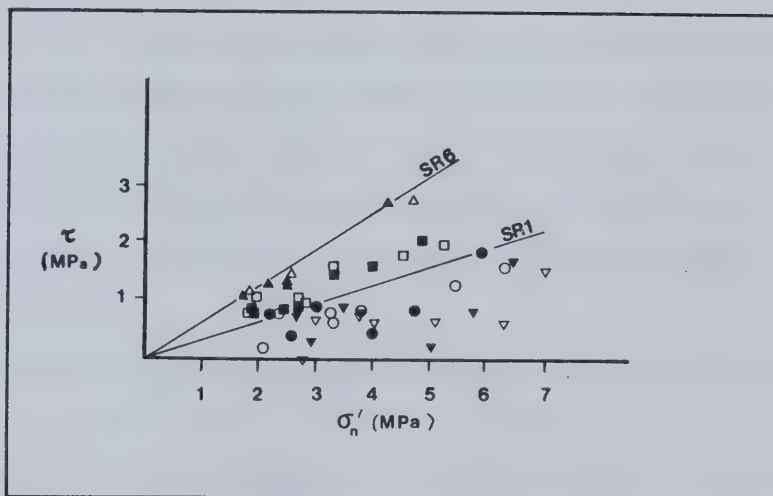
NOTE:

1. RESULTS OF WEDGE ANALYSIS ARE PRESENTED AS POINTS
   REPRESENTING THE AVERAGE EFFECTIVE NORMAL STRESS
   AND THE AVERAGE SHEAR STRESS ON THE BASE OF THE
   PASSIVE WEDGE.

2. SR1 AND SR6 REPRESENT STRENGTH ENVELOPES FOR TWIG
   CREEK TUFF AND SALMON RIVER TUFF FROM THE JUPITER
   CREEK LANDSLIDE SHEAR ZONE AS DISCUSSED IN CHAPTER 6.

Figure 7.7 Summary of all Salmon Valley Wedge Analyses.

1. the analyses assumed that the weakest material had been discovered during the detailed field work in the landslide areas. Discovery of such material was dependent on surface exposures and the possibility exists that material of lower shear strength is present in the slopes analysed but that such material is not exposed.

2. the value of ϕ'_{req} obtained in the analysis is affected by the assumed geometry of the failure surfaces. These were constructed on the basis of field evidence, the form of the re-constructed profile, and kinematic considerations. Thus, they are approximations only.

3. the greatest uncertainty surrounds the effect of water pressures, both within the basal shear zone and in tension cracks which are seen to have an important effect on stability. In the almost semi-arid climate of the areas studied, the slopes are generally dry. Water levels were probably higher at various periods in post-glacial times, as discussed later in this Chapter. After extensive traverses of slopes in the Salmon Valley, only two springs were noted in the valley side slopes in the vicinity of the Shell Creek and Jupiter Creek landslides (Figs. 4. 9 and 4. 16).

4. lateral pressures exerted along the lateral margins of the landslides were ignored in the analyses.

5. the analyses do not consider the possible effects of in-situ horizontal stresses, or seismic processes which, as reviewed in Chapter 3, are active in the region.

It is therefore concluded that given the constraints noted above, and our knowledge of the geology and materials in the slopes analysed, that conditions for translational sliding may have existed in the Salmon Valley and Chasm Creek slopes.

7.3 Evaluation of the Spreading Model

7.3.1 Background

The proposed spreading model demands that complete cap separation takes place during stress relief associated with valley excavation, and that the cap is therefore free to load the subjacent volcaniclastic layer in a manner analogous to the strip loading of a foundation. The presence of extensive tension cracking in the Salmon valley and Chasm Creek slopes may be evidence of this process.

The stability of the cap loading may be analysed as a bearing capacity problem in which the cap is a strip loading of the volcaniclastic foundation. This approach to the stability of slopes has been attempted by Escario (1968), R.S. Evans (1981), and Caine (1982).

Spreading may take place in drained or undrained conditions. The rate of cap loading, during the stress relief process is not known, but it is thought to be slow enough to enable drainage to take place. Therefore, the process of cap loading is considered to be a drained process. Undrained conditions may occur if sudden structural breakdown of the open tuff fabric takes place. This may result from strains initiated by cap loading or as a result of the decrease in structural strength due to diagenesis. Whilst microstructural observations noted in Chapter 5 suggest that this process is possible, definitive laboratory tests have not been carried out. It is thought useful, however, to explore the mechanisms of both drained and undrained spreading.

Attempts at establishing undrained extrusion criteria have been made for soft clays by Jurgensen (1934), Brohms and Bennermark (1968), Brown and Meyerhof (1969), Broms and Bjerke (1972) and Mitchell and Markell (1974). The extrusion criteria proposed by these workers, and by other workers in rock, are summarised in Table 7.2. There appears to be consensus that extrusion takes place when

$$\gamma H = 3q_u \qquad\qquad 7.1$$

where

γ = unit weight of soil

H = height of slope

q_u = uniaxial compressive strength

With regard to the bearing capacity of intact rock , Coates (1970) found that the failure load (q_f) was approximately $3q_u$. Ladanyi (1972) examined the failure of rock under concentrated loadings similar to those envisaged under cap loading. He found a crude lower bound solution in which $q_f = 3q_u$, where q_u is the uniaxial compressive strength of intact rock measured at the same scale as the region beneath the loading surface. In this analysis, Ladanyi (1972) assumes that the largest horizontal confining

Table 7.2 Undrained extrusion criteria for clays and rocks.

SOURCE	MATERIAL	[a]FAILURE LOAD (q_f)
BROHMS AND BENNERMARK (1968)	CLAY	3.00 q_u
BROWN AND MEYERHOF (1969)	CLAY	2.57 q_u
BROHMS AND BJERKE (1972)	CLAY	3.00 q_u
MITCHELL AND MARKELL (1974)	CLAY	3.00 q_u
COATES (1970)	ROCK	3.00 q_u
ESCARIO (1968)	ROCK	2.70 q_u
LADANYI (1972)	ROCK	3.00 q_u

[a]FAILURE LOAD IS GIVEN FOR CONTINUOUS STRIP FOOTINGS

pressure that can be mobilised to support the rock beneath the cap footing is the q_u of the weak layer.

Based on the above, therefore, it appears reasonable to suggest that a lower bound approximation to the undrained extrusion threshold is at an overburden pressure equivalent to $3q_u$ of the rock mass. It is suggested here that this defines the sliding-spreading boundary for intact rock or a jointed rock mass with closed joints. With open joints, Kulhawy and Goodman (1980) suggest that failure is likely to occur by the uniaxial compression of the rock. In this case $q_f \sim q_u$. These criteria are examined with reference to the Salmon Valley and Chasm Creek slopes analysed in the translational sliding model above, using the same generalised slope geometries.

7.3.2 Methods and Assumptions

The stability of the cap loading may be investigated by analogy with a bearing capacity analysis. The magnitude of the stresses required to initiate degradation of the intact rock substance in the spreading layer may be estimated from the theory of Mandel and Salencon (1972), who give a solution for the bearing pressures required to cause extrusion of a soft layer compressed between two rough surfaces. It has been applied to the stability of natural slopes by Vaughan (1976) and to the squeeze of underclays in coal mines by Rockaway (1977). The method is based on limit equilibrium, and plane strain is considered for a material obeying Coulomb's yield criterion. The solution is sensitive to the thickness of the weak layer which, in all cases examined here, was determined on stratigraphic evidence.

Drained and undrained analyses were carried out. The parameters for the analysis were obtained from the appropiate figures in Mandel and Salencon (1972).

7.3.3 Results and Discussion

Results of the drained spreading analysis, using $c=0$ and $o=18°$, indicated that bearing pressures far in excess of those existing in the slopes, were required for extrusion. It is, therefore, considered unlikely that drained cap loading, by itself, could have initiated spreading in the slopes considered.

The results of the undrained spreading analysis are shown in Table 7.3 and Fig. 7.8. Three aspects of the results are discussed below:

1.   the location of the point of initial strength loss (marked by the black dot in Fig. 7.8),

2.   the relationship between the laboratory–measured value of q_u and the value of q_u required to resist extrusion (q_u –REQ) as obtained in the Mandel and Salençon analysis,

3.   the relationship between q_u –REQ and the maximum overburden pressure at the base of the cap.

As a consequence of the slope geometries used in the analysis, the point at which the maximum value of q_u –REQ in the basal layer is generally at a point directly beneath the slope crest, i.e., at a location where the cap block would be expected to separate during stress relief and rebound. If a steeper frontal slope is assumed, then this point migrates toward the slope face as seen in Fig. 7.8E. The interior position of the point of initial strength loss, which corresponds to the point of plastic zone initiation, is also predicted by the analysis of the Turnagain Heights spreading movement by Voight (1973). This point may mark the location of the initiation of structural breakdown which leads to the progressive failure of the slope.

As seen in Table 7.3, the range of q_u –REQ at this point varies between 845.5 kPa and 1535.5 kPa for the slope geometries considered. In column 3 the ratio of q_u estimated from the Point Load Test (q_u –LAB) to q_u –REQ is defined. Values of this ratio are seen to range from 3.06 to 5.7. This corresponds to an undrained factor of safety for extrusion.

The ratio of q_u –LAB to the overburden pressure (P) at the point of the maximum q_u required in Fig. 7.8, is also given in Table 7.3 (column 4). This ratio corresponds to the undrained factor of safety against extrusion for the case of open joints in the basal volcaniclastic layer (Kulhawy and Goodman, 1980). Values of this ratio vary between 0.34 and 0.62 for slopes in the Salmon Valley and between 0.99 and 1.14 for the Chasm Creek slopes.

Several factors influence the interpretation of these ratios as meaningful estimates of cap–loading stability. First, the value of q_u –LAB is uncorrected for the effect of water content which may reduce its value by as much as 3 times (Broch and Franklin, 1972;

Table 7.3 Results of the undrained spreading analysis.

SLOPE ANALYSED	A	1	2	3	4	5	6
JUPITER CREEK 1	SRT	4.70	0.945	4.97	7.56	8.00	0.62
JUPITER CREEK 2	SRT	4.70	1.008	4.66	9.07	9.00	0.52
SHELL CREEK	TWG	7.44	1.379	5.39	13.83	10.02	0.54
SHELL CREEK	SRT	4.70	1.379	3.40	13.83	10.02	0.34
ADELPHI CREEK	TWG	7.44	1.535	4.84	13.04	8.49	0.54
ADELPHI CREEK	SRT	4.70	1.535	3.06	13.04	8.49	0.34
CHASM WEST 1	CC	4.82	0.845	5.70	4.22	5.00	1.14
CHASM WEST 2	CC	4.82	1.220	3.95	4.88	4.00	0.99

KEY TO COLUMNS;

A = MATERIAL ASSUMED TO SPREAD;TWG=TWIG CREEK TUFF, SRT= SALMON RIVER TUFF, CC=CHASM C TUFF.
1 = q_u AS MEASURED IN POINT LOAD TEST (MPa)
2 = MAXIMUM q_u REQUIRED TO RESIST SPREADING OBTAINED IN THE MANDEL-SALENÇON ANALYSIS (MPa)
3 = q_u AVAILABLE AS MEASURED/q_u REQUIRED
4 = OVERBURDEN PRESSURE (P) AT POINT OF MAXIMUM q_u REQUI-RED (MPa)
5 = COLUMN 4/ COLUMN 2
6 = COLUMN 1/ COLUMN 4
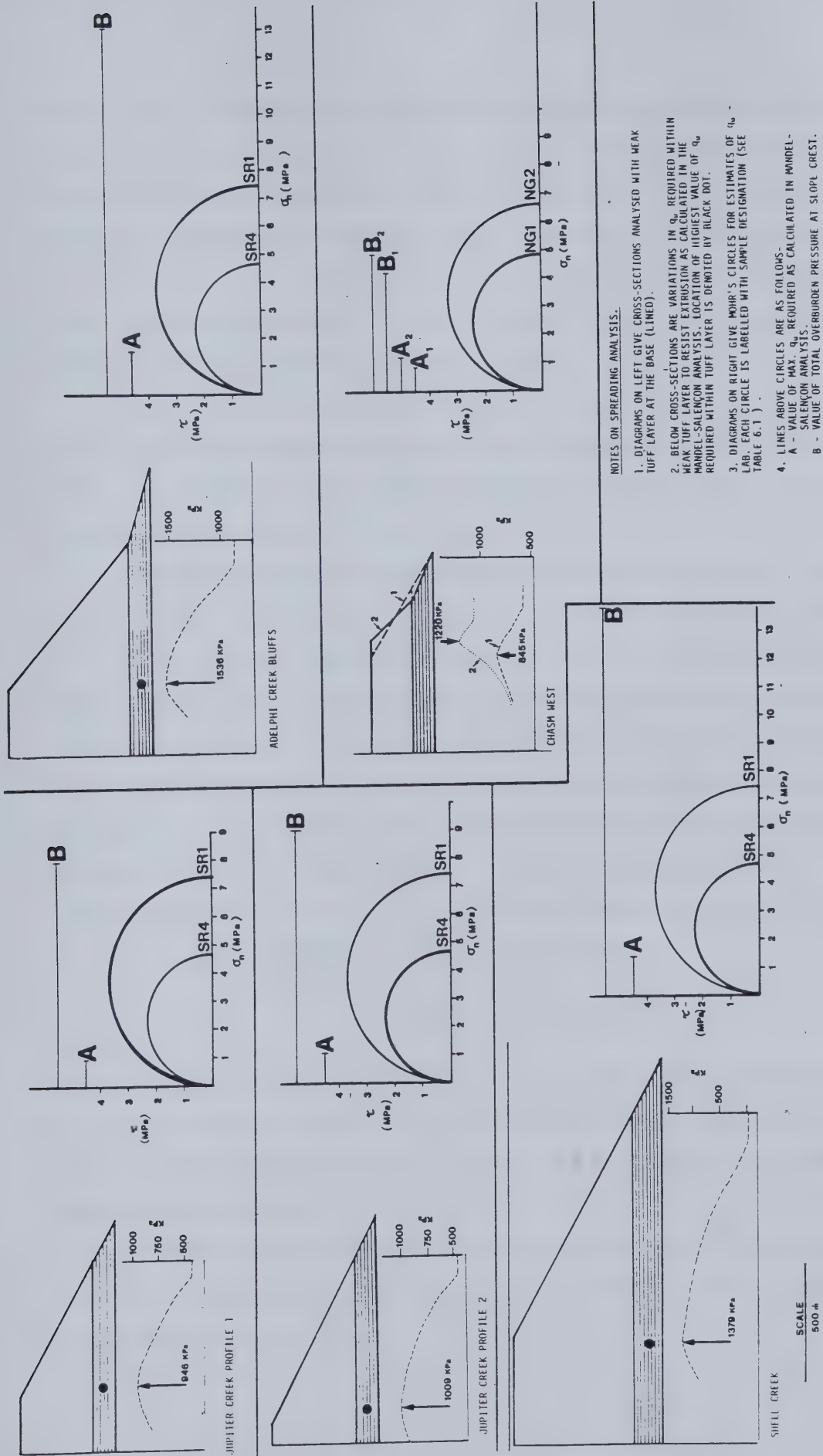
Figure 7.8 Results of the undrained spreading analysis using the method of Mandel and Salencon (1972).

NOTES ON SPREADING ANALYSIS.

1. DIAGRAMS ON LEFT GIVE CROSS-SECTIONS ANALYSED WITH WEAK TUFF LAYER AT THE BASE (LINED).

2. BELOW CROSS-SECTIONS ARE VARIATIONS IN q_u REQUIRED WITHIN WEAK TUFF LAYER TO RESIST EXTRUSION AS CALCULATED IN THE MANDEL-SALENCON ANALYSIS. LOCATION OF HIGHEST VALUE OF q_u REQUIRED WITHIN TUFF LAYER IS DENOTED BY BLACK DOT.

3. DIAGRAMS ON RIGHT GIVE MOHR'S CIRCLES FOR ESTIMATES OF q_u LAB. EACH CIRCLE IS LABELLED WITH SAMPLE DESIGNATION (SEE TABLE 6.1).

4. LINES ABOVE CIRCLES ARE AS FOLLOWS-
   A - VALUE OF MAX. q_u REQUIRED AS CALCULATED IN MANDEL-SALENCON ANALYSIS.
   B - VALUE OF TOTAL OVERBURDEN PRESSURE AT SLOPE CREST.

ADELPHI CREEK BLUFFS

CHASM WEST

JUPITER CREEK PROFILE 1

JUPITER CREEK PROFILE 2

SHELL CREEK

SCALE
500 m

Broch, 1979). As mentioned in Chapter 6, tests were conducted in the air dry state and sample availability did not allow the effects of water content to be examined. Secondly, the problem of applying a laboratory measured q_u (q_u –LAB) to a rock mass (q_u –RM) has not been solved (Kulhawy and Goodman, 1980). Estimates, in the literature, of the scale effect reduction in q_u –LAB differ by orders of magnitude. For example, Hoek and Bray (1977) suggest that the value q_u –RM is approximately $0.25q_u$ –LAB of unweathered rock, whilst Hoek and Brown (1980) estimate it to be $0.001q_u$ –LAB.

In the Mandel and Salencon (1972) analysis (Table 7.2), conditions for undrained spreading in the basal layer require the value of q_u –RM to vary between 0.18 and $0.33q_u$ –LAB. An average of q_u –RM = $0.22q_u$ LAB is obtained which compares favourably to the estimates of Hoek and Bray (1977) noted above.

The relationship between overburden pressure (P) and the value of q_u –REQ is also explored in Table 7.3 (column 5), with respect to the extrusion criteria noted in Section 7.3.1. The ratio between P, and q_u –REQ obtained in the Mandel and Salencon analysis, varies between 8.00 and 10.02 for the Salmon Valley slopes (mean = 9.16) and between 4.0 and 5.00 for Chasm Creek. These values are therefore in excess of the criterion for undrained extrusion of $q_f = 3q_u$ –RM. It is of interest to note that these results are comparable to those of Ladanyi (1972), who found from experiment on intact rock, that the values of a similar ratio varied between 7 and 15. The relationship between P and q_u –REQ is further explored in Fig. 7.9. Only rectilinear slopes were included in the analysis and a linear regression equation was fitted to the data where

$$P = -2.840 + 12.46 \ q_u\text{–REQ} \qquad\qquad 7.2$$

in which r = 0.94154 and is significant at the 1% level. The line for the extrusion criterion $q_f = 3 \ q_u$ –RM is also included in Fig. 7.9. For the range of slope geometries considered, therefore, it is concluded that Equation 7.2 may be more applicable as an undrained spreading threshold criterion than Equation 7.1.

If the Mandel and Salencon analysis approximates conditions for undrained spreading in the Salmon Valley, spreading has occurred where P = 2.04 q_u –LAB which is not corrected for moisture effects.
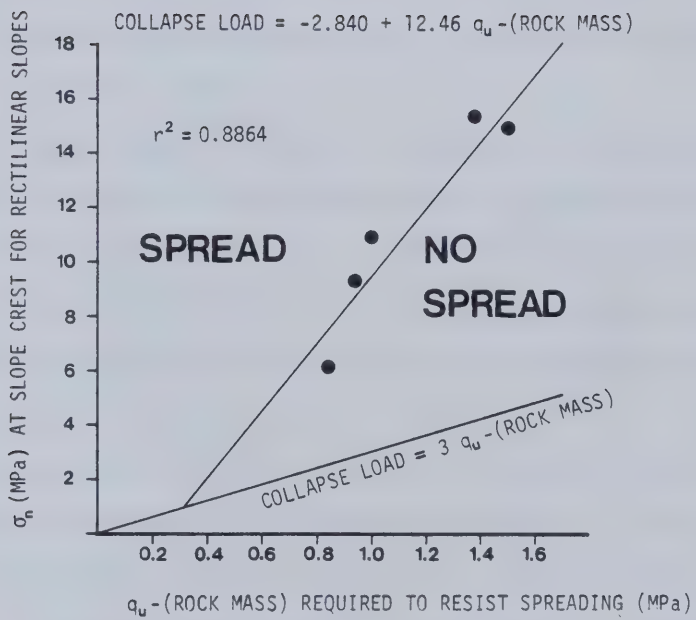
Figure 7.9 Relationship between overburden pressure at the slope crest (P) and q_u –REQ.

If is assumed that q_u —RM represents a form of structural breakdown threshold, and that the value of $q_{u\text{-RM}} = 0.22q_u$ —LAB, the results presented above indicate that undrained spreading is a possible mechanism for the slope movements studied. It is also of interest to note that the total overburden pressure at the slope crest approaches the value of q_u —RM

7.4 Evaluation of Movement Mechanism

The first–approximation to movement mechanism presented above suggests, on the basis of the results of very simple analyses, which utilize what are thought to be reasonable assumptions, that two modes of movement *viz.* translational sliding and undrained spreading are possible mechanisms for slope movements in the Salmon Valley and Chasm Creek. A schematic representation of these possible modes of movement in these slopes is seen in Fig. 7.10.

Although both the nature and number of assumptions that have to be made in this first approximation yield the problem indeterminate, the evidence points to a combination of complex movement mechanisms which results in a general progressive failure of the slopes in question. It is likely that this failure is initiated by a local structural collapse in the volcaniclastic layer, as predicted in the Mandel and Salencon analysis, but that extrusion of the volcaniclastic layer does not take place.

The discussion above illustrates the difficulty with which translational sliding movement may be distinguished from spreading movements (cf. Voight, 1973). It is concluded that the distinction cannot be made on the basis of landslide morphology alone. Observations on the morphology of rupture zones in Chapter 4, as well as on the microstructure of materials from those zones in Chapter 5, indicated that degradation of the intact rock structure has taken place within the basal weak layer. Although this might indicate a spreading movement rather than translation along a discrete surface, the distinction between the two types of movement rests on the interpretation of Varnes' definition of a slide, i.e., a movement in which shear strain occurs along one or several surfaces within a relatively "narrow zone". It may be in the cases examined that the thickness of the "narrow zone" is in excess of the 12–15 m exposed and that degradation of intact rock has taken place within it. If this is the case, the movement mechanism may
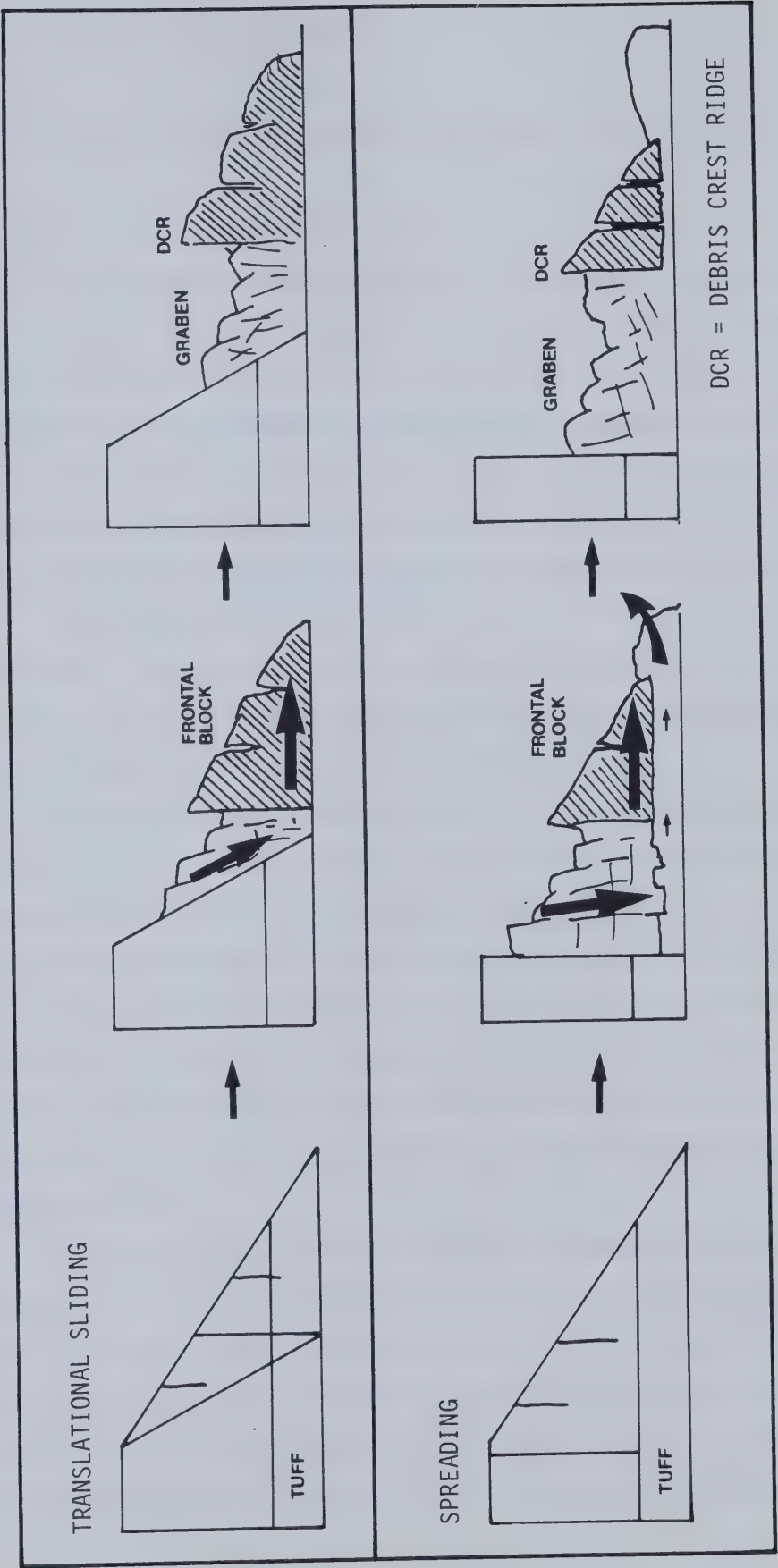
Figure 7.10 Schematic representation of the translational sliding and spreading modes of movement in the Salmon Valley and Chasm Creek slopes.

be interpreted as translational sliding.

7.5 The Timing of Slope Movements and Present Hazard Criteria

7.5.1 The Occurrence of First Time Slides

The landslides analysed in this chapter, as well as all the others examined in this work, give the impression of having occurred a substantial time ago. This impression is based on the existence of a developed organic soil profile on most landslides, the existence of well vegetated debris and scarps in a dry semi-arid climate, and the absence of historical reports of their occurrence. In some cases drainage has been established through the landslide debris and fluvial terraces have developed in the foot of the debris. The geomorphic anomalies normally associated with recent landslides are absent.

Criteria for establishing the absolute age of the landslides is lacking. Suitable exposures of Holocene volcanic ash are limited to those exposures discussed in Chapter 4, and the occurrence of organic material within either landslide debris or associated surficial deposits has not been located in extensive field work.

Fulton (1975) has suggested that most of the landslides occurred in the first few thousand years following deglaciation "as glacially oversteepened and meltwater undercut slopes failed" (p. 30). This is also thought to be the case in other massive deep-seated landslides on the margins of the Thompson study area (e.g., Downie slide, Piteau *et al.* 1978). Ryder (1971) concluded that most of the material in large alluvial fans in the Kamloops-Thompson area was deposited before 6600 yrs. B.P. and that deposition ceased approximately 500-1000 yrs. B.P. Similar observations were made on the rates of talus accumulation in the Similkameen valley to the south of the Thompson study area (Worobey, 1972).

The post-glacial climate of the Thompson study area has been reconstructed by Alley (1976) on the basis of the palynology of a dated core of Holocene peat at Kelowna Bog in the Okanagan Valley. This is summarised in Fig. 7.11 along with an interpretation of active geomorphic processes based on Fulton (1975), Ryder (1971) and Clague (1981). In support of Fulton's (1975) suggestion on the timing of landslides, the period immediately following deglaciation, i.e., 9500-8200 yrs. B.P., was a cool-moist period during which
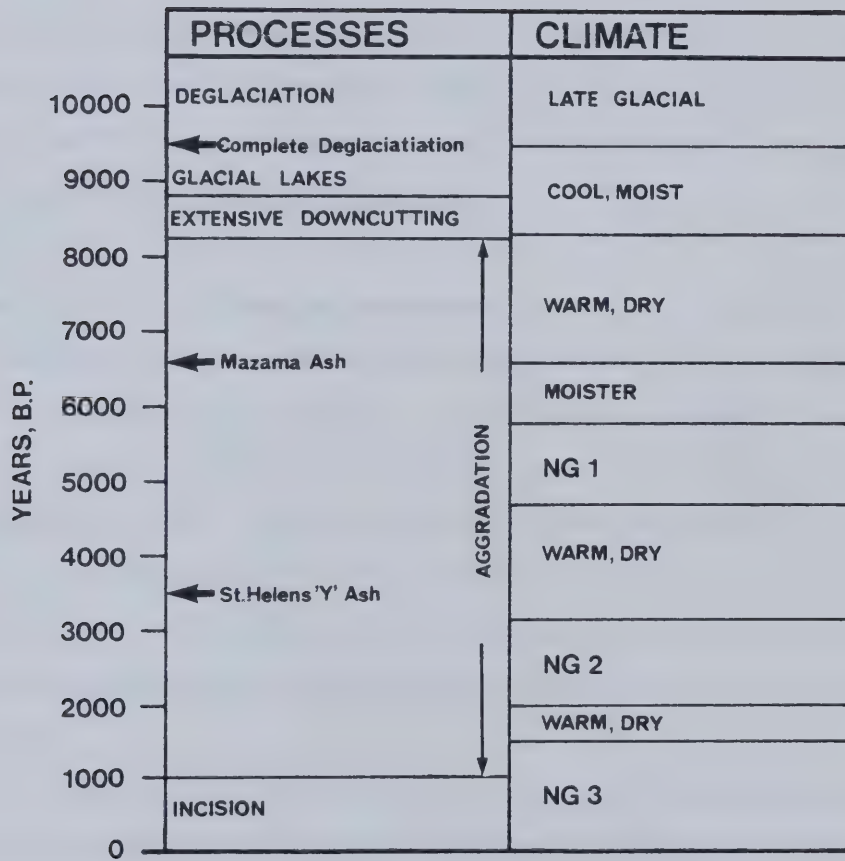
Figure 7.11 Chronology of Post-Glacial processes and climate in the Thompson study area, based on Alley (1976), Fulton (1975), Ryder (1971) and Clague (1981).

the draining of the pro—glacial lakes in the area took place (Fulton, .1969) and which was followed by active downcutting during the establishement of the present drainage. During this time, slope geometry changes due to the passage of meltwater from the drainage of the glacial lakes and stream downcutting, would have led to stress—relief and possible cap loading. These factors would favour the initiation of slope movement which may have been episodic in post—glacial time.

The possibility of first—time landslides occurring in the present environment is one that may be considered. On the basis of field observations and as a result of the analysis presented in this chapter, Adelphi Creek Bluffs is perhaps the slope that is most likely to experience a large first—time landslide. In addition the potential slide masses at Enderby Cliffs, and near the mouth of Gorge Creek, discussed in Chapter 3, are thought to have high potential for first—time slope movement.

7.5.2 Reactivation and Secondary Movements

Little evidence of present day—recent slope movement was observed in the landslides examined in this investigation. Disturbance in the vegetation cover on landslide debris was noted at the Bouleau Lake landslide complex and in several of the Lower Deadman River landslides. At Enderby a secondary flow lobe is presently moving and a family was forced to vacate a house in its path (Plate 3.4). These movements are flows developed in the debris of disintegrated or degraded block movements and constitute the most active slope movements associated with the landslides in the present—day environment.

Secondary scarp failures were noted in the Lower Deadman Valley (Plates 3.8 and 3.15) and a large block is moving down from the scarp at Chasm East landslide (Plate 3.18). At the Jupiter Creek landslide, movement in zone 3 was inferred from the bent trees and depression in the ground surface (Plate 4.13). This is thought to be continued primary movement or secondary block movement. The potential exists in Zone 3 for continued and perhaps large scale movement.

The degradation of landslide masses by weathering and interaction with seepage results in the reduction of the shear strength of areas of landslide debris. Secondary flow movements are thus likely to continue to occur.

7.5.3 Hazard Criteria

An attempt was made to develop hazard criteria that may be used to detect unstable slope geometries. Thus detected the slopes may then be investigated on the ground to establish whether or not a weak basal layer exists and to see if any evidence of slope movement exists.

The geometries of landslides investigated in this work were plotted in Fig. 7.12. In addition the geometries of the reconstructed profiles of the slopes analysed in this chapter are also plotted in Fig. 7.12. Several points arise from an examination of this diagram. First, the reconstructed profiles, in addition to the slopes at Adelphi Creek Bluffs and the incipient landslide mass at Enderby Cliffs, plot to the left of the landslide geometries in what may be called an area of incipient landslide geometry. Block movements plot in an area to the right of the line delineating the incipient landslide geometry and to the right of this is an area of disintegrated and degraded block movement. From Fig. 7.12 it is seen that slopes over 122 m in height which have a mean slope equal to or greater than 26.5° should be investigated for potential slope movements.

Figure 7.12 Landslide geometries for slope movements in the Thompson and Chilcotin

study areas.

8. LANDSLIDES IN VOLCANIC SUCCESSIONS:SUMMARY AND CONCLUSIONS.

8.1 Results of Review

At the outset of this work it was established that slopes developed in layered volcanic successions are particularly susceptible to slope movements. Reports and descriptions of landslides ,in volcanic successions that are mainly Tertiary in age, were reviewed from numerous parts of the world. It was concluded that

a.   landsliding is commonly related to the presence of a weak layer beneath a rigid capping of more resistant lava flows and breccias. The weak layer may consist of weathered Pre-Tertiary material at the basal Tertiary unconformity (e.g., Pre-Cambrian Belt Supergroup in the Spokane area), Mesozoic mudrocks (e.g., Jurassic mudrocks of the Antrim Plateau), or basal volcaniclastic rocks which are frequently deposited before the placement of lava (e.g., John Day Formation, Washington and Oregon)

b.   The effect of geological structure on landsliding is evident in controls on both lateral and headscarp geometries. The volcanic successsions reviewed are characterised by steep to vertical dip-slip and strike-slip faults which provide low strength lateral release surfaces and steep headscarps. Their presence also controls local jointing patterns in the cap and results in block-type slope movements.

c.   movement is frequently in a direction at some angle to the direction of true dip. This suggests that movement takes place along bedding planes (or unit boundaries) at some angle to the true dip, along other low angle discontinuities which are not detected, or by the rupture of intact material within the weak layer. Movement direction is therefore seen to be governed by the orientation of release surfaces in the cap rather than the orientation of the weak layer or discontinuities within it.

d.   initial slope movements are generally of the block type. Successive movements are common. Debris is usually composed of interlocking blocks separated by steep sided depressions. Beneath the steep headscarp a graben commonly occurs. In some slope movements the cap disintegrates during

311

initial movement and the blocks are not preserved. Modification of the debris by secondary flow is frequently observed. The morphology of the landslides is suggestive of two types of slope movement viz. sliding or spreading.

e.   an examination of the phases in landslide development suggest that both sliding and spreading processes are possible. Erosion and stress-relief processes produce structurally defined blocks in the cap which may be free to slide along shear surfaces or load the subjacent weak layer and cause it to extrude by plastic flow or liquefaction.

f.   reports of current slope movements in volcanic successions are generally limited to limited displacements in pre-existing landslides. Few first-time landslides are reported (e.g., Gradot Ridge, Yugoslavia; Kyushu, Japan). Given the prevalence of pre-existing landslide sites it is suggested that the geological conditions (e.g., erosion, groundwater) for the inititiation of first-time slope movements appear to have existed at some time in the geological past rather than in the present geological environment.

8.2 Framework and Objectives of the Present study

To investigate the nature of geological controls on landslides in volcanic successions and the kinematics of the slope movements, a regional landslide study was carried out on slopes developed in Paleogene and Neogene volcanic successions in two areas of the Interior Plateau, British Columbia.

The Paleogene succession is structurally disturbed exhibiting a wide variety of lavas and breccias and volcaniclastic rocks which outcrop in the northern Thompson Plateau. The younger Neogene succession, outcropping in the southern Fraser Plateau is structurally undisturbed and consists of basaltic lava flows overlying a basal volcaniclastic assemblage.

The study had the following objectives;

(a) To establish the regional distribution of landslides, the variation in landslide types and the geomorphic and geological environment of landslides in Paleogene and Neogene volcanic successions in selected areas of the southern Interior Plateau of British Columbia.

(b) To isolate the geological factors (including geomorphology, geological history,

stratigraphy, lithology and structure) contributing to slope movements within a smaller study area with particular emphasis on the characteristics of weak volcaniclastic strata, and to describe landslide morphology, kinematics and movement history.

(c) To investigate the microstructure and geotechnical properties of weak volcaniclastic rocks which are associated with landsliding.

(d) To evaluate sliding and spreading models of slope movement with respect to selected landslides.

(e) To develop a geotechnical basis for the assessment of existing natural slope stability for use in natural hazard evaluations.

8.3 Landslide Distribution and Landslide Types in the Study Areas

A systematic air photo inventory of both the Thompson (16565 km²) and the Chilcotin (6500km²) study areas yielded approximately 32 and 67 landslide sites respectively. The majority of landslides in the study areas are block-type landslides and have volumes in excess of 10^8 m³.

Landslide morphology was used as a basis for landslide classification and four types were distinguished: simple block movements, multiple juxtaposed block movements, complex block movements, and successive block movements.

In the Salmon valley, four landslides were analysed in detail. The landslides are characterised by :

a. high, near vertical head and lateral scarps;

b. the presence of a graben in the debris at the foot of the scarp consisting of interlocking ridges and blocks separated by steep-sided depressions up to 60 m deep.

c. a debris crest ridge which marked the downslope boundary of the graben;

d. a frontal zone of distended blocks downslope of the debris crest ridge which is either terminated by a steep debris slope, as in the case of the Shell Creek and Jupiter Creek landslides, or a gentler slope which blends into surficial deposits at the foot of the debris as at the Adelphi Creek and Stephen's Lake Road landslides.

The debris shows little evidence of rotation and the movement is dominantly horizontal.

The morphology of the landslides is suggestive of translational sliding or lateral spreading.

8.4 Factors Affecting the Spatial Variability of Regional Landslide Response

(a) Stratigraphy: An examination of the geological environment of slope movement sites indicates that landslides have taken place where weak volcaniclastic layers, consisting of tuffs, tuff-breccias, and tuffaceous sediments, were exposed at the base of pre-movement slopes, beneath a capping of lavas, breccias, or dry unaltered volcaniclastic rocks. The properties of the cap determine initial fragmentation characteristics which result in the preservation of blocks in the debris or their disintegration. Properties important in this respect are discontinuity density, which controls cap coherence, and intact rock strength.

(b) Structure: Since the Neogene succession is not structurally disturbed the effect of macrostructure is limited to slope movement sites in Paleogene rocks. Structural control is related to elements of the regional structural fabric which consist of steep, linear dip-slip and strike-slip faults of the Interior Shear Zone. The relationship between the plan geometry of landslides i.e., the orientation of lateral release surfaces and headscarps, and regional structural elements was established both on the regional scale and in detail in the Salmon Valley. Faulting is also important in ensuring the lateral contiguity of the basal weak layer at the base of some pre-movement slopes which accounts for the large volume of some landslides in Palaoegene rocks.

In numerous examples, the direction of slope movement is at some angle to the true dip direction. In some cases this was inferred to be down a surface dipping toward the valley at some angle less than the true dip or on a horizontal surface parallel to the strike. In other cases, movement direction is against the dip implying that the movement has involved the rupture of intact material in the basal weak layer. The dominant control on initial movement direction was found to be the orientation of release surfaces in the cap and not the disposition of the weak layer or discontinuities within it.

In the absence of macro-structural control, landslides in Neogene rocks exhibit curved headscarps, diffuse lateral boundaries and are generally contiguous block movements due to the fact that the basal weak layer is not truncated by faulting.

(c) Geomorphology: Landslides in the Thompson study area appear to be localised along the margins of steep-sided meltwater channels formed, or modified, during de-glaciation by the drainage of pro-glacial lakes, and along oversteepened creek valley slopes. Locally, however, slope development has a complex history. Where the relationship between surficial materials and landslide debris is exposed, it is evident that slope movements were not an immediate response to oversteepening by meltwater or stream activity. This observation implies that the majority of slope movements are delayed failures in relation to the slope geometry change by erosion. This raises the problem of the timing of first-time landslides.

In the Chilcotin study area, landslide debris is found covering benches of glacio-lacustrine silts above the flood plain of the present Chilcotin River. This infers that basal erosion was not an immediate cause of slope movement.

8.5 Microstructure of Volcaniclastic Materials

Because of the association between landsliding in the cap and the occurrence of subjacent volcaniclastic material, an investigation into the microstructure of these materials was carried out. Intact, sheared and remoulded samples were examined.

Volcaniclastic rocks are fragmental systems consisting of grains that occur within a matrix in a hierarchy of microstructural domains which are dominantly matrix-supported. Due to the presence of chemically unstable pyroclastic material, diagenetic changes take place at grain and matrix sites in each domain. Montmorillonite was found to be the dominant product of this alteration and originates in the diagenesis of volcanic glass particles and feldspar crystals. Since these substances make up both grain and matrix elements, the result of the alteration is to degrade the strength of the intact rock material.

The microfabric of volcaniclastic material is also characterised by an open, porous structure at the inter-,intra-, and trans-assemblage scales. Due to the vesiculated nature of some pyroclastic particles, intra-particle porosity is also marked. The open structure

results from a combination of low initial densities, due to airfall deposition, and post-alteration solution which has modified the distribution and volume of pore space by an unknown amount.

8.6 Geotechnical Properties of Volcaniclastic Materials

A range of geotechnical properties was established for selected volcaniclastic materials. They are characterised by:

1. low dry densities ($13.98 - 21.92$ KN/m^3) and high porosities ($9 - 43.3\%$) which are intermediate between soil (e.g., glacio-lacustrine silt, loess) and the more common types of rock. These data reflect the porous structure noted above.

2. low uniaxial compressive strengths ($q_u \leq 13.5$ MPa). The values of q_u were shown to be dependent on porosity and also reflect the extent of replacement by montmorillonite within the intact microstructure.

3. low angles of ultimate frictional resistance ($<20^0$), although these values may be higher in the presence of significant authigenic or pyroclastic silica. Values of ϕ'_{ult}. may be expected to decrease during the alteration process with the development of diagenetic montmorillonite.

8.7 Evaluation of Sliding and Spreading Models

Two models of movement mechanisms were evaluated with reference to three slopes in the Salmon Valley and the Chasm Creek West landslide. In the translational sliding model, the failure surface was assumed to be bi-linear and to consist of a steep back surface controlled by discontinuities in the cap and a sub-horizontal basal shear surface located in the subjacent volcaniclastic layer. A simple wedge analysis was performed on a variety of failure geometries under a range of groundwater conditions.

In the spreading model, extrusion of the subjacent volcaniclastic material takes place, by plastic flow or liquefaction, under cap loading. The cap is free to load the subjacent strata due to cap separation during the stress-relief process. Failure of intact rock is required for spreading and the movement takes place independent of existing discontinuities in the spreading layer. The stability of the cap loading was analysed as a bearing capacity problem and was estimated from the theory of Mandel and Salencon

(1972), which approximates the bearing pressures required to cause the extrusion of a weak subjacent layer. Drained and undrained analyses were carried out. Drained spreading requires overburden stresses far in excess of those existing in the slopes in question. Undrained spreading may be possible if structural collapse of the tuff takes place under cap loading. Although microstructural observations in Chapter 5 suggests this is possible, detailed laboratory tests are not available to confirm this.

The analysis yielded first approximations to slope movement conditions in the slopes selected for both modes of movement. It was found , using reasonable assumptions concerning failure geometry, strength of the rock mass, and groundwater conditions, that conditions for both types of movement may have existed in the Salmon Valley and Chasm Creek slopes prior to movement. The movements have probably resulted from progressive failure initiated by local structural degradation in the weak layer. The analysis illustrates the difficulty with which spreading movements may be distinguished from translational sliding movements.

8.8 Timing, Present Movements, Hazard Criteria.

No direct ages were obtainable for the occurrence of landslides examined in this work. The results of the evaluation of movement mechanism noted above infer that the initiation of slope movements occurred toward the end of the stress–relief phase initiated upon valley modification by erosional events in late–glacial or early post–glacial time. This may in part account for the delay in slope movement, vis–a–vis slope geometry change, noted at the end of Chapter 7. A second time–dependent factor may also have been the changes in the microstructure of the volcaniclastic materials (diagenesis and post–diagenesis solution) brought about by the re-establishment of groundwater flow systems in newly over–deepened valleys following de–glaciation. It is thought, in the absence of absolute dates, that the most likely timing for the initiation of first–time slope movements in the study area is in the early post–glacial period prior to the onset of the Altithermal at approximately 8200 years B.P. The possibility exists that seismic processes may have induced first–time slope movements at any time in post–glacial time.

Present movements are generally secondary flows within the debris which occur as blocks degrade. However, the stability of deeply undercut landslide debris should be

examined further at a number of sites. Tilted trees at Jupiter Creek and Chasm Creek indicate that small scale block movements within existing landslides are currently taking place.

An attempt was made to develop hazard criteria that may be used to detect potentially unstable slope geometries. Reconstructed pre-movement slope geometries and possible incipient landslide masses at Adelphi Creek Bluffs, Gorge Creek, and Enderby Cliffs fall within an incipient landslide geometry field which is defined by slopes over .122 m in height and which have mean slopes equal to or greater than 26.5°.

BIBLIOGRAPHY

Alley, N.F. 1976. The palynology and palaeoclimatic significance of a dated core of Holocene peat, Okanagan Valley, British Columbia. Canadian Journal of Earth Sciences, 13, pp. 1131–1144.

Alley, N.F. and B. Thomson. 1978. Aspects of environmental geology, parts of Graham Island, Queen Charlotte Islands. Bulletin Number 2, Resource Analysis Branch, British Columbia Ministry of Environment, Victoria, 65p.

Almon, W.R., L. B. Fullerton and D.K. Davies. 1976. Pore space reduction in Cretaceous sandstones through chemical precipitation of clay minerals. Journal of Sedimentary Petrology, 46, pp. 89–96.

Anderson, F.W. and K.C. Durham. 1966. The geology of northern Skye. Memoir of the Geological Survey of Scotland, H.M.S.O., Edingurgh, 216 p.

Anderson. R.A. 1971. Stability of slopes in clay shales interbedded with Columbia River Basalt. M.Sc. thesis, University of Idaho, Moscow. 297 p.

Anderson, R.A. and R.L. Schuster. 1970. Stability of slopes in clay shales interbedded with Columbia River Basalt. Proceedings, 8th. Annual Engineering Geology and Soils Engineering Symposium, Pocatello, Idaho, pp. 273–284.

Asai, T. 1968 The post–glacial big landslides in Iceland illustrated by stereographs. Natural Science Reports, Ochanomizu University, Tokyo, 19, pp. 83–88 .

Atlantic Richfield Hanford Co. 1976. Preliminary feasibility study on storage of radioactive wastes in Columbia River Basalt. Vol. 1. ARH–ST–137 (Vol. 1). 183 p.

Attwood, W.W. 1918. Relations of landslide and glacial deposits to reservoir sites in the

San Juan Mountains, Colorado. United States Geological Survey Bulletin 685. 38 p.

Atwood. W.W. and K.F. Mather. 1932. Physiography and Quaternary geology of the San Juan Mountains, Colorado. United States Geological Survey, Professional Paper 166. 176 p.

Bailey, E.B., C.T. Clough, W.B. Wright, J.E. Richey and G.V. Wilson. 1924. Tertiary and post−Tertiary Geology of Mull, Loch Aline and Oban. Memoir of Geological Survey of Scotland, H.M.S.O., 445 p.

Bailey, R.G. 1971. Landslide hazards related to land use planning in Teton National Forest, Northwest Wyoming. United States Department of Agriculture, Forest Service, Intermountain Region, 131 p.

Baker, R.F. and R. Chieruzzi. 1959. Regional concept of landslide occurrence. Highway Research Board, Bulletin 216, pp. 1−16.

Banks, D.C. and R.T. Saucier. 1964. Engineering geology of Buckboard Mesa. Report No. PNE 500IP, U.S. Army Corps. of Engineers, Waterways Experiment Station, Vicksburg, Miss. 147 p.

Barden, L. 1972. The relation of soil structure to the engineering geology of clay soil. Quarterly Journal of Engineering Geology, 5, 85−102.

Barton, M.E. 1977. Landsliding along bedding planes. Bulletin, International Association of Engineering Geology, 16, pp. 5−7.

Barton, N. 1979. Artificial slopes in complex formations: reduced stability with time. Proceedings, Conference on the Geotechnics of Structurally Complex Formations, Capri, Vol. 2, pp.316−320.

Barton, N. and V. Choubey. 1977. The shear strength of rock joints in theory and practice. Rock Mechanics, 10, pp. 1–54.

Bennett, R.H., W.R. Bryant and G.H. Keller. 1981. Clay fabric of selected submarine sediments: fundamental properties and models. Journal of Sedimentary Petrology, 51, pp. 217–232.

Bevier, M.L. 1981. Stratigraphy and petrology of the Miocene plateau lavas of British Columbia. Geological Association of Canada Joint Meeting, Calgary, 1981. Abstracts, 6, p. A–4.

Bieniawski, Z.T. 1974. Estimating the strength of rock materials. Journal of the South African Institute of Mining and Metallurgy, 88, pp.312–320.

Bieniawski, Z.T. 1979. The Geomechanics Classification in rock engineering applications. Proceedings, 4th. International Conference on Rock Mechanics, 2, pp. 41–47.

Bohor, B.F. and R.E. Hughes. 1971. Scanning electron microscopy of clays and clay minerals. Clays and Clay Minerals, 19, pp. 49–54.

Borst, R.L. and W.D. Keller. 1969. Scanning electron micrographs of API reference clay minerals and other selected samples. Proceedings, International Clay Conference, Israel, 1, pp. 871–901.

Bostock, H.S. 1941. Okanagan Falls, British Columbia. Geological Survey of Canada, Map 627A.

Brindley, G.W. and G. Brown. 1980. Crystal structures of clay minerals and their X–ray identification. Mineralogical Society Monograph No. 5.

Broch, E. 1979. Changes in rock strength caused by water. Proceedings, 4th.

International Conference on Rock Mechanics, 1, pp. 71–75.

Broch, E. and J.A. Franklin. 1972. The point load strength test. International Journal of Rock Mechanics and Mining Science, 9, pp. 669–697.

Brohms, B.B. and H. Bennermark. 1967. Stability of clay at vertical openings. Journal of the Soil Mechanics and Foundations Division, American Society of Civil Engineers, 93, pp. 71–94.

Brohms, B.B. and H. Bjerke. 1972. Extrusion of soft clay through a retaining wall. Canadian Geotechnical Journal, 10, pp. 103–109.

Brown, J.D. and G.G. Meyerhof. 1969. Experimental study of bearing capacity in layered clays. Proceedings, 7th. International Conference on Soil Mechanics and Foundation Engineering, 2, pp. 45–51.

Brown, R.W. 1928. Experiments relating to the results of horizontal faulting. American Association of Petroleum Geologist, Bulletin, 12, pp. 715–720.

Bryan, K. 1929. Geology of reservoir and dam sites. United States Geological Survey, Water–Supply Paper 597, pp. 1–38.

Burland, J.B., T.I. Longworth and J.F.A. Moore. 1977. A study of ground movement and progressive failure caused by a deep excavation in Oxford Clay. Geotechnique, 27, pp. 557–591.

Caine, N. 1982. Toppling failures from alpine cliffs on Ben Lomond, Tasmania. Earth Surface Processes and Landforms, 7, pp. 133–152.

Cairnes, C.E. 1932. Mineral resources of north Okanagan Valley, B.C. Geological Survey of Canada, Summary Report for 1931, part A, pp. 66–109.

Campbell, R.B. and H.W. Tipper. 1971. Geology of the Bonaparte Lake map-area, British Columbia. Geological Survey of Canada, Memoir 363. 100 p.

Carr, J.M. 1962. Geology of the Princeton, Merritt, Kamloops area of southern B.C. Western Mines and Oil Review, 35, pp. 46-49.

Carr, J.M. and A.J. Reed. 1976. Afton: A supergene copper deposit. In 'Porphyry deposits of the Canadian Cordillera'. Edited by A. Sutherland-Brown. Canadian Institute of Mining and Metallurgy, Special Volume 15, p. 376-387.

Carroll, D. 1970. Clay minerals: a guide to their X-ray identification. Geological Society of America, Special Paper 126. 80 p.

Chandler, E.C. 1966. Stability of rock excavation underlain by artesian horizons. Proceedings, 4th. Annual Engineering Geology and Soils Engineering Symposium, Moscow, Idaho, pp. 21-47.

Charlesworth, J.K. 1953. The geology of Ireland: an introduction. Oliver and Boyd, London, 276 p. (see pp. 236-237).

Church, B.N. 1973. Geology of the White Lake basin. British Columbia Department of Mines and Petroleum Resources, Bulletin 61. 120 p.

Church, B.N. 1975. Geology of the Hat Creek coal basin (92I/13E). British Columbia Minister of Mines and Petroleum Resources, Geology of British Columbia, 1975, p. G99-G118.

Church, B.N. 1979. Geology of the Terrace Mountain Tertiary outlier. British Columbia Ministry of Energy, Mines and Petroleum Resources. Preliminary Map 37.

Church, B.N. and S.G. Evans. 1983. Basalts of the Kamloops Group in Salmon River area

(82L/5). In 'Geological Fieldwork 1982'. Geological Branch, Mineral Resources Division, Paper 1983, pp. 88–91 , British Columbia Ministry of Energy, Mines and Petroleum Resources .

Clague, J.J. 1981. Late Quaternary geology and geochronology of British Columbia. Part 2: Summary and discussion of radiocarbon–dated Quaternary history. Geological Survey of Canada, Paper 80–35.

Clague, J.J. and J.G. Souther. 1982. The Dusty Creek landslide on Mount Cayley, British Columbia. Canadian Journal of Earth Sciences, 19, pp. 524–539.

Clarke, D.D. 1904. A phenomenal landslide. American Society of Civil Engineers, Transactions, 53, pp. 322–412.

Clarke, D.D. 1918. A phenomenal landslide – supplement. American Society of Civil Engineers, Transactions, 82, pp. 767–801.

Coates, D.F. 1970. Rock mechanics principles. Canada Department of Energy Mines and Resources, Mines Branch Monograph 874.

Coates, D.F. and Y.S. Yu. 1978. Block flow slope instability. CANMET Report 78–10. 112 p.

Cockfield, W.E. 1948. Geology and mineral deposits of Nicola map–area, British Columbia. Geological Survey of Canada, Memoir 249. 164 p.

Collins, K. and A. McGown. 1973. The form and function of microfabric features in a variety of natural soils. Geotechnique, 24, pp. 223–254.

Compton, R.R. 1962. Manual of field geology. John Wiley & Sons, New York. 378 p.

Corns, C.F. and R.H. Nesbitt. 1967. Sliding stability of 3 dams on weak rock foundations. Transactions, 9th. International Congress on Large Dams, 1, pp. 463-486.

Crandell, D.R. and R.K. Fahnestock. 1965. Rockfalls and avalanches from Little Tahoma Peak on Mount Rainier, Washington. United States Geological Survey Bulletin 1221-A. 30 p.

Daly, R.A. 1915. A geological reconnaissance between Golden and Kamloops, along the line of the Canadian Pacific Railway. Geological Survey of Canada, Memoir 68. 260 p.

Davies, D.K., W.R. Almon, S.B. Bonis and B.E. Hunter. 1979. Deposition and diagenesis of Tertiary-Holocene volcaniclastics, Guatemala. Society of Economic Palaeontologists and Mineralogists Special Publication 26, pp. 281-306.

Davis, G.H. 1980. Structural characteristics of metamorphic core complexes, southern Arizona. Geological Society of America, Memoir 153, pp. 35-77.

Davis, S.N. 1969. Porosity and permeability in natural materials. In 'Flow through porous media'. Edited by R.J.M. de Wiest. pp. 53-89. Acedemic Press, New York.

Davis, S.N. and R.J.M. De Wiest. 1966. Hydrogeology. J. Wiley and Sons, N.Y., 463 pp.

Dawson, G.M. 1879. Preliminary report on the physical and geological features of the southern portion of the interior of British Columbia. Geological Survey of Canada, Report of Progress 1877-1878, pp. 1-186B.

Dawson, G.M. 1896. Report on the area of the Kamloops map-sheet, British Columbia. Geological Survey of Canada, Annual Report 1894, v. VII, pt. B. 427 p.

Deere, D.U. and R.P. Miller. 1966. Engineering classification and index properties for

intact rock. Technical Report No. AFNL-TR-65-116 Air Force Weapons Laboratory. New Mexico.

Dishaw, H.E. 1967. Massive landslides. Photogrammetric Engineering, 33, pp. 603-608.

Dreyer, W. 1926. Volcanic formations govern design in Pitt River 3 hydro development. Engineering News Record, 96, pp. 144-149.

Duffel, S. and K.C. McTaggart. 1951. Ashcroft map-area, British Columbia. Geological Survey of Canada, Memoir 262. 122 p.

Dunbavan, M. 1980. Physical modelling of sequential slope failure. 3rd. Australian-New Zealand Conference on Geomechanics, 2, pp. 41-45.

Dyrness, C.T. 1967. Mass soil movements in the H.J. Andrews Experimental Forest. United States Department of Agriculture, Forest Service Research Paper PNW-42, 12 p.

Eisbacher, G.H. 1979. First-order regionalization of landslide characteristics in the Canadian Cordillera. Geoscience Canada, 6, p. 69-79.

Erskine, C.F. 1973. Landslides in the vicinity of the Fort Randall Reservoir, South Dakota. United States Geological Survey, Professional Paper 675. 65 p.

Escario, V. 1968. Failure patterns in a rock cut resting on clay. Proceedings, International Symposium on Rock Mechanics, Madrid, pp. 237-242.

Esu, F. 1966. Short-term stability of slopes in unweathered jointed clays. Geotechnique, 16, pp. 321-328.

Evans, R.S. 1981. An analysis of secondary toppling rock failures - the stress

redistribution method. Quarterly Journal of Engineering Geology, 14, pp. 77-86.

Ewing, T.E. 1979. Geology of the Kamloops Group (92I/9,10,15,16) Geological
    Fieldwork, 1978. Paper 79-1, B.C. Ministry of Energy and Petroleum Resources.
    pp. 119-123.

Ewing, T.E. 1980. Palaeogene tectonic evolution of the Pacific Northwest. Journal of
    Geology, 88, pp. 619-638.

Ewing, T.E. 1981(a). Regional stratigraphy and structural setting of the Kamloops Group,
    south-central British Columbia. Canadian Journal of Earth Sciences, 18, pp.
    1464-1477.

Ewing, T.E. 1981(b). Petrology and geochemistry of the Kamloops Group volcanics, British
    Columbia. Canadian Journal of Earth Sciences, 18, pp. 1478-1491.

Flint, R.F.and C.S. Denny. 1958. Quaternary geology of Boulder Mountain, Aquarius
    Plateau, Utah. United States Geological Survey, Bulletin 1061-D, pp. 103-164.

Elygenring, P., P.R. Palmason and C.K. Willey. 1976. Slurry trench cutoffs through lava
    and underlying interbeds. Transactions, 12th. International Conference on Large
    Dams, 1, pp. 1-18.

Fookes, P.G. 1965. Orientation of fissures in stiff overconsolidated clay of the Siwalik
    System. Geotechnique, 15, pp. 195-206.

Fookes, P.G., W.R. Dearman and J.A. Franklin. 1971. Some engineering aspects of rock
    weathering with field examples from Dartmoor and elsewhere. Quarterly Journal of
    Engineering Geology, 4, pp. 139-185.

Foster, R.H. and P.K. De. 1971. Optical and electron microscopic investigation of shear

induced structures in lightly consolidated (soft) and heavy consolidated (hard) kaolinite. Clays and Clay Minerals, 19, pp. 31-47.

Franklin, J.A. and R. Chandra. 1972. The slake-durability test. International Journal of Rock Mechanics and Mining Science, 9, pp. 325-341.

Fulton, R.J. 1965 . Silt depostion in late-glacial lakes of southern British Columbia. American Journal of Science, v. 263, no. 7, p. 553-570.

Fulton, R.J. 1967. Deglaciation studies in Kamloops region, an area of moderate relief, British Columbia. Geological Survey of Canada, Bulletin 154, 36 p.

Fulton, R.J. 1969. Glacial lake history, southern Interior Plateau, British Columbia. Geological Survey of Canada, Paper 69-37, 14 p.

Fulton, R.J. 1975. Quaternary geology and geomorphology, Nicola-Vernon area, British Columbia (82L W.1/2 and 92I E.1/2). Geological Survey of Canada, Memoir 380, 50 p.

Fulton, R.J. 1976. Quaternary history south-central British Columbia and correlations with adjacent areas. In 'Quaternary Glaciations in the Northern Hemisphere'. Ed. D.J. Easterbrook and V. Sibrava. IUGS-UNESCO International Geological Correlation Programme, Project 73-1-24, Report no. 3, p. 62-89.

Fulton, R.J. and G.W. Smith. 1978. Late Pleistocene stratigraphy of south-central British Columbia. Canadian Journal of Earth Sciences, 15, pp. 971-980.

Gibb, J.G. 1979. A coastal landslide. Soil and Water (N.Z.), 15, pp. 20-21.

Geikie, A. 1903. Textbook of geology, Vol. 1. MacMillan, London, 702 p. (see pp. 480-481).

Geikie, J. 1880. On the geology of the Fareoe Islands. Transactions, Royal Society of Edinburgh, 30, pp. 217–269.

Geological Survey of Greenland. 1976. Qutdligssat:70 V.ISYD(1:1000000 Map)

Goodman, R.E. 1976. Methods of geological engineering in discontinuous rocks. West Publishing Company, New York, 472 p.

Goodman, R.E. 1980. Introduction to rock mechanics. John Wiley and Sons, New York. 478 p.

Graham, P.S.W. and D.G.F. Long. 1979. The Tranquille Beds of the Kamloops Group: A Tertiary (Middle Eocene) coal bearing sequence in the vicinity of Kamloops Lake, British Columbia. In 'Current Research, Part A'. Geological Survey of Canada, Paper 79-A, pp. 357–360.

Griggs, A.B. 1976. The Columbia River Basalt Group in the Spokane quadrangle, Washington, Idaho, Montana. United States Geological Survey, Bulletin 1413. 39 p.

Gullixson, R.L. 1958. Foundation grouting, McNary Dam, Oregon and Washington. Geological Society of America, Engineering Geology Case Histories, 2, pp. 5–8.

Hadley, J.B. 1978. Madison Canyon rockslide, Montana , U.S.A. In 'Rockslide and Avalanches, 1 '. Edited by B. Voight, Elsevier, New York, pp. 167–180.

Hall, W.B. 1960. Mass–gravity movements in the Madison and Gallatin Ranges, southwestern Montana. Billings Geological Society Guidebook, 11th. Annual Field Conference, pp. 200–206.

Hamrol, A. 1961. A quantitative classification of the weathering and weatherability of rocks. Proceedings, 5th. International Conference on Soil Mechanics and

Foundation Engineering, 2, pp. 771-774.

Harp, E.L., R.C. Wilson and G.F. Wieczorek. 1981. Landslides from the February 4, 1976, Guatemala Earthquake. United States Geological Survey, Professional Paper 1204-A. 35 p.

Heginbottom, J.A. 1972. Surficial geology of the Taseko Lakes map-area, British Columbia. Geological Survey of Canada, Paper 72-14, 9 p.

Heiken, G.H. 1972. Morphology and petrology of volcanic ashes. Geological Society of America, Bulletin, 83, pp. 1961-1988.

Heiken, G.H. 1974. An atlas of volcanic ash. Smithsonian Contributions to the Earth Sciences, 12, 101 p.

Heitfeld K-H., R. Azzam and H. Dullman. 1980. Deformability and shear strength of swellable tuffitic sediments. Bulletin of the International Association of Engineering Geology, 22, pp. 195-199.

Hills, L.V. and H. Baadsgaard, H. 1967. Potassium-argon dating of some Lower Tertiary strata in British Columbia. Bulletin of Canadian Petroleum Geology, v. 15, p. 138-149.

Hinds, N.E.A. 1938. Large landslides in the Colorado Plateau. Geological Society of America Proceedings for 1937, pp. 241-242.

Hodge, R.A.L. 1977. Regional geology, groundwater flow systems and slope stability. Unpublished M.Sc. Thesis, University of British Columbia, Vancouver, B.C., 121 p.

Hoek, E. and J.W. Bray. 1977. Rock slope engineering. Institution of Mining and Metallurgy, London. 402 p.

Hoek, E. and E.T. Brown. 1980. Empirical strength criterion for rock masses. Journal of the Geotechnical Engineering Division, American Society of Civil Engineers, 106, pp. 1013–1035.

Hogensen, G.M. 1964. Geology and ground water resources, Umatilla River basin, Oregon. United States Geological Survey Water–Supply Paper 1620, 162 p.

Howe, E. 1909. Landslides in the San Juan Mountains, Colorado. United States Geological Survey, Professional Paper 67, 55 p.

Hutchinson, J.N. 1967. The free degradation of London Clay cliffs. Proceedings, Geotechnical Conference, Oslo, 1, pp. 113–118.

International Society For Rock Mechanics. 1978. Commission on standardisation of laboratory and field tests: suggested methods for the quantitative description of discontinuities in rock masses. International Journal of Rock Mechanics, Mining Science and Geomechanics Abstracts, 15, pp. 319–368.

International Society For Rock Mechanics. 1979. Commission on standardisation of laboratory and field tests: suggested methods for determining water content, porosity, density, absorption and related properties and swelling and slakedurability index properties. International Journal of Rock Mechanics, Mining Science and Geomechanics Abstracts, 16, pp. 141–156.

Japan Society of Landslide. 1972. Landslides in Japan. National Conference of Landslide Control. 40 p.

Jones, A.G. 1959. Vernon map–area, British Columbia. Geological Survey of Canada, Memoir 196. 186 p.

Jorgensen, G. 1972. An area of solifluction on Suduroy, the Faeroe Islands. Bulletin,

Geological Society of Denmark, 21, pp. 368–373.

Jorgensen, G. 1978. Landslides and related phenomena on Suduroy, the Faeroe Islands. Bulletin of the Geological Society of Denmark, Vol. 27, Special Issue, pp. 85–89.

Jurgenson, L. 1934. The application of theories of elasticity and plasticity to foundation problems. In "Contributions to Soil Mechanics. 1925–1940." Boston Society of Civil Engineers, 1940, pp. 148–183.

Kanji, M.A. 1979. Transition materials and weak discontinuities as structurally complex formations. Proceedings, Conference on the Geotechnics of Structurally Complex Formations, Capri, 2, pp. 255–262.

Kanji, M.A., G. Re, R.A. Abrahao, F.O. Moura and N.F. Midea. 1977. Complex structures as dam foundations: geomechanical characteristics (A. Vermelha). Proceedings, Conference on the Geotechnics of Structurally Complex Formations, Capri, pp. 297–305.

Keefer, W.R. and J.K. Love. 1956. Landslides along the Gros Ventre River, Teton County, Wyoming. Wyoming Geological Association Guidebook, 11th. Annual Field Conference, pp. 24–28.

Keller, G.V. 1960. Physical properties of tuffs of the Oak Spring Formation, Nevada. United States Geological Survey, Professional Paper 400B, pp. B396–B400.

Kelley, V.C. 1979. Geomorphology of the Espanola Basin. In 'Guidebook of Santa Fe County', New Mexico Geological Society, 30th. Field Conference. Ed. R.V. Ingersoll, pp. 281–288.

Khoury, H.N. and D.B. Eberl. 1979. Bubble wall shards altered to montmorillonite. Clays and Clay Minerals, 27, pp. 291–292.

Koons, E.D. 1945. Geology of the Uinkaret Plateau, Northern Arizona. Geological Society of America, Bulletin, 56, pp. 151–180.

Krahn, J. and N.R. Morgenstern. 1979. The ultimate frictional resistance of rock discontinuities. International Journal of Rock Mechanics, Mining Science and Geomechanics Abstracts, 16, pp. 127–133.

Kuenen, Ph. H. 1935. Contributions to the geology of the East Indies from the Snellius Expedition, Part I, Volcanoes. Leidsche Geologische Mededeelingen, 7, 273–283.

Kulhawy, F.H. and R.E. Goodman. 1980. Design of foundations on discontinuous rock. Proceedings, International Conference on Structural Foundations on Rock, Sydney, 1, pp. 209–220.

Ladanyi, B. 1972. Rock failure under concentrated loading. Proceedings, 10th. Symposium on Rock Mechanics, pp. 363–387.

Lambe, T.W., F.Silva and W.A. Marr. 1981. Instability of Amuay cliffside. Journal of the Geotechnical Engineering Division, American Society of Civil Engineers, 107, pp. 1505–1520.

La Rochelle, P., J.Y. Chagnon and G. Lefebvre. 1970. Regional geology and landslides in the marine clay deposits of eastern Canada. Canadian Geotechnical Journal, 7, pp. 145–156.

Lawrence, R.D. 1979. Tectonic significance of regional jointing in Columbia River Basalt, north–central Oregon. Northwest Science, 53, 1979, pp. 33–42.

Lee, C.F. and K.Y. Lo. 1976. Rock squeeze study of two deep excavations at Niagara Falls. Proceedings, American Society of Civil Engineers Specialty Conference, Rock Engineering For Foundations and Slopes, 1, pp. 116–140.

Lensen, G.J. 1958. A method of graben and horst formation. Journal of Geology, 66, pp. 579-587.

Liang, T. and D.J. Belcher. 1958. Airphoto interpretation. In "Landslides and engineering practice", Highway Research Board Special Report 29, pp. 69-92.

Locker, J.G. 1973. Petrographic and engineering properties of fine-grained rock of Central Alberta. Alberta Research Council Bulletin, 30, 144 p.

Long, D.G.F. 1981. Dextral strike-slip faults in the Canadian Cordillera and depositional environments of related fresh-water intermontane coal basins. In 'Sedimentation and tectonics in alluvial basins'. Edited by A.D. Miall. Geological Association of Canada Special Paper 23, pp. 153-186.

Lupini, J.F., A.E. Skinner and P.R. Vaughan. 1981. The drained residual strength of cohesive soils. Geotechnique, 31, pp. 181-213.

Lutton, R.J. and D.C. Banks. 1970. Study of clay shale slopes along the Panama Canal - East Culebra and West Culebra slides and the model slope. U.S. Army Engineers Waterways Experiment Station, Technical Report No. S-70-9, Report 1 (Corps. of Engineers, Vicksburg, Miss.), WES Report 2.

Lutton, R.J., C.C. Banks and W.E. Strohm. 1979. Slides in Gaillard Cut, Panama Canal Zone. In 'Rockslides and Avalanches, 2'. Edited by B. Voight. Elsevier, Amsterdam, pp. 151-224.

Macdonald, G.A. 1972. Volcanoes. Prentice-Hall, Inc., Englewood Cliffs, N.J. 510 p.

Mahr, T. and J. Malgot. 1977. Influence of soil physio-mechanical properties on the landslides development. 5th. Danube European Conference on Soil Mechanics and Foundation Engineering, Proceedings, pp. 211-224.

Malgot, J. and J. Otepka. 1977. Gravitational slope deformations near Handlova. Bulletin, International Association of Engineering Geology, 15, pp. 63-65.

Mandel, J. and J. Salencon. 1972. Force portante d'un sol sur une assise rigide (etude theoretique). Geotechnique, 22, pp. 79-93.

Manning, P.I., J.A. Robbie and H.E. Wilson. 1970. Geology of Belfast and the Lagan Valley. Government of Northern Ireland, Memoirs of the Geological Survey, 242 p.

Matheson, D.S. and S. Thomson. Geological implications of valley rebound. Canadian Journal of Earth Sciences, 10, pp. 961-978.

Mathews, W.H. 1952. Ice-dammed lavas from Clinker Mountain, southwestern British Columbia. American Journal of Science, 250, pp. 553-565.

Mathews, W.H. 1964. Potassium-argon age determination of Cenozoic volcanic rocks from British Columbia. Geological Society of America Bulletin, 75, pp. 465-468.

Mathews, W.H. 1968. Geomorphology, southwestern British Columbia. In 'Guidebook for geological field trips in southwestern British Columbia'. Edited by W.H. Mathews. Department of Geology, The University of British Columbia, Vancouver, B.C., Report No. 6, pp. 18-24.

Mathews, W.H. 1979. Landslides of Central Vancouver Island and the 1946 Earthquake. Bulletin of the Seismological Society of America, 69, pp. 445-450.

Mathews, W.H. 1981. Early Cenozoic resetting of potassium-argon dates and geothermal history of north Okanagan area, British Columbia. Canadian Journal of Earth Sciences, 18, pp. 1310-1319.

Mathews, W.H. and K.C.McTaggart. 1978. Hope rockslides, British Columbia, Canada. In

'Rockslides and Avalanches, 1'. Edited by B. Voight. Elsevier, New York, pp. 259–279.

Mathews, W.H. and G.E. Rouse. 1963. Late Tertiary volcanic rocks and plant–bearing deposits in British Columbia. Geological Society of America Bulletin, v. 74, p. 55–60.

McKyes, E. and R.N. Yong. 1971. Three techniques for fabric viewing as applied to shear distortion of a clay. Clays and Clay Minerals, 19, pp. 289–293.

Mitchell, J.K. 1976. Fundamentals of soil behavior. John Wiley and Sons, New York, 422 p.

Mitchell, R.J. and A.R. Markell. 1974. Flowsliding in sensitive soils. Canadian Geotechnical Journal, pp. 11–31.

Miyagi, T. 1979. Landslide in Miyagi Prefecture, Northeast Japan. Tohoku University, Sendai, Science Reports 57, Geography. pp. 91–101.

Mokievsky–Zubok, O. 1977. Glacier–caused slide near Pylon Peak, B.C. Canadian Journal of Earth Sciences, 14, pp. 2657–2662.

Moore, D.P. and W.H. Mathews. 1978. The Rubble Creek landslide, southwestern British Columbia. Canadian Journal of Earth Sciences, 15, pp. 1039–1052.

Morgenstern, N.R., G.E. Blight, N.Janbu, and D. Resendiz. 1977. State–of–the–art–report:slopes and excavations. Proceedings, 9. International Conference of Soil Mechanics and Foundation Engineering, 2, pp. 547–604.

Morgenstern, N.R. and D.M. Cruden. 1977. Description and classification of geotechnical complexities. General Report, Session 2, International Symposium on the Geotechnics of Structurally Complex Formations, 18 p.

Morgenstern, N.R. and J.S. Tchalenko. 1967. Microstructural observations on shear zones from slips in natural clays. Proceedings, Oslo Geotechnical Conference, 1, pp. 147–152.

Morgenstern, N.R. and D.A. Sangrey. 1978. Methods of stability analysis. In 'Landslides:Analysis and Control.' Edited by R.L.Schuster and R.J. Krizek. Transportation Research Board, National Research Council, Special Report 176, pp. 155–171.

Morland, L.W. and C.R. Hastings. 1973. A void–collapse model for dry porous tuffs. Engineering Geology, 7, pp. 81–97.

Nakamura, S. 1976. Landslides and subsurface valleys around the pyroclastic deposits. Science Reports, Tohoku University, 7th Series (Geography), 26, pp. 113–125.

Nemcok, A. 1964. Geological construction of slopes and its influence on the origin and distribution of landslides in the west Carpathians. Geologicky Sbornik, 15, pp. 147–155.

Newcomb, R.C. 1959. Some preliminary notes on ground water in the Columbia River Basalt. Northwest Science, 33, pp. 1–18.

Newcomb, R.C. 1961. Storage of groundwater behind subsurface dams in the Columbia River Basalt, Washington, Oregon and Idaho. United States Geological Survey, Professional Paper 383–A, 15 p.

Newcomb, R.C. 1969. Effects of tectonic structure on the occurrence of groundwater in the Basalt of the Columbia River Group of The Dalles Area, Oregon and Washington. United States Geological Survey, Professional Paper 383–C, 33 p.

Niccum, M.R. 1967., A guide for foundation investigations in the basalts at the National

Reactor Testing Station, Idaho. Proceedings, 5th Annual Engineering Geology and Soils Engineering Symposium, Pocatello, Idaho. pp. 65–92.

Nieble, C., N.F. Midea, F. Fujimura and S.B. Neto. 1974. Shear strength of typical features of basaltic rock masses – Parana Basin – Brazil. Proceedings, 3rd. International Society Rock Mechnanics Conference, 2A, pp. 294–301.

Okulitch, A.V. 1979. Thompson–Shuswap–Okanagan. Geological Survey of Canada, Open–File Report 637.

Ollier, C. 1969. Volcanoes. M.I.T. Press, Cambridge, Mass. 177 p.

Parsons, W.H. 1974. Volcanic rocks of the Absaroka–Yellowstone region. In "Rock Mechanics:The American Northwest." Edited by B. Voight, pp. 94–101.

Pasek, J. and B. Kostak. 1977. Block type slope movements (in Czechoslovakian with English Summary). Rozpravy Ceskoslovenske Akademie Ved, Rada Matematickych a Prirodnich Ved, Rocnik 87–Sesit 3, 58 p.

Patton, F.D. 1976. The Devastation Glacier slide, Pemberton, B.C. Geological Association of Canada, Cordilleran Section, Programme and Abstracts, pp. 26–27.

Paeth, R.C., M.E. Harward, E.G. Knox and C.T. Dyrness. 1971. Factors affecting mass movement of four soils in the western Cascades of Oregon. Soil Science Society of America, Proceedings, 35, pp. 943–947.

Palmer, L. 1977. Large landslides of the Columbia River Gorge, Oregon and Washington. Geological Society of America, Reviews in Eengineering Geology, 3, pp. 69–83.

Pearson, R.C. and J.D. Obradovich. 1977. Eocene rocks in northeast Washington – radiometric ages and correlation. United States Geological Survey, Bulletin 1433, 41

p.

Pettijohn, F.J. 1975. Sedimentary Rocks. 3rd Edition, Harper and Row, Inc., New York. 628
    p.

Pevear, D.R., V.E. Williams and G.E. Mustoe. 1980. Kaolinite, smectite, and K-rectorite in
    bentonites: relation to Coal rank at Tulameen, British Columbia. Clays and Clay
    Minerals, 28, pp. 241-254.

Phillips, F.C. 1971. The Use of Stereographic Projection in Structural Geology. 3rd
    Edition, Arnold, London, 90 p.

Pierce, W.G. 1968. The Carter Mountain landslide area, northwest Wyoming. United
    States Geological Survey, Professional Paper 600-D, pp. D235-D241.

Piper, A.M. 1932. Geology and groundwater resources of The Dalles region, Oregon.
    United States Geological Survey, Water Supply Paper 659-B, pp. 107-189.

Pope, R.J. and M.W. Anderson. 1960. Strength properties of clays derived from volcanic
    rocks. Proceedings, A.S.C.E. Research Conference on Shear Strength in Cohesive
    Soils, University of Colorado. pp. 315-340.

Preto, V.E. 1973. Afton: Pothook. B.C. Department of Mines and Petroleum Resources;
    Geology, Exploration and Mining, 1972, pp. 209-220.

Prior, D.B., N. Stephens and D.R. Archer. 1968. Composite mudflows of the Antrim
    coast of northeast Ireland. Geografiska Annaler, 50A, pp. 65-78.

Pusch, R. 1970. Microstructural changes in soft quick clay at failure. Canadian
    Geotechnical Journal, 7, pp. 1-7.

Radbruch-Hall, D.H., D.J. Varnes and W.Z. Savage. 1976. Gravitational spreading of steep-sided ridges ('sackung') in western United States. Bulletin, International Association of Engineering Geology, 14, pp. 23-35.

Rands, H.A. 1915. Grouted cut-off for the Estacada Dam. Transactions, American Society of Civil Engineers, 78, pp. 447-482.

Raphael, J.M. and R.E. Goodman. 1979. Strength and deformability of highly fractured rock. Journal of the Geotechnical Engineering Division, American Society of Civil Engineers, 105, pp. 1285-1300.

Ratterman, N.G. and R.C. Surdam. 1981. Zeolite mineral reaction in a tuff in the Laney Member of the Green River Formation, Wyoming. Clays and Clay Minerals, 29, pp. 365-377.

Ray, R.G. 1960. Aerial photographs in geologic interpretation and mapping. United States Geological Survey, Professional Paper 373, 230 p.

Read, P.B. 1980. Stratigraphy and structure: Thor-Odin to Frenchman Cap domes, Vernon east-half map area, southern British Columbia. Geological Survey of Canada, Paper 80-1A, pp. 19-25.

Read, P.B. and A.V. Okulitch. 1977. The Triassic unconformity of south-central British Columbia. Canadian Journal of Earth Sciences, 14, pp. 606-638.

Resendiz, D. and J. Zonana. 1969. The short-term stability of open excavations in Mexico City clay. In 'Nabor Carillo;The Subsidence of Mexico City and Texcoco Project'. Secretaria de Hacienda y Credito Publico, Mexico, pp. 203-227.

Rib, H.T. and T. Liang. Recognition and identification. In 'Landslides: Analysis and Control'. Edited by R.L. Schuster and R.J. Krizek. Transportaion Research Board, National

Research Council, Special Report 176, pp. 34–80.

Riglin, L.D. 1976. The Perpetual landslide, Summerland, British Columbia. Unpublished
    M.Sc. Thesis, U.B.C., Vancouver, 146 p.

Rocha, M. 1964. Mechanical behaviour of rock foundations in concrete dams.
    Transactions, 8th. International Congress on Large Dams, Edinburgh, 1, pp.
    785–831.

Rocha, M., S. Brito and C. Nieble. 1974. Application of advanced techniques to the study
    of the foundations of Sao Simao Dam. Proceedings, 3rd. International Society for
    Rock Mechanics Conference, Vol. 2A, pp. 913–921.

Ross, J.V. 1975. A Tertiary thermal event in south–central British Columbia: reply.
    Canadian Journal of Earth Sciences, 12, pp. 899–902.

Rouse, G.E. and W.H. Mathews. 1961. Radioactive dating of Tertiary plant–bearing
    deposits. Science, v. 133, p. 1079–1080.

Ruiz, M.D., F.P. Camargo, N.F. Midea and C.M. Nieble. 1968. Some considerations
    regarding the shear strength of rock masses. Proceedings, International symposium
    on Rock Mechanics, Madrid. pp. 159–169.

Ruiz, M.D., G. Re, T.B. Celestino and M.A. Buosi. 1979. A synthesis of the geomechanical
    characteristics of basaltic masses as dam foundations. Proceedings, 4th. Congress
    International Society of Rock Mechanics, 1, pp. 287–292.

Russell, I.C. 1893. A geological reconnaissance in central Washington. United States
    Geological Survey, Bulletin 108, 108 p.

Russell, I.C. 1898. Topographic features due to landslides. Popular Science Monthly, 53,

pp. 480-489.

Russell, I.C. 1899. A preliminary paper on the geology of the Cascade mountains in northern Washington. United States Geological Survey, 20. Annual Report, 1898-99, Part 2, pp. 83-210.

Russell, I.C. 1901. Geology and water resources of Nez Perce Co., Idaho, Part 1. United States Geological Survey, Water Supply Paper 53, 85 p.

Russell, I.C. 1902. Geology and water resources of the Snake River Plains of Idaho. United States Geological Survey, Bulletin 199, 192 p.

Ryder, J.M. 1971. The stratigraphy and morphology of para-glacial alluvial fans in south-central British Columbia. Canadian Journal of Earth Sciences, 8, pp. 279-298.

Ryder, J.M. 1976. Terrain inventory and Quaternary geology, Ashcroft, British Columbia. Geological Survey of Canada Paper 74-49, 17 p.

Ryder, J.M. 1978. Geomorphology and Late Quarternary history of the Lillooet area. Archaeological Survey of Canada Paper 73, Report of the Lillooet Archaeological Project. pp. 56-57.

Sarna-Wojicki, A.M., S. Shipley, R.B. Waitt, D. Dzurisin, and S.H. Wood. Areal distribution, thickness, mass, volume, and grain size of air-fall ash from the six major eruptions of 1980. In 'The 1980 Eruptions of Mount St. Helens.' Edited by P.W. Lipman and D.R. Mullineaux. United States Geological Survey Professional Paper 1250, pp. 577-600.

Schau, M.P. 1968. Geology of the Upper Triassic Nicola Group in southcentral British Columbia. Unpublished Ph.D. thesis, U.B.C., Vancouver, 211 p.

Schmid, R. 1981. Descriptive nomenclature and classification of pyroclastic deposits and fragments: Recommendations of the IUGS Subcommission on the Systematics of Igneous Rocks. Geology, 9, pp. 41-43.

Schmidt, V. and D.A. McDonald. 1979. Texture and recognition of secondary porosity in sandstones. Society of Economic Palaeontologists and Mineralogists, Special Publication, No. 26, pp. 209-225.

Scott, J.S. and E.W. Brooker. 1968. Geological and engineering aspects of Upper Cretaceous shales in western Canda. Geological Survey of Canada, Paper 66-37, 75 p.

Serafim, J.L. 1964. Rock mechanics considerations in the design of concrete dams. In 'State of Stress in the Earth's Crust'. Edited by W.R. Judd. American Elsevier Co., New York, pp. 611-650.

Sharma, S.C. 1975. Landslips in the Deccan Traps with special reference to the western Ghats. Proceedings, Seminar on Landslides and Toe Erosion Problems with Special Reference to Himalayan Region, Sikkim, 1975. pp.

Shroder, J.F. 1971. Landslides in Utah. Utah Geological and Mineralogical Survey, Bulletin 90, 51 p.

Simonett, D.S. 1967. Landslide distribution and earthquakes in the Bewani and Torricelli Mountains, New Guinea. In 'Landform Studies from Australia and New Guinea'. Edited by J.N. Jennings and J.A. Mabbitt, Australia National University Press, Canberra, pp. 64-84.

Sissons, J.B. 1967. The Evolution of Scotland's Scenery. Oliver and Boyd, London, 259 pp.

Skempton, A.W. 1966. Some observations on tectonic shear zones. Proceedings, 1st. International Conference on Rock Mechanics, 1, pp. 329–335.

Smith, G.O. 1903. Contributions to the geology of Washington – geology and physiography of central Washington. United States Geological Survey, Professional Paper 19, 101 p.

Squier, L.R. and J.H. Versteeg. 1971. The history and correction of the OMSI–Zoo landslide. 9th. Annual Symposium Engineering Geology and Soils Engineering, Proceedings, Boise, Idaho, pp. 237–256.

Stanley, K.O. and L.V. Benson. 1979. Early diagenesis of High Plains Tertiary vitric and arkosic sandstone, Wyoming and Nebraska. Society of Economic Palaeontologists and Mineralogists, Special Publication 26, pp. 401–423.

Staples, L.W. 1957. Landslide at north abutment of Lookout Point Dam, Oregon. Geological Society of America, Engineering Geology Case Histories, No. 1, pp. 43–48.

Stearns, H.T., L. Crandall and W.G. Steward. 1938. Geology and water resources of the Snake River Plain in southeastern Idaho. United States Geological Survey, Water Supply Paper 774, 268 p.

Stephens, N. 1958. The evolution of the coastline of northeast Ireland. The Advancement of Science, 14, pp. 389–391.

Stewart, J.H. 1979. Basin–range structure in western North America: a review. In 'Cenozoic Tectonics and Regional Geophysics of the Western Cordillera', Edited by R.B. Smith and G.P. Eaton. Geological Society of America, Memoir 152, pp. 1–15.

Stimpson, B. and G. Walton. 1967. Clay mylonites in English Coal Measures – their

significance in open cast slope stability. International Association Engineering
Geology, 1st International Congress, Paris 1970, Proceedings, Vol. 2, pp.
1388-1393.

Suklje, L. and S. Vidmar. 1961. A landslide due to long term creep. Proceedings, 5th.
International Conference Soil Mechanics and Foundation Engineering, 2, pp.
727-735.

Surdam, R.C. and J.R. Boles. 1979. Diagenesis of volcanic sandstones. Society of
Economic Palaeontologists and Mineralogists, Special Publication No. 26, pp.
227-242.

Swanson, F.J. and M.E. James. 1975. Geology and geomorphology of the H.J. Andrews
Experimental Forest, western Cascades, Oregon. United States Department of
Agriculture Forest Service Research Paper PNW-188, 14 p.

Swanston, D.N. and F.J. Swanson. 1976. Timber harvesting, mass erosion and steepland
forest geomorphology in the Pacific Northwest. In 'Geomorphology and
Engineering', Ed. D.R. Coates, pp. 199-221, Dowden Hutchison and Ross, Inc.,
Stroudsburg, Pa.

Tchalenko, J.S. 1972. Similarities between shear zones of different magnitudes.
Geological Society of America, Bulletin, 81, pp. 1625-1640.

Thompson, C.D. and J.J. Emery. 1977. Influence of a Localised Plastic Layer on
Embankment Stability. Canadian Geotechnical Journal, 14, pp. 524-530.

Thomson, S. and N.R. Morgenstern. 1977. Factors affecting distribution of landslides
along rivers in southern Alberta. Canadian Geotechnical Journal, 14, pp. 508-523.

Thomson, S. and N.R. Morgenstern. 1979. Landslides in argillaceous bedrock, Prairie

Provinces, Canada. In 'Rockslides and Avalances 2.' Edited by B. Voight. Elsevier, Amsterdam, pp. 515–540.

Thorarinsson, S. 1967. The eruptions of Hekla in historical times. Societas Scientiarum Islandica, Reykavik, 183 p.

Thorarinsson, S., T. Einarsson and G. Kjartansson. 1959. On the geology and geomorphology of Iceland. Geografiska Annaler, 41, pp. 135–169.

Thorez, J. 1976. Practical Identification of Clay Minerals. Lelotte, Dison, Belgium. 90 p.

Tipper, H.W. 1959. Quesnel. Geological Survey of Canada Map 12–1959.

Tipper, H.W. 1963. Taseko Lakes. Geological Survey of Canada Map 29–1963.

Trettin, H.P. 1961. Geology of the Fraser River valley between Lillooet and Big Bar Creek. British Columbia Department of Mines and Petroleum Resources, Bulletin, 44, 109 p.

Trimble, D. E. 1963. Geology of Portland, Oregon, and adjacent areas. United States Geological Survey, Bulletin 1119, 119 p.

Trollope, D.H. 1980. The Vajont slope failure. Rock Mechanics, 13, pp. 71–88.

Tryggvason, T. 1957. The rock series at Irafoss. Water Power, 9, pp. 13–19.

Uglow, W.L. 1923. Cretaceous age and Early Eocene uplift of a peneplain in southern British Columbia. Bulletin of the Geological Society of America, 34, pp. 561–572.

UNAM. 1976. Behavior of dams built in Mexico. Instituto de Ingervieria, UNAM, Ciudad Universitaria, Mexico. 587 p.

Underwood, L.B. 1964. Chalk foundations at 4 major dams in the Missouri River basin. Transactions, 8th. International Conference on Large Dams, 1, pp. 23–45.

Underwood, L.B., S.T. Thorfinson and W.T. Black. 1964. Rebound in the design of the Oahe Dam hydraulic structure. Journal of the Soil Mechanics and Foundation Engineering Division, American Society of Civil Engineers, 90, pp. 65–86.

Vandine, D.F. 1980. Engineering geology and geotechnical study of Drynoch landslide, British Columbia. Geological Survey of Canada, Paper 79–31, 34 p.

Van Horn, R. 1972. Surficial and bedrock geologic map of the Golden quadrangle, Jefferson County, Colorado., United States Geological Survey Map I–761–A.

Varnes, D.J. 1978. Slope movement types and processes. In 'Landslides: Analysis and Control'. Edited by R.L. Schuster and R.J. Krizek. Transportation Research Board, National Research Council, Special Report 176, pp. 11–33.

Vaughan, P.R. 1976. Appendix: The deformations of the Empingham valley slope. Philosophical Transactions of the Royal Society of London, A, 283, pp. 451–462.

Vaughan, P.R. and H.J. Walbancke. 1973. The stability of cut and fill slopes in boulder clay. Proceedings of Symposium on Engineering Behavior of Glacial Materials, pp. 209–219, Birmingham.

Vesic, A.S. 1975. Bearing capacity of shallow foundations. In 'Foundation Engineering Handbook'. Edited by H.F. Winterkorn and H–Y Fang, Van Nostrand Reinhold Co., pp. 121–147.

Voight, B. 1973. The mechanics of retrogressive block–gliding, with emphasis on the evolution of the Turnagain Heights landslide, Anchorage, Alaska. In 'Gravity and Tectonics'. Edited by K.A. de Jong and R. Scholten, John Wiley and Sons, New York,

pp. 97–121.

Voight, B., H. Glicken, R.J. Janda and P.M. Douglass. 1981. Catastrophic rockslide avalanche of May 18. In 'The 1980 Eruptions of Mount St. Helens'. Edited by P.W. Lipman and D.R. Mullineaux. United States Geological Survey Professional Paper 1250, pp. 347–377.

Waldrop, H.A. and H.J. Hyden. 1963. Landslides near Gardiner, Montana. United States Geological Survey, Professional Paper 450–E, pp. E11–E14.

Walker, G.P.L. and R. Croasdale. 1971. Characteristics of some basaltic pyroclastics. Bulletin Volcanologique, 35, pp. 303–317.

Wallace, R.E. 1950. Determination of dip and strike by indirect observation in the field and from aerial photographs: a solution by stereographic projection. Journal of Geology, 58, pp. 269–280.

Walton, A.W. 1975. Zeolitic diagenesis in Oligocene volcanic sediments, Trans–Pecos, Texas. Geological Society of America Bulletin, 86, pp. 615–624.

Walton, A.W., W.E. Galloway and C.D. Henry. 1981. Release of Uranium from volcanic glass in sedimentary sequences: An analysis of two systems. Economic Geology, 76, pp. 69–88.

Watari, M. 1967. On the landslide mechanism in altered volcanic rock. Proceedings, 3rd. Asian Regional Conference on Soil Mechanics and Foundation Engineering, 1, pp. 369–373.

Waters, A.C. 1955. Geomorphology of south–central Washington, illustrated by the Yakima–East quadrangle. Bulletin of the Geological Society of America, 66, pp. 663–684.

Waters, A.C. 1973. The Columbia River Gorge; basalt stratigraphy, ancient lava dams, and landslide dams. Oregon Department of Geology and Mineral Industries, Bulletin 77, pp. 133–154.

Watson, R.A. and H.E. Wright. 1963. Landslides on the east flank of the Chuska Mountains, northwestern New Mexico. American Journal of Science, 261, pp. 525–548.

Weymouth, J.H. and W.O. Williamson. 1953. The effects of extrusion and some other processes on the microstructure of clay. American Journal of Science, 251, pp. 89–108.

Williams, H. and A.R. McBirney. 1979. Volcanology. Freeman, Cooper & Co. San Francisco. 397 p.

Wilson, M.D. and E.D. Pittman. 1977. Authigenic clays in sandstones: recognition and influence on reservoir properties and palaeoenvironmental analysis. Journal of Sedimentary Petrology, 47, pp. 3–31.

Windom, K.E., D.C. Stewart and C.P. Thornton. 1981. Development of columnar–spheroidal structures by meteoric water in a New Mexico basalt. Geology, 9, pp. 73–76.

Witkind, I.J. 1969. Geology of the Tepee Creek quadrangle, Montana–Wyoming. United States Geological Survey Professional Paper 609, 101 p.

Worobey, G. 1972. An investigation of talus slope development in the Similkameen Valley, near Keremeos, British Columbia. Unpublished M.A. Thesis, University of British Columbia, Vancouver, 170 p.

Wright, H.E. 1946. Tertiary and Quaternary geology of the Lower Rio Puerco area, New

Mexico. Geological Society of America, Bulletin, 57, pp. 383-456.

Yatsu, E. 1966. Rock Control in Geomorphology. Sozosha, Tokyo, 135 p.

Yeend, W.E. 1969. Quatenary Geology of the Grand and Battlement Mesas Area, Colorado. United States Professional Paper 617, 50 p.

Yeend, W.E. 1973. Slow-sliding slumps, Grand Mesa, Colorado. The Mountain Geologist, 10, pp. 25-28.

Zaruba, Q. and V. Mencl. 1969. Landslides and their Control. Elsevier, New York, 205 p.